

# **Neuroprotective effects of amantadine-flavonoid conjugates**

**P.M. FOURIE**

*Dissertation submitted in partial fulfilment of the requirements for the degree*

**Magister Scientiae**

*in*

*Pharmaceutical Chemistry*

*at the North-West University, Potchefstroom Campus*

Supervisor: Prof. S.F. Malan

Co-Supervisor: Prof. S. Van Dyk

Assistant Supervisor: Prof. D.W. Oliver

# **Neurobeskermde effekte van amantadien-flavonoïd konjugate**

**P.M. FOURIE**

*Verhandeling voorgelê ter gedeeltelike vervulling van die vereistes vir die graad*

**Magister Scientiae**

*in*

*Farmaseutiese chemie*

*by die Noordwes-Universiteit, Potchefstroom Kampus*

Promotor:	Prof. S.F. Malan
Mede-promotor:	Prof. S. Van Dyk
Hulp promotor:	Prof. D.W. Oliver



## Abstract

Neurodegenerative disorders like Parkinson's and Alzheimer's disease affect millions of people around the world. Oxidative stress has been implicated in the pathogenesis of a number of neurodegenerative disorders, cancer and ischemia. The brain is particularly vulnerable to oxidative damage because of its high utilisation of oxygen, high levels of polyunsaturated fatty acids, relatively high levels of redox transition metal ions and low levels of antioxidants. Oxidative stress occurs due to an imbalance in the pro-oxidant and antioxidant levels. Reactive oxygen/nitrogen species (ROS/RNS) is a collective term used for free radicals and related molecules, promoting oxidative stress within cells and ultimately leading to neurodegeneration. Antioxidants counteract the excess in ROS/RNS, and is therefore of interest in the treatment and prevention of neurodegenerative disorders.

Monoamine oxidases, especially monoamine oxidase B (MAO-B), also play an important role in neurodegenerative disorders. MAO-B is the main enzyme responsible for the oxidative deamination of dopamine in the substantia nigra of the brain. By inhibiting MAO-B, dopamine is increased in the brain providing symptomatic relief in Parkinson's disease.

The focus of the current study was to synthesise multifunctional compounds that could be used in the treatment and/or prevention of neurodegenerative diseases. In this study flavonoids were selected because of their wide spectrum of biological activities, including antioxidant activity and its monoamine oxidase inhibition. Flavones and chalcones are both classified under flavonoids and both structures were included. The amantadine moiety was included because of its known ability to inhibit calcium flux through the N-methyl-D-aspartate (NMDA) receptor channel. Six amantadine-flavonoid derivatives were synthesised using standard laboratory procedures and structures were determined with standard methods such as NMR, IR and mass spectrometry. The synthesised compounds were tested in a selection of biological assays, to establish the relative antioxidant properties and MAO inhibitory activity.

The biological assays employed to test antioxidant properties were the thiobarbituric acid (TBA) and nitro-blue tetrazolium (NBT) assays. The TBA assay relies on the assessment of lipid peroxidation, induced *via* hydroxyl anions ( $\text{OH}\cdot$ ), generating a pink colour with the complex formation between malondialdehyde (MDA) and TBA, which is measured spectrophotometrically at 532 nm. The principal of the NBT assay is the reduction of NBT to nitro-blue diformazan (NBD), producing a purple colour in the presence of superoxide anions ( $\text{O}_2^-$ ).

The synthesised compounds were also evaluated for their MAO inhibitory activity toward recombinant human MAO-A and –B and inhibition values were expressed as IC<sub>50</sub> values.

The experimental data obtained in the NBT and TBA assay indicated a weak but a significant ability to scavenge O<sub>2</sub><sup>•-</sup> and OH<sup>•</sup>. In the NBT assay N-(adamantan-1-yl)-2-{3-hydroxy-4-[(2E)-3-(3-methoxyphenyl)pro-2-enoyl]phenoxy}acetamide (**6**) had the best results with a 50.47 ± 1.31 µM/mg protein reduction in NBD formation, indicating that the hydroxyl group contributed to activity. The synthesised compounds were compared to the toxin (KCN) with a reduction in NDB formation of 69.88 ± 1.59 µM/mg protein. Results obtained from the TBA assay indicated that the flavone moiety had better OH<sup>•</sup> scavenging ability than that of the chalcone moiety with N-(adamantan-1-yl)-2-[(5-hydroxy-4-oxo-2-phenyl-4H-chromen-7-yl)oxy]acetamide (**3**) showing the best activity at 0.967 ± 0.063 nmol MDA/mg tissue. The synthesised compounds were compared to the toxin (H<sub>2</sub>O<sub>2</sub>) 1.316 ± 0.028 nmol MDA/mg tissue. None of the test compounds could be compared to the results obtained with Trolox<sup>®</sup>. The IC<sub>50</sub> values obtained for inhibition of recombinant human MAO indicated that the chalcone moiety (N-(adamantan-1-yl)-4-[(1E)-3-oxo-3-phenylpro-1-en-1-yl]benzamide (**5**)) showed the best inhibition of MAO-B with an IC<sub>50</sub> of 0.717 ± 0.009 µM and of MAO-A with an IC<sub>50</sub> of 24.987 ± 5.988 µM. It was further confirmed that N-(adamantan-1-yl)-4-[(1E)-3-oxo-3-phenylpro-1-en-1-yl]benzamide (**5**) binds reversible to MAO-B and that the mode of inhibition is competitive. Docking studies revealed that N-(adamantan-1-yl)-4-[(1E)-3-oxo-3-phenylpro-1-en-1-yl]benzamide (**5**) traverses both cavities of MAO-B with the chalcone moiety orientated towards the FAD co-factor while the amantadine moiety protrudes into the entrance cavity.

The observation that the synthesised compounds containing the chalcone moiety inhibited both MAO-A and –B and showed some degree of superoxide anion scavenging ability, make them ideal candidates for further research and possible multifunctional drug design.

Key terms: antioxidant, monoamine oxidase inhibitors, amantadine, flavonoids, neuroprotective.

## Uittreksel

Neurodegeneratiewe toestande soos Parkinson en Alzheimer se siekte beïnvloed miljoene mense om die wêreld. Oksidatiewe stres is geïmpliseer in die patogenese van 'n aantal neurodegeneratiewe siektes, kanker en in beperking in bloedvoorsiening. Die brein is veral kwesbaar vir oksidatiewe skade as gevolg van sy hoë suurstofbenutting, hoë vlakke van polionversadigde vetsure, relatief hoë vlakke van redoks-oorgangsmetaalione en lae vlakke van anti-oksidente. Oksidatiewe stres vind plaas as gevolg van 'n wanbalans in pro-oksident en anti-oksident vlakke. Reaktiewe suurstof/stikstof spesies (RSS) is 'n versamelterm vir vryradikale en verwante molekules wat oksidatiewe stres binne selle bevorder en uiteindelik neurodegenerasie veroorsaak. Die oormaat RSS word teengewerk deur anti-oksidente en is dus van belang in die behandeling en voorkoming van neurodegeneratiewe siektes. Monoamienoksidases, veral monoamienoksidase-B (MAO-B), speel 'n belangrike rol in die neurodegeneratiewe siektes en MAO-B is 'n belangrike ensiem verantwoordelik vir die oksidatiewe deaminering van dopamien in die substantia nigra van die brein. Deur MAO-B te inhibeer word dopamienvlakke in die brein verhoog en simptomatiese verligting in Parkinson se siekte verkry.

Die fokus van die huidige studie was om 'n multifunksionele verbinding te sintetiseer wat gebruik kan word in die behandeling en/of voorkoming van neurodegeneratiewe siektes. Flavonoïede is in hierdie studie gekies omdat hulle 'n wye spektrum van biologiese aktiwiteit insluitende anti-oksident aktiwiteit en inhibisie van monoamineoksidase vertoon. Flavone en chalkone word geklassifiseer as flavonoïede en beide is ingesluit in die ondersoek. Die amantadienstruktuur is ingesluit omdat dit bekend is dat dit kalsiumfluks inhibeer deur die N-metiel-D-aspartaat (NMDA) reseptorkanaal. Amantadien-flavonoïedkonjugate is met standaard laboratoriumprosedures gesintetiseer en strukture is met standaard metodes soos kernmagnetiese resonansspektroskopie, infrarooispektroskopie en massaspektrometrie bevestig. Die gesintetiseerde verbindings is geëvalueer vir anti-oksidentaktiwiteit en monoamienoksidaseinhibisie.

Die biologiese analise wat gebruik is om anti-oksident eienskappe te toets is die tiobarbituursuur- en nitro-bloutetrasoliumanalises. Die tiobarbituursuuranalise is gebaseer op die bepaling van lipiedperoksidase d.m.v induksie van hidroksieradikale ( $\text{OH}^\bullet$ ) in rotbreinhomogenaat met waterstofperoksied ( $\text{H}_2\text{O}_2$ ) as toksien. Dit vorm 'n kompleks tussen malondialdehid (MDA) en tiobarbituursuur met 'n pienk kleur wat dan gelees word by 532 nm. Die NBT-analise meet die reaksie van NBT na nitro-bloudiformasan (NBD) wat 'n pers kleur produseer in die teenwoordigheid van superoksiedradikale ( $\text{O}_2^-$ ) in die rotbreinhomogenaat.

Die gesintetiseerde verbindings is ook getoets vir hul MAO-inhiberende aktiwiteit met rekombinante mensmonoamienoksidase en inhibisie is uitgedruk as  $IC_{50}$ -waardes.

Die eksperimentele data verkry met die NBT en tiobarbituursuuranalise het aangedui dat die gesintetiseerde verbindings 'n swak, maar noemenswaardige vermoë het om  $OH^\bullet$  en  $O_2^-$  op te ruim. N-(adamantaan-1-iel)-2-{3-hidroksi-4-[(2E)-3-(3-metoksifeniel)pro-2-enol]fenoksi}asetamied (**6**) het die beste resultate gelever in die NBT toets met 'n  $50,47 \pm 1,31 \mu M$  / mg proteïen vermindering in NBD vorming, wat daarop dui dat die hidroksielgroep bydra tot beter aktiwiteit. Die gesintetiseerde verbindings is vergelyk met die toksien, KCN, wat 'n afname in NBD vorming van  $69,88 \pm 1,59 \mu M$  / mg proteïen veroorsaak. Die uitslae van die tiobarbituursuuranalise het aangedui dat verbindings met die flavoonstruktuur beter  $OH^\bullet$  opriemingsvermoë het as die chalkoonderivate. N-(adamantaan-1-iel)-2-[(5-hidroksi-4-okso-2-feniel-4H-chromeen-7-iel)oksi]asetamied (**3**) het die beste aktiwiteit getoon met  $0,967 \pm 0,063$  nmol MDA / mg weefsel. Die gesintetiseerde verbindings is vergelyk met die toksien,  $H_2O_2$ , met  $1,316 \pm 0,028$  nmol MDA / mg weefsel. Nie een van die toets verbindings kan vergelyk word met die resultate wat met Trolox<sup>®</sup> verkry is nie. Uit die  $IC_{50}$ -waardes van MAO-inhibisie blyk dit dat die chalkoonderivaat (N-(adamantaan-1-iel)-4-[(1E)-3-okso-3-fenielpro-1-en-1-iel]bensamied (**5**)) die beste inhibisie van MAO-B, met 'n  $IC_{50}$  waarde van  $0,717 \pm 0,009 \mu M$ , en MAO-A, met 'n  $IC_{50}$  waarde van  $24,987 \pm 5,988 \mu M$ , toon. N-(adamantaan-1-iel)-4-[(1E)-3-okso-3-fenielpro-1-en-1-iel]bensamied (**5**) bind omkeerbaar met MAO-B en die modus van die inhibisie is mededingend. Rekenaarmodeleringstudies het gewys dat N-(adamantaan-1-iel)-4-[(1E)-3-okso-3-fenielpro-1-en-1-iel]bensamied (**5**) albei holtes in die MAO-B aktiewe setel beset met die chalkoonstruktuur gerig na die FAD-kofaktor in die substraatholte terwyl die amantadienderivaat tot in die ingangsholte strek.

Die verbindings met die chalkoonstruktuur inhibeer beide MAO-A en -B en dit het ook 'n mate van superoksiedanioonopriemingsvermoë. Dit maak hierdie konjugate ideale kandidate vir verdere navorsing en multifunksionele geneesmiddelontwerp.

Sleuteltermes: anti-oksidant, monoamienoksidase inhibeerder, flavonoïed, amantadien, neurobeskermd.

# Table of Contents

<b>Abstract.....</b>	<b>i</b>
<b>Uittreksel.....</b>	<b>iii</b>
<b>Table of Contents .....</b>	<b>v</b>
<b>List of Figures, Schemes &amp; Tables .....</b>	<b>xi</b>
<b>List of Abbreviations .....</b>	<b>xvi</b>
<b>Chapter 1. Introduction .....</b>	<b>1</b>
<b>1.1        Neurodegenerative disorders .....</b>	<b>1</b>
1.1.1       Parkinson's disease .....	1
1.1.2       Alzheimer's disease .....	1
1.1.3       Huntington's disease.....	2
<b>1.2       Oxidative stress .....</b>	<b>2</b>
<b>1.3       Monoamine oxidase.....</b>	<b>3</b>
<b>1.4       Research Objective.....</b>	<b>4</b>
1.4.1       Objectives for this Study: .....	4
<b>1.5       Proposed Series of Test Compounds .....</b>	<b>4</b>
<b>Chapter 2. Literature Review .....</b>	<b>6</b>
<b>2.1       Free Radicals, Reactive Oxygen Species and Reactive Nitrogen Species .....</b>	<b>6</b>
2.1.1       Reactive Oxygen Species and Free Radicals.....	7



2.1.1.1	Single Oxygen and Molecular oxygen.....	7
2.1.2	Hydrogen peroxide.....	8
2.1.3	Reactive Nitrogen Species.....	9
<b>2.2</b>	<b>Mitochondria as ROS source.....</b>	<b>10</b>
<b>2.3</b>	<b>Oxidative Stress.....</b>	<b>12</b>
2.3.1	Mechanisms of lipid peroxidation .....	14
2.3.2	Mechanisms of protein oxidation.....	16
2.3.3	DNA oxidation .....	17
<b>2.4</b>	<b>Oxidative modification in Alzheimer's disease.....</b>	<b>17</b>
<b>2.5</b>	<b>Oxidative modifications in Parkinson's disease.....</b>	<b>19</b>
<b>2.6</b>	<b>Antioxidants .....</b>	<b>20</b>
2.6.1	Enzymatic antioxidants .....	21
2.6.1.1	Superoxide dismutase .....	22
2.6.1.2	Glutathione peroxidase .....	22
2.6.1.3	Catalase .....	23
2.6.2	Non-enzymatic antioxidants .....	23
2.6.2.1	Natural Plant Antioxidants.....	24
2.6.2.1.1	Chalcones .....	24
2.6.2.1.2	Flavonoids.....	25
<b>Chapter 3.....</b>		<b>28</b>
<b>3.1</b>	<b>Monoamine Oxidase .....</b>	<b>28</b>

<b>3.2</b>	<b>Characteristics of Monoamine oxidase .....</b>	<b>29</b>
3.2.1	Three dimensional structure.....	30
<b>3.3</b>	<b>Physiological role of Monoamine oxidase B and inhibitors thereof .....</b>	<b>33</b>
3.3.1	Neurotoxins and models of neurodegeneration .....	34
3.3.2	Monoamine oxidase B inhibitors .....	36
3.3.3	MAO-B substrate.....	38
<b>3.4</b>	<b>Enzyme kinetics .....</b>	<b>38</b>
3.4.1	Introduction .....	38
3.4.2	$K_m$ determination .....	38
3.4.3	$K_i$ determination .....	40
3.4.4	$IC_{50}$ value calculation .....	42
<b>Chapter 4. Experimental.....</b>		<b>43</b>
<b>4</b>	<b>Standard Experimental Procedures .....</b>	<b>43</b>
4.1.1	Instrumentation .....	43
4.1.1.1	Nuclear Magnetic Resonance (NMR) Spectroscopy.....	43
4.1.1.2	Mass Spectrometry (MS) .....	43
4.1.1.3	Infrared Spectroscopy (IR) .....	43
4.1.1.4	Melting Point (MP) Determination .....	43
4.1.2	Chromatographic Techniques .....	43
4.1.2.1	Thin Layer Chromatography (TLC) .....	44
4.1.2.2	Column Chromatography .....	44
<b>4.2</b>	<b>Synthesis of Selected Compounds .....</b>	<b>44</b>

4.2.1	Synthesis of Amantadine-flavone conjugates .....	44
4.2.2	Synthesis of Amantadine-chalcone conjugates .....	44
<b>4.3</b>	<b>Synthesis .....</b>	<b>46</b>
4.3.1	N-(adamantan-1-yl)-2-[(4-oxo-2-phenyl-4H-chromen-3-yl)oxy]acetamide (1).....	46
4.3.2	N-(adamantan-1-yl)-2-[(4-oxo-2-phenyl-4H-chromen-7-yl)oxy]acetamide (2).....	47
4.3.3	N-(adamantan-1-yl)-2-[(5-hydroxy-4-oxo-2-phenyl-4H-chromen-7-yl)oxy]acetamide (3).....	48
4.3.4	N-(adamantan-1-yl)-2-[(4-oxo-2-phenyl-4H-chromen-6-yl)oxy]acetamide (4).....	49
4.3.5	N-(adamantan-1-yl)-4-[(1E)-3-oxo-3-phenylpro-1-en-1-yl]benzamide (5) .....	50
4.3.6	N-(adamantan-1-yl)-2-{3-hydroxy-4-[(2E)-3-(3-methoxyphenyl)pro-2-enoyl]phenoxy}acetamide (6).....	51
<b>4.4</b>	<b>Structure elucidation .....</b>	<b>52</b>
<b>4.5</b>	<b>Lipid Peroxidation.....</b>	<b>54</b>
4.5.1	Introduction .....	54
4.5.2	Assay Procedure.....	55
4.5.3	Materials and Methods.....	56
4.5.3.1	Chemicals and Reagents.....	56
4.5.3.2	Animals .....	57
4.5.3.3	Instrumentation .....	57
4.5.3.4	Malondialdehyde Calibration Curve .....	57
4.5.3.5	Preparation of Whole Rat Brain Homogenate.....	58

4.5.3.6	Method .....	58
4.5.3.7	Statistical Analysis .....	58
4.5.4	Results .....	59
4.5.5	Discussion.....	61
<b>4.6</b>	<b>Superoxide Anion Scavenging Activity .....</b>	<b>61</b>
4.6.1	Introduction .....	61
4.6.2	Assay Procedure.....	61
4.6.3	Materials and Methods.....	63
4.6.3.1	Chemicals and Reagents .....	63
4.6.3.2	Animals .....	63
4.6.3.3	Instrumentation .....	63
4.6.3.4	Preparation of standards.....	63
	BSA standard .....	63
	Nitro-Blue Difformazan Calibration Curve .....	64
4.6.3.5	Preparation of Whole Rat Brain Homogenate.....	65
4.6.3.6	Method .....	65
4.6.3.7	Statistical Analysis .....	65
4.6.4	Results .....	66
4.6.5	Discussion.....	67
<b>4.7</b>	<b>IC<sub>50</sub> determination for the inhibition of Human MAO .....</b>	<b>68</b>
4.7.1	Introduction .....	68
4.7.2	Assay procedure .....	68

4.7.3	Materials and Methods.....	69
4.7.3.1	Chemicals and Reagents.....	69
4.7.3.2	Instrumentation .....	69
4.7.3.3	Materials and Method .....	69
4.7.4	Results .....	70
4.7.5	Reversibility study .....	72
4.7.5.1	Method .....	72
4.7.5.2	Results .....	72
4.7.6	K <sub>i</sub> determination .....	73
4.7.6.1	Method .....	73
4.7.6.2	Results .....	74
4.7.7	Discussion.....	75
<b>4.8</b>	<b>Molecular modelling .....</b>	<b>75</b>
4.8.1	Introduction .....	75
4.8.2	Experimental .....	75
4.8.3	Results and discussion .....	76
<b>Chapter 5. Discussion and Conclusion .....</b>		<b>77</b>
<b>References.....</b>		<b>80</b>
<b>Appendix.....</b>		<b>103</b>
<b>Acknowledgements.....</b>		<b>129</b>

## List of Figures, Schemes & Tables

Figure 1.1	Basic flavonoid structure.	4
Figure 1.2	Test compounds ( <b>1 - 6</b> ) used in this study.	5
Figure 2.1	The mitochondrial electron transport chain. This simplified diagram of the electron transport chain on the inner mitochondrial membrane shows the direction of electron ( $e^-$ ) flow along the chain (black arrows) and the direction of flow (red arrows) of hydrogen ions ( $H^+$ ) across the mitochondrial membrane. Dotted arrows show ROS production as a result of the electron leak. UQ refers to ubiquinone; Cyt C refers to cytochrome c (directly extracted from Al Ghouleh <i>et al.</i> , 2011).	10
Figure 2.2	Reactive oxygen species (ROS) generated from mitochondria can damage cells. Free radicals generated by the electron transport chain can result in oxidative damage to mitochondrial DNA, proteins and lipid peroxidation. Enzymatic antioxidants include copper-zinc-containing superoxide dismutases (Cu-Zn-SOD); manganese-containing superoxide dismutases (Mn-SOD); glutathione peroxidase (GPx) and catalase (directly extracted from Yamada & Harashima, 2008).	11
Figure 2.3	Nitration of the 3-position of tyrosine by peroxynitrite.	13
Figure 2.4	Schematic diagram of lipid peroxidation mechanism applied to any polyunsaturated fatty acid. Arachidonic acid is used as an example (directly extracted from Catalá, 2010).	15
Figure 2.5	Involvement of Methionine 35 of $\beta$ -amyloid (1-42) in lipid peroxidation. The sulphur (S)-atom of Methionine 35 of the $\beta$ -amyloid (1-42) peptide can undergo one-electron oxidation to form a sulfuranyl radical cation within the bilayer, which has the ability to abstract a labile, allylic H-atom from the unsaturated acyl chains of lipid molecules, leading to initiation of the lipid peroxidation process (Butterfield <i>et al.</i> , 2010).	18
Figure 2.6	Classification of antioxidants. Some non-enzymatic antioxidants like uric acid, vitamin E, glutathione and CoQ10 are synthesised in the human body and they can also be derived from dietary sources. Polyphenols are the major class of antioxidants which are derived from diet (directly extracted from Venkat Ratnam <i>et al.</i> , 2006)	21

Figure 2.7	Schematic representation of antioxidant enzymes (adapted from Real <i>et al.</i> , 2010).	22
Figure 2.8	Basic flavone synthetase (Adapted from Gantet & Memelink, 2002).	25
Figure 3.1	MAO catalyses the oxidative deamination of monoamines. Monoamines are degraded by MAO to their correspondent aldehydes (R-CHO). This reaction produces ammonia (NH <sub>3</sub> ) and hydrogen peroxide (H <sub>2</sub> O <sub>2</sub> ). Aldehydes are further oxidised by aldehyde dehydrogenase (ALDH) into carboxylic acids (R-COOH). NADH is a critical cofactor for the latter reaction (directly extracted from Bortolato <i>et al.</i> , 2008).	28
Figure 3.2	The three dimensional structure of MAO-B dimer.	30
Figure 3.3	Ribbon diagram of monomeric unit of human MAO-B structure. The covalent flavin moiety is shown in a ball and stick model in yellow. The flavin binding domain is in blue, the substrate domain in red and the membrane domain in green (Edmondson <i>et al.</i> , 2007).	31
Figure 3.4	Ribbon diagram of the human MAO-A structure (Edmondson <i>et al.</i> , 2007).	32
Figure 3.5	Comparison of the active site cavities of human MAO-A and -B. Clorgyline is present in MAO-A's active site and Deprenyl in MAO-B's active site. Both form covalent N(5) flavocyanine adducts with the respective flavin coenzymes. The active site "shaping loop" structures is denoted in red for MAO-A and green for MAO-B (Edmondson <i>et al.</i> , 2007).	32
Figure 3.6	The pathways of hydrogen peroxide formation and reactive hydroxyl radical generation <i>via</i> iron Fenton Chemistry (adapted from Youdim <i>et al.</i> , 2004).	33
Figure 3.7	The neurotoxin MPTP is oxidised by MAO-B to give MPDP <sup>+</sup> and subsequently MPP <sup>+</sup> . MAO inhibitors and antioxidants exert neuroprotective actions by decreasing toxin activation and reducing oxidative stress (directly extracted from Heraiz & Guillén, 2011).	34
Figure 3.8	Mechanism of actions of various toxins used to produce Parkinson's disease models. MPTP is transported across the BBB and is converted to MPDP <sup>+</sup> by MAO-B. MPDP <sup>+</sup> is then oxidised to the toxic form MPP <sup>+</sup> in astrocytes. MPP <sup>+</sup> is released into the extracellular milieu by the plasma membrane transporter Oct3 and subsequently enters dopamine neurons by specific dopamine	

	transporters. This causes oxidative stress followed by cellular death. Abbreviations: ATP: Adenosine triphosphate; Oct3: organic cation transporter 3; BBB: Blood brain barrier; DAT: dopamine transporter; UPS: ubiquitin proteasome system (adapted from Cicchetti <i>et al.</i> , 2009).	35
Figure 3.9	Structures of selected MAO-B inhibitors.	37
Figure 3.10	Graphical presentation of the Michealis-Menten equation ( $V_i$ vs $[S]$ ).	39
Figure 3.11	A Lineweaver-Burke plot ( $1/V_i$ vs $1/[S]$ ).	40
Figure 3.12	The double reciprocal plot in the presence of different pre-set concentrations of a competitive inhibitor.	41
Figure 3.13	Secondary plot of the slopes from the double reciprocal plot versus inhibitor concentration.	41
Figure 3.14	Graphical representation of $IC_{50}$ value.	42
Figure 4.1	Correlations seen in HMQC of N-(adamantan-1-yl)-2-[(4-oxo-2-phenyl-4H-chromen-3-yl)oxy]acetamide ( <b>1</b> )	52
Figure 4.2	The Mechanism of the typical free radical chain reaction.	55
Figure 4.3	The reaction of Malondialdehyde with Thiobarbituric acid to yield a pink TBA2-MDA Complex.	55
Figure 4.4	MDA Calibration Curve indicating the MDA/TBA-complex formed.	57
Figure 4.5	The attenuation of lipid peroxidation by different concentrations of the synthesised compounds in whole rat brain homogenates <i>in vitro</i> . Each bar represents the mean $\pm$ S.E.M.; n = 10. ***p < 0.0001 vs toxin (#).	59
Figure 4.6	Reduction of NBT to NBD.	62
Figure 4.7	Bovine Serum Albumin Calibration Curve.	64
Figure 4.8	Nitro-blue Diformazan Calibration Curve.	64
Figure 4.9	The superoxide scavenging properties of the synthesised compounds in the presence of KCN in rat brain homogenate. Each bar represents the mean $\pm$ S.E.M.; n = 10. ***p < 0.0001 vs toxin (#).	66



Figure 4.10	The oxidation of kynuramine by MAO-A and –B.	69
Figure 4.11	The IC <sub>50</sub> calculation of N-(adamantan-1-yl)-4-[(1E)-3-oxo-3-phenylpro-1-en-1-yl]benzamide ( <b>5</b> ) towards human MAO-B: Log [I] = -0.147, which is equal to [I] = 0.717 $\mu$ M. The rate is expressed as nmol product formed/min•mg protein.	71
Figure 4.12	Rate of kynuramine oxidation by recombinant human MAO-B for each of the pre-incubation periods (0 – 60 minutes). The rate (V) is expressed as nmol product formed/min/mg protein.	73
Figure 4.13	Lineweaver-Burke plots of the oxidation of kynuramine by recombinant human MAO-B in the absence (diamond) and presence of various concentrations of compound <b>5</b> (square, 0.179 $\mu$ M; triangle, 0.358 $\mu$ M and cross, 0.717 $\mu$ M). The rate (V) is expressed as nmol product formed/min/mg protein.	74
Figure 4.14	Representation of compound <b>5</b> docked within MAO-B. The FAD co-factor is displayed in green, the inhibitor in blue, the pi bond in orange and Tyr435 in yellow.	76
Figure 5.1	Test compounds ( <b>1</b> - <b>6</b> ) synthesised in this study	78
Scheme 1	Synthetic route of amantadine-flavone conjugates.	44
Scheme 2	Synthetic route of amantadine-chalcone ( <b>5</b> ).	45
Scheme 3	Synthetic route of amantadine-chalcone ( <b>6</b> ).	45
Table 2.1	Some selected antioxidants and their mechanisms of action.	24
Table 2.2	Chemical structures of flavonoids and some examples.	26
Table 3.1	Substrates of MAO-A and MAO-B.	38
Table 4.1	<sup>1</sup> H and <sup>13</sup> C (DMSO-D <sub>6</sub> ) correlations observed in N-(adamantan-1-yl)-2-[(4-oxo-2-phenyl-4H-chromen-3-yl)oxy]acetamide ( <b>1</b> ).	53
Table 4.2	Lipid Peroxidation of Rat Brain Homogenate in the presence of Flavonoids.	60
Table 4.3	Scavenging of KCN-induced superoxide anion in the presence of Flavonoids.	67

Table 4.4      IC<sub>50</sub> values for the inhibition of human MAO-A and MAO-B by test compounds.

71

## List of Abbreviations

$\beta$ A42	-	$\beta$ -amyloid peptide 42
$\mu$ l	-	Microlitres
$\mu$ M	-	Micromolar
•NO	-	Nitric Oxide
$^{13}\text{C}$ NMR	-	Carbon-thirteen Nuclear Magnetic Resonance Spectroscopy
$^1\text{H}$ NMR	-	Proton/Hydrogen-one Nuclear Magnetic Resonance Spectroscopy
3-NT	-	3-nitrotyrosine
5-HT	-	Serotonin
AChE	-	Acetylcholinesterase
Acrolein	-	2-propen-1-al
ALDH	-	Aldehyde Dehydrogenase
ALR	-	Aldehyde Reductase
Arg	-	Arginine
ATP	-	Adenosine Triphosphate
BHT	-	2,6-Di-tert-butyl-4-methylphenol
CAT	-	Catalase
$\text{CH}_2\text{Cl}_2$	-	Dichloromethane
$\text{CH}_3\text{CN}$	-	Acetonitrile
$\text{CHCl}_3$	-	Chloroform
CHI	-	Chalcone Isomerase
CHS	-	Chalcone Synthase
CNS	-	Central Nervous System

COMP	-	Catechol O-Methyltransferase
Cu-Zn-SOD	-	Copper, zinc superoxide dismutase
Cys	-	Cysteine
DA	-	Dopamine
DAT	-	Dopamine Transporter
DMF	-	Dimethylformamide
DMSO	-	Dimethyl sulfoxide
Eq	-	Equation
ESI	-	Electron Spray Ionisation
ETC	-	Electron transport chain
EtOAc	-	Ethyl acetate
FAD	-	Flavin adenine dinucleotide
GAA	-	Glacial Acetic Acid
GPx	-	Glutathione peroxidase
GSH	-	Glutathione
H <sup>+</sup>	-	Proton/Hydrogen atom
H <sub>2</sub> O	-	Water molecule
H <sub>2</sub> O <sub>2</sub>	-	Hydrogen Peroxide
His	-	Histidine
HMBC NMR	-	Heteronuclear Multiple-bond Correlation Nuclear Magnetic Resonance
HNE	-	4-hydroxy-2- <i>trans</i> -nonenal
HSQC NMR	-	Heteronuclear Single Quantum Correlation Nuclear Magnetic
IC <sub>50</sub>	-	Half Maximal Inhibitory Concentration

Ile	-	Isoleucine
iNOS	-	Inducible Nitric Oxide Synthase
IR	-	Infrared Spectroscopy
KCl	-	Potassium Chloride
L•	-	Lipid Radical
L-DOPA	-	Levodopa
LO•	-	Lipid Alkoxyl Radical
LOO•	-	Lipid Peroxyl Radical
LOOH	-	Lipid Hydroperoxide
Lys	-	Lysine
MDA	-	Malondialdehyde
Met	-	Methionine
ml	-	Millilitres
Mn-SOD	-	Manganese superoxide dismutase
MOA	-	Monoamine Oxidase
MPDP <sup>+</sup>	-	1-methyl-4-2,3-dihydropyridinium
MPP <sup>+</sup>	-	1-methyl-4-phenylpyridinium
MPTP	-	1-methyl-4-phenyl-1,2,3,6-tetrahydropyridine
MS	-	Mass Spectrometry
mtDNA	-	Mitochondrial DNA
NAD <sup>+</sup>	-	Nicotinamide Adenine Dinucleotide
NADH	-	Reduced Nicotinamide Adenine Dinucleotide
NBD	-	Nitro-blue Diformazan

NBT	-	Nitro-blue Tetrazolium
NE	-	Norepinephrine
NFT	-	Neurofibrillary Tangles
NMDA	-	N-methyl-D-aspartate
nNOS	-	Neuronal Nitric Oxide Synthase
$\text{NO}^-$	-	Nitroxyl Anion
NOS	-	Nitric Oxide Synthase
O	-	Oxygen atom
$\text{O}_2$	-	Molecular Oxygen
$\text{O}_2^-$	-	Superoxide Anion
Oct3	-	Organic Cation Transporter 3
$\text{OH}^-$	-	Hydroxyl anion
OH	-	Hydroxyl group
$\text{OH}^\bullet$	-	Hydroxyl Radical
$\text{ONOO}^-$	-	Peroxynitrite Anion
PBS	-	Phosphate Buffer Solution
PE	-	Petroleum Ether
Pro	-	Proline
Prx	-	Peroxiredoxine
$\text{R}^\bullet$	-	Organic Radical
		Resonance Spectroscopy
RH	-	Organic Molecule
RNS	-	Reactive Nitrogen Species

ROO•	-	Peroxyl Radical
ROOH	-	Hydroperoxide
ROS	-	Reactive Oxygen Species
S.E.M.	-	Standard Error of the Mean
SOD	-	Superoxide Dismutase
Sp	-	Senile Plaques
TBA	-	Thiobarbituric acid
TBARS	-	Thiobarbituric Acid-reactive Substances
TCA	-	Trichloroacetic acid
Thr	-	Threonine
TLC	-	Thin Layer Chromatography
TLC	-	Thin Layer Chromatography
TMP	-	1,1,3,3-tetramethoxypropane
TPQ	-	Topaquinone
Trolox <sup>®</sup>	-	(±)-6-Hydroxy-2,5,7,8-tetramethylchromane-2-carboxylic acid
Tyr	-	Tyrosine
UPS	-	Ubiquitin Proteasome System

# Chapter 1. Introduction

## 1.1 Neurodegenerative disorders

Most neurodegenerative disorders are age dependent and are on an increase because of an overall increased age of the population. Ageing is a biological process characterised by a gradual decline in physiological functions that affect many tissues, with a more significant impact on the brain. Neurological diseases contribute to a large number of deaths, disability and financial expenses worldwide (Blennow *et al.*, 2006). Parkinson's disease, Alzheimer's disease and Huntington's disease are the most common neurodegenerative diseases and Parkinson's disease and Alzheimer's disease have received significant research attention in recent years.

### 1.1.1 Parkinson's disease

James Parkinson first described Parkinson's disease in 1817. The term Parkinsonism refers to a clinical syndrome comprising of a combination of motor problems: bradykinesia, resting tremor, muscle rigidity, loss of postural reflexes, flexed posture and freezing phenomena as included in the review by Lang & Lozano (1998). Fahn & Sulzer (2004) reviewed the link between Parkinson's disease and environmental as well as genetic factors. Parkinson's disease is a slowly progressing syndrome that begins insidiously, gradually worsens in severity, and usually affects the body on one side before spreading to the other. Pathological hallmarks include the partial loss of dopaminergic neurons within the substantia nigra pars compacta and the presence of Lewy bodies whose primary component include fibrillar  $\alpha$ -synuclein and ubiquitin (Spillantini *et al.*, 1997). Accompanying this neuronal loss is an increase in glial cells in the substantia nigra with a loss of neuromelanin, the pigment contained in the substantia nigra dopaminergic neurons (Fahn & Sulzer, 2004). Clinical symptoms of Parkinson's disease appear when dopamine levels are reduced below 60 % that of normal (Bernheimer *et al.*, 1973). Hely *et al* (2000) reviewed the current treatment of Parkinson's disease which includes levodopa, dopamine agonists, monoamine oxidation B (MAO-B) inhibitors, catechol o-methyltransferase (COMT) inhibitors and anticholinergics.

### 1.1.2 Alzheimer's disease

Alzheimer's disease was first described by Alois Alzheimer in 1901. It is the most common cause of dementia and ranks fourth as the cause of mortality in western countries (Blennow *et al.*, 2006).



Alzheimer's disease patient's most common and morbid complication is agitation and it causes their caretakers increased distress (Tariot *et al.*, 2002). Alzheimer's disease has been shown to have a significant genetic component with both familial and sporadic forms (Blennow *et al.*, 2006). It's a slowly progressing disorder with insidious onset and progressive impairment of episodic memory with instrumental signs including a loss of recognition ability and/or productive speech, the ability to perform complex moves, together with impaired cognitive symptoms such as impaired judgment, decision-making and orientation.

At microscopic level, the characteristic pathologies of Alzheimer's disease are senile or neuritic plaques ( $\beta$ -amyloid plaques) and neurofibrillary tangles. Tau hyperphosphorylation leads to tangle formation in the medial temporal lobe and the cortical areas of the brain, together with degeneration of neurons and synapses (Blennow *et al.*, 2006). The disease is diagnosed from patient history, based on the presence of neurological tests together with advanced medical imaging such as positron emission tomography. The current treatment includes acetylcholinesterase (AChE) inhibitors and N-methyl-D-aspartate (NMDA) receptor antagonists (Blennow *et al.*, 2006).

### **1.1.3 Huntington's disease**

Huntington's disease is characterised by excessive choreic movements of the extremities, head and torso, with a cognitive decline and emotional disturbances over a period of 30 years (Paulsen, 2009). The Huntington's Disease Collaborative Research Group (1993) explained the origin of the disease as "an expansion of the trinucleotide cytosineadenineguanine in the 5'-translated region of the IT15 gene on the short arm of chromosome four and length of trinucleotide cytosineadenineguanine expansion which is inversely correlated with age at diagnosis" (Duyao *et al.*, 1993). The current treatment includes antipsychotics and dopamine antagonists (Naarding *et al.*, 2001).

## **1.2 Oxidative stress**

Although initially speculated about, the occurrence of free radicals in living organisms was demonstrated half a century ago (Commoner *et al.*, 1954) and has therefore become a rationale for the free radical theory of ageing (Harman, 1956). Oxygen is essential for the survival of cells, as it is the terminal acceptor of electrons during respiration, which is the main source of energy through the production of ATP in the mitochondria. The body has developed several antioxidant systems to curb the production of free radicals generated as toxic by-products of energy production.

Acute exposure to relatively high levels of these oxidants, especially in the presence of  $\text{Ca}^{2+}$ , impairs mitochondrial function and contributes to cytotoxicity *via* necrosis and/or apoptosis (Crompton, 1999). Antioxidants are substances that counteract free radicals and prevent the damage they cause. As the organism age, free radical production increases and antioxidant systems fail to regulate the oxidative status effectively. This results in the progressive decline, in cellular and tissue function, and in turn insufficient supply of energy and/or increased susceptibility to apoptosis (Linnane *et al.*, 1989). Human perception depends on the ability of the central nervous system (CNS) to maintain high levels of energy production while maintaining a healthy internal electrochemical environment. Cognitive and memory deficits are thus consequences of imbalances between free radical production and antioxidant capacity within the brain (Ames, 2006) and an unbalanced accumulation of oxidative modifiers in the brain potentiates neurodegeneration and impairs cognitive function (Radak *et al.*, 2007). It is therefore essential to lessen the oxidative burden on neurons through antioxidants, preventing the damage caused by free radicals.

Chalcones are intermediary compounds in the biosynthetic pathway of flavonoids. Flavones are a class of flavonoids, and both chalcones and flavones exhibit antioxidant activity.

### 1.3 Monoamine oxidase

Monoamine oxidase is one of the enzymes controlling the amine neurotransmitter levels in cells. Monoamine oxidase A and B (MAO-A and -B) are mitochondrial bound flavin adenine dinucleotide (FAD) containing enzymes which catalyse the  $\alpha$ -carbon oxidation of a variety of endogenous (Kumar *et al.*, 2003) and dietary aminyl substrates in the brain and peripheral tissues (Binda *et al.*, 2002). The catalysed oxidation of the amines results in the formation of the corresponding aldehydes, ammonia and hydrogen peroxide ( $\text{H}_2\text{O}_2$ ). MAO-B inhibitors thus block the central production and accumulation of potentially neurotoxic species such as dopaldehyde and  $\text{H}_2\text{O}_2$  which are formed during the MAO-B catalysed metabolism of dopamine (Gesi *et al.*, 2001; Marchitti *et al.*, 2007). Since MAO-B is a major dopamine metabolising enzyme, inhibitors of MAO-B are employed to increase dopamine levels in the treatment of Parkinson's disease (Binda *et al.*, 2002). These properties of MAO-B inhibitors may be of relevance since the density and activity of MAO-B increases with age in most brain regions (Kumar *et al.*, 2003).

Lately the focus of drug design studies shifted to developing multifunctional drugs i.e. a moiety targeting two or more sites of action. NMDA receptor antagonists, monoamine oxidase B (MAO-B) inhibitors and antioxidants have separately been focused on in the past. In this study the combination as a multifunctional drug is investigated.

## 1.4 Research Objective

### 1.4.1 Objectives for this Study:

- To synthesise multifunctional compounds designed for both antioxidant and monoamine oxidase inhibitory activity. The inclusion of the amantadine moiety could also contribute to NDMA receptor antagonism.
- To confirm the identity of the compounds with NMR, IR and MS techniques.
- To establish the extent of antioxidant activity of the synthesised flavonoid series when compared to the correlating flavone series, by employing superoxide anion (NBT) and lipid peroxidation (TBA) assays.
- To evaluate monoamine oxidase activity and specificity of the synthesised flavonoid series, by employing biological evaluations, MAO-A and –B assays.

## 1.5 Proposed Series of Test Compounds

Flavonoids are a class of dietary antioxidants found in nature. Antioxidant activity may be attained with various substitutions to the basic flavonoid structure (figure 1.1), one of which is hydroxyl substitution.

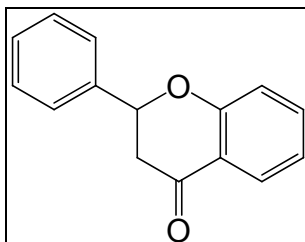
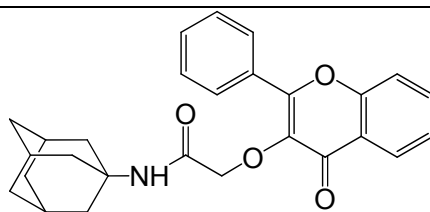


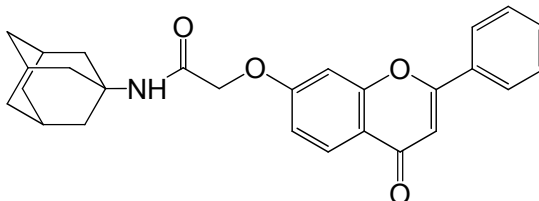
**Figure 1.1:** Basic flavonoid structure.

Amantadine falls in a class of organic polycyclic cage compounds that has intrigued medical chemists over the past decades. These compounds have important potential pharmaceutical applications in neurodegenerative disorders such as Parkinson's and Alzheimer's disease (Geldenhuys *et al.*, 2005). Amantadine increases extracellular dopamine levels and also binds to the NMDA receptor/ion channel complex, blocking uptake of calcium ions into neurons (Parsons *et al.*, 1999).

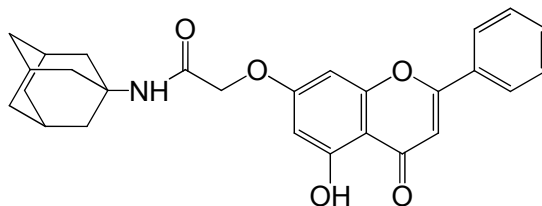
The complete series of compounds (figure 1.2) in this study consisted of amantadine-flavone (1 to 4) and amantadine-chalcone conjugates (5-6).



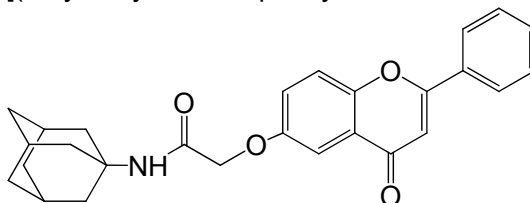
N-(adamantan-1-yl)-2-[(4-oxo-2-phenyl-4H-chromen-3-yl)oxy]acetamide (1)



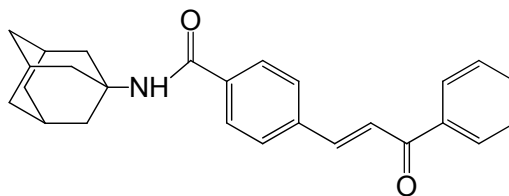
N-(adamantan-1-yl)-2-[(4-oxo-2-phenyl-4H-chromen-3-yl)oxy]acetamide (2)



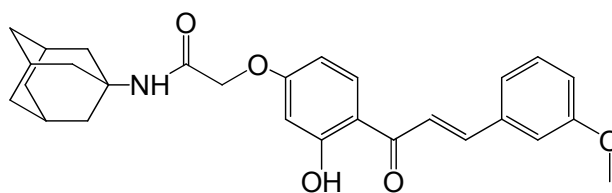
N-(adamantan-1-yl)-2-[(5-hydroxy-4-oxo-2-phenyl-4H-chromen-7-yl)oxy]acetamide (3)



N-(adamantan-1-yl)-2-[(4-oxo-2-phenyl-4H-chromen-6-yl)oxy]acetamide (4)



N-(adamantan-1-yl)-4-[(1E)-3-oxo-3-phenylpro-1-en-1-yl]benzamide (5)



N-(adamantan-1-yl)-2-{3-hydroxy-4-[(2E)-3-(3-methoxyphenyl)pro-2-enoyl]phenoxy}acetamide (6)

**Figure 1.2:** Test compounds (1 - 6) used in this study.

## Chapter 2. Literature Review

### 2.1 Free Radicals, Reactive Oxygen Species and Reactive Nitrogen Species

Free radicals are chemical species (atom, ion or molecule) containing an unpaired or odd number of electrons with the ability to bring about oxidation of molecules, either by directly abstracting electrons or indirectly through the production of highly reactive intermediates. Oxygen is essential to energy production, cellular metabolism and a common source of free radicals which are produced in a number of pathways (Halliwell & Gutteridge, 1989). The Mitochondria are the most abundant source of production and these free radicals can cause significant damage to biological tissue. In the mitochondria oxygen is reduced to water through a number of sequential steps producing a small quantity of short-lived intermediates including superoxide ( $O_2^-$ ), hydrogen peroxide ( $H_2O_2$ ) and the hydroxyl radical ( $OH^\bullet$ ). Both  $O_2^-$  and  $OH^\bullet$  are highly reactive because of the free electron in their outer orbit. Hydrogen peroxide is also toxic to cells and a source of additional free radical production, especially when reacting with reduced transition metals to form hydroxyl radicals (Wickens, 2001).

Free radicals and related species are mainly derived from oxygen (Reactive oxygen species/ROS) but also from nitrogen (reactive nitrogen species/RNS). These free radicals are generated as by-products of biological oxidation of normal metabolism. The mitochondria are both the main intracellular source of ROS and the target of oxyradical attack. According to the mitochondrial theory of ageing, ROS produced by the mitochondrial electron transport chain (ETC), attack mitochondrial membrane constituents including proteins, mitochondrial DNA (mtDNA) and lipids (Butterfield & Stadtman, 1997). The progressive oxidative damage to mtDNA during aging can lead to mtDNA mutations, subsequently impairing the ETC, further increasing ROS production and resulting in additional mtDNA mutations (Wei, 1992). The result is a vicious cycle accounting for the increased oxidative damage during ageing and leads to the progressive decline in cellular and tissue function (Linnane *et al*, 1989).

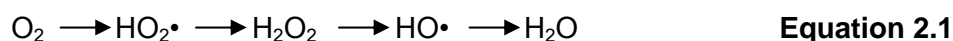
In the presence of  $Ca^{2+}$ , acute exposure to high oxidant levels can induce the mitochondrial permeability transition pore, leading to uncoupled oxidative phosphorylation with catastrophic effects on mitochondrial bioenergetics and cytotoxicity *via* necrosis and/or apoptosis (Crompton, 1999; Leung & Halestrap, 2008; Iverson & Orrenius, 2004). Mitochondrial membranes in the brain contain large amounts of phospholipids, these lipids modulate oxidative stress and molecular integrity during aging (Pamplona, 2008).

It has been suggested that the imbalances between local reactive oxygen species and anti-oxidant levels within the brain cause cognitive or memory defects (Ames, 2006; Corbetta *et*

*al*, 2008) and the accumulation of oxidative modified proteins potentiates neurodegeneration and impairs cognitive function (Radak *et al*, 2007).

### 2.1.1 Reactive Oxygen Species and Free Radicals

ROS is formed when oxygen molecules (O<sub>2</sub>) are converted to water molecules (Markesbery *et al.*, 2001) in the aerobic organism.



Produced free radicals are beneficial for cells as they are a prerequisite to carry out certain biological reactions. With an overproduction or a weakening in the antioxidant defence system, cellular damage can appear (Halliwell & Gutteridge, 1989; Halliwell & Gutteridge, 1984).

#### 2.1.1.1 Single Oxygen and Molecular oxygen

Oxygen is essential as it is the terminal acceptor of electrons during respiration and is the main source of energy in aerobes (Halliwell & Gutteridge, 1989). Singlet oxygen (<sup>1</sup>O<sub>2</sub>) readily reacts with most molecules as it is in the same quantum state, thus making it highly reactive. Two forms of singlet oxygen consist: delta singlet oxygen and sigma singlet oxygen. The former is not a free radical because unpaired electrons are not present as the outer two electrons occupy the same orbital and have opposing directions, making it more biologically significant due to its long life.

In contrast, sigma singlet oxygen has electrons of antiparallel spins occupying different orbitals. These species are highly reactive but has a short half-life because it decays immediately after being formed to the delta singlet oxygen state (Halliwell & Gutteridge, 1989; Cadenas, 1989). It is formed *in vivo* by enzymatic activation of oxygen through peroxidases or lipo-oxygenase activity during prostaglandin biosynthesis.

Physicochemical reactions such as the reaction with ozone (O<sub>3</sub>) within the human body fluids and interactions between hydrogen peroxide and peroxynitrite or during the respiratory burst of phagocytes can also produce sigma singlet oxygen. This entity induces various mutagenic, genotoxic and carcinogenic effects through its effect on polyunsaturated fatty acids and DNA (Cui *et al.*, 2004).

Molecular oxygen, also called triplet oxygen is the ground state of the O<sub>2</sub> molecule. The molecular electron configuration consists of two unpaired electrons occupying two degenerative molecular orbits. The reactivity of molecular oxygen is very low due to the parallel directions of electron spin. When oxygen oxidises a non-radical atom or molecule, it accepts a pair of electrons with parallel spin to fit into the free electron orbitals, but any pair of electrons must necessarily have opposite spins (Pauli's principle). Nevertheless, oxygen reactivity can be increased by inverting the spin of one of its two outer orbitals or by its sequential and univalent reduction to free radicals (Martínez-Cayuela, 1995). The free radical superoxide anion (O<sub>2</sub><sup>•-</sup>) is formed by the addition of one electron to ground state dioxygen (O<sub>2</sub>). Superoxide anions produced are unstable in aqueous solutions and are reduced by the enzyme superoxide dismutase (SOD) yielding hydrogen peroxide (H<sub>2</sub>O<sub>2</sub>) and molecular oxygen (Cadenas, 1989; Halliwell & Gutteridge, 1984) as illustrated in equation 2.2.



### 2.1.2 Hydrogen peroxide

Hydrogen peroxide is not a free radical but is included into the category of ROS because of its ability to oxidise unsaturated double bonds. It can be produced *in vivo* by several oxidising enzymes such as superoxide dismutase. Together with ROS, it damages several cellular components. The metal catalysed Haber-Weiss reaction (equation 2.3 – 2.5) is responsible for hydroxyl radicals and oxygen that is produced from hydrogen peroxide, they are formed by the Fenton reaction (Equation 2.4) and initiate lipid peroxidation (Wang *et al.*, 2007). This reaction between hydrogen peroxide and the reduced, ferrous ions (Fe<sup>2+</sup>) produces the hydroxyl radical (OH•).

These are highly reactive chemical species reacting with any biological molecule (Chance *et al.*, 1979), or initiating chain reactions which could become self-sustained through the regeneration of propagating radicals (Yu, 1994; Beckman, 1996).



Free iron in tiny amounts is normally present in healthy individuals, but they are sequestered by specialised proteins such as ferritin, so that virtually no OH• is produced.

Copper also reacts with  $\text{H}_2\text{O}_2$  to produce  $\text{OH}\cdot$  with a greater rate constant than iron (Halliwell & Gutteridge, 1984). Free copper is not normally available inside the body, but is tightly bound to serum albumin or incorporated into caeruloplasmin (Simpson *et al.*, 1988). Hydroxyl radicals can react with hydrogen peroxide to produce other radicals, and may also combine with each other to produce hydrogen peroxide as illustrated below (Walling, 1975).



The hydroxyl radical mediated chain reaction (equation 2.8 – 2.10) is initiated when a hydrogen atom is abstracted from an organic molecule (RH). An organic radical is formed ( $\text{R}\cdot$ ) and reacts with oxygen producing a peroxy radical ( $\text{ROO}\cdot$ ). The latter reacts with a second organic radical forming hydroperoxide ( $\text{ROOH}$ ), and another radical that propagates the chain reactions (Nappi & Vass, 1998). Terminating the radicals sustaining the propagation or scavenging the initial radical is the most effective protection against these processes (Nappi & Vass, 1998).



Radical damage can be circumvented *in vivo* by antioxidant defences that sequester or chelate metal ions and scavenge ROS, preventing their interactions with catalytic metals (Yu, 1994; Beckman, 1996).

### 2.1.3 Reactive Nitrogen Species

Nitric oxide ( $\cdot\text{NO}$ ) is the only known biological molecule that can react with  $\text{O}_2^-$  fast enough to exceed SOD function (Beckman, 1996). The bimolecular coupling of  $\cdot\text{NO}$  and  $\text{O}_2^-$  forms the peroxynitrite anion ( $\text{ONOO}^-$ ; equation 2.11), which is an important endogenous vasodilator (Markesbery *et al.*, 2001).



$\text{ONOO}^-$  is regarded to be a potent oxidant and nitrating agent capable of attacking and modifying proteins (Greenacre & Ischiropoulos, 2001), lipids (Radi *et al.*, 1991) and DNA (Bumey *et al.*, 1999), as well as depleting antioxidant defences.



## 2.2 Mitochondria as ROS source

In aerobic organisms, the role of energy production is accomplished by the mitochondrial electron transport chain (ETC). The ETC is located in the mitochondria inner membrane (MIM) and consists of five protein complexes: NADH dehydrogenase (complex I), succinate dehydrogenase (complex II), ubiquinone-cytochrome c oxidoreductase (complex III), cytochrome c oxidase (complex IV) and ATP-synthase (complex V). Complexes I, III and IV, pump protons across the inner mitochondrial space, creating an electrochemical gradient, which is then utilised by complex V for ATP generation (Paradies *et al.*, 2011) as illustrated by figure 2.1.

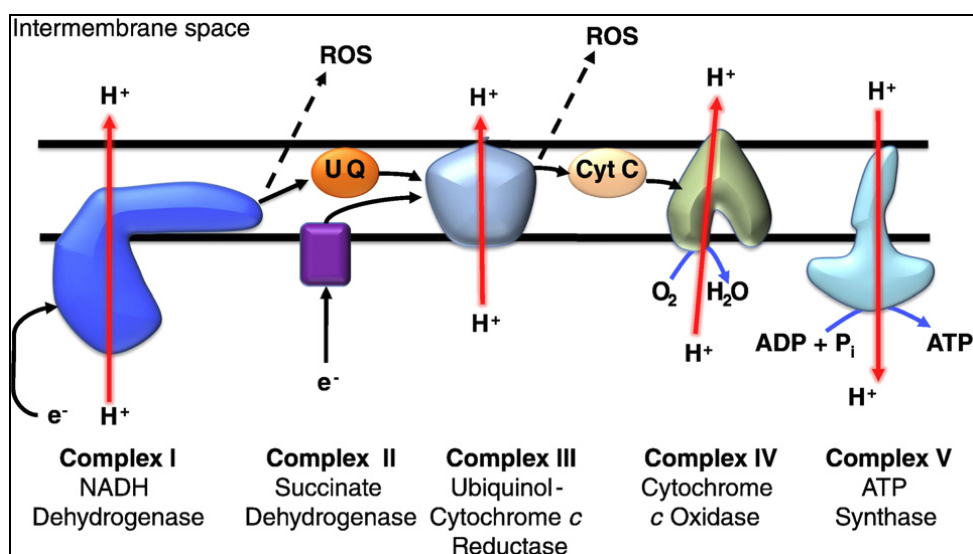


**Figure 2.1:** The mitochondrial electron transport chain. This simplified diagram of the electron transport chain on the inner mitochondrial membrane shows the direction of electron (e<sup>-</sup>) flow along the chain (black arrows) and the direction of flow (red arrows) of hydrogen ions (H<sup>+</sup>) across the mitochondrial membrane. Dotted arrows show ROS production as a result of the electron leak. UQ refers to ubiquinone; Cyt C refers to cytochrome c (directly extracted from Al Ghoulah *et al.*, 2011).

The ETC is a significant source of ROS as around 90 % of the cell's oxygen is consumed by the mitochondria to support oxidative phosphorylation. It is estimated that approximately 0.2-2 % of the oxygen consumed by the cell is converted to ROS through the production of superoxide anions (Boveris & Chance, 1973).

Oxidative phosphorylation, however, comes with additional costs, namely the production of potentially harmful ROS (Paradies *et al.*, 2011). The electron transport chain within the mitochondria is the main source of ROS as illustrated in figure 2.2.

Superoxide anion ( $O_2^-$ ) is the primary ROS generated, which is then converted by spontaneous dismutation or superoxide dismutase (SOD) to hydrogen peroxide ( $H_2O_2$ ). Hydrogen peroxide in turn is converted into water by glutathione peroxidase or catalase. If  $H_2O_2$  is not converted into water it produces hydroxyl radicals ( $OH^\bullet$ ) in the presence of divalent cations (Fenton reaction), this can be even more damaging to the mitochondrial biomolecules (Giuseppe *et al*, 2011).

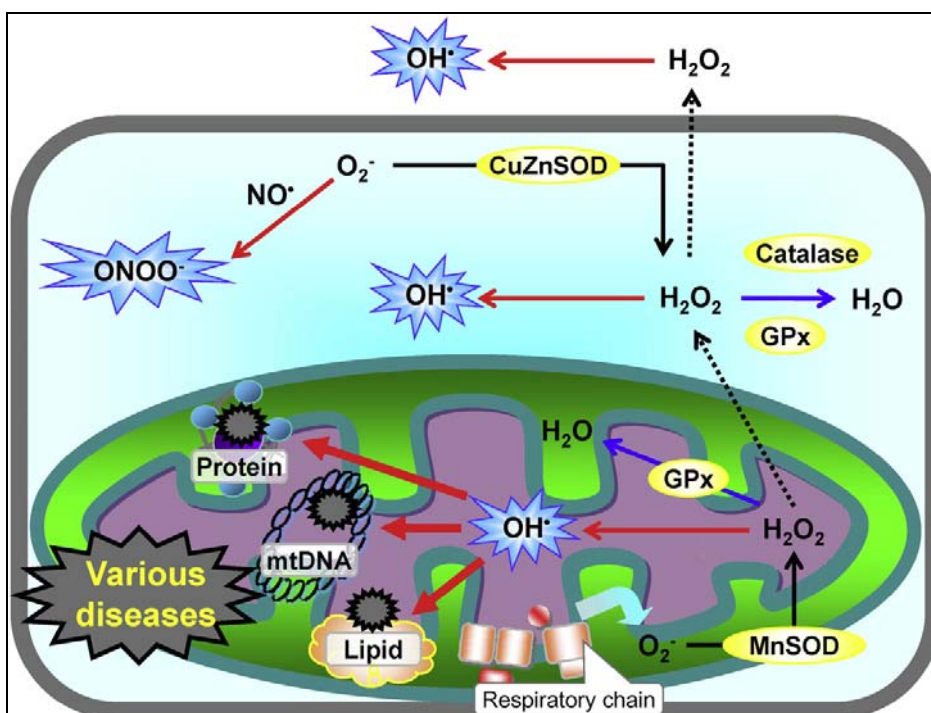


**Figure 2.2:** Reactive oxygen species (ROS) generated from mitochondria can damage cells. Free radicals generated by the electron transport chain can result in oxidative damage to mitochondrial DNA, proteins and lipid peroxidation. Enzymatic antioxidants include copper-zinc-containing superoxide dismutases (Cu-Zn-SOD); manganese-containing superoxide dismutases (Mn-SOD); glutathione peroxidase (GPx) and catalase (directly extracted from Yamada & Harashima, 2008).

The respiratory chain and superoxide anion production sites have been subjected to many studies (Murphy, 2009). Complex I and complex III are the two major sites of  $O_2^-$  production (figure 2.1). Mitochondria produce superoxide anions, predominantly from complex I, and when the matrix  $NADH/NAD^+$  ratio is high, it results in a reduced FMN site on complex I. When ATP is not produced, it causes a reverse in the electron transport resulting in a high proton motive force ( $\Delta p$ ) and reduced coenzyme Q pool (Paradies *et al.*, 2011). Superoxide

production is likely caused at complex III by cytochrome b (Nohl & Stolze, 1992) or unstable ubisemiquinone molecules (Turrens *et al.*, 1985).

ROS is also produced outside of the mitochondria but to a lesser degree. These reactions include xanthine oxidase, d-amino oxidase, the p-450 cytochromes and proline and lysine hydroxylase (Paradies *et al.*, 2011).

Nitric oxide ( $\bullet\text{NO}$ ) might modulate the ROS production in the mitochondria and convert it to various reactive nitrogen species (RNS) such as the nitroxyl anion ( $\text{NO}^-$ ) or toxic peroxynitrite ( $\text{ONOO}^-$ ). At low levels  $\text{O}_2^-$  and  $\text{H}_2\text{O}_2$  production can be increased by NO at the cytochrome c oxidase level. This is done through modulation of oxygen consumption (Sarkela *et al.*, 2001). In contrast at high levels of NO, it reacts with  $\text{O}_2^-$  resulting in  $\text{ONOO}^-$  formation by inhibiting  $\text{H}_2\text{O}_2$  production (Markesbery *et al.*, 2001).

The antioxidant defence system counteracts the burden of ROS production. Manganese-superoxide dismutase (Mn-SOD), in the mitochondrial matrix, converts  $\text{O}_2^-$  to  $\text{H}_2\text{O}_2$  which is further metabolised by glutathione peroxidase (Gpx I) and peroxiredoxine (Prx III), or diffused into the cytosol.  $\text{O}_2^-$  can only diffuse through the mitochondrial membrane in the protonated form (Paradies *et al.*, 2011). Part of the respiratory chain produced  $\text{O}_2^-$  can be released into the inner membrane space producing  $\text{H}_2\text{O}_2$  via copper-zinc superoxide dismutase (Cu-Zn-SOD). The  $\text{O}_2^-$  that is present in the intermembrane space can diffuse through voltage dependent anion channels into the cytosol or be scavenged by cytochrome c (Madesh & Hajnóczky, 2001).  $\text{O}_2^-$  can also form highly reactive peroxynitrite by reacting with nitric oxide. Mitochondrial antioxidant protection is also exerted by glutathione (GSH) and multiple GSH-linked antioxidant enzymes. Among GSH-linked enzymes involved in mitochondrial antioxidant defence are Gpx 1 and Gpx 4 (phospholipid hydroperoxide glutathione peroxidase). Gpx 1 is located predominantly in the cytosol whereas Gpx 4 is membrane associated, possibly at the contact sites of the two membranes, with a fraction localised to the mitochondria (Paradies *et al.*, 2011). These enzymes catalyse the reduction of lipid hydroperoxides and  $\text{H}_2\text{O}_2$ .

The peroxiredoxins are a group of non-seleno thiol-specific peroxidases contributing to cellular redox control via their hydroperoxide and  $\text{H}_2\text{O}_2$  eliminating ability (Rhee *et al.*, 2005).

## 2.3 Oxidative Stress

Oxidative stress plays a crucial role in the pathogenesis of a number of diseases, including neurodegenerative disorders, cancer and ischemia (Butterfield *et al.*, 2002). The brain is particularly vulnerable because of its high utilisation of oxygen, increased polyunsaturated

fatty acids, high levels of redox transition metal ions and low levels of antioxidants (Butterfield *et al*, 2002; Butterfield *et al*, 2001; Markesbery, 1997).

In an oxygen-rich environment, the presence of iron ions can further lead to an enhanced hydroxyl free radical production and ultimately to a cascade of oxidative events (Butterfield *et al*, 2007). The imbalance between pro-oxidant and antioxidant levels cause oxidative stress. Reactive oxygen species and reactive nitrogen species (RNS) are highly reactive with biomolecules, including proteins, lipids, carbohydrate, DNA and RNA (Butterfield & Stadtman, 1997). Commonly used markers of oxidative stress include protein carbonyls and 3-nitrotyrosine for protein oxidation. Lipid peroxidation markers include: thiobarbituric acid-reactive substances (TBARS), free fatty acid release, 4-hydroxy-2-*trans*-nonenal (HNE), iso- and neuroprostane formation, and 2-propen-1-al (acrolein). Other markers include: advanced glycation end products for carbohydrates; 8-OH-guanosine and 8-OH-2'-deoxyguanosine and other oxidized bases, and altered DNA repair mechanisms for DNA and RNA oxidation. Earliest of these changes after an oxidative insult are increased levels of toxic carbonyls, 3-nitrotyrosine (3-NT) and HNE (Butterfield *et al*, 2001; Butterfield *et al*, 2007; Lovel *et al*, 2001; Castegna *et al*, 2003; Smith *et al*, 1997; Sultana *et al*, 2006; Sultana *et al*, 2006b).

The irreversible nitration of tyrosine (Tyr) residues by peroxynitrite (figure 2.3) has profound functional and structural consequences (Beckman, 1996). The produced 3-NT can potentially compromise various cellular activity mechanisms. This is done by blocking the protein activation/deactivation, switching it sterically and/or electronically *via* phosphorylation/dephosphorylation events involving tyrosine's 4-OH group (Butterfield & Kanski, 2001). By making the aromatic moiety more hydrophilic the nitro group is able to alter the tertiary structure and folding patterns of proteins.

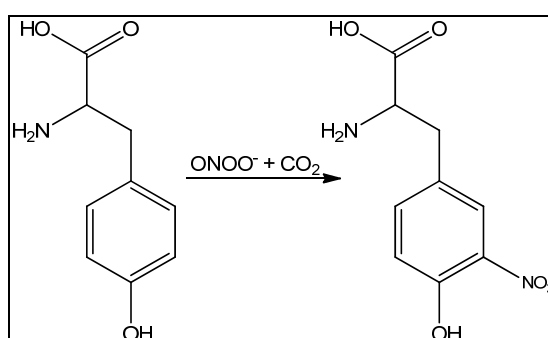


**Figure 2.3:** Nitration of the 3-position of tyrosine by peroxynitrite.

Overexpression of inducible nitric oxide synthase (iNOS) and action of constitutive neuronal NOS (nNOS) can cause additional damage to the brain. This increases nitric oxide (NO)

production *via* catalytic conversion of arginine to citrulline. In term nitric oxide reacts with superoxide anion ( $O_2^-$ ) at a diffusion-controlled rate to produce peroxynitrite ( $ONOO^-$ ). Peroxynitrite is highly reactive, has a very short half-life, and can undergo a variety of chemical reactions depending upon its cellular environment, the presence of  $CO_2$  and the availability of reactive targets forming modifications such as 3-NT (Koppenol *et al*, 1992; Murphy *et al*, 1998).

Protein carbonyl groups are generated by a wide range of oxidation reactions (Butterfield *et al.*, 2007) such as the direct oxidation of certain amine acid side chains [i.e., lysine (Lys), arginine (Arg), proline (Pro), threonine (Thr) and histidine (His)], peptide backbone scission, etc (Berlett & Stadtman, 1997; Butterfield *et al.*, 2007; Dalle-Donne *et al.*, 2006; Dalle-Donne *et al*, 2005; Stadtman & Levine, 2003)). This oxidation can lead to the aggregation or dimerisation of proteins, thereby exposing the more hydrophobic residues to aqueous environment and causing loss of structural or functional activity and protein aggregation. In Alzheimer's disease the protein aggregation causes accumulation of the oxidised proteins as cytoplasmic inclusions and  $\beta$ -amyloid aggregation (Butterfield & Kanski, 2001; Berlett & Stadtman, 1999). This causes additional damage such as alterations in protein expression and gene regulation, induction of apoptosis and necrosis to name a few. This suggests the physiological and pathological significance of protein oxidation (Abdul & Butterfield, 2007; Butterfield *et al.*, 2007; Naoi *et al*, 2005).

### **2.3.1 Mechanisms of lipid peroxidation**

Lipids are a heterogeneous group of compounds with a number of significant functions in the body (Benedetti *et al.*, 1980). The oxidising of lipids without release of energy results in the contamination of unsaturated lipids. This is caused by oxidative deterioration of lipids when they react with molecular oxygen (Catalá, 2010). The process of introducing an oxygen molecule that is catalysed by free radicals (non-enzymatic lipid peroxidation) or enzymes (enzymatic lipid peroxidation) is called lipid peroxidation (Halliwell & Gutteridge, 1990; Halliwell & Chirico, 1993; Gutteridge, 1995).

Lipid peroxidation consists of three stages: the initiation, propagation and termination (Catalá, 2006). During the initiation phase a hydrogen atom is abstracted from membrane lipids, mainly phospholipids, by several species including radicals hydroxyl ( $\bullet OH$ ), alkoxyl ( $RO\bullet$ ), peroxy ( $ROO\bullet$ ), and possibly  $HO_2\bullet$  (Gutteridge, 1988). During the extraction of a hydrogen atom, an unpaired electron is formed on the carbon,  $-CH-$ . This leads to the subtraction of  $H\bullet$  (Catalá, 2010) and the production of a lipid radical ( $L\bullet$ ), which in turn reacts with molecular oxygen to form a lipid peroxy radical ( $LOO\bullet$ ). This radical can abstract

hydrogen from an adjacent fatty acid producing a lipid hydroperoxide (LOOH) and a second lipid radical (Catalá, 2006; Catalá, 2010).

Reduced metals such as  $\text{Fe}^{2+}$  can cleave the LOOH, producing the lipid alkoxyl radicals ( $\text{LO}\cdot$ ). Both the alkoxyl and peroxy radicals stimulate the chain reaction of lipid peroxidation by abstracting additional hydrogen atoms (Buettner, 1993).

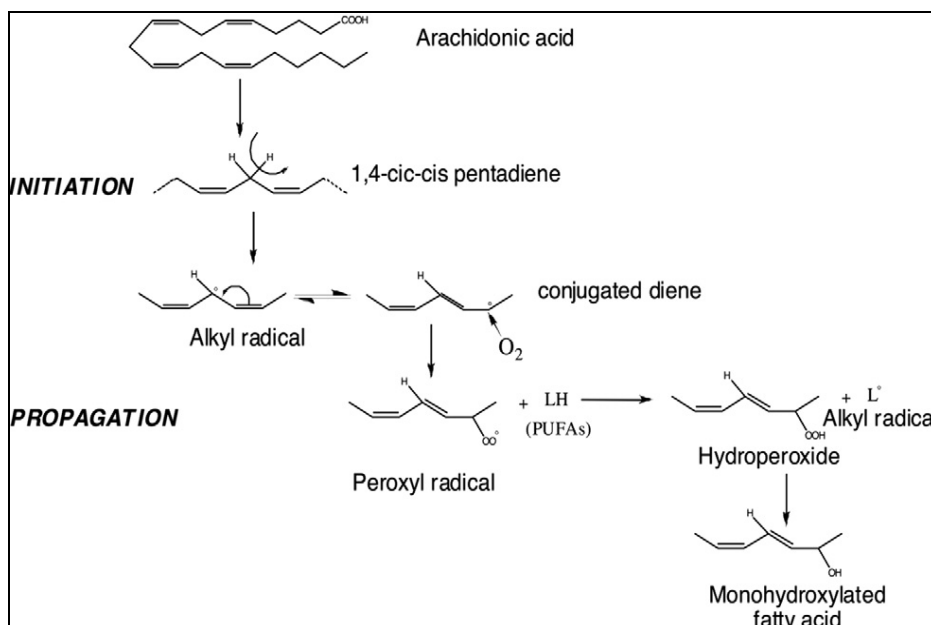


**Figure 2.4:** Schematic diagram of lipid peroxidation mechanism applied to any polyunsaturated fatty acid. Arachidonic acid is used as an example (directly extracted from Catalá, 2010).

Peroxidation of lipids can agitate the membrane assembly, causing changes in permeability and fluidity, ion transport alterations and inhibition of metabolic processes (Nigam & Schewe, 1998). Injured mitochondria, induced by lipid peroxidation, can lead to further ROS generation (Green & Reed, 1998).

With the degradation of lipid hydroperoxides, a great diversity of aldehydes are formed. The highly reactive nature of some of these aldehydes can disseminate and augment the initial free radical events. HNE is known to be the main aldehyde formed during lipid peroxidation of n-6 polyunsaturated fatty acids, such as linoleic acid C18:2 n-6 and arachidonic acid C20:4 n-6. Malondialdehyde (MDA) and 4-Hydroxy-2-alkenals represent the most prominent aldehyde substances generated during lipid peroxidation. Lipid peroxidation of membrane phospholipids generates hydroxyl-alkenals and oxidized phospholipids that are active in physiological and/or pathological conditions (Catalá, 2009; Catalá, 2010).

### 2.3.2 Mechanisms of protein oxidation

Backbone oxidation leads to the formation of carbon-centred radicals and is initiated by the  $\alpha$ -carbon abstraction of hydrogen. The peroxy radical is formed in the presence of oxygen and can further lead to the formation of an alkoxyl radical and subsequently hydroxylation of the peptide backbone (Butterfield & Stadtman, 1997). These reactions can be mediated by  $\text{Cu}^+$ ,  $\text{Fe}^{2+}$  or hydroperoxyl radicals ( $\text{HOO}\cdot$ ).

Protein cross-linking and/or peptide bond cleavage is also caused by protein oxidation, this occurs *via* diamide or  $\alpha$ -amidation pathways. Cleavage of the peptide bond will result in the formation of carbonyl groups that are often used as protein oxidation markers (Berlett & Stadtman, 1997; Dalle-Donne *et al.*, 2006; Stadtman & Levine, 2003; Butterfield, 1997). By abstracting hydrogen from a carbon of the same or another peptide, another carbon-centred radical is formed, thus maintaining the free radical initiated oxidation between and across proteins (Butterfield & Stadtman, 1997).

The oxidation of amino acid side-chains greatly depends on their structure. Oxidation can target most amino acid side-chains, but the products of only a few have been fully characterised (Butterfield & Stadtman, 1997). These include lysine, histidine, tyrosine, phenylalanine, tryptophan, methionine, arginine, cysteine, threonine, proline, and glutamic acid. For instance, sulphur-containing amino acids (Cys, Met) are easily and reversibly oxidised under relatively mild conditions, leading to disulfides and methionine sulfoxide, respectively (Butterfield & Kanski, 2001).

Experimental evidence has found that the protective mechanism of methionine oxidation can serve as a buffer for more extensive oxidative stress (Requena *et al.*, 2004). Methionine sulfoxide reductase enzymes further support this (Berlett & Stadtman, 1997).

The amino acid side-chain can undergo another modification following oxidative stress. This mechanism is associated with products of the lipid peroxidation processes which involves Michael addition to electron-rich Cys, His, or Lys residues by various reactive aldehydes including 4-hydroxynonenal, 2-porpenal, malondialdehyde, and others (Butterfield & Kanski, 2001; Esterbauer *et al.*, 1991). There is a covalent addition of an aldehyde carbon group to the peptide chain when these alkenals react with nucleophilic side-chains of Cys, His, or Lys residues, thus altering the membrane proteins function and conformation. Schiff base formation between the carbonyl functionality on the alkenal and an amine on an adjacent protein can also occur, cross-linking the protein (Butterfield & Kanski, 2001; Butterfield & Stadtman, 1997).

### 2.3.3 DNA oxidation

The ROS oxidative damage to DNA results in strand breaks in DNA-DNA, DNA-protein cross-linking and sister-chromatic exchange and translocation (Crawford *et al.*, 2002; Davies, 1995). Lipid peroxidation products HNE and acrolein attack DNA bases, resulting in the formation of bulky exocyclic adducts. Oxidised base adducts such as 8-hydroxy-2-deoxyguanine are produced by the ROS mediated DNA oxidation (Cooke *et al.*, 2003). These modifications can cause inappropriate base pairing that alters protein synthesis.

## 2.4 Oxidative modification in Alzheimer's disease

As mentioned previously, Alzheimer's disease is an age-related neurodegenerative disorder characterised histopathologically by the presence of senile plaques (SP), neurofibrillary tangles (NFT) and synapse loss (Selkoe, 2001). Senile plaques are extracellular deposits of amyloid while neurofibrillary tangles consist of a protein called tau. There is considerable evidence of oxidative stress in the pathology of Alzheimer's disease (Markesbery, 1997; Markesbery & Carney, 1999) and the increase in ROS/RNS may cause further damage to biomolecules, leading to loss of function and consequently to apoptosis.

The main component of senile plaques,  $\beta$ -amyloid peptide [40 and 42 amino acids; ( $\beta$ A40 or  $\beta$ A42)], is generated by the proteolytic cleavage of amyloid precursor protein by the action of  $\beta$ - and  $\gamma$ -secretases.  $\beta$ A42 was shown to induce oxidative stress in both *in vitro* and *in vivo* studies (Boyd-Kimball *et al.*, 2004; Boyd-Kimball *et al.*, 2005).  $\beta$ A42 exists in various aggregated states of which the oligomeric form is highly toxic (Glabe, 2005).

The methionine at residue 35 of  $\beta$ A42 was shown to be particularly important for its oxidative role (Butterfield *et al.*, 2007; Butterfield *et al.*, 2010). Methionine can form a sulfuranyl radical cation when oxidised, this has the ability to abstract an allylic H-atom from the unsaturated acyl chains of lipid molecules, thereby leading to the initiation of lipid peroxidation (figure 2.5; Butterfield *et al.*, 2002; Lauderback *et al.*, 2001).

In  $\beta$ A42-mediated lipid peroxidation, methionine35 (Met35) has a helical secondary structure (Butterfield & Boyd-kimball, 2005) with the Ile31 backbone carbonyl located within a van der Waals distance of the S-atom in  $\beta$ A42. Since the electronegativity of oxygen is higher than that of sulphur, the lone electron pair on sulphur is drawn towards oxygen. These electrons are more vulnerable to a one-electron oxidation forming the sulfuranyl radical cation. This radical can abstract a labile allylic H-atom from an unsaturated acyl lipid chain forming a carbon-centered free radical.



The latter can immediately form a peroxy free radical by binding paramagnetic and non-polar oxygen, this in turn can abstract another acyl chain-resident labile allylic H-atom, continuing the chain reaction. There is a large amplification effect of free radicals on  $\beta$ A42 that is mediated by the chain reaction within the lipid phase of the membrane. The lipid acyl hydroperoxide formed by these reactions can lead directly to HNE formation (Butterfield *et al.*, 2010).

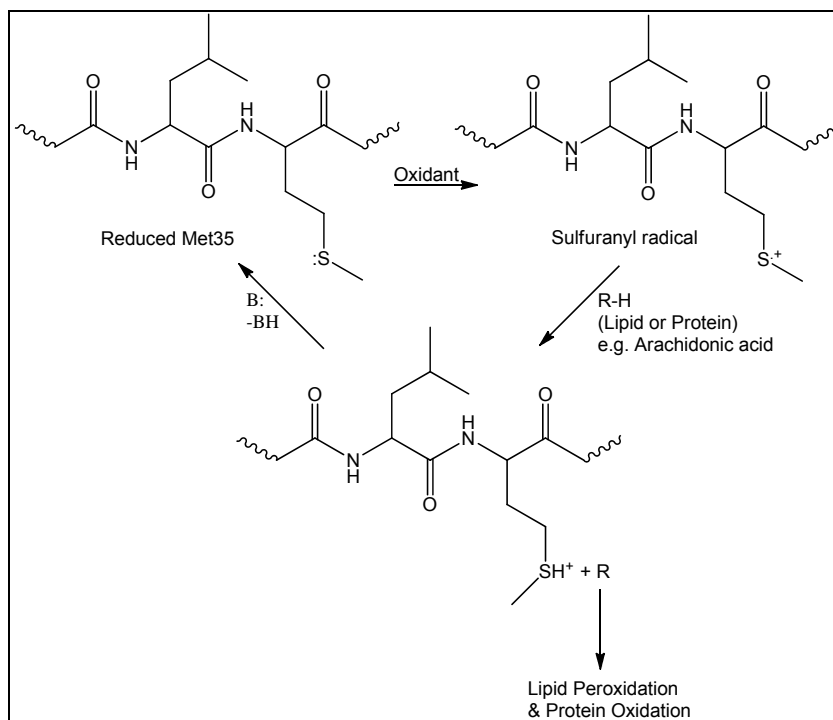


**Figure 2.5:** Involvement of Methionine35 of  $\beta$ -amyloid (1-42) in lipid peroxidation. The sulphur (S)-atom of Methionine35 of the  $\beta$ -amyloid (1-42) peptide can undergo one-electron oxidation to form a sulfuranyl radical cation within the bilayer, which has the ability to abstract a labile, allylic H-atom from the unsaturated acyl chains of lipid molecules, leading to initiation of the lipid peroxidation process (Butterfield *et al.*, 2010).

$\beta$ A42 has been reported to be located in mitochondrial membranes (Reddy, 2009; Sultana & Butterfield, 2009) and may initiate lipid peroxidation by similar processes as discussed above. This may lead to lipid membrane component alterations and also affect membrane embedded proteins. Lipid peroxidation may also cause alterations in membrane fluidity and eventually to alteration in membrane functions. This can cause alterations to the mitochondrial membrane leading to leakage of cytochrome c, an apoptosis inducing molecule, as well as alterations in protein functions involved in the electron transport system. This causes an increase in ROS/RNS release and production.

In addition, the up regulation of  $\beta$ -secretase 1 expression caused by increased lipid peroxidation production causes increased  $\beta$ A42 production (Tamagno *et al.*, 2005; Butterfield *et al.*, 2010). Lipid peroxidation products and  $\beta$ A42 have been shown to induce c-Jun N-terminal protein kinase pathways, leading to neuronal apoptosis (Tang *et al.*, 2008).

Lipid peroxidation results in the production of HNE, malondialdehyde, and the  $\alpha$ ,  $\beta$ -unsaturated aldehyde, acrolein, which are diffusible and highly reactive with other biomolecules thus making this process neurotoxic (Esterbauer *et al.*, 1991). The aldehydic products of lipid peroxidation are highly reactive and bind covalently to proteins through Michael addition to protein cysteines, lysines, and histidines, altering their structure and function (Pocernich & Butterfield, 2003; Drake *et al.*, 2003; Butterfield *et al.*, 2010) as discussed in section 2.3.2.

## **2.5 Oxidative modifications in Parkinson's disease**

As previously mentioned, Parkinson's disease is partly caused by the deficiency of striatal dopamine levels, this is due to the degeneration of dopaminergic neurons in the substantia nigra pars compacta. Dopaminergic neurons in the substantia nigra are more vulnerable to oxidative modification than that of areas such as the ventral tegmental area (VTA). Dopamine is either degraded by monoamine oxidase or auto-oxidation. Degradation *via* MAO produces dihydroxyphenylacetic acid and  $H_2O_2$  which occurs with the consumption of  $O_2$  and  $H_2O$  (Gesi *et al.*, 2001; Maker *et al.*, 1981), while intracellular auto-oxidation of dopamine generates  $H_2O_2$  and dopamine-quinone (Graham, 1978).

The produced  $H_2O_2$  can be converted into hydroxyl radicals by the Fenton reaction in the presence of ferrous iron. Iron mediated catalysis of hydroxyl radicals could contribute to oxidative stress in Parkinson's disease, given that iron levels are higher in the substantia nigra, but also increased in Parkinson's disease patients (Dexter *et al.*, 1989; Sofic *et al.*, 1988).

Dopamine-quinone, however participates in nucleophilic addition reactions with protein sulfhydryl groups (Graham, 1978), leading to reduced glutathione (GSH) levels and protein modifications. Dopamine-quinones promote  $H^+$  leakage from mitochondria, inhibit synaptosome glutamate and dopamine transporter function (Berman & Hastings, 1997) and inhibit tyrosine hydroxylase in cell free systems (Kuhn *et al.*, 1999). The mitochondria's  $H^+$  loss result in the uncoupling of respiration to ATP synthesis (Berman & Hastings, 1999).

The first familial Parkinson's disease gene discovered was *α-synuclein* (Munoz *et al.*, 1997; Polymeropoulos *et al.*, 1997). In Parkinson's disease oxidative damaged *α-synuclein* is deposited in Lewy Body's (Jenner *et al.*, 1992). *α-synuclein* modulates synaptic vesicle trafficking under normal physiological conditions, owing to its ability to bind to synaptic vesicles at the synaptic terminal (Goedert, 2001). Nitrated *α-synuclein* is prone to aggregation, more resistant to proteolysis, has less solubility and a reduced lipid binding tendency (Hodara *et al.*, 2004). *α-synuclein* can undergo other oxidative modifications (Danielson & Anderson, 2008) with the addition of a dopamine adduct on *α-synuclein* gaining the most attention. This modification stabilises toxic *α-synuclein* protofibrils and prevent further aggregation (Norris *et al.*, 2004; Mazzulli *et al.*, 2006). The permeabilisation of synaptic vesicles is mediated by *α-synuclein* protofibrils (Mazzulli *et al.*, 2006; Mosharov *et al.*, 2006) and increases intracellular dopamine levels, further enhancing dopamine modifications of *α-synuclein* (Mosharov *et al.*, 2006). These studies provide the potential mechanism of how oxidative stress and *α-synuclein* contribute to the neurodegenerative process in Parkinson's disease (Tsang & Chung, 2009).

## 2.6 Antioxidants

Antioxidants counteract free radicals formed during the mitochondrial ETC, preventing the damage they can cause. Neutralising free radicals before they react with biological targets by breaking the chain or preventing their formation from oxygen can significantly reduce their adverse effects (Azzi *et al.*, 2004). Chain-breakers act by scavenging already produced radicals, mostly hydroxyl radicals thereby inhibiting the chain of oxidative stress. Preventing this activation of oxygen occurs through inhibition of superoxide anion production, hydrogen peroxide degradation and metal ion chelation or reduction. The body has developed several endogenous antioxidant systems to counteract the production of reactive species.

Antioxidants are classified into two categories, enzymatic and non-enzymatic (figure 2.6). The endogenously produced enzymes are responsible for the conversion of  $O_2^-$  into  $H_2O_2$  and then converting it to  $H_2O$  and  $O_2$ , but this isn't sufficient in combating increased free radical formation. Many of the non-enzymatic antioxidants are obtained from dietary sources which are classified into various groups (Liu, 2004). Polyphenols is a major class in dietary oxidants consisting of phenolic acid and flavonoids. The other classes of dietary antioxidants include vitamins, carotenoids, organosulfural compounds and minerals (Venkat Ratnam *et al.*, 2006).

In order to scavenge the radicals, it is postulated that the antioxidant must act as a hydrogen-donor in order to reduce the oxidising free radical, thus quenching the ability of the radical to oxidise biological matter. The antioxidant should form a stable radical in order not to harm biological matter itself. Therefore, antioxidants containing hydroxyl donating groups, promises enhanced antioxidant activity through the scavenging of radicals (Ammar *et al.*, 2009).

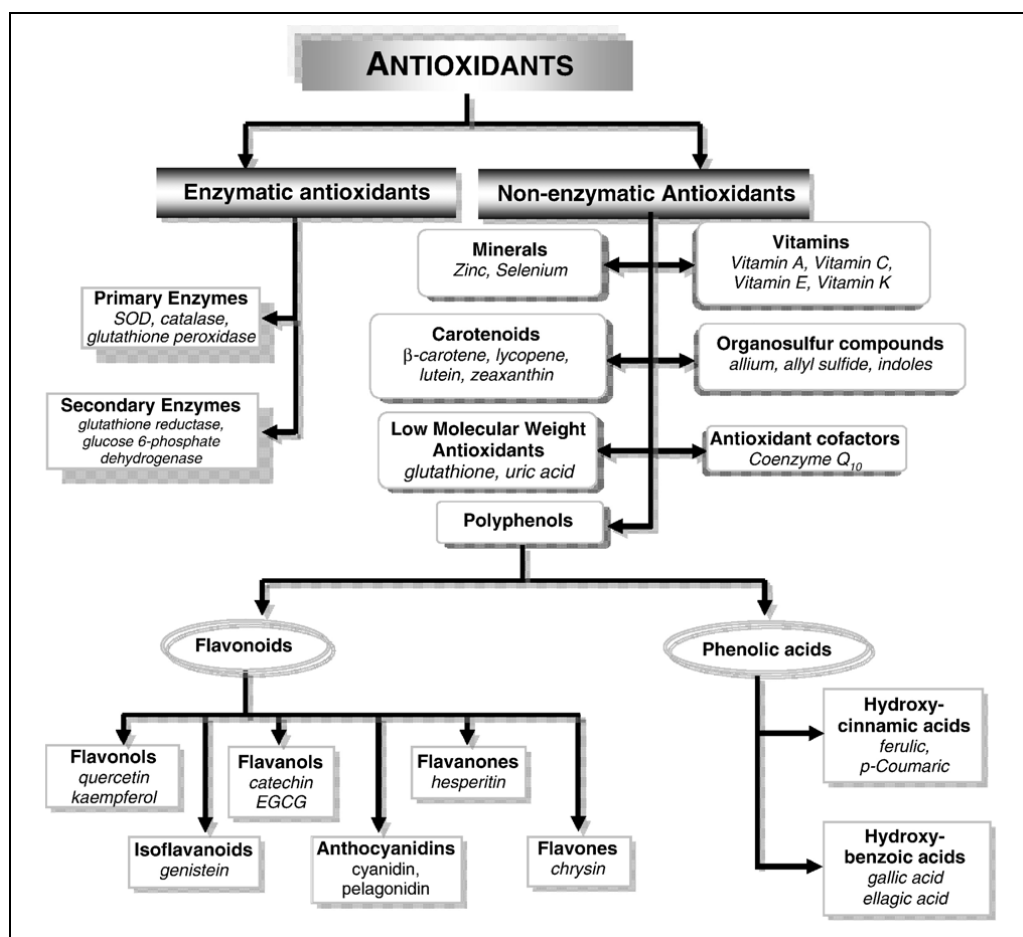


**Figure 2.6:** Classification of antioxidants. Some non-enzymatic antioxidants like uric acid, vitamin E, glutathione and CoQ10 are synthesised in the human body and they can also be derived from dietary sources. Polyphenols are the major class of antioxidants which are derived from diet (directly extracted from Venkat Ratnam *et al.*, 2006).

### 2.6.1 Enzymatic antioxidants

Enzymatic antioxidants are the body's main source of dealing with oxidative stress. These include:

- Copper, zinc superoxide dismutase (Cu-Zn-SOD; Fridovich, 1995), the enzyme responsible for the conversion of superoxide anion into hydrogen peroxide, present in the cytoplasm and the mitochondrial intermembrane space (Okado-Matsumoto & Fridovich, 2001);
- Manganese superoxide dismutase (Mn-SOD; Fridovich, 1995), with the same action as Cu-Zn-SOD, but is only found in the mitochondrial matrix;
- Glutathione peroxidase (GPx), a peroxidase responsible for the reduction of hydrogen peroxide and hydroperoxides that utilises reduced glutathione as hydrogen donor (Ursini *et al.*, 1995);
- Catalase (CAT), the enzyme that catalyses the dismutation of hydrogen peroxide to oxygen and water (Chance *et al.*, 1979).

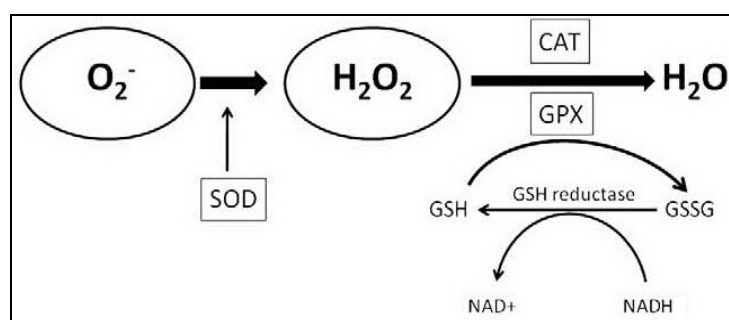


**Figure 2.7:** Schematic representation of antioxidant enzymes (adapted from Real *et al.*, 2010).

### 2.6.1.1 Superoxide dismutase

Superoxide dismutase is present in almost every cell in the body, playing a pivotal role in protecting cells and tissues against oxidative stress. SOD appears in three forms as described above. Cu-Zn-SOD and Mn-SOD are present intracellularly, while a second Cu-Zn-SOD is located extracellularly to inhibit the reduction of nitric oxide by superoxide anions in blood vessels (Fukai, 2009). The common mechanism of SOD is the dismutation of  $O_2^-$  to a less potent  $H_2O_2$  (equation 2.2; section 2.1). SOD is fundamental in the processing of superoxide anions that would otherwise lead to the reduction of  $Fe^{3+}$  to  $Fe^{2+}$ , thereby promoting  $OH^\bullet$  formation.

### 2.6.1.2 Glutathione peroxidase

GPx, a family of selenium dependent and independent antioxidant enzymes, can be divided into two groups, namely cellular and extracellular (Rahman *et al.*, 2006).

GPx is present in the cytoplasm and mitochondria (Andersen, 2004). The glutathione redox cycle is a central mechanism for reduction of intracellular hydroperoxides (equation 2.12).



The activity of GPx requires reduced glutathione (GSH) which is oxidised during the reduction of peroxides (GSSG). Thus, a separate enzyme, glutathione reductase (equation 2.13), is required for the NADH-dependent reduction of oxidised glutathione (Turrens, 2004). Nicotinamide adenine dinucleotide ( $\text{NAD}^+$ ) is an oxidising agent, it accepts electrons from other molecules and are reduced (NADH). The capacity to recycle GSH makes the GSH cycle pivotal to the antioxidant defence mechanism of a cell (Heffner & Repine, 1989).

### 2.6.1.3 Catalase

This antioxidant enzyme is a homotetrameric protein decomposing hydrogen peroxide into water and oxygen (equation 2.14).



Catalase is concentrated in the liver and erythrocytes, while the brain, heart and skeletal muscle contain only small amounts. Catalase is also found in peroxisomes and in the cytoplasm (Rahman *et al.*, 2006).

By reducing hydrogen peroxide, catalase and GPx conserve SOD; and SOD, by reducing superoxide, in turn conserves catalase and GPx. A steady low level state of SOD, GPx and catalase, as well as superoxide and hydrogen peroxide are thus maintained by such a feedback mechanism (Rahman *et al.*, 2006).

### 2.6.2 Non-enzymatic antioxidants

Oxidative stress is reduced by a complex network of antioxidants, among which dietary antioxidants play a fundamental role (reviewed in Vertuani *et al.*, 2004). Vitamin C and E are well known for their exogenous antioxidant activity (Lu & Liu, 2002).

Vitamin C, or ascorbic acid, is a hydrophilic antioxidant and has the ability to regenerate vitamin E from its tocopheroxyl radical form and thereby restore its free radical scavenging capacity (Benzie *et al.*, 1999). It also inhibits peroxidation of membrane phospholipids and acts as a scavenger of free radicals.

Vitamin E, or  $\alpha$ -tocopherol, is a lipophilic antioxidant. It is responsible for terminating free radical chain reactions that result from the oxidation of polyunsaturated fatty acids (Lu & Liu, 2002). Deficiency in Vitamin E influences the activities of SOD, catalase and GPx and is thus very important for the enzymatic antioxidant defence of the body. Both these vitamins though contribute to the oxidative health of the brain and are well-known strategies against neurodegeneration.

**Table 2.1:** Some selected antioxidants and their mechanisms of action.

<b>Some selected antioxidants and their mechanisms of action</b>	
<b>Antioxidant</b>	<b>Mechanism of action</b>
Superoxide dismutase (SOD)	Dismutation of superoxide to $H_2O_2$
Catalase (CAT)	Decomposes $H_2O_2$ to molecular oxygen and water
N-acetyl cysteine (NAC)	Scavenging of $H_2O_2$ and peroxide Deacetylation of precursor for GSH synthesis
Glutathione (GSH)	Intracellular reducing agent
Epigallocatechin-3-O-gallate (EGCG)	Metal chelation Scavenging of superoxide, $H_2O_2$ , OH and singlet oxygen Tocopherol regeneration
Lycopene	Trapping of singlet oxygen
Ellagic acid	Scavenging of $H_2O_2$ Stimulation of glutathione-S-transferase
Coenzyme Q10 (CoQ10)	Inhibition of lipid peroxidation Reduces mitochondrial oxidative stress
Indole-3-carbinol (I3C)	Inhibition of DNA-carcinogen adduct formation Suppression of free radical production
Genistein	$H_2O_2$ scavenging
Quercetin	$H_2O_2$ scavenging, one of the potent antioxidant among polyphenols
Vitamin C	Scavenging of superoxide anion by forming semidehydroascorbate radical which is subsequently reduced by GSH
Vitamin E	Direct scavenging of superoxide Upregulation of antioxidant enzymes Inhibition of lipid peroxidation

## 2.6.2.1 Natural Plant Antioxidants

### 2.6.2.1.1 Chalcones

Chalcones are intermediary compounds in the biosynthetic pathway of a very large and widespread group of plant constituents known collectively as flavonoids (Harborne, 1986).

Flavonoids are synthesised *via* phenylalanine metabolic pathways, well known pathways in plant secondary metabolism. Chalcone synthase (CHS) together with chalcone isomerase (CHI) are important regulation factors of flavonoid biosynthesis and are key enzymes in this pathway. The chalcone isomerase reaction can occur spontaneously and reversibly without enzymatic intervention. In brief, chalcone synthase is the entry point of the flavonoid pathway, which catalyses 4-coumaroyl-CoA and malonyl-CoA to chalcone (figure 2.8).

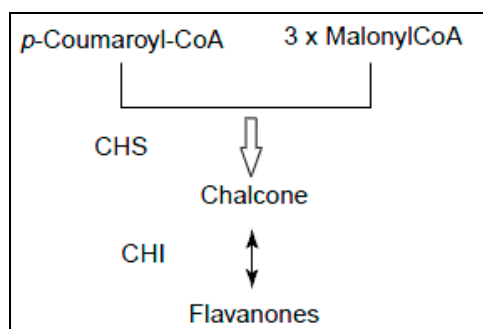


**Figure 2.8:** Basic flavone synthetase (Adapted from Gantet & Memelink, 2002).

This leads the phenylpropanoids pathway to flavonoid biosynthesis, in which chalcone isomerase catalyses chalcone to flavone, which in succession turns into many other bioactive flavonoids (Dixon & Paiva, 1995; Weisshaar & Jenkins, 1998). Chalcones have been shown to possess antioxidant (Nakamura *et al.*, 2003), oxygen scavenging, monoamine oxidase inhibitory and anti-inflammatory properties in a variety of experimental systems (Alcaraz *et al.*, 2004).

Among the naturally occurring chalcones (Middleton *et al.*, 2000) and their synthetic analogues (Dimmock *et al.*, 1999) several compounds displayed cytotoxic (cell growth inhibitor) activity towards cultured tumor cells. Chalcones are also effective *in vivo* as cell proliferation inhibitors, anti-tumor promoting and chemopreventive agents (Middleton *et al.*, 2000; Dimmock *et al.*, 1999).

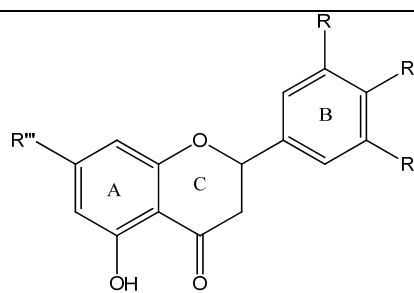
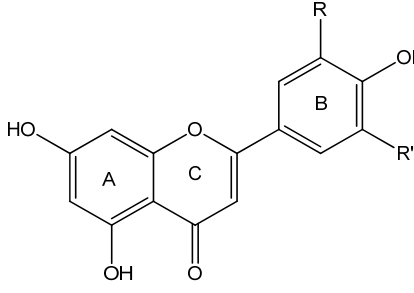
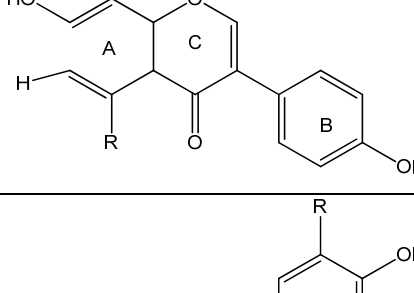
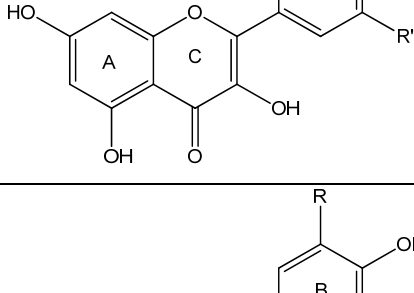
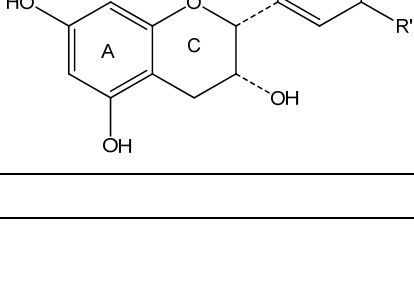
#### 2.6.2.1.2 Flavonoids

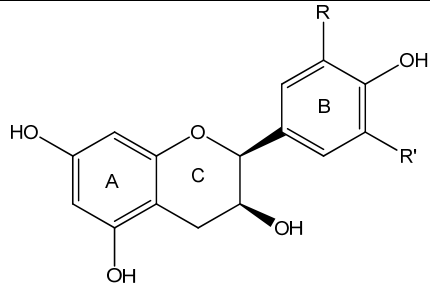
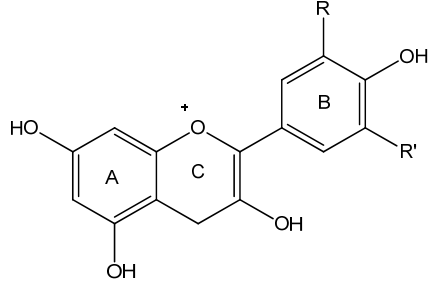
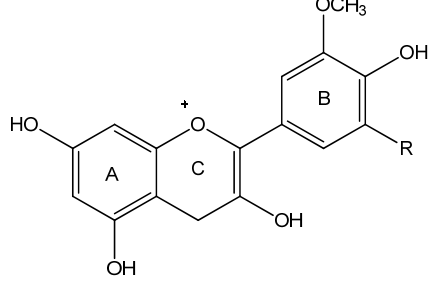
Flavonoids are a large family of secondary plant metabolites, widespread in roots, leaves, flowers, barks, seeds and nuts (Wollenweber & Dietz, 1981; Peterson & Dwyer, 1998). It forms a class of benzo- $\gamma$ -pyrone derivatives which are ubiquitous in plants. The immediate family members of flavonoids include flavones, flavanes, flavonols, anthocyanidins and catechins as illustrated in table 2.2. They possess a wide spectrum of biological activity including remarkable antioxidant (Siddaiah *et al.*, 2006), antiviral and anticancer (Deschner *et al.*, 1991; Elangovan *et al.*, 1994) activity. Flavonoids also possess antiischemic (Rump *et al.*, 1995), antiallergic, anti-inflammatory (Gil *et al.*, 1994) activity and monoamine oxidase



inhibition ability (Chimenti *et al.*, 2010). A recent study reported that the elderberry extract inhibited Human Influenza A infection *in vitro* (Roschek *et al.*, 2009). Current interest in these substances was stimulated by the potential health benefits arising from their antioxidant activity. These are the result of their high propensity to transfer electrons to chelate ferrous ions and to scavenge reactive oxygen species (Robak & Gryglewski, 1996).

**Table 2.2:** Chemical structures of flavonoids and some examples.

Classes	Structural formula	Examples
Flavanones		R=R'=H, R''=R'''=OH; Naringenin R=OH, R'=H, R''=R'''=OH; Eriodyctiol R=R'=OH, R''=R'''=OH; 5 <sup>1</sup> -OH-Eriodyctiol
Flavones		R=R'=H; Apigenin R=OH, R'=H; Luteolin R=R'=OCH <sub>3</sub> ; Tricetin
Isoflavones		R=OH; Genistein R=H; Daidzein
Flavonols		R=R'=H; Kaempferol R=OH, R'=H; Quercetin R=R'=OH; Myricetin
Flavanols		R=OH, R'=H; (-)-Epicatechin R=R'=OH; (-)-Epigallocatechin R=OH, R'=H; (+)-Catechin R=R'=OH; (+)-Gallocatechin

		$R=OH, R'=H$ ; (+)-Epicatechin $R=R'=OH$ ; (+)-Epigallocatechin $R=OH, R'=H$ ; (-)-Catechin $R=R'=OH$ ; (-)-Gallocatechin
Anthoxyanidins		$R=OH, R'=H$ ; Cyanidin $R=R'=OH$ ; Dephinidin $R=R'=OCH_3$ ; Malvidin $R=R'=H$ ; Pelargonidin
		$R=H$ ; Peonidin $R=OH$ ; Petunidin

The damage caused by reactive oxygen species has serious and lethal consequences. It is therefore necessary to reduce and/or prevent the production of these free radicals. Flavonoid's wide spectrum of biological activity especially against oxidative stress makes them the ideal compounds in treating and preventing ROS damage that ultimately leads to neurodegeneration.

## Chapter 3

### 3.1 Monoamine Oxidase

Amine oxidases have traditionally been divided into two main groups, based on the chemical nature of the attached cofactor. The flavin adenine dinucleotide (FAD) containing enzymes (Monoamine oxidase A and B and polyamine oxidase) are intracellular enzymes (Shih *et al.*, 1998). The other class of amine oxidases contain a cofactor possessing one or more carbonyl groups, which is topaquinone (TPQ) in most cases. These include diamine oxidases, lysyl oxidase, plasma membrane bound and soluble monoamine oxidases (Salmi *et al.*, 2001). The FAD containing monoamine oxidases (MOA; E.C. 1.4.3.4) are located at the outer membranes of mitochondria in the brain, liver, intestinal mucosa, and other organs. The prominent function of MOA is that it catalyses the oxidative deamination of both endogenous and exogenous substances influencing the concentration of dietary amines, monoamine neurotransmitters and hormones. This broad array includes several notable biogenic amines: indoleamines such as serotonin (5-hydroxytryptamine, 5-HT) and tryptamine; catecholamines such as dopamine (DA), norepinephrine (NE) and epinephrine; trace amines such as  $\beta$ -phenylethylamine, tyramine, octopamine and MPTP neurotoxin (Bortolato *et al.*, 2008). The end products are aldehydes and  $H_2O_2$  that are involved in oxidative cellular processes (Wouters, 1998).

The rapid deterioration of brain monoamines, such as 5-HT, NE and DA is essential for the proper functioning of synaptic neurotransmission. Monoamine signalling is regarded as a key mechanism for the modulation of mood and emotion, perceptual and cognitive function as well as motor control (Bortolato *et al.*, 2008).

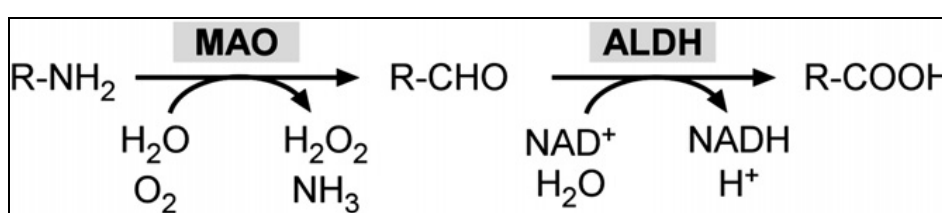


**Figure 3.1:** MAO catalyses the oxidative deamination of monoamines. Monoamines are degraded by MAO to their correspondent aldehydes ( $R-CHO$ ). This reaction produces ammonia ( $NH_3$ ) and hydrogen peroxide ( $H_2O_2$ ). Aldehydes are further oxidised by aldehyde dehydrogenase (ALDH) into carboxylic acids ( $R-COOH$ ).  $NADH$  is a critical cofactor for the latter reaction (directly extracted from Bortolato *et al.*, 2008).

MAO catalyses the  $\alpha$ -carbon oxidation of amines to imines and iminiums with simultaneous reduction of the covalently bound FAD cofactor. The reaction assists in the degradation of monoamines into their corresponding aldehydes, which are then oxidised into acids by aldehyde dehydrogenase (ALDH) or converted into alcohols or glycols by aldehyde reductase (ALR). The enzyme is regenerated by oxidation of the reduced FAD with synchronised reduction of molecular oxygen to hydrogen peroxide. Each mole of substrate oxidised produces one mole of hydrogen peroxide. By-products of these reactions include a number of neurotoxic species, such as ammonia and as mentioned above, hydrogen peroxide. In particular, hydrogen peroxide can trigger the production of reactive oxygen species and induce mitochondrial damage and neuronal apoptosis (Bortolato *et al.*, 2008).

### 3.2 Characteristics of Monoamine oxidase

Two isoforms of the enzyme have been characterised, MAO-A and MAO-B, differing in their substrate specificity and susceptibility to specific inhibitors (Kalgutkar *et al.*, 1995). These isoforms catalyse the biotransformation by oxidation of endogenous neurotransmitter monoamines and also the metabolism of various exogenous primary, secondary and tertiary amines in the CNS as well as peripheral tissues (Kopin, 1985). MAO-A is irreversibly inhibited by low concentrations of clorgyline (Johnston, 1968) and preferentially deaminates 5-hydroxytryptamine, norepinephrine and epinephrine. MAO-B is irreversibly inhibited by (R)-deprenyl (Knoll & Magyar, 1972) and preferentially deaminates  $\beta$ -phenylethylamine and benzylamine. The metabolism of dopamine and other monoamines (such as tryptamine and tyramine) are generally contributed to by both isoforms. Notably, however, is that DA is mainly degraded by MAO-A in the rodent brain, while MAO-B plays a substantial role in this process in humans and other primates. The activity of MAO-B was shown to be enhanced in aging and Alzheimer's disease patients (Saura *et al.*, 1994).

Both the MAO-A and -B genes are located in the chromosome X (Xp 11.23), in opposite directions with tail-to-tail orientation, and display identical number of exons (15) and intron exon organisation (Lan *et al.*, 1989). The deduced primary sequences of the two isoenzymes have 70 % identity, and contain a pentapeptidic sequence binding the FAD cofactor through a thioester covalent linkage to the cysteine (Bach *et al.* 1988). The primary sequence is highly critical for the differences in catalytic activity between MAO-A and -B (Bortolato *et al.*, 2008). The internal segment (between aminoacids 152 and 366) grants inhibitor and substrate specificities (Shih *et al.*, 1998; Tsugeno *et al.*, 1995). Both MAO-A and -B are located in the outer membrane of the mitochondria, to which they are anchored by the C-terminal domain (Rebrin *et al.*, 2001).

Both MAO-A and -B play a pivotal role in the metabolism of monoamine neurotransmitters and are therefore of considerable pharmacological interest. Inhibitors of MAO are of therapeutic interest for the treatment of psychiatric and neurological disorders. Reversible MAO-A inhibitors are used as antidepressant and anxiolytic drugs (Amrein *et al.*, 1999) while selective inhibitors of MAO-B are important in the treatment of both Parkinson's and Alzheimer's disease (Saura *et al.*, 1994). All these findings support the clinical importance of MAO inhibitors in the treatment of several neurological and psychiatric disorders. Furthermore, MAO-B is of considerable pharmacological interest due to its role as the catalyst that mediates the bio-activation of the pro-neurotoxin MPTP.

### 3.2.1 Three dimensional structure

The crystal structure of MAO-B (520 amino acids) was modelled (Geha *et al.*, 2001) and first solved by Binda and coworkers (2002) to a resolution of 3 Å (figure 3.2).



**Figure 3.2:** The three dimensional structure of MAO-B dimer.

Human MAO-B crystallises as a dimer and exhibits hydrodynamic properties of a dimeric form in two different detergent solutions (Edmondson *et al.*, 2007). The structure of a single monomer of the dimeric form is illustrated in figure 3.3.

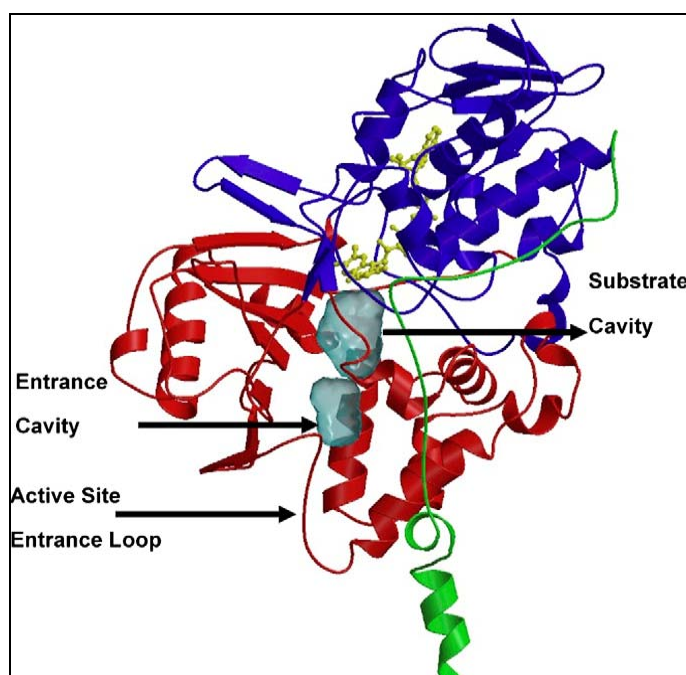


**Figure 3.3:** Ribbon diagram of monomeric unit of human MAO-B structure. The covalent flavin moiety is shown in a ball and stick model in yellow. The flavin binding domain is in blue, the substrate domain in red and the membrane domain in green (Edmondson *et al.*, 2007).

For a substrate molecule to reach the flavin centre, it must first negotiate a protein loop at the entrance to one of two cavities before reaching the flavin coenzyme. The first cavity is the “entrance cavity”, which is hydrophobic in nature and exhibits a volume of 290 Å<sup>3</sup>. Isoleucine199 separates it from the “substrate cavity” which is similarly hydrophobic and exhibits a volume of 390 Å<sup>3</sup>. The isoleucine199 side chain serves as a “gate” between the two cavities and can either exist in an open or closed form, depending on the substrate or bound inhibitor. This is crucial as it helps in defining the inhibitor specificity of human MAO-B (Hubálek *et al.*, 2005). FAD coenzyme is covalently bound in an 8 $\alpha$ -thioether linkage (Kearney *et al.*, 1971) at the end of the substrate to cysteine397. A hydrophilic area exists near the FAD co-factor with sites for favourable amine binding. This aromatic cage is formed by FAD and two residues, tyrosine398 and tyrosine435 (Li *et al.*, 2006).

Human MAO-A crystallises as a monomer and has a cavity size of 550 Å<sup>3</sup> (figure 3.4). It differs from human MAO-B in that it only has a single substrate binding cavity with protein loops at the entrance.

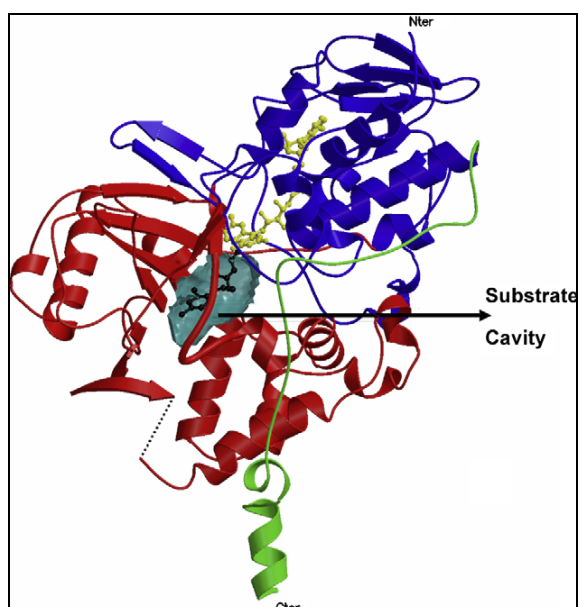


**Figure 3.4:** Ribbon diagram of the human MAO-A structure (Edmondson *et al.*, 2007).

A comparison of the active sites for human MAO-A and –B are shown in figure 3.5. MAO-B has a bipartite elongated cavity that occupies a combined volume close to 700 Å when the side chain of isoleucine199 is in the open conformation. MAO-A has a single cavity exhibiting a rounder shape and larger volume. Analysis of residue side chains in either active site shows the substrate to have less freedom for rotation in the MAO-B site than in MAO-A (Edmondson *et al.*, 2007).

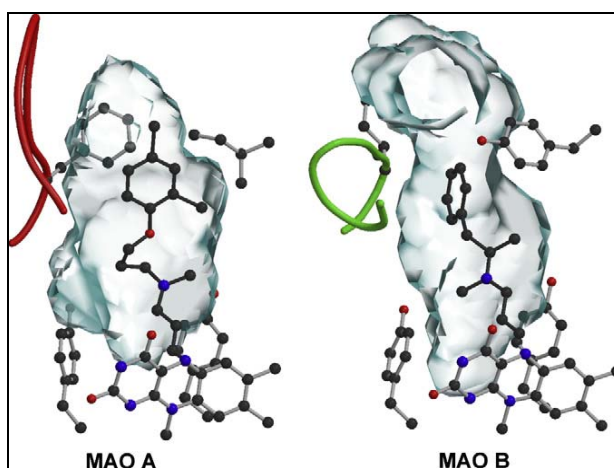


**Figure 3.5:** Comparison of the active site cavities of human MAO-A and –B. Clorgyline is present in MAO-A's active site and Deprenyl in MAO-B's active site. Both form covalent N (5) flavocyanyne adducts with the respective flavin coenzymes. The active site "shaping loop" structures is denoted in red for MAO-A and green for MAO-B (Edmondson *et al.*, 2007).

### 3.3 Physiological role of Monoamine oxidase B and inhibitors thereof

The primary goal of MAO-B inhibitors is to increase the availability of the neurotransmitters at nerve terminals. MAO-B inhibitors increase the basal dopamine levels in the dopaminergic input pathway by inhibiting the metabolism of dopamine by MAO-B. MAO-B inhibition thus helps to conserve the depleted supply of dopamine in Parkinson's disease. In patients with advanced Parkinson's disease, the simultaneous administration of MAO-B inhibitor (R)-deprenyl with levodopa (L-DOPA) potentiated the action of L-DOPA, leading to a reduction of required L-DOPA (Birkmayer *et al.*, 1975). A lower dose of L-DOPA is desirable, as L-DOPA, despite its excellent initial improvements, is associated with long term side effects, including motor fluctuations, dyskinesia and dystonia. Inhibition of MAO-B also results in the reduction of hydrogen peroxide production, which is believed to play a crucial role in the aetiology of Parkinson's disease.

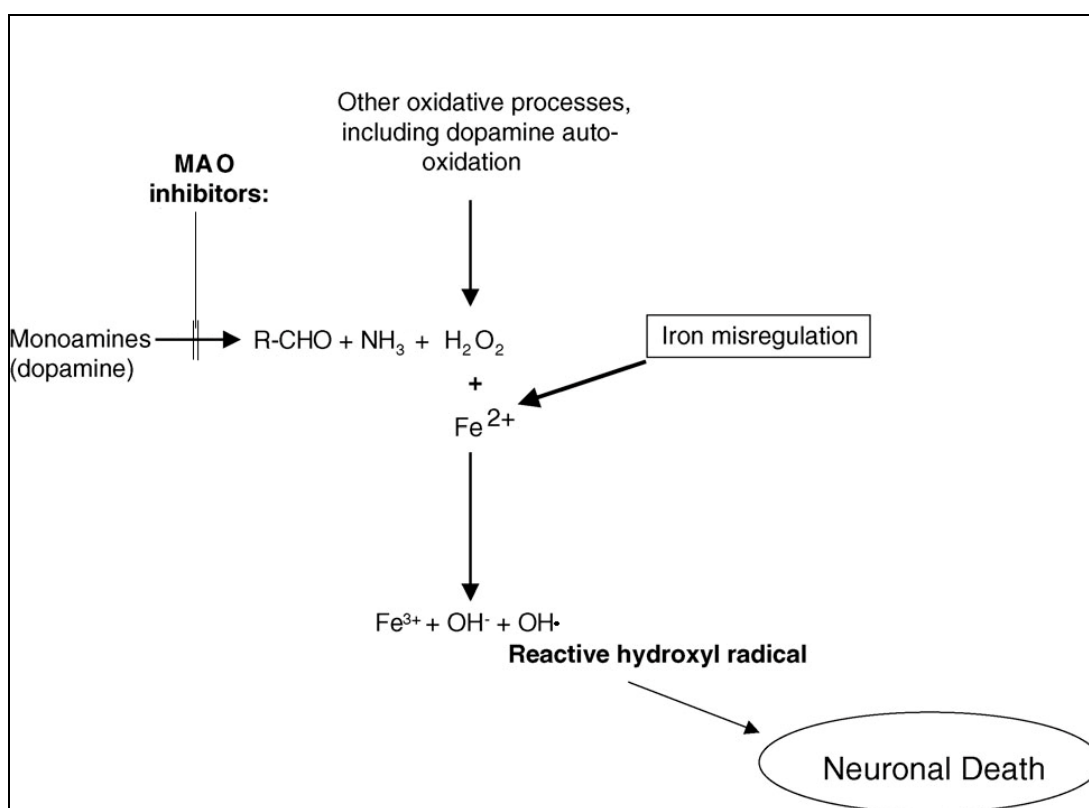


**Figure 3.6:** The pathways of hydrogen peroxide formation and reactive hydroxyl radical generation *via* iron Fenton Chemistry (adapted from Youdim *et al.*, 2004).

MAO-catalysed oxidation of DA results in the formation of H<sub>2</sub>O<sub>2</sub>, normally a harmless cellular metabolite. In the presence of iron (II), however, it can be converted by the Fenton reaction to the highly reactive hydroxyl radical as (figure 3.6). Inhibitors of MAO-B reduce the oxidative stress in healthy dopaminergic neurons in humans by reducing H<sub>2</sub>O<sub>2</sub> production,



thus functioning as a neuroprotective agent (Foley *et al.*, 2000). MAO-B inhibitors are also important since they prevent MAO-B from oxidising 1-methyl-4-phenyl-1,2,3,6-tetrahydropyridine (MPTP) to 1-methyl-4-phenylpyridinium (MPP<sup>+</sup>) which is a highly toxic compound (Langston *et al.*, 1984) illustrated in figure 3.7.

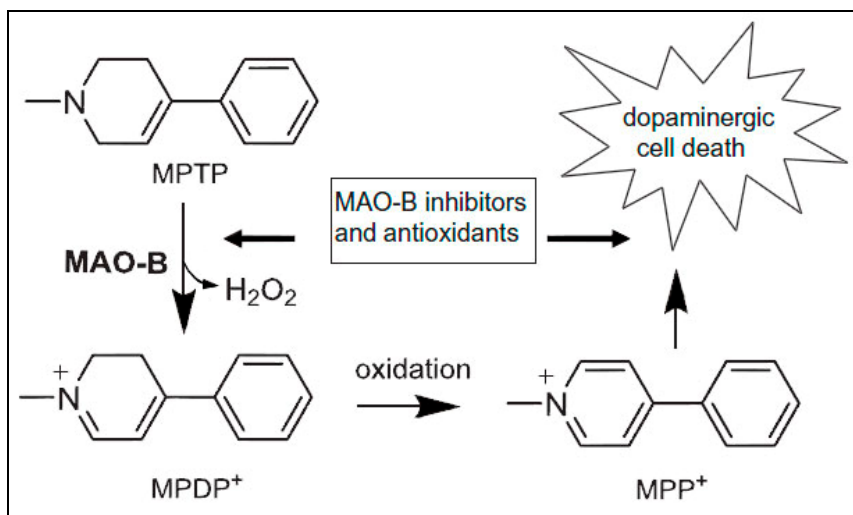


**Figure 3.7:** The neurotoxin MPTP is oxidised by MAO-B to give MPDP<sup>+</sup> and subsequently MPP<sup>+</sup>. MAO inhibitors and antioxidants exert neuroprotective actions by decreasing toxin activation and reducing oxidative stress (directly extracted from Herraiz & Guillén, 2011).

Research has shown that MAO inhibitors play an important role in various physiological and pathological processes, thus designating MAO-B as an important drug target.

### 3.3.1 Neurotoxins and models of neurodegeneration

The ultimate causes underlying Parkinson's disease are unknown, although several environmental toxins (figure 3.8) such as rotenone, MPTP, 2-methyl- $\beta$ -carboline, isoquinolines, and pesticides might be involved (Drechsel & Patel, 2008; Henchcliffe & Beal, 2008). The neurotoxin MPTP (figure 3.7) has attracted particular interest as a parkinsonism-inducing neurotoxin (Langston *et al.*, 1983). MPTP was discovered when a drug addict, preparing a meperidine analogue, inadvertently synthesised MPTP as an impurity. After injection of the drug the person, still in his twenties, rapidly developed Parkinson's disease like symptoms. MAO-B inhibitors are important since they prevent the formation of MAO-B from oxidising MPTP to 1-methyl-4-2,3-dihydropyridinium (MPDP<sup>+</sup>; Langston *et al.*, 1984), which was found when the MAO-B inhibitor ((R)-deprenyl) protected the nigrostriatal neurons in mice against damage caused by MPTP (Heikkilä *et al.*, 1984).

This led to MPTP and other tetrahydropyridinyl substrates becoming popular agents for neuroprotective studies in the field of Parkinson's disease.

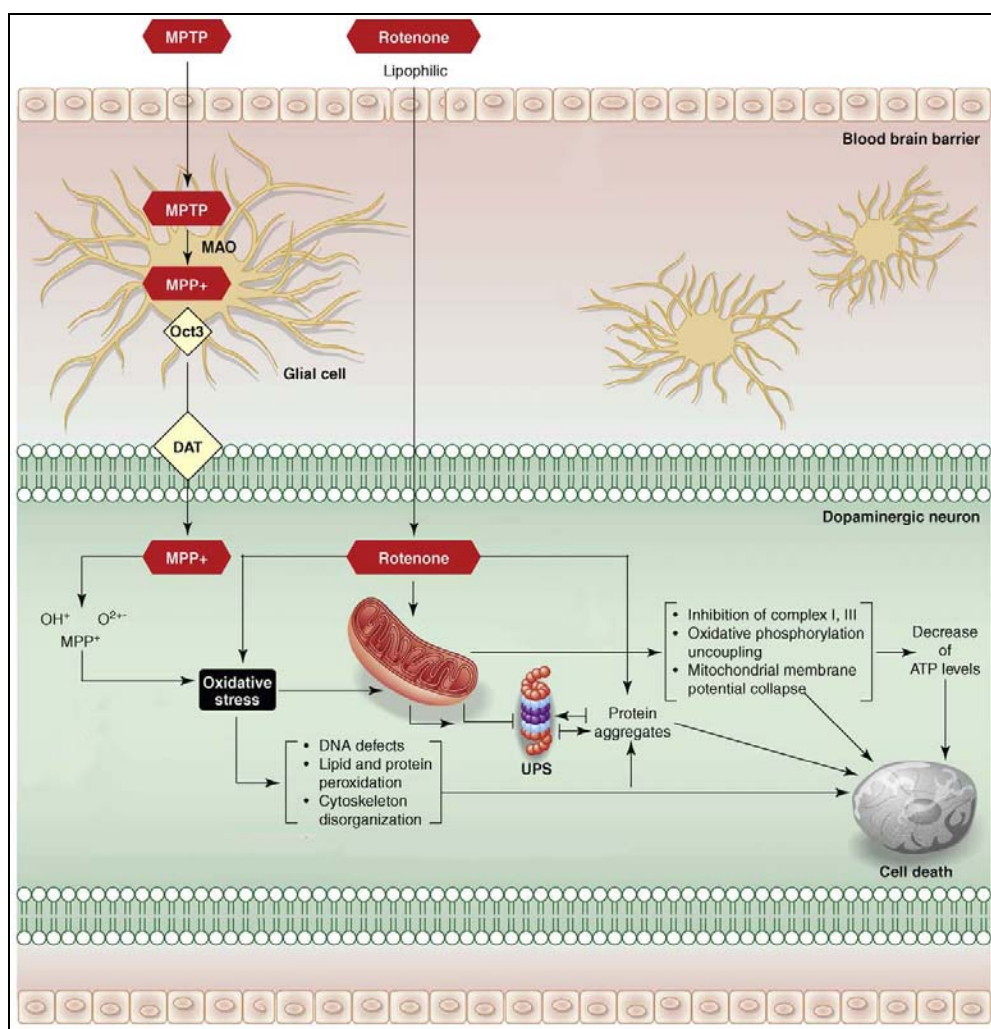


**Figure 3.8:** Mechanism of actions of various toxins used to produce Parkinson's disease models. MPTP is transported across the BBB and is converted to MPDP<sup>+</sup> by MAO-B. MPDP<sup>+</sup> is then oxidised to the toxic form MPP<sup>+</sup> in astrocytes. MPP<sup>+</sup> is released into the extracellular milieu by the plasma membrane transporter Oct3 and subsequently enters dopamine neurons by specific dopamine transporters. This causes oxidative stress followed by cellular death. Abbreviations: ATP: Adenosine triphosphate; Oct3: organic cation transporter 3; BBB: Blood brain barrier; DAT: dopamine transporter; UPS: ubiquitin proteasome system (adapted from Cicchetti *et al.*, 2009).

The mechanism of toxicity is mediated by MAO enzymes that bioactivate MPTP to toxic metabolites (Langston *et al.*, 1983). MPTP easily crosses the blood-brain barrier and is preferentially metabolised by MAO-B to MPDP<sup>+</sup> in the glial cells.

This metabolite is subsequently oxidised to MPP<sup>+</sup>, which is selectively taken up by dopaminergic cells *via* the dopamine transporter (DAT) resulting in the inhibition of mitochondrial complex I of the electron transport system and leading to depletion of ATP and cell death (Langston *et al.*, 1984). MPDP<sup>+</sup>/MPP<sup>+</sup> species induce oxidative stress through dopamine efflux and auto-oxidation whereas free radicals including OH•, superoxide, and NO•, are likely involved in dopaminergic neurotoxicity (Adams *et al.*, 1993; Chiueh *et al.*, 1992; Drechsel & Patel, 2008; Seet *et al.*, 2010; Smith & Bennett, 1997). These biochemical features might be attenuated in the presence of antioxidants (Gonzalez-Polo *et al.*, 2004; Herraiz & Guillèn, 2011; Lee *et al.*, 2011). MPP<sup>+</sup> has also been shown to induce apoptosis *via* cytochrome c release and activation of caspases, properties that may contribute further to its neurotoxicity (Yoshinaga *et al.*, 2000).

### 3.3.2 Monoamine oxidase B inhibitors

MAO inhibitors have been characterised into two groups, MAO-A and MAO-B. Two classes of MAO-B inhibitors can be distinguished

- Reversible, competitive inhibitors that are structurally related to MAO substrates, and can thus bind to the active site of the enzyme, but are metabolised comparatively slowly (Foley *et al.*, 2000).
- Irreversible,  $k_{cat}$  or “suicide” inhibitors, initially binding to MAO in a reversible, competitive manner, but are then oxidised by the enzyme forming the active inhibitor, which covalently binds the enzyme active site *via* the FAD cofactor, thus rendering it permanently unavailable for amine metabolism. The inhibition is more persistent than that achieved by reversible inhibitors (weeks rather than hours), as its effects can only be overcome by the *de novo* synthesis of the enzyme (Abeles & Maycock, 1976; Foley *et al.*, 2000).

Rasagiline and (R)-deprenyl are irreversible inhibitors of MAO-B while lazabemide is a reversible inhibitor (The Parkinson Study Group, 1993). These compounds were used in Parkinson’s disease therapy (Rabey *et al.*, 2000) but their usage has decreased. Both of the irreversible MAO-B inhibitors were found to be neuroprotective in MPTP treated animals (Heikkila *et al.*, 1984). (R)-deprenyl had a neuroprotective effect by slowing the rate of degeneration in dopaminergic neurons when combined with L-DOPA (Birkmayer *et al.*, 1977).

Although the current inhibitors used in the clinical treatment of Parkinson's disease are irreversible, irreversible inhibitors have a number of disadvantages (Prins *et al.*, 2010). These include the loss of isoform selectivity as a result of repeated drug administration and a slow and variable rate of enzyme recovery following withdrawal of the drug (Tipton *et al.*, 2004). In contrast, for reversible inhibition, enzyme activity is recovered when the inhibitor is eliminated from the tissues and the risk of loss of selectivity is reduced because of the shorter duration of action (Strydom *et al.*, 2011). When the mode of inhibition is competitive, the inhibition may be relieved when the substrate concentration is increased.

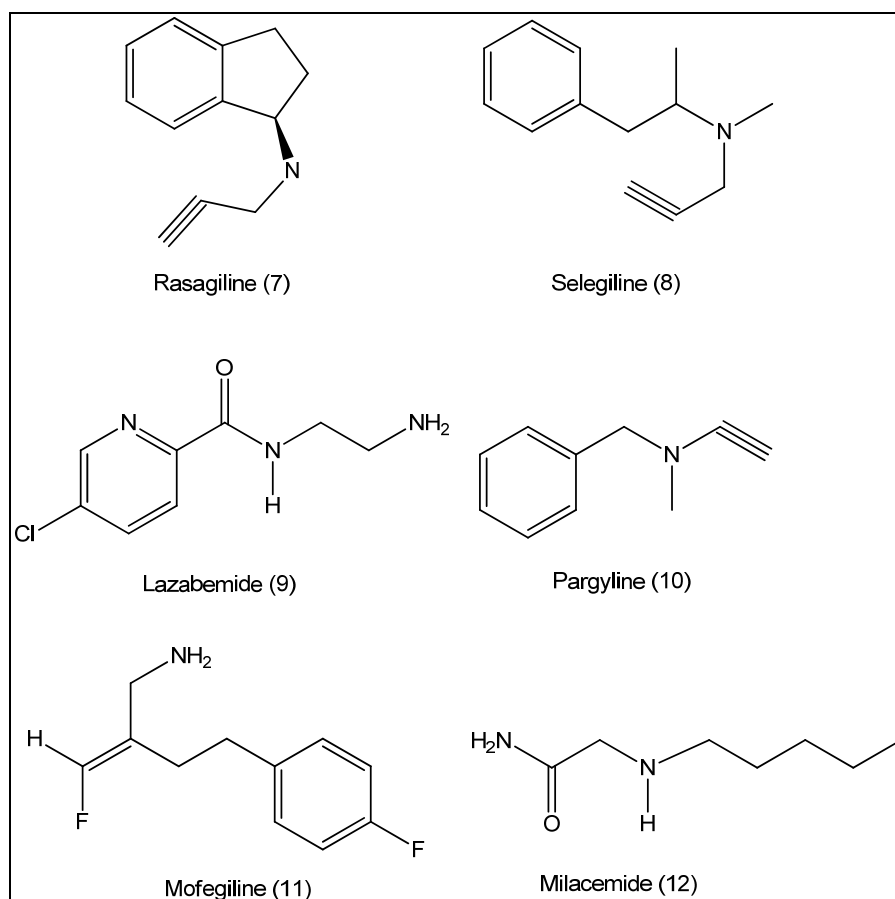


**Figure 3.9:** Structures of selected MAO-B inhibitors.

An overdose of irreversible MAO-B inhibitors can lead to serious side effects, because the inhibitor is irreversibly bound to the FAD co-factor of the enzyme. The enzyme activity can only be regained *via de novo* synthesis of new MAO-B proteins, a process that may require several days. For this reason several research groups are currently attempting to identify new MAO-B inhibitors that are reversible while retaining its selectivity for MAO-B.

### 3.3.3 MAO-B substrate

The active sites of the MAO-A and MAO-B exhibit a 93.9 % sequence identity (Grimsby *et al.*, 1991); however it is the secondary binding sites of the two molecules and possibly their lipid environment which confer their substrate selectivity (Fowler *et al.*, 1980; Kalir *et al.*, 1981; Shih *et al.*, 1998).

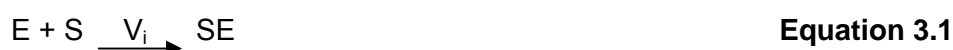
**Table 3.1:** Substrates of MAO-A and MAO-B.

MAO-A	MAO-B	MAO-A/B
Serotonin Octopamine Adrenaline Noradrenaline	Benzylamine Phenylethylamine Methylhistamine N-acetylputrescine MPTP n-Phenylamine Octylamine Milacemide	Tyramine Dopamine Tryptamine Kynuramine 3-Methoxytyramine

## 3.4 Enzyme kinetics

### 3.4.1 Introduction

The general equation for the chemical reaction between an enzyme (E) and substrate (S), producing the enzyme substrate complex (SE), is illustrated in equation 3.1.



The velocity of the forward reaction is indicated by  $V_i$ . When the substrate is in excess compared to the enzyme,  $V_i$  will be directly proportionate to the enzyme concentration ( $v_i \propto [E]$ ). If the concentration of the enzyme substrate [S] is increased while all other conditions are kept constant, the initial velocity ( $V_i$ ) of an enzymatic reaction will increase to a maximum value  $V_{max}$ . At  $V_{max}$  the enzyme is saturated with substrate and  $V_i$  is unchanged by further increases in substrate concentration.

### 3.4.2 $K_m$ determination

The substrate concentration [S] that produce half-maximal velocity ( $V_{max}/2$ ), is the  $K_m$  value or Michaelis constant (Marangoni, 2003) and is determined experimentally by graphing  $V_i$  vs [S] (figure 3.10). With certain assumptions, the  $K_m$  value resemble the dissociation (binding) constant ( $K_d$ ) for the enzyme-substrate complex. Because the affinity of an enzyme for its substrate is equal to the inverse of  $K_d$ , a numerically small  $K_m$  indicates a high affinity of the substrate for the enzyme (Rodwell, 1993).

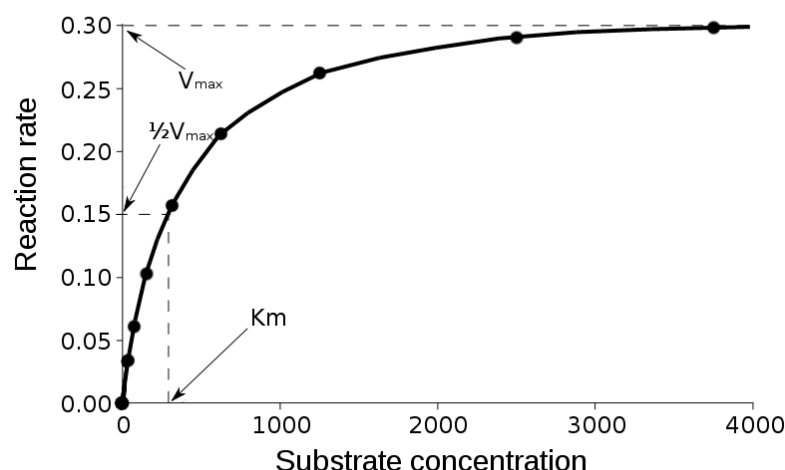


**Figure 3.10:** Graphical presentation of the Michaelis-Menten equation ( $V_i$  vs  $[S]$ ).

The Michaelis-Menten equation expresses the behaviour of various enzymes under the influence of different substrate concentrations (equation 3.2)

$$V_i = \frac{V_{\max} \times [S]}{K_m + [S]}$$

**Equation 3.2**

Numerous enzymes give saturation curves that do not permit exact measurement of  $V_{\max}$  (and therefore  $K_m$ ) when  $V_i$  is plotted against  $[S]$ . By inversion of the Michaelis-Menten equation (equation 3.3) and graphing the inverse of the initial velocity ( $1/V_i$ ) as a function of the inverse of substrate concentration ( $1/[S]$ ), a straight line is obtained. The resulting plot is called a double reciprocal plot or Lineweaver-Burke plot (figure 3.11). The  $K_m$  and  $V_{\max}$  values can easily be obtained from this plot since the y-axis intercept is equal to  $1/V_{\max}$  and the slope is  $K_m/V_{\max}$ . The x-axis intercept is equivalent to  $-1/K_m$  (Segel, 1993).

When  $[S]$  is approximately equivalent to  $K_m$ ,  $V_i$  is very receptive to changes in substrate concentrations and the presence of inhibitors. For that reason, when examining the MAO-B catalytic rate the substrate concentrations that bracket the apparent  $K_m$  value are used.

$$\frac{1}{V} = \frac{K_m}{V_{\max}} \times \frac{1}{[S]} + \frac{1}{V_{\max}}$$

**Equation 3.3**

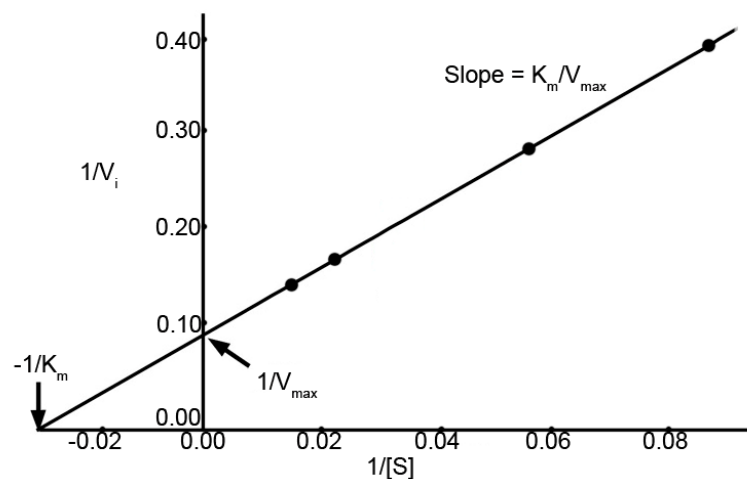


**Figure 3.11:** A Lineweaver-Burke plot ( $1/V$ , vs  $1/[S]$ ).

### 3.4.3 $K_i$ determination

Classic competitive inhibition takes place at the substrate-binding site of an enzyme in a mode that prevents the substrate from binding. The inhibitor and substrate are mutually exclusive, this means that they compete for binding at the identical site and that the association of the inhibitor and the enzyme is reversible (Marangoni, 2003). Competitive inhibition is represented graphically by the Lineweaver-Burke plot (figure 3.11). The addition of a competitive inhibitor to an enzyme substrate reaction increases the slope of the straight line while the y-axis intercept remains unchanged. The intercept on the x-axis increases and becomes less negative (van den Berg *et al.*, 2006). Therefore a competitive inhibitor raises the apparent  $K_m$  value of the substrate while  $V_{max}$  remains unchanged (Marangoni, 2003). The form of the Michaelis-Menten equation describing the inhibitor-substrate enzyme relationship for many enzymes is illustrated in equation 3.4.

$$V_i = \frac{V_{max} \times \frac{[S]}{K_m}}{1 + \frac{[S]}{K_m} + \frac{[I]}{K_i}}$$

**Equation 3.4**

The inverse of this equation expresses the double reciprocal plot in the presence of a competitive inhibitor as described in equation 3.5.

$$\frac{1}{V} = \frac{K_m}{V_{max}} \left( 1 + \frac{[I]}{K_i} \right) \times \frac{1}{[S]} + \frac{1}{V_{max}}$$

**Equation 3.5**

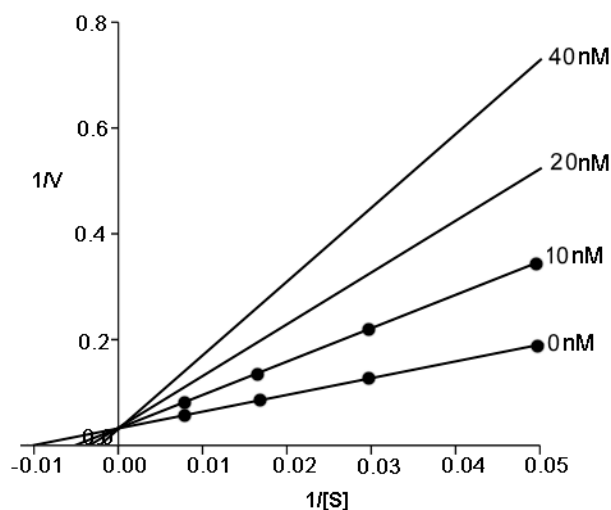


**Figure 3.12:** The double reciprocal plot in the presence of different pre-set concentrations of a competitive inhibitor.

The  $K_i$  value of a competitive inhibitor is used to describe the affinity of the inhibitor for the active site of the enzyme. In a series of competitive inhibitors, those with the lowest  $K_i$  values will cause the highest level of inhibition at a fixed concentration of inhibitor  $[I]$ . The  $K_i$  value for an inhibitor can be determined from the secondary plot in which the slope of each reciprocal plot is graphed vs the corresponding inhibitor concentration (figure 3.13). The x-axis value is equal to  $-K_i$ . In the presence of a concentration of inhibitor  $[I]$  that is approximately equal to  $K_i$ , the substrate concentration has to double to maintain the same original velocity as in the absence of the inhibitor (van den Berg *et al.*, 2006).

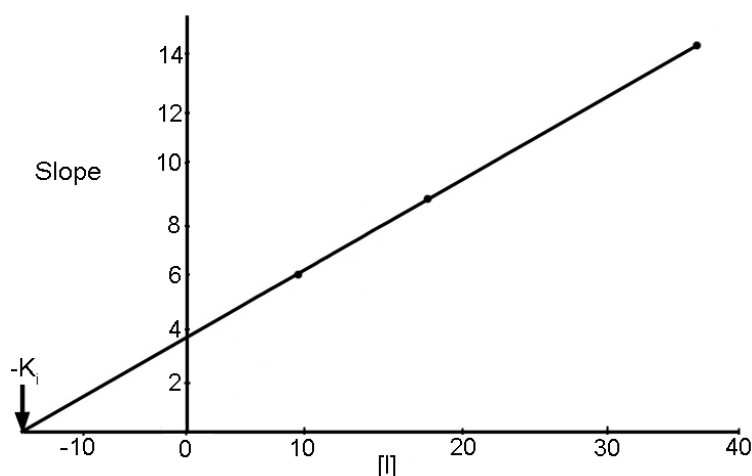


**Figure 3.13:** Secondary plot of the slopes from the double reciprocal plot versus inhibitor concentration.



If the plasma or tissue concentrations of a competitive inhibitor are larger than  $K_i$ , an interaction is expected with the enzymes leading to a physiological effect. On the contrary, if the plasma or tissue concentrations are lower than  $K_i$ , an interaction between the inhibitor and the enzyme is unlikely to lead to a physiological significant effect (Kakkar *et al.*, 1999).

#### 3.4.4 $IC_{50}$ value calculation

Another way of expressing inhibitor potency is through  $IC_{50}$  value. The  $IC_{50}$  value represents the concentration of a drug that is required for 50 % inhibition *in vitro* (figure 3.14).

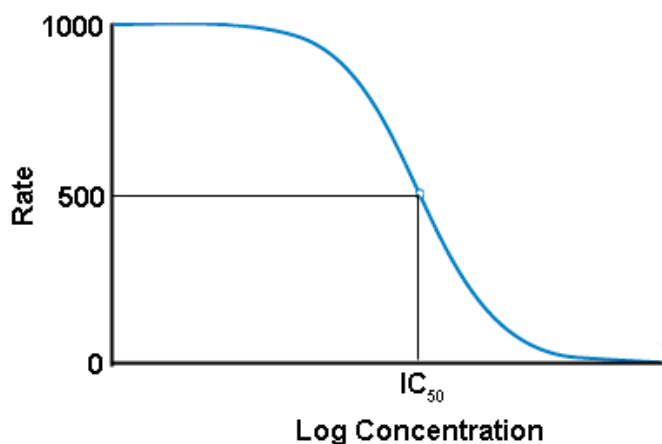


**Figure 3.14:** Graphical representation of  $IC_{50}$  value.

The relationship between  $K_i$  and  $IC_{50}$  value can be expressed by equation 3.6 (Cheng *et al.*, 1973).

$$K_i = IC_{50} / (1 + [S]/K_m) \quad \text{Equation 3.6}$$

For this study the enzymes used are recombinant human MAO-A and -B, with substrate concentration of 45  $\mu$ M and 30  $\mu$ M and  $K_m$  values of  $16.1 \pm 0.21 \mu$ M and  $22.66 \pm 0.72 \mu$ M (Strydom *et al.*, 2010).

Monoamine oxidases inhibitors are important in the treatment of several neurological disorders by inhibiting the MAO catalysed oxidative deamination of amines. These include an important neurotransmitter dopamine necessary for normal brain function. The MAO-B inhibitory activity of flavonoids prevent this depletion of dopamine, the combined antioxidant and MAO-B inhibitory effects make this group of compounds interesting in treating and preventing neurodegeneration.

## Chapter 4. Experimental

### 4 Standard Experimental Procedures

#### 4.1.1 Instrumentation

Spectral graphs are available in the appendix section of this dissertation.

##### 4.1.1.1 Nuclear Magnetic Resonance (NMR) Spectroscopy

NMR spectra ( $^1\text{H}$ ,  $^{13}\text{C}$ , DEPT, HSQC, HMBC and COSY) were obtained with a Bruker Advance 600 spectrometer, in a 14,09 Tesla magnetic field, using an ultra-shield plus magnet.  $^1\text{H}$  NMR and  $^{13}\text{C}$  NMR spectra were recorded at frequencies of 600 MHz and 150 MHz, respectively. Spectra were measured in DMSO- $\text{D}_6$  and  $\text{CDCl}_3$  and chemical shifts were measured in parts per million (ppm). Spectra were referenced to the residual solvent peak.  $^1\text{H}$  NMR signal multiplicity was denoted as s (singlet), br s (broad singlet), d (doublet), dd (doublet of doublets), t (triplet), td (triplet of doublets), q (quartet) or m (multiplet).

##### 4.1.1.2 Mass Spectrometry (MS)

The low resolution spectra were acquired on the thermo Finnigan LXQ ion trap mass spectrometer in electrospray ionisation (ESI) positive mode. The accurate mass spectra were acquired on the Thermo Electron DFS dual focussing magnetic sector mass spectrometer and the Waters Synapt G2 mass spectrometer in electrospray ionisation (ESI) positive mode.

##### 4.1.1.3 Infrared Spectroscopy (IR)

IR spectra were recorded on a Nicolet Nexus 470-FT-IR spectrometer (Madison, Wisconsin, USA). Samples were prepared using KBr disks.

##### 4.1.1.4 Melting Point (MP) Determination

Melting points were determined using a Stuart melting point SMP10 apparatus and capillary tubes holding the sample in the heating chamber. A plateau temperature was quickly reached after which the exact melting point was observed by  $1^\circ\text{C}/\text{min}$  ramping to the melting point of the compound.

#### 4.1.2 Chromatographic Techniques

Mobile phases used were prepared on a volume-to-volume basis and suitable mobile phases were determined using the Prism model (Nyiredy *et al*, 1985).

#### 4.1.2.1 Thin Layer Chromatography (TLC)

Analytical TLC was performed on 0.20 mm thick aluminium silica gel sheets (Alugram® SIL G/UV254, Kieselgel 60, Macherey-Nagel, Düren, Germany). Visualisation was achieved using UV light (254 nm), a spray reagent containing ninhydrin in ethanol or iodine vapours, with mobile phases as indicated for each compound.

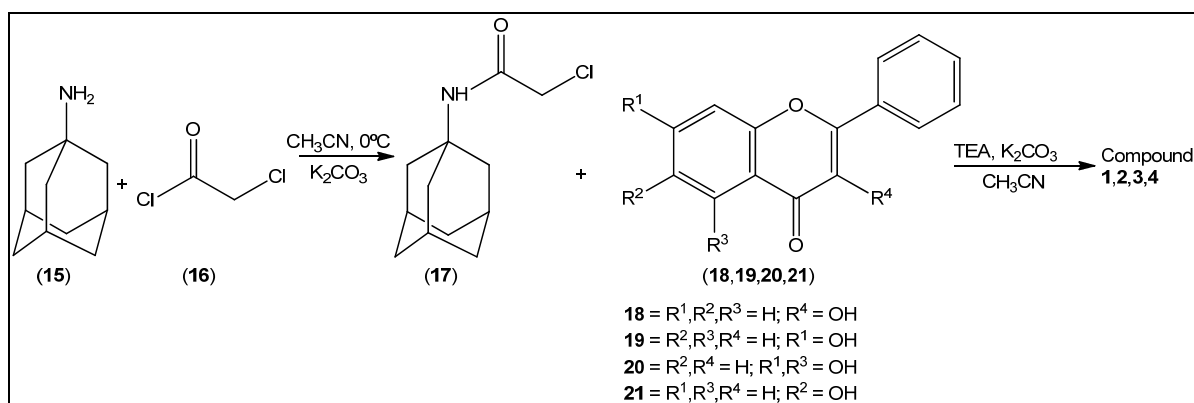
#### 4.1.2.2 Column Chromatography

All compounds were purified using a standard glass column, 71 cm in length and with an inner diameter of 4 cm. The stationary phase used was silica gel (0.063-0.200 mm/70-230 mesh ASTM, Macherey-Nagel, Düren, Germany) with mobile phases as indicated for each compound.

### 4.2 Synthesis of Selected Compounds

#### 4.2.1 Synthesis of Amantadine-flavone conjugates

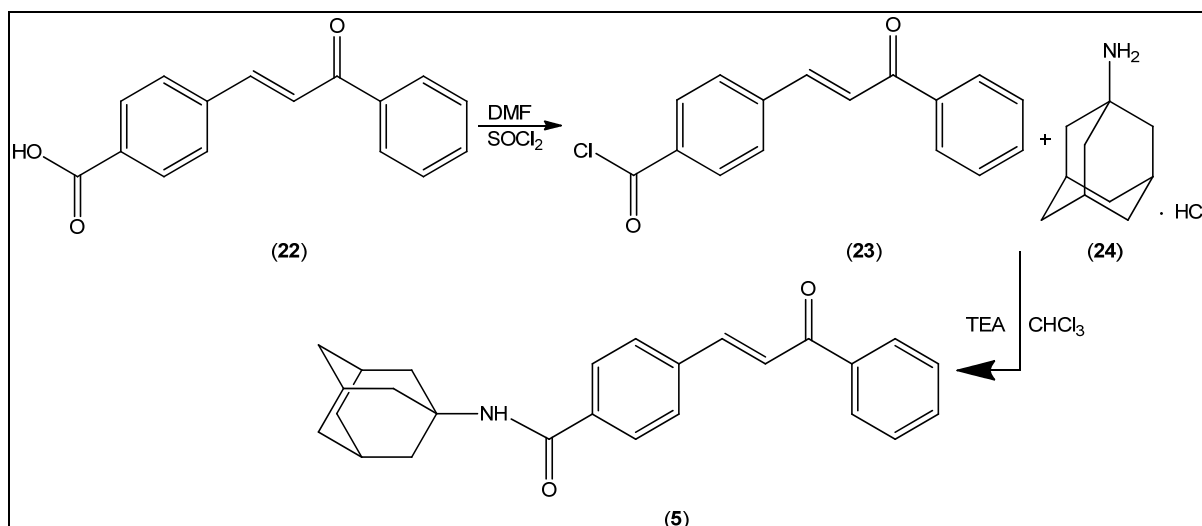
Amantadine free base (**15**) was obtained with an acid base extraction. This was reacted with chloroacetyl chloride (**16**) under Schotten-Baumann conditions (Paczal *et al.*, 2006) to form the amide derivative (**17**). The chloride acts as a good leaving group and promotes amide formation. The amide was then reacted with the hydroxyl group (Brown *et al.*, 1989) of various flavones (**18,19,20,21**) under basic conditions to yield the amide ether (**1,2,3,4**) illustrated in scheme 1.



**Scheme 1:** Synthetic route of amantadine-flavone conjugates.

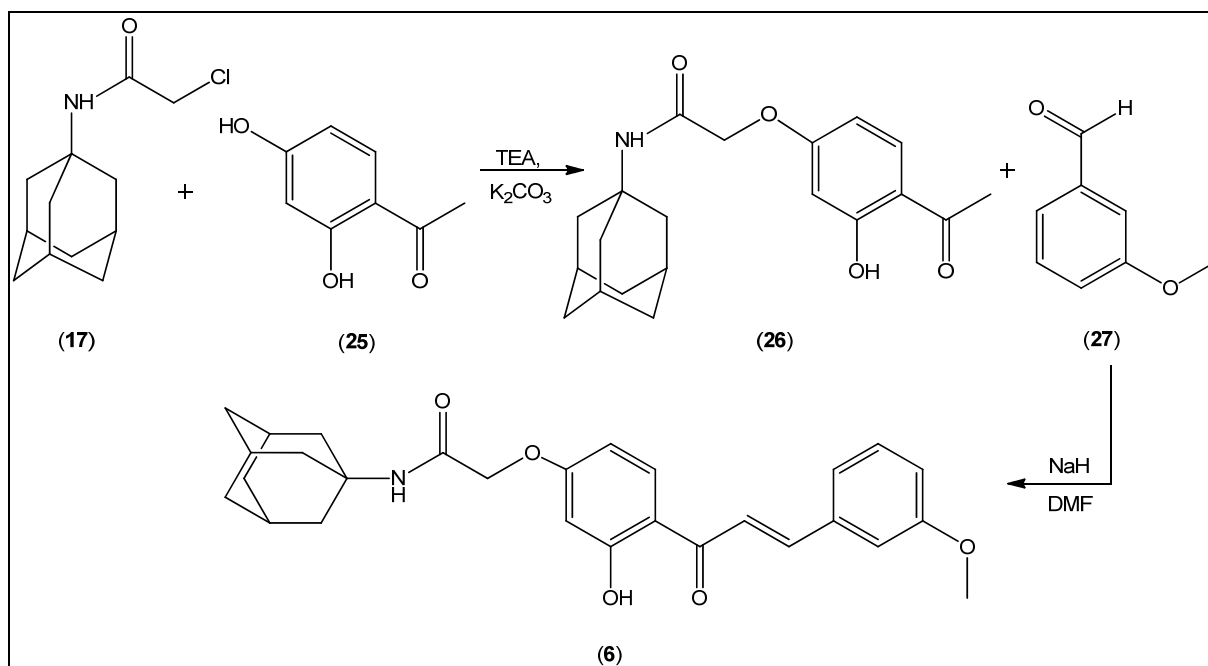
#### 4.2.2 Synthesis of Amantadine-chalcone conjugates

Chalcone (**22**) was reacted with thionyl chloride (Dimmock *et al.*, 2002), converting it to the acid chloride (**23**). This was conjugated to amantadine hydrochloride (**24**) under basic conditions (Manetti *et al.*, 2003) to yield the amide (**5**) illustrated in scheme 2.



**Scheme 2:** Synthetic route of amantadine-chalcone (5).

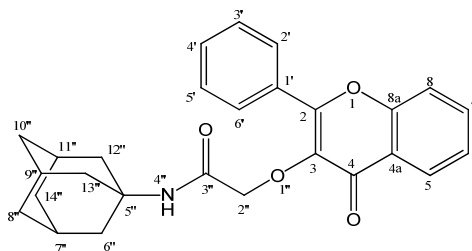
Chalcone derivative (6) was obtained by reacting the amide derivative (17) with the hydroxyl group of 2,4'-dihydroxyacetophenone (25) to yield the monosubstituted amide ether (26). The amide ether (26) was reacted with 3-anisaldehyde (27) using an aldol condensation (Lourens, 2008) to yield enone (6) (scheme 3).



**Scheme 3:** Synthetic route of amantadine-chalcone (6).

## 4.3 Synthesis

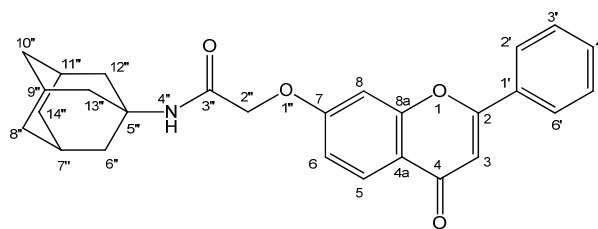
### 4.3.1 N-(adamantan-1-yl)-2-[(4-oxo-2-phenyl-4H-chromen-3-yl)oxy]acetamide (1)



**Synthetic method:** To a chilled (0 °C) solution of chloroacetyl chloride (0.520 ml, 6.0 mmol) and potassium carbonate (1.800 g, 13 mmol) in CH<sub>3</sub>CN (15 ml) was added amantadine free base (1.000 g, 6.0 mmol). The reaction mixture was stirred for a further 2 hours at 0 °C. The reaction mixture was then filtered and the filtrate was evaporated to yield (**17**) as a white powder (0.350 g, 35 %), which was used without further purification. The amide (**17**) and triethylamine (0.170 ml, 1.2 mmol) was dissolved in CH<sub>3</sub>CN (30 ml) with potassium carbonate (1.800 g, 13.0 mmol). A solution of 3-hydroxyflavone (0.293 g, 1.2 mmol) in CH<sub>3</sub>CN (30 ml) was added dropwise over a period of an hour to the reaction mixture. The mixture was heated at reflux temperature under a nitrogen atmosphere for 48 hours. The reaction was monitored by TLC and after completion it was concentrated in vacuo. The residue was dissolved in EtOAc (100 ml) and the organic fraction washed with brine (30 ml). The organic fractions were combined and concentrated. The residue was purified by column chromatography (EtOAc/petroleum ether 2:7) to yield (**1**) as a white powder (EtOAc:PE, 2:7, R<sub>f</sub> = 0.32, yield: 0.108 g, 36 %).

**Physical data:** C<sub>27</sub>H<sub>27</sub>NO<sub>4</sub>; **mp:** 134 °C; **<sup>1</sup>H NMR** (600MHz, DMSO-D<sub>6</sub>) δH (Spectrum 1): 8.13 (dd, 1H, *J* = 8.0, 1.4 Hz, H-5), 8.08-8.06 (m, 2H, H-2', H-6'), 7.86-7.83 (m, 1H, H-7), 7.77 (d, 1H, *J* = 8.4 Hz, H-8), 7.65 (br s, 1H, H-4''), 7.60-7.59 (m, 3H, H-3', H-4', H-5'), 7.52-7.50 (m, 1H, H-6), 4.28 (s, 2H, H-2''), 1.99 (br s, 3H, H-7'', H-9'', H-11''), 1.91 (br s, 6H, H-6'', H-12'', H-13''), 1.60 (br s, 6H, H-8'', H-10'', H-14''); **<sup>13</sup>C NMR** (150 MHz, DMSO-D<sub>6</sub>) δC (Spectrum 2): 174.17 (C-4), 166.65 (C-3''), 155.38 (C-2), 154.81 (C-8a), 140.04 (C-3), 134.33 (C-7), 131.10 (C-4'), 130.23 (C-1'), 128.76 (C-2', C-6'), 128.58 (C-3', C-5'), 125.25 (C-5), 125.04 (C-6), 123.24 (C-4a), 118.49 (C-8), 71.68 (C-2''), 50.79 (C-5''), 40.87 (C-6'', C-12'', C-13''), 35.90 (C-8'', C-10'', C-14''), 28.76 (C-7'', C-9'', C-11''); **HRESIMS** (positive ionization mode), *m/z* (Spectrum 9): 430.20115 [M+H]<sup>+</sup> (calc. for C<sub>27</sub>H<sub>28</sub>NO<sub>4</sub>: 430.20183); **MS** (ESI, positive ionization mode, 70 eV) *m/z* (Spectrum 8): 430 (M<sup>+</sup>); **IR** (KBr) ν<sub>max</sub> (Spectrum 7): 3271, 1670, 1631, 1106, 1080 cm<sup>-1</sup>.

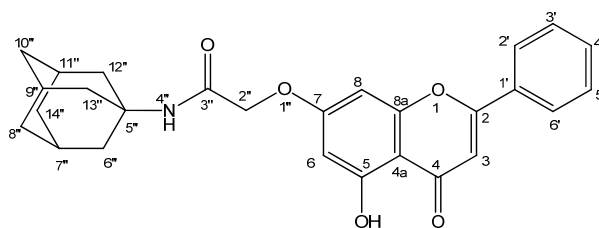
### 4.3.2 N-(adamantan-1-yl)-2-[(4-oxo-2-phenyl-4H-chromen-7-yl)oxy]acetamide (2)



**Synthetic method:** The amide (**17**; 0.350 g, 1.5 mmol) was prepared *in situ* and dissolved with triethylamine (0.140 ml, 1.0 mmol) in CH<sub>3</sub>CN (30 ml) with potassium carbonate (1.8 g, 13 mmol). A solution of 7-hydroxyflavone (0.244 g, 1.0 mmol) in CH<sub>3</sub>CN (30 ml) was added dropwise over a period of an hour to the reaction mixture. The mixture was refluxed under nitrogen for 48 hours. The reaction was monitored by TLC and after completion it was concentrated in vacuo. The residue was dissolved in EtOAc (100 ml) and the organic fraction washed with brine (30 ml). The organic fractions were combined and concentrated. The residue was purified by column chromatography (EtOAc /petroleum ether 3:4) to yield (**2**) as a white powder (EtOAc:PE, 3:4, R<sub>f</sub> = 0.39, yield: 0.121 g, 49 %).

**Physical data:** C<sub>27</sub>H<sub>27</sub>NO<sub>4</sub>; **mp**: 146 °C; **<sup>1</sup>H NMR** (600MHz, DMSO-D<sub>6</sub>) δH (Spectrum 10): 8.06 (d, 2H, *J* = 6.9 Hz, H-2', H-6'), 7.95 (d, 1H, *J* = 8.8 Hz, H-5), 7.58-7.56 (m, 3H, H-3', H-4', H-5'), 7.52 (s, 1H, H-4''), 7.25 (d, 1H, *J* = 2.5 Hz, H-8), 7.10-7.09 (dd, 1H, *J* = 8.8, 2.5 Hz, H-6), 6.95 (s, 1H, H-3), 4.59 (s, 2H, H-2''), 2.00 (br s, 3H, H-7'', H-9'', H-11''), 1.96 (br s, 6H, H-6'', H-12'', H-13''), 1.60 (br s, 6H, H-8'', H-10'', H-14''); **<sup>13</sup>C NMR** (150 MHz, DMSO-D<sub>6</sub>) δC (Spectrum 11): 176.39 (C-4), 165.75 (C-3''), 162.48 (C-2 or C-7), 162.20 (C-2 or C-7), 157.21 (C-8a), 131.69 (C-4'), 131.16 (C-1'), 129.11 (C-3', C-5'), 126.21, 126.16 (C-5, C-2', C-6'), 117.43 (C-4a), 114.82 (C-6), 106.84 (C-3), 102.00 (C-8), 67.36 (C-2''), 51.17 (C-5''), 40.92 (C-6'', C-12'', C-13''), 35.93 (C-8'', C-10'', C-14''), 28.80 (C-7'', C-9'', C-11''); **HRESIMS** (positive ionization mode), *m/z* (Spectrum 18): 430.20132 [M+H]<sup>+</sup> (calc. for C<sub>27</sub>H<sub>28</sub>NO<sub>4</sub>: 430.20183); **MS** (ESI, 70 eV) *m/z* (Spectrum 17): 430 (M<sup>+</sup>); **IR** (KBr) ν<sub>max</sub> (Spectrum 16): 3264, 1672, 1618, 1127 cm<sup>-1</sup>.

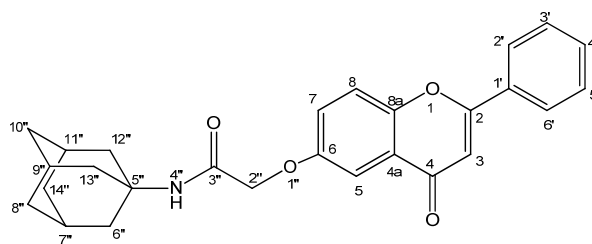
### 4.3.3 N-(adamantan-1-yl)-2-[(5-hydroxy-4-oxo-2-phenyl-4H-chromen-7-yl)oxy]acetamide (**3**)



**Synthetic method:** The amide (**17**; 0.350 g, 1.5 mmol) was prepared *in situ* and dissolved with triethylamine (0.140 ml, 1.0 mmol) in CH<sub>3</sub>CN (30 ml) with potassium carbonate (1.8 g, 13.0 mmol). A solution of chrysin (0.260 g, 1.0 mmol) in CH<sub>3</sub>CN (30 ml) was added dropwise over a period of an hour to the reaction mixture. The mixture was heated to reflux temperature under nitrogen atmosphere for 48 hours. The reaction was monitored by TLC and after completion it was concentrated in vacuo. The residue was dissolved in EtOAc (100 ml) and the organic fraction washed with brine (30 ml). The organic fractions were combined and concentrated. The residue was purified by column chromatography (EtOAc /petroleum ether 2:3) to yield (**3**) as a yellow powder (EtOAc:PE, 2:3, R<sub>f</sub> = 0.67, yield: 0.110 g, 42 %).

**Physical data:** C<sub>27</sub>H<sub>27</sub>NO<sub>5</sub>; mp: 220 °C; <sup>1</sup>H NMR (600MHz, DMSO-D<sub>6</sub>) δH (Spectrum 19): 12.80 (s, 1H, 5-OH), 8.08 (d, 2H, *J* = 7.2 Hz, H-2', H-6'), 7.63-7.57 (m, 3H, H-3', H-4', H-5'), 7.49 (s, 1H, H-4''), 7.04 (s, 1H, H-3), 6.78 (d, 1H, *J* = 2.2 Hz, H-8), 6.41 (d, 1H, *J* = 2.2 Hz, H-6), 4.55 (s, 2H, H-2''), 2.01 (br s, 3H, H-7'', H-9'', H-11''), 1.96 (br s, 6H, H-6'', H-12'', H-13''), 1.61 (br s, 6H, H-8'', H-10'', H-14''); <sup>13</sup>C NMR (150 MHz, DMSO-D<sub>6</sub>) δC (Spectrum 20): 182.07 (C-4), 165.64 (C-3''), 163.95 (C-2), 163.53 (C-7), 161.15 (C-5), 157.12 (C-8a), 132.18 (C-4'), 130.58 (C-1'), 129.17 (C-3', C-5'), 126.43 (C-2', C-6'), 105.40 (C-3), 105.10 (C-4a), 98.50 (C-6), 93.72 (C-8), 67.27 (C-2''), 51.14 (C-5''), 40.91 (C-6'', C-12'', C-13''), 35.92 (C-8'', C-10'', C-14''), 28.77 (C-7'', C-9'', C-11''); **HRESIMS** (positive ionization mode), *m/z* (Spectrum 27): 446.19512 [M+H]<sup>+</sup> (calc. for C<sub>27</sub>H<sub>28</sub>NO<sub>5</sub>: 446.19674); **MS** (EI, 70 eV) *m/z* (Spectrum 26): 446 (M<sup>+</sup>), ; **IR** (KBr) ν<sub>max</sub> (Spectrum 25): 3643, 3417, 1681, 1655, 1080 cm<sup>-1</sup>.

#### 4.3.4 N-(adamantan-1-yl)-2-[(4-oxo-2-phenyl-4H-chromen-6-yl)oxy]acetamide (4)

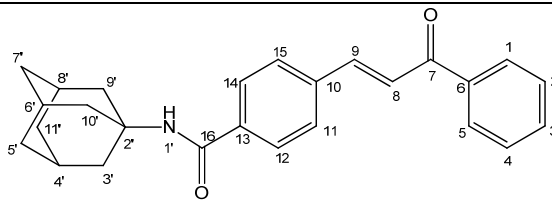


**Synthetic method:** The amide (**17**; 0.350 g, 1.5 mmol) was prepared *in situ* and dissolved with triethylamine (0.140 ml, 1.0 mmol) in CH<sub>3</sub>CN (30 ml) with potassium carbonate (1.8 g, 13.0 mmol). A solution of 6-hydroxyflavone (0.244 g, 1.0 mmol) in CH<sub>3</sub>CN (30 ml) was added dropwise over a period of an hour to the reaction mixture. The mixture was heated to reflux temperature under nitrogen atmosphere for 48 hours. The reaction was monitored by TLC and after completion it was concentrated in vacuo. The residue was dissolved in EtOAc (100 ml) and the organic fraction washed with brine (30 ml). The organic fractions were combined and concentrated. The residue was purified by column chromatography (EtOAc /petroleum ether 2:3) to yield (**4**) as a white powder (EtOAc:PE, 2:3, R<sub>f</sub> = 0.51, yield: 0.151 g, 61 %).

**Physical data:** C<sub>27</sub>H<sub>27</sub>NO<sub>4</sub>; **mp:** 188 °C; **<sup>1</sup>H NMR** (600MHz, DMSO-D<sub>6</sub>) δH (Spectrum 28): 8.11-8.10 (dd, 2H, *J* = 6.7, 1.59 Hz, H-2', H-6'), 7.78 (d, 1H, *J* = 9.1 Hz, H-8), 7.63-7.57 (m, 3H, H-3', H-4', H-5'), 7.54 (s, 1H, H-4''), 7.47 (dd, 1H, *J* = 9.1, 3.1 Hz, H-7), 7.43 (d, 1H, *J* = 3.1 Hz, H-5), 7.02 (s, 1H, H-3), 4.54 (s, 2H, H-2''), 2.01 (br s, 3H, H-7'', H-9'', H-11''), 1.97 (br s, 6H, H-6'', H-12'', H-13''), 1.62 (br s, 6H, H-8'', H-10'', H-14''); **<sup>13</sup>C NMR** (150 MHz, DMSO-D<sub>6</sub>) δC (Spectrum 29): 176.77 (C-4), 166.08 (C-3''), 162.36 (C-2), 155.27 (C-6), 150.54 (C-8a), 131.75 (C-4'), 131.20 (C-1'), 129.12 (C-3', C-5'), 126.30 (C-2', C-6'), 123.93 (C-4a), 123.59 (C-7), 120.06 (C-8), 106.16 (C-5 or C-3), 106.05 (C-5 or C-3), 67.30 (C-2''), 51.07 (C-5''), 40.91 (C-6'', C-12'', C-13''), 35.94 (C-8'', C-10'', C-14''), 28.78 (C-7'', C-9'', C-11'') Tentative assignment of quaternary carbons based on previous derivatives and literature values of similar compounds (Burns *et al.*, 2007) as HMBC was not obtained; **HRESIMS** (positive ionization mode), *m/z* (Spectrum 34): 430.2018 [M+H]<sup>+</sup> (calc. for C<sub>27</sub>H<sub>28</sub>NO<sub>5</sub>: 430.20183); **IR** (KBr) ν<sub>max</sub> (Spectrum 33): 3413, 1687, 1671, 1087 cm<sup>-1</sup>.



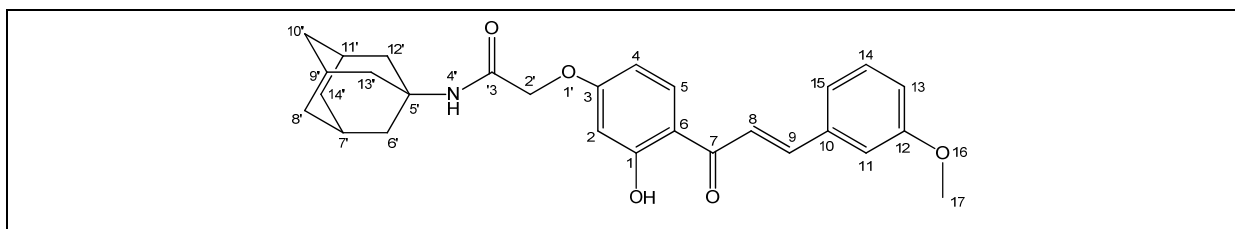
#### 4.3.5 N-(adamantan-1-yl)-4-[(1E)-3-oxo-3-phenylpro-1-en-1-yl]benzamide (5)



**Synthetic method:** To a solution of chalcone (0.500 g, 2.4 mmol) and DMF (0.026 ml, 0.3 mmol) in dry  $\text{CH}_2\text{Cl}_2$  (30 ml) was added thionyl chloride (0.332 ml, 5.5 mmol) and the reaction mixture subsequently heated at reflux temperature for 2 hours. After evaporation of the solvent, the residue was dissolved in  $\text{CHCl}_3$  (30 ml). Amantadine hydrochloride (0.377 g, 2.0 mmol) and triethylamine (0.560 ml, 4.0 mmol) was dissolved in  $\text{CHCl}_3$  (10 ml) and was then added dropwise over a period of an hour. The reaction mixture was stirred for a further 2 hours at room temperature and then diluted with  $\text{CHCl}_3$  (100 ml). The organic fraction was washed with distilled water (30 ml) and concentrated. The residue was purified by column chromatography ( $\text{CHCl}_3/\text{CH}_3\text{OH}$  99:1) to yield (5) a white powder (EtOAc:PE, 8:2,  $R_f$  = 0.83, yield: 0.105 g, 21 %).

**Physical data:**  $\text{C}_{26}\text{H}_{27}\text{NO}_2$ ; mp: 176 °C;  $^1\text{H NMR}$  (600MHz,  $\text{CDCl}_3$ )  $\delta\text{H}$  (Spectrum 35): 8.01 (dd, 2H,  $J$  = 8.0, 1.06 Hz, H-1, H-5), 7.78 (d, 1H,  $J$  = 15.7 Hz, H-9), 7.74 (d, 2H,  $J$  = 8.2 Hz, H-12, H-14), 7.66 (d, 2H,  $J$  = 8.2 Hz, H-11, H-15), 7.60-7.49 (m, 4H, H-2, H-3, H-4, H-8), 5.81 (s, 1H, H-1'), 2.12 (br s, 9H, H-3', H-4', H-6', H-8', H-9', H-10'), 1.71 (br s, 6H, H-5', H-7', H-11');  $^{13}\text{C NMR}$  (150 MHz,  $\text{CDCl}_3$ )  $\delta\text{C}$  (Spectrum 36): 190.24 (C-7), 165.74 (C-16), 143.39 (C-9), 137.91 (C-6), 137.46 (C-10 or C-13), 137.34 (C-10 or C-13), 132.98 (C-3), 128.68, 128.51, 128.40 (C-1, C-2, C-4, C-5, C-11, C-15), 127.35 (C-12, C-14), 123.38 (C-8), 52.50 (C-2'), 41.62 (C-3', C-9', C-10'), 36.32 (C-5', C-7', C-11'), 29.46 (C-4', C-6', C-8'); **HRESIMS** (positive ionization mode),  $m/z$  (Spectrum 42): 386.2122  $[\text{M}+\text{H}]^+$  (calc. for  $\text{C}_{26}\text{H}_{28}\text{NO}_2$ : 386.21200); **IR** (KBr)  $\nu_{\text{max}}$  (Spectrum 41): 3319, 1662, 1643  $\text{cm}^{-1}$ .

#### 4.3.6 N-(adamantan-1-yl)-2-{3-hydroxy-4-[(2E)-3-(3-methoxyphenyl)pro-2-enoyl]phenoxy}acetamide (6)



**Synthetic method:** Compound (**17**; 0.720 g, 3.1 mmol) was prepared *in situ* and 2'4'-Dihydroxyacetophenone (0.287 g, 2.1 mmol) in CH<sub>3</sub>CN (30 ml) was added dropwise over a period of an hour. The mixture was heated to reflux temperature under nitrogen atmosphere for 48 hours. The reaction was monitored by TLC and after completion it was concentrated in vacuo and dissolved in EtOAc (100 ml). The organic fraction was washed with brine (30 ml) and concentrated. The residue was purified by column chromatography (EtOAc/PE 2:3) to yield (**26**) as a white powder (yield: 0.121 g, 42 %). The residue (**26**) was dissolved in DMF (7 ml) under nitrogen atmosphere and cooled to 0 °C. To the solution sodium hydride (0.012 g, 0.7 mmol) was slowly added while stirring over the period of 15 min. 3-Anisaldehyde (0.050 ml, 4.2 mmol) was dissolved in DMF (2 ml) and added dropwise over a period of 30 minutes. The reaction mixture was stirred for a further 3 hours at 0 °C, quenched by the addition of ice water and acidified with 1 M HCl. The precipitate was filtered and purified by column chromatography (AcOEt/petroleum ether 2:4) to yield (**6**) as a yellow powder (AcOEt:PE, 2:4, R<sub>f</sub> = 0.66, yield: 0.050 g, 41 %).

**Physical data:** C<sub>27</sub>H<sub>27</sub>NO<sub>4</sub>; **mp:** 177 °C; **<sup>1</sup>H NMR** (600MHz, CDCl<sub>3</sub>) δH (Spectrum 43): 13.29 (s, 1H, 1-OH), 7.85 (d, 1H, *J* = 8.90 Hz, H-5), 7.83 (d, 1H, *J* = 15.4 Hz, H-9), 7.53 (d, 1H, *J* = 15.4 Hz, H-8), 7.33 (t, 1H, *J* = 7.9 Hz, H-14), 7.23 (d, 1H, *J* = 7.9 Hz, H-15), 7.13 (s, 1H, H-11), 6.96 (dd, 1H, *J* = 7.9, 2.2 Hz, H-13), 6.49 (dd, 1H, *J* = 8.90, 2.46 Hz, H-4), 6.46 (d, 1H, *J* = 2.46 Hz, H-2), 6.10 (br s, 1H, H-4'), 4.38 (s, 2H, H-2'), 3.84 (s, 3H, H-17), 2.08 (br s, 3H, H-7', H-9', H-11'), 2.02 (br s, 6H, H-6', H-12', H-13'), 1.67 (br s, 6H, H-8', H-10', H-14'); **<sup>13</sup>C NMR** (150 MHz, CDCl<sub>3</sub>) δC (Spectrum 44): 191.92 (C-7), 166.31 (C-3 or C-3'), 165.76 (C-3 or C-3'), 163.23 (C-1), 159.91 (C-12), 144.83 (C-9), 135.93 (C-10), 131.62 (C-5), 129.97 (C-14), 121.14 (C-15), 120.27 (C-8), 116.40 (C-13), 115.08 (C-6), 113.69 (C-11), 106.91 (C-4), 102.77 (C-2), 67.40 (C-2'), 55.34 (C-17), 52.09 (C-5'), 41.48 (C-6', C-12', C-13'), 36.18 (C-8', C-10', C-14'), 29.35 (C-7', C-9', C-11'); **HRESIMS** (positive ionization mode), *m/z* (Spectrum 50): 462.2271 [M+H]<sup>+</sup> (calc. for C<sub>28</sub>H<sub>32</sub>NO<sub>5</sub>: 462.22804); **IR** (KBr) ν<sub>max</sub> (Spectrum 49): 3420, 3122, 1692, 1648, 1417, 1042 cm<sup>-1</sup>.

#### 4.4 Structure elucidation

Structure elucidation was done by employing various techniques. Chemical shifts, multiplicities, integration (for  $^1\text{H}$  NMR) and correlations observed in two-dimensional NMR spectra such as the COSY, HSQC and HMBC spectra were used to assign  $^1\text{H}$ - and  $^{13}\text{C}$  NMR peaks. Mass spectrometry and infrared spectroscopy were further employed to confirm structures. As an example, the structure elucidation of compound **1** will be discussed.

The high-resolution mass spectrometry of compound **1** confirmed the molecular formula of  $\text{C}_{27}\text{H}_{27}\text{O}_4\text{N}$  with a molecular mass of 430.20 in the positive ionization mode. This correlated with the calculated  $\text{C}_{27}\text{H}_{28}\text{O}_4\text{N}$  molecular mass of 430.20115. The IR spectrum (KBr, spectrum 7) indicated the presence of the NH ( $3271\text{ cm}^{-1}$ ), the amide carbonyl ( $1631\text{ cm}^{-1}$ ) and the carbonyl of the ketone ( $1670\text{ cm}^{-1}$ ). Bands in the  $1650 - 1050\text{ cm}^{-1}$  range are typical of a flavone skeleton (Antri *et al.*, 2004). In the  $^{13}\text{C}$  NMR spectrum (spectrum 2) there are 19 peaks present which represents 27 carbon atoms, excluding solvent peaks. Twelve of these (14 carbon atoms) are in the aromatic region, 5 peaks (11 carbon atoms) are in the aliphatic region, one is a ketone carbonyl and one is an amide carbonyl. Inspection of the DEPT NMR spectrum (spectrum 3) revealed the presence of three  $\text{CH}_2$  signals and eight CH signals. In the  $^1\text{H}$  NMR (spectrum 1) four aromatic protons:  $\delta_{\text{H}}$  8.13, 7.52-7.50, 7.86-7.83 and 7.77, that are characteristic of the protons of the A ring of 3-hydroxyflavone, occur (Burns *et al.*, 2007) and is illustrated in figure 4.1. Although a doublet of doublets peak was expected at  $\delta_{\text{H}}$  7.77, only a doublet was observed in the overlapping spectra as the peaks were quite broad. The chemical shifts, splitting pattern and integration of the signals at  $\delta_{\text{H}}$  8.08-8.06 and 7.60-7.59 confirm the presence of an unsubstituted B ring (Burns *et al.*, 2007). In the aliphatic region, 3 signals at  $\delta_{\text{H}}$  1.99, 1.91 and 1.60 are characteristic of the protons of amantadine (SDBSWeb). The proton signal at  $\delta_{\text{H}}$  7.65 suggests the presence of an ether linking the amantadine to the 3-hydroxyflavone group.

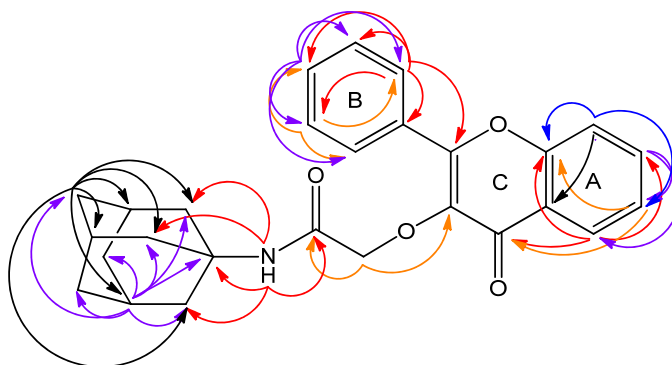


**Figure 4.1:** Correlations seen in HMBC of N-(adamantan-1-yl)-2-[(4-oxo-2-phenyl-4H-chromen-3-yl)oxy]acetamide (**1**)

Two-dimensional NMR experiments (COSY – spectrum 4, HSQC – spectrum 5, HMBC – spectrum 6) were employed in further assignment of NMR signals (Table 4.1).

**Table 4.1:**  $^1\text{H}$  and  $^{13}\text{C}$  (DMSO- $\text{D}_6$ ) correlations observed in N-(adamantan-1-yl)-2-[(4-oxo-2-phenyl-4H-chromen-3-yl)oxy]acetamide (**1**).

Position	$\delta_{\text{H}}$	$\delta_{\text{C}}^{\text{a}}$ (HSQC correlations)	Correlation ( $\delta_{\text{C}}$ ) observed in HMBC	$^{13}\text{C}$ NMR assignment of HMBC correlated carbon
2		155.38 (C)		
3		140.04 (C)		
4		174.17 (C)		
4a		123.24 (C)		
5	8.13 (8.0, 1.4)	125.25 (CH)	134.33, 154.81, 174.17	7, 8a, 4
6	7.52-7.50	125.04 (CH)	118.49, 123.24	8, 4a
7	7.86-7.83	134.33 (CH)	125.25 or 125.04, 154.81	5 or 6, 8a
8	7.77 (8.4)	118.49 (CH)	154.81 or 125.04, 123.24	8a or 6, 4a
8a		154.81 (C)		
1'		130.23 (C)		
2', 6'	8.08-8.06	128.76 (CH)	130.23, 155.38, 128.58, 131.10	1', 2, 3', 6', 4'
3', 5'	7.60-7.59	128.58 (CH)	128.76, 131.10	2', 6', 4'
4'	7.60-7.59	131.10 (CH)	128.76, 128.58	2', 6', 3', 5'
1''				
2''	4.28	71.68 ( $\text{CH}_2$ )	140.04, 166.65	3, 3''
3''		166.65 (C)		
4''	7.65		40.87, 166.65, 50.79	(6'', 12'', 13''), 3'', 5''
5''		50.79 (C)		
6'', 12'', 13''	1.91	40.87 ( $\text{CH}_2$ )	35.90, 50.79	(8'', 10'', 14''), 5''
7'', 9'', 11''	1.99	28.76 (CH)	35.90, 40.87, 50.79	(8'', 10'', 14''), (6'', 12'', 13''), 5''
8'', 10'', 14''	1.60	35.90 ( $\text{CH}_2$ )	28.76, 40.87, 35.90	(7'', 9'', 11''), (6'' 12'', 13''), (8'', 10'', 14'')

<sup>a</sup> HSQC correlated carbons where protons are present, multiplicity determined by DEPT indicated in parentheses.

The position of the ether link between the flavone and amantadine moieties was confirmed with HMBC correlations (spectrum 6). Correlations were observed between H-2''  $\delta_{\text{H}}$  4.28 (the protons of the linker) and C-3 of the flavone moiety ( $\delta_{\text{C}}$  140.04) as well as the amide

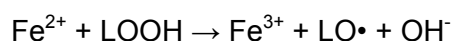
carbonyl, C-3" ( $\delta_C$  166.65). These correlations thus indicated that the ether link connecting the amantadine and flavone moieties was attached to C-3 of the flavone C ring and the amantadine amide. The correlations observed between the NH (H-4",  $\delta_H$  7.65) and carbons 6", 12" and 13" ( $\delta_C$  40.87), as well as the correlations observed between the proton signal at  $\delta_H$  1.91 (H-6", 12" and 13") and C-5" (the quaternary carbon of the amantadine moiety,  $\delta_C$  50.79) were useful in the assignment of the CH<sub>2</sub> peaks of the amantadine moiety. The structure elucidation of compounds **2,3,4,5** and **6** were done in a similar manner.

## 4.5 Lipid Peroxidation

### 4.5.1 Introduction

Oxidative stress has been implicated to play a crucial role in the pathogenesis of a number of diseases, including neurodegenerative disorders, cancer and ischemia (Butterfield, 2002). Oxygen radicals can cause severe damage to cellular structures and functions, which can lead to cell death (Linden *et al.*, 2008). One of the consequences of oxidative stress is the peroxidation of lipids that are easily oxidised by reactive oxygen species. Lipids are particularly vulnerable to oxidation and the brain is rich in polyunsaturated fatty acids. Polyunsaturated fatty acids are essential for normal neural cell membrane function because many membrane properties, such as fluidity and permeability, are closely related to the presence of unsaturated and polyunsaturated side chains. During lipid peroxidation various reactive electrophilic aldehydes are generated with malondialdehyde (MDA) as the most abundant species (Esterbauer & Cheeseman, 1990).

This phenomenon occurs through ongoing free radical chain reactions until termination occurs (Reed, 2011) as illustrated in figure 4.2. The "X" in the figure represents the hydroxyl radical. Free radicals attack an allylic carbon to form a carbon-centered radical (step 1). This radical reacts with O<sub>2</sub> to produce peroxy radicals (step 2). These peroxy radicals can react with adjacent lipids, forming lipid hydroperoxide and, through the Fenton reaction (equation 4.1), lipid alkoxyl radicals (LO•), which are all reactive oxygen species, thus repeating the cycle (step 3). Decomposing lipid hydroperoxide produces multiple lipid peroxidation products such as acrolein and its derivative, MDA.



**Equation 4.1**

Lipid peroxidation can be terminated by two radicals reacting to form a nonradical and oxygen (step 4). Vitamin E ( $\alpha$ -tocopherol) acts as a "chain-breaking" antioxidant and can terminate propagation steps of lipid peroxidation.

When the hydrogen is abstracted in step 1,  $\alpha$ -tocopherol radicals forms (step 5) that can be reverted back to vitamin E by the potent antioxidants vitamin C (ascorbic acid) and glutathione (step 6). Cadenas *et al.* (1983) hypothesized this mechanism using HNE as the reactive aldehyde upon observation of the cellular effects of HNE and vitamin E pretreatment of rat hepatocytes.

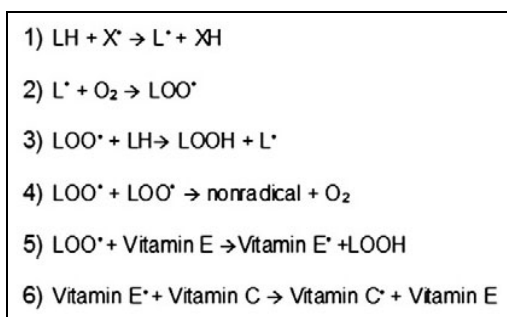


**Figure 4.2:** The Mechanism of the typical free radical chain reaction.

#### 4.5.2 Assay Procedure

Determination of MDA by thiobarbituric acid (TBA) is one of the most common assays used to assess lipid peroxidation. TBA reacts with the aldehyde products of lipid peroxidation at high temperatures in a 2:1 ratio, to produce a pink-coloured complex which is spectrophotometrically measured at a wavelength of 532 nm (Ottino & Duncan, 1997) illustrated in figure 4.3.

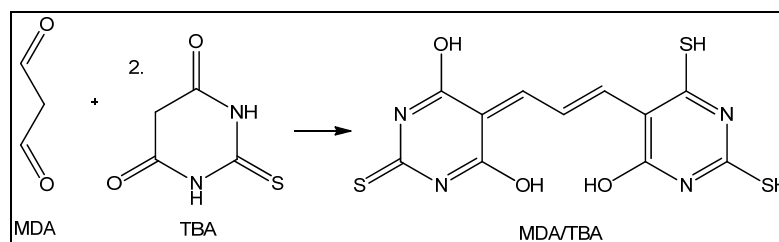


**Figure 4.3:** The reaction of Malondialdehyde with Thiobarbituric acid to yield a pink TBA2-MDA Complex.

All aldehydes produced during lipid peroxidation are thiobarbituric acid-reactive substances (TBARS), able to form complexes with TBA and will therefore give unreliable measurements of MDA levels (Esterbauer *et al.*, 1991). TBARS are consequently expressed as malondialdehyde equivalents, and only the amount of free MDA equivalents will be measured in this assay (Draper & Hadley, 1990). The assay was adapted from Ottino & Duncan (1997) to evaluate the amount of lipid peroxidation taking place by measuring the amount of malondialdehyde equivalents produced after incubation with the toxin.

The assay was performed on whole rat brain homogenate as a model for lipid peroxidation. The homogenate was incubated in a toxin-solution, consisting of hydrogen peroxide, iron(III)chloride and vitamin C. Although vitamin C is an antioxidant *in vivo*, it interacts with metal ions *in vitro* to produce hydroxyl and lipid alkoxyl radicals (Carr & Frei, 1999). This combination of chemicals induces the Fenton reaction, leading to the production of destructive hydroxyl radicals, which is responsible for initiation of the lipid peroxidation reactions.

A range of test compounds with and without hydroxyl substitution was therefore assessed for inhibition of MDA production and consequently lipid peroxidation. Flavones were included as reference antioxidants. Trolox<sup>®</sup>, a water-soluble derivative of vitamin E and well known antioxidant was used as a positive control.

### **4.5.3 Materials and Methods**

#### **4.5.3.1 Chemicals and Reagents**

1,1,3,3-Tetramethoxypropane (TMP), thiobarbituric acid (TBA), trichloroacetic acid (TCA) and (±)-6-hydroxy-2,5,7,8-tetramethylchroman-2-carboxylic acid (Trolox<sup>®</sup>) were purchased from Sigma Aldrich Chemical Corporation, Steinheim, while iron(III)chloride hexahydrate (FeCl<sub>3</sub>.6H<sub>2</sub>O), methanol, ethanol and 8-hydroxyquinoline were purchased from Merck, Darmstadt, Germany. 2,6-Di-tert-butyl-4-methylphenol (BHT), chrysin, 6-hydroxyflavone and 7 hydroxyflavone were purchased from Sigma Aldrich, St. Louis. Potassium chloride (KCl), di-sodium hydrogen orthophosphate anhydrous (Na<sub>2</sub>HPO<sub>4</sub>), potassium Dihydrogen orthophosphate (KH<sub>2</sub>PO<sub>4</sub>), hydrochloric acid, butanol, dimethyl sulphoxide (DMSO) and ascorbic acid were purchased from Saarchem (PTY) Ltd., Wadeville. Sodium chloride (NaCl) was purchased from BHD, Midrand and hydrogen peroxide (H<sub>2</sub>O<sub>2</sub>) from Alpha Pharmaceuticals, Durban, South Africa. Double distilled water was used throughout this experiment.

The phosphate buffer solution (PBS) constituted of 137 mM NaCl, 2.7 mM KCl, 10 mM Na<sub>2</sub>HPO<sub>4</sub> and 2 mM KH<sub>2</sub>PO<sub>4</sub>, dissolved in 1 L double distilled water and the pH adjusted to 7.4. The BHT (0.5 g/L) was dissolved in methanol; TCA (10 %) and TBA (0.33 %) were prepared in double distilled water. TBA is light sensitive and was always prepared fresh and protected from light by covering the container in aluminium foil. Hydrogen peroxide (5 mM H<sub>2</sub>O<sub>2</sub>) was used, as the toxin, to generate OH• and initiate lipid peroxidation in the rat brain homogenates (Sewerynek *et al.*, 1995). Ascorbic acid (1.4 mM) and FeCl<sub>3</sub> (4.88 mM) were added to increase the generation of OH• according to the Fenton reaction (Equation 7.1) in

section 1.4.1. (Cui *et al.*, 2004). The final concentration of the negative control was 10 % ethanol. The final concentration of the positive control was 1 mM Trolox® in DMSO.

The test compounds were dissolved in DMSO to achieve final concentrations of 0.4 mM, 0.2 mM and 0.1 mM in DMSO.

#### 4.5.3.2 Animals

Ethics approval was obtained by the North-West University Ethics Committee for the use of rats in this assay with ethic number 05D05. Rat brain homogenate was prepared from adult Sprague Dawley rats weighing 200 to 250 g. The rats were bred and maintained in a controlled environment in the North-West University Laboratory Animal Centre. Rats were decapitated and the brains removed by a trained laboratory animal professional.

#### 4.5.3.3 Instrumentation

A labsystem Original Multiscan RC plate-reader and Genesis software was used to determine absorbances in this experiment at 530 nm.

#### 4.5.3.4 Malondialdehyde Calibration Curve

The MDA standard is provided as 1,1,3,3-tetramethoxypropane (TMP) because MDA is not stable. The TMP is hydrolysed during the acid incubation step at 60 °C . A standard solution of 50 nmol/L TMP in double distilled water was used in the calibration curve as a standard, and diluted with PBS to achieve TMP concentrations ranging between 0 and 25 nmol/L with 5 nmol/L intervals.

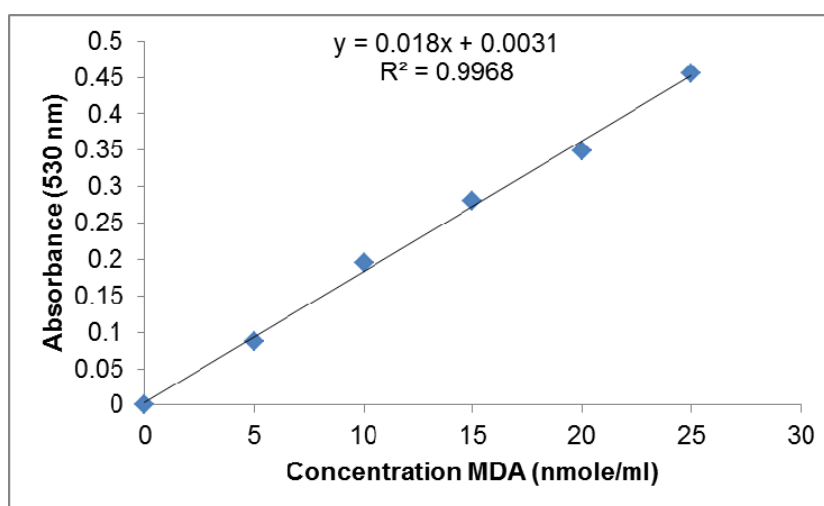


**Figure 4.4:** MDA calibration curve indicating the MDA/TBA-complex formed.



Before incubation at 60 °C, TCA and TBA solutions were added. After cooling on ice, a butanol extraction was completed by centrifuging at 2000 x g for 5 minutes. From the top butanol layer, 200 µl was transferred into a 96-well plate and the absorbance measured at a wavelength of 530 nm. Butanol was used as a blank to establish the effect of the well plate and butanol on absorption values. A calibration curve was generated by plotting the absorbance of the TBA/MDA-complex against the concentration MDA (figure 4.4).

#### **4.5.3.5 Preparation of Whole Rat Brain Homogenate**

Two whole rat brains were homogenised to yield a medium rich in lipids. Decapitation was performed by a trained laboratory animal professional with a guillotine and the skull opened without injuring the brain. The homogenate was prepared with a manual glass-Teflon homogeniser to yield a 10 % PBS (v/w) concentration and kept on ice at all times.

#### **4.5.3.6 Method**

The assay was performed to determine the possible antioxidant activity of the synthesised compounds. Each Eppendorf tube contained 0.160 µl rat brain homogenate, 10 µl H<sub>2</sub>O<sub>2</sub>, 5 µl FeCl<sub>3</sub>, 5 µl ascorbic acid and varying concentrations of synthesised compound (0.4 mM, 0.2 mM and 0.1 mM drug concentrations in DMSO solutions). These were incubated in an oscillating water bath for 60 minutes at 37 °C, in order to induce lipid peroxidation. After incubation the content was centrifuged at 2000 x g for 20 min, this was done to remove all insoluble protein. The supernatant was removed from each tube and the termination of the incubation period was followed by the addition of 100 µl BHT, 200 µl TCA and 100 µl TBA to this fraction. Amplification of lipid peroxidation during the assay was prevented by adding the chain-breaking antioxidant BHT to the sample, TCA to start the acid-heating hydrolysis and TBA to bind to the formed MDA and form the pink chromogen. The tubes were sealed and the mixture heated to 60 °C in a water bath for 60 min, to release the protein-bound MDA through hydrolysis. Following the incubation, the samples were cooled on ice until it reached room temperature and the TBA-MDA complexes were extracted with 2ml butanol and centrifuged at 2000 x g for 10 minutes. The absorbance was read at 530 nm.

The absorbance values noted were converted to the amount malondialdehyde equivalents produced, using the MDA calibration curve (figure 3). The extent of lipid peroxidation was assessed by calculating nanomoles MDA produced per 1 milligram tissue.

#### **4.5.3.7 Statistical Analysis**

The *in vitro* experiment was repeated 5 times on 2 rat brains. Hydrogen peroxide was included as the toxin in every assay and used as a point of reference. Graphpad Prism was

used to statistically analyse data in the Unpaired Student-Newman Keuls t-test and to determine the standard error of the means (S.E.M.). Results were expressed as the mean value  $\pm$  S.E.M. of the 10 runs. Significant differences were obtained when  $p < 0.05$ .

#### 4.5.4 Results

In this experiment good antioxidant activity is indicated by a lower absorbance value of MDA, indicating lipid peroxidation inhibition. The ability of the studied compounds to inhibit toxin induced lipid peroxidation is presented in table 4.2, figure 4.5.

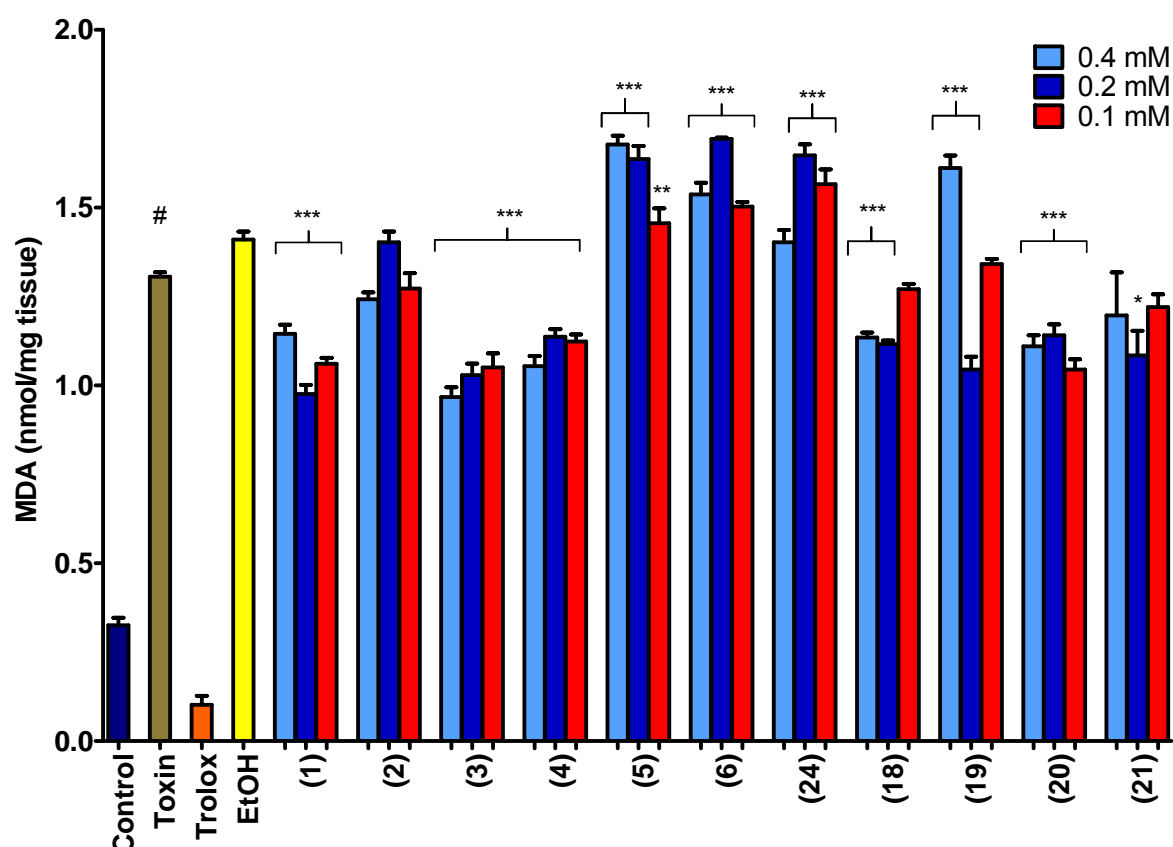


**Figure 4.5:** The attenuation of lipid peroxidation by different concentrations of the synthesised compounds in whole rat brain homogenates *in vitro*. Each bar represents the mean  $\pm$  S.E.M.;  $n = 10$ . \*\*\* $p < 0.0001$  vs toxin (#).

**Table 4.2:** Lipid Peroxidation of Rat Brain Homogenate in the presence of Flavonoids.

Test Compounds	Concentration (mM)	Lipid Peroxidation (nmol MDA/mg tissue)	± S.E.M.
Control		0.325	0.048
Toxin		1.316	0.028
Trolox®		0.102	0.057
EtOH		1.41	0.049
Compound 1	0.4	1.145	0.058
	0.2	0.975	0.059
	0.1	1.061	0.037
Compound 2	0.4	1.242	0.044
	0.2	1.402	0.068
	0.1	1.272	0.097
Compound 3	0.4	0.967	0.063
	0.2	1.03	0.071
	0.1	1.051	0.088
Compound 4	0.4	1.055	0.063
	0.2	1.137	0.047
	0.1	1.123	0.044
Compound 5	0.4	1.677	0.055
	0.2	1.636	0.082
	0.1	1.456	0.093
Compound 6	0.4	1.537	0.073
	0.2	1.693	0.009
	0.1	1.502	0.03
Amantadine (24)	0.4	1.402	0.078
	0.2	1.647	0.069
	0.1	1.566	0.094
3-hydroxyflavone (18)	0.4	1.134	0.031
	0.2	1.116	0.022
	0.1	1.27	0.033
7-hydroxyflavone (19)	0.4	1.611	0.078
	0.2	1.045	0.081
	0.1	1.341	0.031
Chrysin (20)	0.4	1.11	0.068
	0.2	1.141	0.069
	0.1	1.045	0.064
6-hydroxyflavone (21)	0.4	1.196	0.270
	0.2	1.084	0.155
	0.1	1.219	0.081

#### 4.5.5 Discussion

The toxin showed an increase in MDA equivalent production of more than double that found in the control ( $p < 0.0001$ ). This indicates that the combination of hydrogen peroxide, iron(III)chloride and vitamin C was effective in inducing lipid peroxidation. The toxin was used in all sample-containing groups to induce lipid peroxidation in the presence of the test compounds, displaying the ability of the compounds to act as chain-breaking antioxidants by scavenging hydroxyl radicals. Not all the test compounds showed significant attenuation of toxin-induced lipid peroxidation inhibition. It is noted however that the solvent DMSO also showed lipid peroxidation inhibition and this was therefore taken into account by adding DMSO to the control and toxin.

The synthesised compounds (**1** - **4**) containing a flavone structure showed better activity when compared to the compounds containing a chalcone structure (**5** - **6**). The chalcone structures further seem to act as pro-oxidants. Compound **3** and **4** showed concentration dependent inhibition of toxin-induced lipid peroxidation. None of the synthesised compounds could be compared to the results obtained from the positive control Trolox<sup>®</sup>.

Compound **1**, **3** and **4** showed equal inhibition to 3-hydroxyflavone (**18**), chrysin (**20**) and 6-hydroxyflavone (**21**). Compound **2** displayed no increase in inhibition when compared to 7-hydroxyflavone (**19**).

### 4.6 Superoxide Anion Scavenging Activity

#### 4.6.1 Introduction

Aerobic organisms utilise oxygen for respiration and energy productions. Oxygen taken into living cells is changed into several harmful reactive oxygen species and free radicals. Once formed, free radicals can start a chain reaction leading to formation of more free radicals. Superoxide anion radical ( $O_2^-$ ) is one of the strongest reactive oxygen species among the free radicals generated (Al-Mamun *et al.*, 2007).  $O_2^-$  is changed into other harmful reactive oxygen species and free radicals such as hydrogen peroxide and hydroxyl radicals.

#### 4.6.2 Assay Procedure

The nitro-blue tetrazolium (NBT) assay of Ottino & Duncan (1997), determines the presence of superoxide anions and other free radicals. In this method, radical production is induced in whole rat brain homogenate by potassium cyanide (KCN). Cyanide causes cell death by inhibiting the mitochondrial electron transport chain at complex IV, thereby preventing the conversion of superoxide to hydrogen peroxide and producing surplus superoxide anions in the mitochondria (Ottino & Duncan, 1997). This blockade of complex IV causes inhibition of

oxidative phosphorylation and ATP production, causing the cell to die due to a lack of ATP. Cyanide is therefore ideal for the generation of superoxide anion in this assay. The radicals produced by cyanide are able to reduce yellow NBT to purple, water insoluble nitro-blue diformazan (NBD), which has an absorption maximum at 560 nm (figure 4.6). It is therefore possible to detect the amount of radicals present in the reaction, by quantifying the amount of NBD produced. The capacity of antioxidants to scavenge radicals is determined by the amount of NBD produced in the presence of cyanide and antioxidant. The ability of the test compounds to scavenge cyanide-induced free radicals can thus also be determined using this colorimetric assay.

Flavones were included as reference antioxidants. Trolox<sup>®</sup>, a water-soluble derivative of vitamin E and well known antioxidant was used as a positive control.

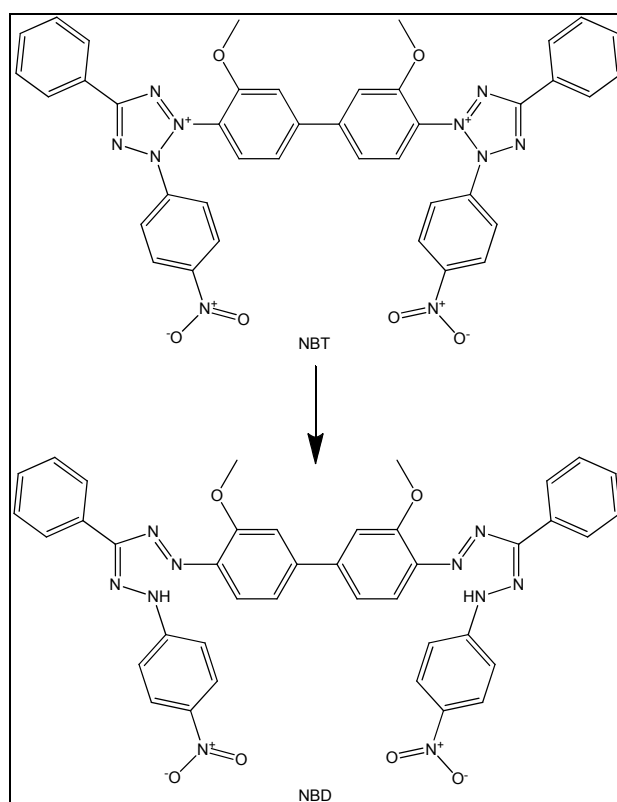


**Figure 4.6:** Reduction of NBT to NBD.

The capacity of antioxidants to scavenge radicals is determined by the amount of NBD produced in the presence of cyanide and antioxidant. The ability of the test compounds to scavenge cyanide-induced free radicals could thus be determined. This colorimetric assay quantified scavenging ability according to the intensity of the purple colour generated by free radicals.

### **4.6.3 Materials and Methods**

#### **4.6.3.1 Chemicals and Reagents**

Potassium cyanide (KCN), glacial acetic acid (GAA), potassium chloride (KCl), di-sodium hydrogen orthophosphate anhydrous ( $\text{Na}_2\text{HPO}_4$ ), potassium dihydrogen orthophosphate ( $\text{KH}_2\text{PO}_4$ ) and dimethyl sulphoxide (DMSO) were purchased from Saarchem (PTY) Ltd., Wadeville. Bovine serum albumin (BSA), ( $\pm$ )-6-hydroxy-2,5,7,8-tetramethylchroman-2-carboxylic acid (Trolox<sup>®</sup>), nitro-blue diformazan (NBD) and nitro-blue tetrazolium (NBT) were purchased from Sigma Aldrich Chemical Corporation, Steinheim. Chrysin, 3-hydroxyflavone, 6-hydroxyflavone and 7-hydroxyflavone were purchased from Sigma Aldrich, St. Louis. Sodium chloride (NaCl) was purchased from BHD, Midrand. Double distilled water was used throughout this experiment. Ethanol was purchased from Merck, Darmstadt, Germany.

The phosphate buffer solution (PBS) constituted of 137 mM NaCl, 2.7 mM KCl, 10 mM  $\text{Na}_2\text{HPO}_4$  and 2 mM  $\text{KH}_2\text{PO}_4$ , dissolved in 1 L double distilled water and the pH adjusted to 7.4. The potassium cyanide solution consisted of 5.6 mM in double distilled water. NBT solution of 20 ml consisted of 0.02 g NBT, 0.4 ml Ethanol in 19.6 ml double distilled water. The NBD solution consisted of 0.0075 g NBD in 25 ml glacial acetic acid (GAA), both NBT and NBD were always prepared fresh and protected from light by covering the container in aluminium foil. The final concentration of the positive control was 1 mM Trolox<sup>®</sup> in DMSO, the same solvent as the drugs.

The test compounds were dissolved in DMSO to achieve final concentrations of 0.4 mM, 0.2 mM and 0.1 mM in DMSO.

#### **4.6.3.2 Animals**

As described in 4.5.3.2

#### **4.6.3.3 Instrumentation**

A lab system Original Multiscan RC plate-reader and Genesis software was used to determine absorbances in this experiment at 560 nm.

#### **4.6.3.4 Preparation of standards**

##### **BSA standard**

The NBT assay is dependent on the amount of protein in the specific rat brain used in the assay, therefore the Bradford protein assay was performed on every rat brain. A bovine serum albumin standard was prepared with phosphate buffer solution in concentrations of 0, 0.1, 0.4, 0.7, 1.0 and 1.4 mg/ml, of which 5  $\mu\text{l}$  was placed in a 96-well plate in triplicate. After

adding 250  $\mu$ l Bradford Reagent, the well plate was shaken by the plate-reader's mixing function for 30 seconds at room temperature to ensure even mixing. A lag time of 15 minutes ensued, after which the absorbance was measured at 560 nm. This generated a standard curve (figure 4.7) of known concentration protein as a function of absorbance intensity at 560 nm.

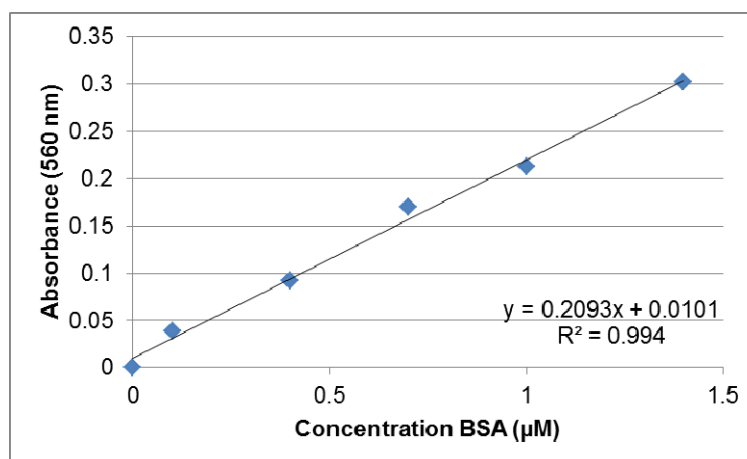


**Figure 4.7:** Bovine Serum Albumin calibration curve.

#### Nitro-Blue Diformazan Calibration Curve

In the NBT assay, reduction of tetrazolium to diformazan is measured as a colorimetric indicator of the superoxide anions present. A NBD calibration curve (figure 4.8) was generated to assist in the calibration of the amount of diformazan produced in the NBT assay. Concentrations of NBD between 0 and 400  $\mu$ M, with 100  $\mu$ M intervals, were prepared in glacial acetic acid to the volume of 255  $\mu$ l and the absorbance measured at 560 nm.

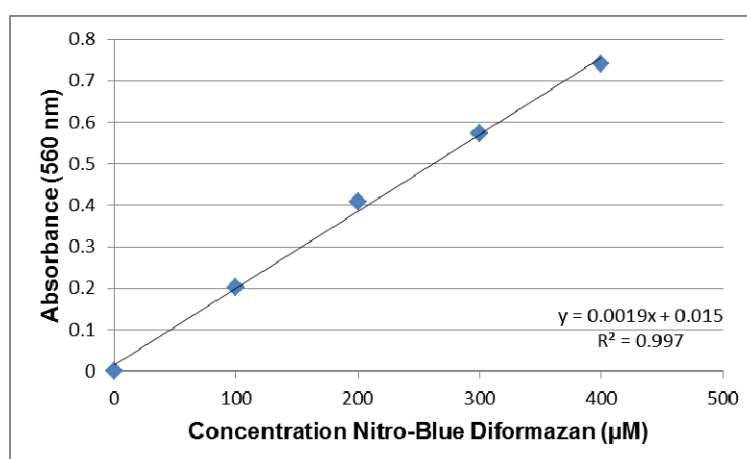


**Figure 4.8:** Nitro-blue Diformazan calibration curve.

#### **4.6.3.5 Preparation of Whole Rat Brain Homogenate**

Two whole rat brains were obtained from rats decapitated by a trained laboratory animal professional with a guillotine and the skull opened without injuring the brain. The homogenate was prepared with a manual glass-Teflon homogeniser to yield a 10 % PBS (v/w) concentration and kept on ice at all times.

#### **4.6.3.6 Method**

The assay was performed to determine the amount of diformazan produced from tetrazolium, thereby establishing the amount of superoxide anions scavenged in the presence of the test compounds when compared to the calibration curve.

Whole rat brain homogenate, 100  $\mu$ l, was incubated at 37 °C in an oscillating water bath with 50  $\mu$ l KCN and 50  $\mu$ l test compounds after adding 80  $\mu$ l of 0.1 % (w/v) NBT solution. The produced free radicals were able to reduce NBT to a water insoluble, purple NBD, which was extracted from the homogenate pellet after centrifugation, by glacial acetic acid. The top 255  $\mu$ l of the glacial acetic acid layer was removed into a 96-well plate and the absorbance measured at 560 nm, using GAA as a blank. The absorbance values were converted to micromoles diformazan, by interpolating into the NBD calibration curve and were expressed as micromoles diformazan per milligram protein, by also employing the Bradford Protein Assay to establish the amount of protein present in each run.

The assay measured the concentration tetrazolium reduced to diformazan as a result of superoxide anion production by cyanide in the presence of the test compounds, using the NBD calibration curve (figure 7), while the concentration diformazan produced per milligram protein was determined by interpolating into the BSA calibration curve (figure 6). The final data was expressed as micromoles NBD per milligram protein. Blank homogenate was tested as control in order to estimate the effect of natural enzymes present in the homogenate on scavenging activity.

#### **4.6.3.7 Statistical Analysis**

The *in vitro* experiment was repeated 5 times on 2 rat brains. A toxin group was included in every assay and used as a point of reference. Graphpad Prism was used to statistically analyse data in the unpaired Student-Newman Keuls t-test and to determine the standard error of the means (S.E.M.). Results were expressed as the mean value  $\pm$  S.E.M. of the 10 runs. Significant differences are obtained when  $p < 0.05$ .



#### 4.6.4 Results

In the NBT assay, potassium cyanide increased the NBD absorbance value of the blank homogenate, while the studied drugs reduced the increased absorbance according to their ability to scavenge cyanide-induced superoxide anions (table 4.3 and figure 4.9).

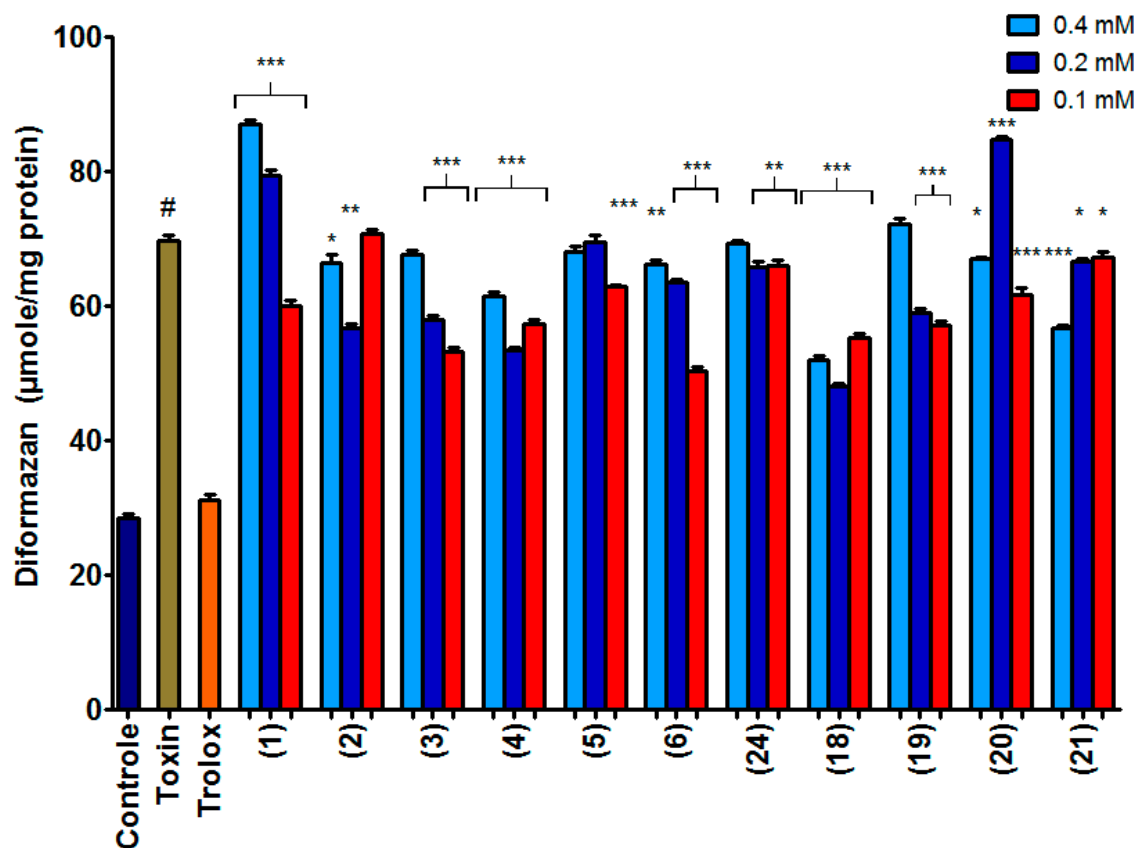


**Figure 4.9:** The superoxide scavenging properties of the synthesised compounds in the presence of KCN in rat brain homogenate. Each bar represents the mean  $\pm$  S.E.M.; n = 10. \*\*\*p < 0.0001 vs toxin (#).

**Table 4.3:** Scavenging of KCN-induced superoxide anion in the presence of Flavonoids.

Test Compounds	Concentration (mM)	Diformazan ( $\mu\text{M}/\text{mg}$ protein)	$\pm$ S.E.M.
Control		28.63	$\pm 1.33$
Toxin	5.6	69.88	$\pm 1.59$
Trolox <sup>®</sup>	1	31.16	$\pm 1.88$
Compound 1	0.4	87.03	$\pm 1.59$
	0.2	79.39	$\pm 1.87$
	0.1	60.03	$\pm 1.74$
Compound 2	0.4	66.57	$\pm 2.67$
	0.2	56.83	$\pm 1.31$
	0.1	70.74	$\pm 1.39$
Compound 3	0.4	67.62	$\pm 1.45$
	0.2	58.06	$\pm 1.28$
	0.1	53.2	$\pm 1.63$
Compound 4	0.4	61.5	$\pm 1.58$
	0.2	53.56	$\pm 0.99$
	0.1	57.31	$\pm 1.74$
Compound 5	0.4	68.22	$\pm 1.54$
	0.2	69.66	$\pm 2.27$
	0.1	63.05	$\pm 0.51$
Compound 6	0.4	66.19	$\pm 1.4$
	0.2	63.62	$\pm 0.85$
	0.1	50.47	$\pm 1.31$
Amantadine (24)	0.4	69.33	$\pm 1.2$
	0.2	65.95	$\pm 1.84$
	0.1	66.03	$\pm 1.96$
3-hydroxyflavone (18)	0.4	52.03	$\pm 1.3$
	0.2	48.04	$\pm 0.89$
	0.1	55.31	$\pm 1.47$
7-hydroxyflavone (19)	0.4	72.23	$\pm 1.88$
	0.2	59.1	$\pm 1.5$
	0.1	57.16	$\pm 1.58$
Chrysin (20)	0.4	67.2	$\pm 0.14$
	0.2	84.85	$\pm 0.94$
	0.1	61.77	$\pm 2.12$
6-hydroxyflavone (21)	0.4	56.69	$\pm 1.33$
	0.2	66.78	$\pm 0.47$
	0.1	67.27	$\pm 1.83$

#### 4.6.5 Discussion

The blockade of complex IV by cyanide causes inhibition of oxidative phosphorylation and ATP production, causing the cell to die due to a lack of ATP. The induction of superoxide

anion production by potassium cyanide is evident when the tetrazolium reduction ability of KCN group is compared to that of the control ( $p < 0.0001$ ). The addition of the test compounds was consequently responsible for respective reductions in superoxide and diformazan production.

All the compounds showed weak inhibition of cyanide-induced superoxide production. None of the compounds could be compared to the results obtained from Trolox<sup>®</sup>. Compound **1**, **3** and **6** showed a concentration dependent decrease in activity, which may be attributed to toxicity of this system at higher concentrations. Compound **1** and **2** had slightly weaker inhibition compared to 3-hydroxyflavone (**18**) and 7-hydroxyflavone (**19**) respectively, while compound **3** and **4** showed better inhibition when compared to chrysin (**20**) and 6-hydroxyflavone (**21**). All the compounds showed better inhibition than amantadine (**24**). At a concentration of 0.1 mM compound **6** had the lowest value, inhibiting cyanide-induced superoxide production the best. Only 6-hydroxyflavone (**21**) showed a concentration dependent increase in activity.

The reason for the decrease in activity with higher concentrations of the other compounds is not clear. It is proposed that higher concentrations of the test compounds may in some way have had a toxic effect on cells, thereby increasing superoxide production, or that solubility was decreased, causing interference. This assay indicates that lower concentrations of the test compounds in the brain will be effective in scavenging radicals and decrease the risk of developing radical-induced neurodegeneration. The effects/toxicity of these compounds at higher concentrations however needs to be investigated further.

## **4.7 IC<sub>50</sub> determination for the inhibition of human MAO**

### **4.7.1 Introduction**

The primary function of MAO is that it catalyses the oxidative deamination of both endogenous and exogenous sources influencing the concentration of dietary amines, monoamine neurotransmitters and hormones. The reaction degrades monoamines into their corresponding aldehydes, which are then oxidised into acids by aldehyde dehydrogenase or converted into alcohols or glycols by aldehyde reductase. By inhibiting MAO the basal dopamine levels in the brain is increased.

### **4.7.2 Assay procedure**

This method is based on the fact that certain MAO-B substrates are oxidised to fluorescent products. The substrate used in this study was kynuramine which is oxidised to 4-hydroxyquinoline (figure 4.10).

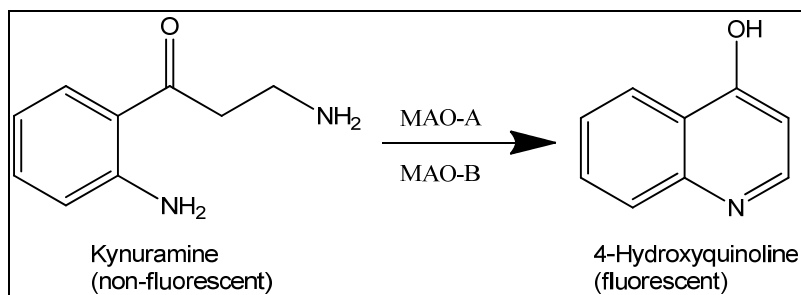


**Figure 4.10:** The oxidation of kynuramine by MAO-A and –B.

The generation of this product can subsequently be measured with a fluorescence spectrophotometer (Zhou *et al.*, 1996). This fluorometric method is frequently used to determine the activities of recombinant human MAO-A and MAO-B. It has the advantage that it is more sensitive than the spectrophotometric method (Matsumoto *et al.*, 1985) and is therefore more suitable to measure activities of recombinant human MAO-A and MAO-B (Strydom *et al.*, 2010). Inhibitor potencies are expressed as an  $IC_{50}$  value for each inhibitor.

### 4.7.3 Materials and Methods

#### 4.7.3.1 Chemicals and Reagents

Potassium dihydrogen orthophosphate ( $KH_2PO_4$ ), potassium chloride (KCl) and dimethyl sulphoxide (DMSO) were purchased from Saarchem (PTY) Ltd., Wadeville. Recombinant human MAO-A and MAO-B were obtained from Sigma Aldrich, St. Louis.

The potassium phosphate buffer consisted of 100 mM  $KH_2PO_4$ , the pH was adjusted to 7.4 and it was made isotonic with KCl. Recombinant human MAO-A (5 mg/ml) and MAO-B (5 mg/ml) was pre-aliquoted and stored at  $-70\text{ }^{\circ}\text{C}$ . Before use MAO-A and –B was diluted to 0.075 mg/ml in the potassium phosphate buffer.

The test compounds were dissolved in DMSO to give various concentrations between 0 – 100  $\mu\text{M}$ .

#### 4.7.3.2 Instrumentation

A Varian Cary Eclipse fluorescence spectrophotometer was used to determine the fluorescence at an excitation wavelength of 310 nm and an emission wavelength of 400 nm.

#### 4.7.3.3 Materials and Method

All reactions were prepared in potassium phosphate buffer containing various concentrations of the test inhibitor (0 – 100  $\mu\text{M}$ ), kynuramine (substrate) and the respective MAO enzyme. Kynuramine added to the incubations resulted in final concentrations of 45  $\mu\text{M}$  for MAO-A

and 30  $\mu\text{M}$  for MAO-B. The final volumes of the incubations were 1900  $\mu\text{l}$ . Stock solutions of the test inhibitors were prepared to give a 4 % (v/v) DMSO in the final incubations. The final concentrations of MAO-A and -B in each incubation were 0.0075 mg/ml.

The enzyme reaction was incubated at 37 °C for 20 minutes, then terminated with the addition of 400  $\mu\text{l}$  NaOH (2 N) and 1000  $\mu\text{l}$  distilled water. After centrifugation at 16,000 g for 10 minutes, the fluorescence of the MAO generated 4-hydroxyquinoline in the supernatant fractions were measured at an excitation wavelength of 310 nm and an emission wavelength of 400 nm. To determine the concentrations of 4-hydroxyquinoline, a linear calibration curve was constructed from solutions of 4-hydroxyquinoline (0.047-1.50  $\mu\text{M}$ ) in a mixture of DMSO (5 %) and potassium phosphate buffer (950  $\mu\text{l}$ ). The calibration standards were prepared to a volume of 1900  $\mu\text{l}$  and contained 400  $\mu\text{l}$  NaOH (2 N) and 1000  $\mu\text{l}$  distilled water.

The initial rate of MAO catalysis was plotted against the logarithm of the inhibitor concentrations to obtain a sigmoidal dose-response curve. Each curve was constructed from 6 different inhibitor concentrations spanning a least 3 orders of magnitude. This data was fitted to the one site competition model incorporated into GraphPad Prism software and the  $\text{IC}_{50}$  values determined in triplicate and are expressed as mean  $\pm$  standard deviation (SD).

#### **4.7.4 Results**

All the  $\text{IC}_{50}$  values obtained from the various MAO enzymes are listed in table 4.4 and are expressed in  $\mu\text{M}$ . Synthesised compounds exhibiting very weak inhibition are expressed in percentage inhibition at 100  $\mu\text{M}$ . The most potent value (lowest  $\text{IC}_{50}$ ) for each enzyme is highlighted in grey with Selegiline (Desideri *et al.*, 2011) as standard reference.

The  $\text{IC}_{50}$  value is obtained as explained earlier by calculating the concentration of the inhibitor which results in a reduction of 50 % of the rate obtained in the absence of inhibitor.

**Table 4.4:** IC<sub>50</sub> values for the inhibition of human MAO-A and MAO-B by test compounds.

Compounds	MAO-A IC <sub>50</sub> (μM)	MAO-B IC <sub>50</sub> (μM)
Selegiline	67.25 ± 1.02	0.019 ± 0.86
Compound (1)	84.157 ± 2.127	No inhibition
Compound (2)	143.833 ± 44.775	48.10 % inhibition at 100 μM
Compound (3)	28.683 ± 1.176	61.15 % inhibition at 100 μM
Compound (4)	50.027 ± 3.218	31.79 % inhibition at 100 μM
Compound (5)	24.987 ± 5.988	0.717 ± 0.009
Compound (6)	39.410 ± 6.809	13.657 ± 0.365

A typical graph for the measurement of IC<sub>50</sub> values is shown in figure 4.11. The catalytic rate of the enzyme is plotted against the logarithm of the inhibitor concentration. This graph is for N-(adamantan-1-yl)-4-[(1E)-3-oxo-3-phenylpro-1-en-1-yl]benzamide (5) which was the most potent inhibitor for human B with an IC<sub>50</sub> of 0.717 ± 0.009 μM.

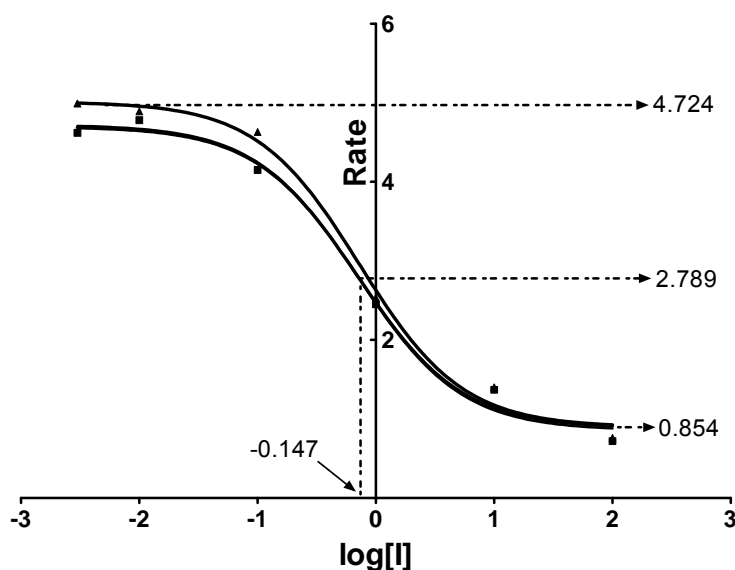


**Figure 4.11:** The IC<sub>50</sub> calculation of N-(adamantan-1-yl)-4-[(1E)-3-oxo-3-phenylpro-1-en-1-yl]benzamide (5) towards human MAO-B: Log [I] = -0.147, which is equal to [I] = 0.717 μM. The rate is expressed as nmol product formed/min.mg protein.

#### 4.7.5 Reversibility study

For safety considerations, reversibility is an important requirement for MAO inhibitors. Compound **5** was selected as the representative inhibitor in the reversibility study with recombinant human MAO-B. In this study the inhibitor was pre-incubated with the enzyme for various periods of time and the rate of substrate oxidation subsequently measured. The rate of substrate oxidation versus the range of pre-incubation times was plotted on a bar graph.

A constant oxidation rate for all the incubation times is an indication of inhibitor reversibility. In contrast, an irreversible inhibitor will exhibit a time-dependent decrease in the rate of enzyme catalysis.

##### 4.7.5.1 Method

Recombinant human MAO-B was prepared as described in section 4.7.3.1 and it was incubated with compound **5** for periods of 0, 15, 30 and 60 minutes at 37 °C. MAO-B was used in concentrations of 0.0326 mg/ml. The incubations were prepared in potassium phosphate buffer. The final concentration of 30 µM kynuramine for MAO-B was incubated for 15 minutes at 37 °C with the pre-incubated enzyme complex. After the incubation period the reactions were stopped with 400 µl of NaOH (2 N) and 1000 µl distilled water. The final volume of the incubations was 1900 µl. The incubations were then centrifuged for 10 minutes at 16 000 g.

The concentration of 4-hydroxyquinoline in each incubation was determined fluorometrically by measuring the fluorescence of the supernatant at an excitation wavelength of 310 nm and an emission wavelength of 400 nm. The PMT voltage was set to medium with an excitation slit of 5 nm and an emission slit of 10 nm. A calibration curve was prepared for each data set as described in the inhibition studies.

##### 4.7.5.2 Results

Reversible inhibition of recombinant human MAO-B by compound **5** was observed. The graph showed no decline in the rate of kynuramine oxidation as a function of incubation time (figure 4.12). Inhibition of recombinant human MAO-B by compound **5** was therefore reversible.

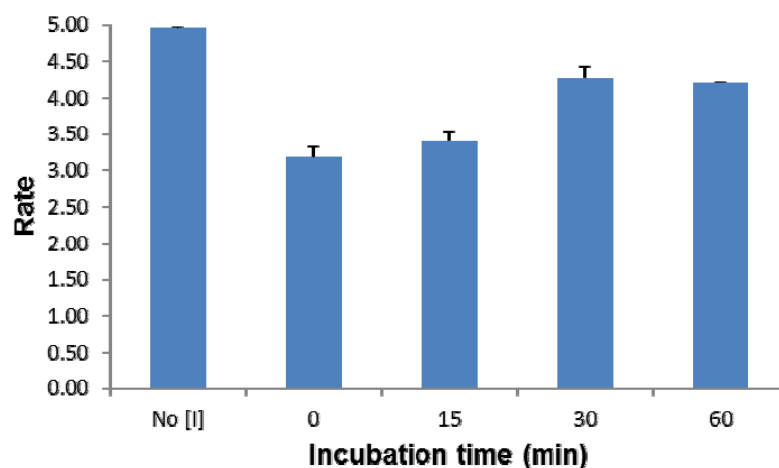


**Figure 4.12:** Rate of kynuramine oxidation by recombinant human MAO-B for each of the pre-incubation periods (0 – 60 minutes). The rate (V) is expressed as nmol product formed/min/mg protein.

#### 4.7.6 $K_i$ determination

In this study the inhibitor activities are expressed as  $IC_{50}$  values. The purpose of this study was to determine whether compound **5** exhibited a competitive mode of inhibition by constructing Lineweaver-Burk plots. As discussed earlier, an intersecting set of Lineweaver-Burk plots are an indication of competitive inhibition.

##### 4.7.6.1 Method

Recombinant human MAO-B was prepared as described in section 4.7.3.1.

All reactions were prepared in potassium phosphate buffer with kynuramine concentrations of 15, 30, 60 and 90  $\mu$ M, recombinant human MAO-B enzyme and compound **5** as inhibitor. The final concentration for MAO-B was 0.0075 mg/ml, while the inhibitor concentrations were 0, 0.179, 0.358 and 0.717  $\mu$ M. Stock solutions of the test inhibitor were prepared in DMSO. The reactions were incubated for 20 minutes at 37 °C and terminated with 400  $\mu$ l NaOH (2 N). 1000  $\mu$ l Distilled water was added to each incubation before it was centrifuged for 10 minutes at 16 000 g.

A calibration curve was prepared by measuring the fluorescence of increasing concentrations of 4-hydroxyquinoline (0.047-1.50  $\mu$ M) in a mixture of DMSO (5 %) and potassium phosphate buffer. To each calibration standard a volume of 400  $\mu$ l NaOH (2 N) and 1000  $\mu$ l distilled water was added. The values obtained for the calibration curve displayed a linear curve.



Lineweaver-Burk plots were constructed from the data sets and the slopes were replotted against the inhibitor concentration. Using this graph the  $K_i$  value could be obtained from the x intercept.

The concentration of 4-hydroxyquinoline in each incubation was determined fluorometrically by measuring the fluorescence of the supernatant at an excitation wavelength of 310 nm and an emission wavelength of 400 nm. The PMT voltage was set to medium with an excitation and emission slit with of 5 nm each.

#### 4.7.6.2 Results

The Lineweaver-Burk plots for inhibition of recombinant human MAO-B by compound **5** indicates that inhibition is competitive (figure 4.13).

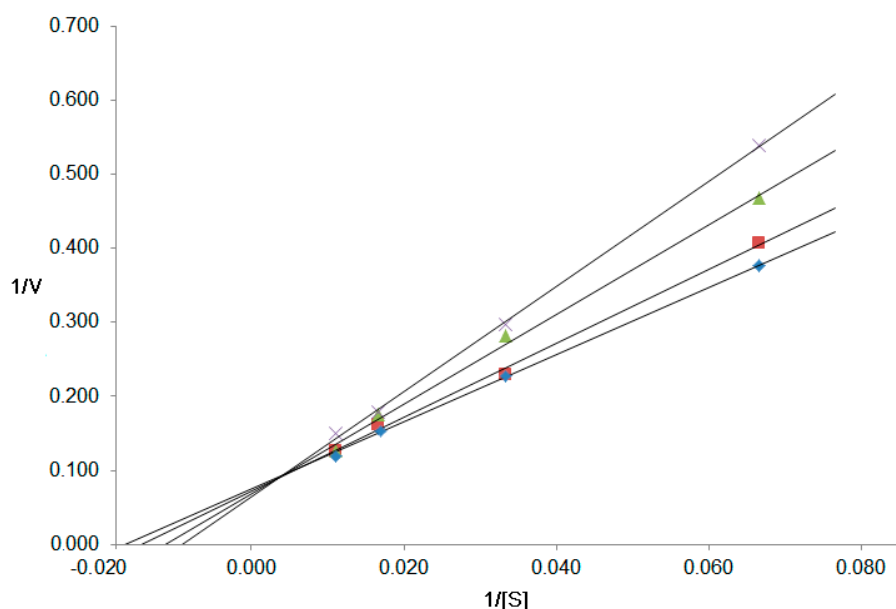


**Figure 4.13:** Lineweaver-Burke plots of the oxidation of kynuramine by recombinant human MAO-B in the absence (diamond) and presence of various concentrations of compound **5** (square, 0.179  $\mu$ M; triangle, 0.358  $\mu$ M and cross, 0.717  $\mu$ M). The rate (V) is expressed as nmol product formed/min/mg protein.

The  $K_i$  value for the inhibition of recombinant human MAO-B by compound **5** was calculated with the following equation:

$$K_i = IC_{50} / (1 + [S]/K_m) \quad \text{Equation 3.6}$$

The substrate concentration used for MAO-B was 30  $\mu$ M with a  $K_m$  value of 22.66  $\mu$ M. The calculated  $K_i$  value for compound **5** is 0.308  $\mu$ M.

#### 4.7.7 Discussion

The synthesised compounds (**1** - **4**) containing a flavone structure displayed almost no MAO-B inhibitory activity. Their inhibition of MAO-A was slightly better than that of MAO-B. Compounds containing a chalcone structure (**5** – **6**) were found to inhibit both MAO-A and MAO-B with more selectivity towards MAO-B. It can be concluded that compound **5** is a competitive, reversible inhibitor of MAO-B. The proposed reason for the increased activity of the chalcone over that of the flavones may be due to extended length of the chalcone structure. The flavone structures may be too large to fit into MAO-B's active site.

### 4.8 Molecular modelling

#### 4.8.1 Introduction

Molecular docking is the method that predicts the orientation of one molecule when bound to another to form a stable complex. Molecular docking is used in developing new drugs, examining the interaction between the drug and the active site of an enzyme and to enhance drugs already in use. Due to the increased availability of high resolution structural data on proteins and enzymes, docking studies have become an integral part of drug discovery (Knegtel *et al.*, 1997). Sildenafil was used as control compound for MAO-B.

#### 4.8.2 Experimental

The molecular docking studies were carried out in Windows based Discovery Studios 3.1. The inhibitor was drawn in DS Visualizer Pro and prepared for docking with the 'Prepare Ligand' protocol within Discovery Studios. MAO-B (2V5Z.pdb) enzyme model was obtained from Brookhaven Protein Data Bank, co-crystallised with sildenafil. After the enzyme was prepared with the 'Clean Protein' function, it was typed with the CHARMM forcefield. A series of three minimisations were carried out on the enzyme while the backbone was kept fixed. The first minimisation was the steepest decent minimisation followed by the conjugate gradient and adopted basis NR minimisations. During the minimisations the implicit distance-dependant dielectrics solvent model was used with the dielectric constant set to 4. Existing ligands were erased from the enzyme and the backbone constraints removed. The binding site was identified within enzyme before the ligand was docked using the 'Ligand fit' protocol. *In situ* ligand minimisation was used on the docked ligand with the 'Smart Minimizer' algorithm. Ten possible docking poses were calculated for each inhibitor.

### 4.8.3 Results and discussion

Using the above described protocol, only compound **5** could be docked. The remaining compounds did not fit into MAO-B's active site cavity. This correlated with the experimental results in section 4.7.4, effectively explaining the remaining compounds having weak to no MAO-B inhibition.

Compound **5** traversed both the entrance and binding site cavities. It was shown that compound **5** bind to MAO-B with the chalcone moiety oriented towards the FAD co-factor while the amantadine moiety protrudes into the entrance cavity. This is a similar orientation to that of safinamide, a potent MAO-B inhibitor. The Ile199 residue which acts as a gate was in an open conformation. Pi bonding occurred between the chalcone moiety and Tyr435.

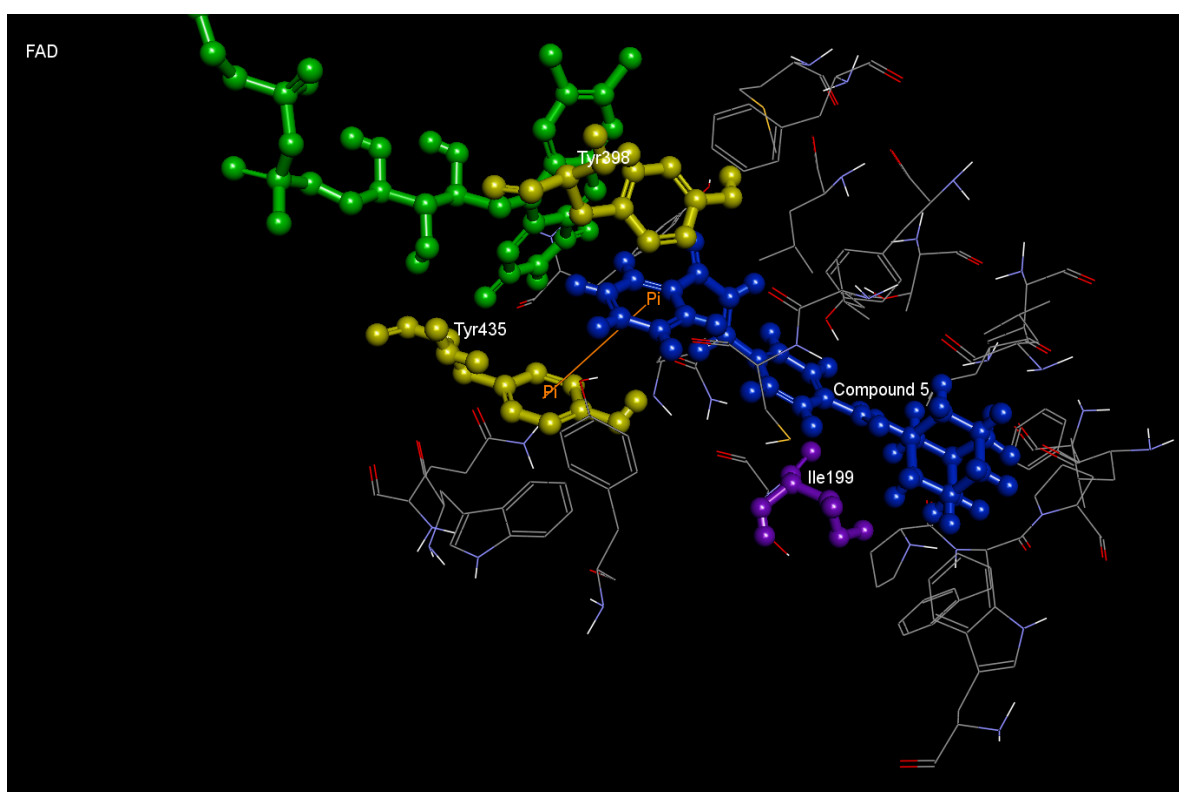


**Figure 4.14:** Representation of compound **5** docked within MAO-B. The FAD co-factor is displayed in green, the inhibitor in blue, the pi bond in orange, Ile199 in purple, Tyr435 and Tyr398 in yellow.

## Chapter 5. Discussion and Conclusion

Reactive oxygen species are a group of oxygen-derived molecules generated as by-products of biological oxidation of normal metabolism. These radicals are responsible for a chain of oxidation reactions, causing oxidation of lipids, proteins and DNA (Butterfield & Stadtman, 1997). These consequences of oxidative damage construct the molecular basis of a wide range of disorders including neurodegenerative disorder and are best avoided. The body's endogenous antioxidant system is unable to effectively counteract the free radical increase with aging. This ultimately leads to the progressive decline in cellular and tissue function thus causing neurodegeneration. It is therefore important to curb the destruction caused by the increased oxygen radicals before the damage to the brain becomes evident, thereby removing the contributing factor in neurodegeneration.

A series of compounds was proposed based on the antioxidant and MAO inhibitory activity of flavonoids (Nakamura *et al.*, 2003; Siddaiah *et al.*, 2006, Chimenti *et al.*, 2010) and synthesised. The amantadine moiety was included because it is known to inhibit calcium flux through the NMDA receptor channel (Parsons *et al.*, 1999). The flavones were selected as lead compound because of their antioxidant ability. These antioxidants contain hydrogen-donating groups reducing the free radical oxidising effect, thus quenching the ability of the radical to oxidise biological matter.

In this study six amantadine-flavonoid conjugates were synthesised and characterised by NMR, MS and IR. The compounds were evaluated for antioxidant activity, using lipid peroxidation (TBARS) and superoxide anion (NBT) assays, and for inhibition of recombinant human MAO-A and -B using a kynuramine oxidation assay.

The results obtained in the superoxide anion nitro-blue tetrazolium (NBT) assay (figure 4.9 in section 4.6.9) indicated the ability of the test compounds to scavenge superoxide anions and showed the order of decreasing scavenging ability to be: compound **6**, **3**, **4**, **2**, **1**, **5**. None of the compounds performed better than Trolox<sup>®</sup>. As expected, the test compounds containing free hydroxyl group showed the best superoxide scavenging ability. Higher concentrations of the test compounds may in some way have had a toxic effect on the cells, or poor solubility may have influenced the assay. Compound **1** and **2** had slightly weaker inhibition than 3-hydroxyflavone (**18**) and 7-hydroxyflavone (**19**) respectively, while compound **3** and **4** showed better inhibitions than chrysin (**20**) and 6-hydroxyflavone (**21**). All the compounds showed better inhibition than amantadine (**24**). The synthesised compound **6** had the best scavenging ability indicating that the one hydroxyl group contributed to better activity.

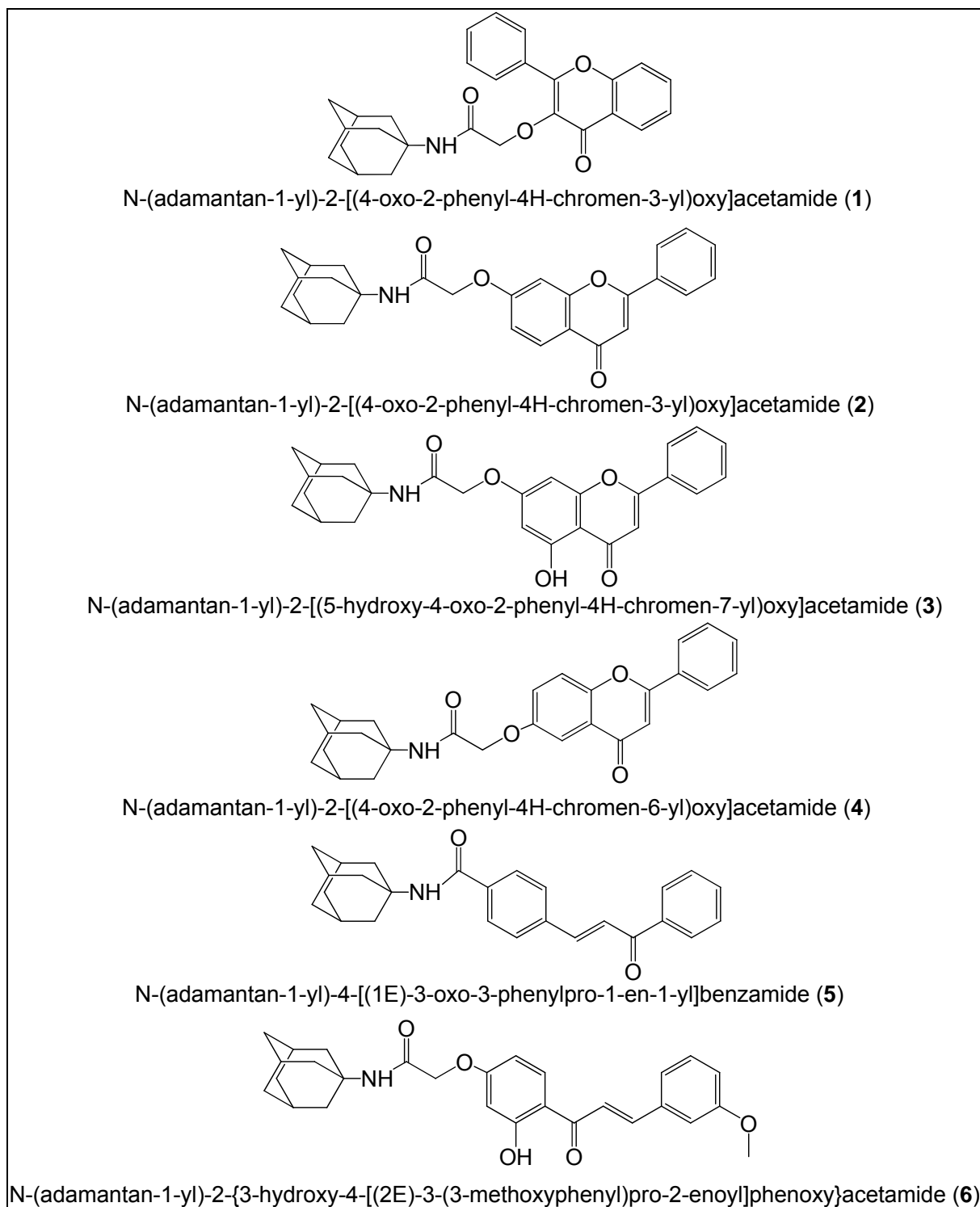


**Figure 5.1:** Test compounds (1 - 6) used in this study.

Lipid peroxidation is a consequence of the amount of superoxide anions produced further up the cascade of oxidative events leading to hydroxyl radical production. Even through the tested compounds may not show the best superoxide scavenging ability, they might still act as antioxidants by scavenging the hydroxyl radicals in the lipid peroxidation assay. The results (figure 4.5 in section 4.5.9) obtained for the synthesised compounds in decreasing

order of activity are: **3>4>1>2>5>6**. In general the compounds containing a flavone structure displayed better results when compared to structures containing the chalcone structure. Compound **1** and **3** showed equal but weak inhibition when compared to 3-hydroxyflavone (**18**) and chrysin (**20**) respectively. Compound **2** and compound **4** had better lipid peroxidation inhibition than 6-hydroxyflavone (**21**), its free flavonoid analogue. Compound **3**, containing an aromatic 5-hydroxyl group, showed the best lipid peroxidation inhibition. None of the test compounds showed activity comparable to Trolox<sup>®</sup>.

The results (table 4.4 in section 4.7.4) obtained for the synthesised compounds in decreasing order of MAO-B activity are: **5>6>4>2>3>1**. The synthesised compounds' MAO-A activity in decreasing order are: **5>3>6>4>1>2**. Compound **5** ( $IC_{50} = 0.717 \mu M$  and  $24.987 \mu M$ ) and **6** ( $IC_{50} = 13.657 \mu M$  and  $39.41 \mu M$ ) containing a chalcone structure inhibited both MAO-A and -B. Compound **5** was further characterised as enzyme inhibitor and found to be reversible ( $K_i = 0.24 \mu M$ ) and competitive in its inhibition of recombinant human MAO-B. The rest of the compounds showed very weak to no MAO-B inhibition. Compound **1 – 4** showed slight MAO-A inhibition.

The docking studies provided insight into the binding of compound **5** within the active site of MAO-B. It was confirmed that compound **5** traverse both cavities of MAO-B. The chalcone moiety is oriented towards the FAD co-factor in the substrate cavity while the amantadine moiety extended into the entrance cavity. This mode of binding is thought to be necessary for the selective inhibition of MAO-B (Hubálek *et al.*, 2005).

From the results obtained, it can be concluded that compound **5** could be an ideal candidate for further research into the neuroprotective effects as a multifunctional drug containing both antioxidant and MAO-B inhibitory activity.

## References

- ABDUL, H.M. & BUTTERFIELD, D.A. 2007. Involvement of PI3K/PKG/ERK1/2 signalling pathways in cortical neurons to trigger protection by cotreatment of acetyl-L-carnitine and  $\alpha$ -lipoic acid against HNE-mediated oxidative stress and neurotoxicity: implications for Alzheimer's disease. *Free Radical Biology and Medicine*, 42:371-384.
- ABELES, R.H. & MAYCOCK, A.L. 1976. Suicide enzyme inactivators. *Accounts of Chemical Research*, 9:313-319.
- ADAMS, J.J.D., KLAIDMAN, L.K. & LEUNG, A.C. 1993. MPP+ and MPDP+ induced oxygen radical formation with mitochondrial enzymes. *Free Radical Biology and Medicine*, 15:181-186.
- AL GHOLEH, I., KHOO, N.K.H., KNAUS, U.G., GRIENDLING, K.K., TOUYZ, R.M., THANNICKAL, V.J., BARCHOWSKY, A., NAUSEEF, W.M., KELLEY, E.E., BAUER, P.M., DARLEY-USMAR, V., SHIVA, S., CIFUENTES-PAGANO, E., FREEMAN, B.A., GLADWIN, M.T. & PAGANO, P.J. 2011. Oxidases and peroxidases in cardiovascular and lung disease: New concepts in reactive oxygen species signaling. *Free Radical Biology and Medicine*, 51:1271-1288.
- AL-MAMUN, M., YAKAMI, K., MASUMIZU, T., NAKAI, Y., SAITO, K., SANO, H. & TAMURA, Y. 2007. Superoxide anion radical scavenging activities of herbs and pastures in northern japan determined using electron spin resonance spectrometry. *International Journal of Biological Sciences*, 3:349-355.
- ALCARAZ, M.J., VICENTE, A.M., ARAICO, A., DOMINIGUEZ, J.N., TERCENCIO, M.C. & FERRANDIZ, M.L. 2004. Role of nuclear factor-kB and heme oxygenase-1 in the mechanism of action of anti-inflammatory chalcone derivate in RAW 264.7 cells. *British Journal of Pharmacology*, 142:1191-1199.
- AMES, B.N. 2006. Low micronutrients intake may accelerate the degenerative diseases of aging through allocation of scarce micronutrients by triage. *Proceedings of the National Academy of Sciences USA*, 103:17598-17594.
- AMMAR, R.B., BHOURI, W., SGHAIER, M.B., BOUBAKER, J., SKANDRANI, I., NEFFATI, A., BOUHLEL, I., KILANI, S., MARIOTTE, A., CHEKIR-GHEDIRA, L., DIJOUX-FRANCA, M. & GHEDIRA, K. 2009. Antioxidant and free radical-scavenging properties of three flavonoids isolated from the leaves of *Rhamnus alaternus* L. (Rhamnaceae): A structure-activity relationship study. *Food Chemistry*, 116:258-264.

- AMREIN, R., MARTIN, J.R. & CAMERON, A.M. 1999. Moclobemide in patients with dementia and depression. *Advances in Neurology*, 509-519.
- ANDERSEN, J.K. 2004. Oxidative stress in neurodegeneration: Cause or consequence? *Nature Reviews Neuroscience*, S18-S25.
- ANTRI, A.E., MESSOURI, I., TLEMCANI, R.C., BOUKTAIB, M., ALAMI, R.E., BALI, B.E. & LACHKER, M. 2004. Flavone glycosides from *Calycotome Villosa* Subsp. *Intermedia*. *Molecules*, 9:568-573.
- AZZI, A., DAVIES, K.J.A. & KELLY, F. 2001. Free radical biology-terminology and critical thinking. *FEBS Letters*, 558:3-6.
- BACH, A.W.J., LAN, N.C., JOHNSON, D.L., ABELL, C.W., BEMKENEK, M.E., KWAN, S.-W., SEEBURG, P.H. & SHIH, J.C. 1988. cDNA cloning of human liver monoamine oxidase A and B: molecular basis of differences in enzymatic properties. *Proceedings of the National Academy of Sciences U.S.A.*, 85:4934-4938.
- BECKMAN, J.S. 1996. Oxidative damage and tyrosine nitration from peroxynitrite. *Chemical Research in Toxicology*, 9:836-844.
- BENEDETTI, A., COMPORTI, M. & ESTERBAUER, H. 1980. Identification of 4-hydroxynonenal as a cytotoxic product originating from the peroxidation of liver microsomal lipids. *Biochimica et Biophysica Acta*, 620:281-296.
- BENZIE, I.F.F., CHUNG, W.Y. & STRAIN, J.J. 1999. "Antioxidant" (reducing) efficiency of ascorbate in plasma is not affected by concentration. *The Journal of Nutritional Biochemistry*, 10:146-150.
- BERLETT, B.S. & STADTMAN, E.R. 1997. Protein oxidation in aging, disease, and oxidative stress. *The Journal of Biological Chemistry*, 272:20313-20316.
- BERMAN, S.B. & HASTINGS, T.G. 1997. Inhibition of glutamate transport in synaptosomes by dopamine oxidation and reactive oxygen species. *Journal of Neurochemistry*, 69:1185-1195.
- BERMAN, S.B. & HASTINGS, T.G. 1999. Dopamine oxidation alters mitochondrial respiration and induces permeability transition in brain mitochondria: implications for Parkinson's disease. *Journal of Neurochemistry*, 73:1127-1137.



- BERNHEIMER, H., BIRKMAYER, W., HORNYKIEWICZ, O., JELLINGER, K. & SEITELBERGER, F. 1973. Brain dopamine and the syndromes of Parkinson and Huntington. Clinical, morphological and neurochemical correlations. *Journal of the Neurological Sciences*, 20:415-455.
- BINDA, C., NEWTON-VINSON, P., HUBALE, F., EDMONDSON, D.E. & MATTEVI, A. 2002. Structure of human monoamine oxidase B, a drug target for the treatment of neurological disorders. *Nature Structural Biology*, 9:22-26.
- BIRKMAYER, W., RIEDERER, P., AMBROZI, L. & YODIM, M.B.H. 1977. Implications of combined treatment with 'Madopar' and L-deprenil in Parkinson's disease. A long-term study. *Lancet*, 1:439-443.
- BIRKMAYER, W., RIEDERER, P., YODIM, M.B.H. & LINAUER, W. 1975. The potentiation of the antiakinetic effect after L-Dopa treatment by an inhibitor of MAO-B, deprenyl. *Journal of Neural Transmission*, 36:303-326.
- BLENNOW, K., DE LEON, M.J. & ZETTERBERG, H. 2006. Alzheimer's disease. *Lancet*, 368:387-403.
- BORTOLATO, M., CHEN, K. & SHIH, J.C. 2008. Monoamine oxidase inactivation: From pathophysiology to therapeutics. *Advanced Drug Delivery Reviews*, 60:1527-1533.
- BOVERIS, A. & CHANCE, B. 1973. The mitochondrial generation of hydrogen peroxide. General properties and effect of hyperbaric oxygen. *Biochemical Journal*, 134:707-716.
- BOYD-KIMBALL, D., MOHAMMAD ABDUL, H., REED, T., SULTANA, R. & BUTTERFIELD, D.A. 2004. Role of phenylalanine 20 in Alzheimer's amyloid beta-peptide (1-42)-induced oxidative stress and neurotoxicity. *Chemical Research in Toxicology*, 17:1743-1749.
- BOYD-KIMBALL, D., SULTANA, R., POON, H.F., LYNN, B.C., CASAMENTI, F., PEPEU, G., KLEIN, J.B. & BUTTERFIELD, D.A. 2005. Proteomic identification of proteins specifically oxidized by intracerebral injection of amyloid beta-peptide (1-42) into rat brain: implications for Alzheimer's disease. *Neuroscience*, 132:313-324.
- BROWN, F.J., BERNSTEIN, P.R., CRONK, L.A., DOSSET, D.L., HEBBEL, K.C., MADUSKUIE, T.P., SHAPIRO, H.S., VACEK, E.P., YEE, Y.K., WILLARD, A.K., KRELL, R.D. & SNYDER, D.W. 1989. Hydroxyacetophenone-derived antagonists of the peptidoleukotrienes. *Journal of Medicinal Chemistry*, 32:807-811.

- BUETTNER, G.R. 1993. The pecking order of free radicals and antioxidants lipid peroxidation alpha-tocopherol and ascorbate. *Archives of Biochemistry and Biophysics*, 300:535-543.
- BUMEY, S., NILES, J.C., DEDON, P.C. & TANNENBAUM, S.R. 1999. DNA damage in deoxynucleosides and oligonucleotides treated with peroxynitrite. *Chemical Research in Toxicology*, 12:513-520.
- BURNS, D.C., ELLIS, D.A. & MARCH, R.E. 2007. A predictive tool for assessing <sup>13</sup>C NMR chemical shifts of flavonoids. *Magnetic Resonance in Chemistry*, 45:835-845.
- BUTTERFIELD, D.A. & BOYD-KIMBALL, D. 2005. The critical role of methionine 35 in Alzheimer's amyloid beta-peptide (1-42)-induced oxidative stress and neurotoxicity. *Biochimica et Biophysica Acta*, 1703:149-156.
- BUTTERFIELD, D.A. & KANSKI, J. 2001. Brain protein oxidation in age-related neurodegenerative disorders that are associated with aggregated proteins. *Mechanisms of Ageing and Development*, 122:945-962.
- BUTTERFIELD, D.A. & STADTMAN, E.R. 1997. Protein oxidation processes in aging brain. *Advances in Cell Aging and Gerontology*, 1:161-191.
- BUTTERFIELD, D.A. 1997. B-Amyloid-associated free radical oxidative stress and neurotoxicity: implications for Alzheimer's disease. *Chemical Research in Toxicology*, 10:495-506.
- BUTTERFIELD, D.A., CASTEGNA, A., LAUDERBACK, C.M. & DRAKE, J. 2002. Evidence that amyloid beta-peptide-induced lipid peroxidation and its sequelae in Alzheimer's disease brain contribute to neuronal death. *Neurobiology of Aging*, 23:655-664.
- BUTTERFIELD, D.A., DRAKE, J., POCERNICH, C. & CASTEGNA, A. 2001. A Evidence of oxidative damage in Alzheimer's disease brain: central role for amyloid beta-peptide. *Trends in Molecular Medicine*, 7:548-554.
- BUTTERFIELD, D.A., GALVAN, V., LANGE, M.B., TANG, H., SOWELL, R.A., SPILMAN, P., FOMBONNE, J., GOROSTIZA, O., ZHANG, J., SULTANA, R. & BREDESEN, D.E. 2010. In vivo oxidative stress in brain of Alzheimer's disease transgenic mice: requirement for methionine 35 in amyloid beta-peptide of APP. *Free Radical Biology and Medicine*, 48:136-144.

- BUTTERFIELD, D.A., REED, T., NEWMAN, S.F. & SULTANA, R. 2007. Roles of amyloid  $\beta$ -peptide-associated oxidative stress and brain protein modifications in the pathogenesis of Alzheimer's disease and mild cognitive impairment. *Free Radical Biology and Medicine*, 43:658-677.
- CADENAS, E. 1989. Biochemistry of oxygen toxicity. *Annual Review of Biochemistry*, 51:79-110.
- CADENAS, E., MULLER, A., BRIGELIUS, R., ESTERBAUER, H. & SIES, H. 1983. Effects of 4-hydroxynonenal on isolated hepatocytes: studies on chemiluminescence response, alkane production and glutathione status. *Biochemical Journal*, 214:479-487.
- CARR, A. & FREI, B. 1999. Does vitamin C act as a pro-oxidant under physiological conditions? *Journal of the Federation of American Societies for Experimental Biology*, 13:1007-1024.
- CASTEGNA, A., THONGBOONKERD, V., KLEIN, J.B., LYNN, B., MARKESBERY, W.R. & BUTTERFIELD, D.A. 2003. Proteomic identification of nitrated proteins in Alzheimer's disease brain. *Journal of Neurochemistry*, 85:1394-1401.
- CATALÁ, A. 2006. An overview of lipid peroxidation with emphasis in outer segments of photoreceptors and the chemiluminescence assay. *The International Journal of Biochemistry & Cell Biology*, 38:1482-1495.
- CATALÁ, A. 2009. Lipid peroxidation of membrane phospholipids generates hydroxyalkenals and oxidized phospholipids active in physiological and/or pathological conditions. *Chemistry and Physics of Lipids*, 157:1-11.
- CATALÁ, A. 2010. A synopsis of the process of lipid peroxidation since the discovery of the essential fatty acids. *Biochemical and Biophysical Research Communications*, 399:318-323.
- CHANCE, B., SIES, H. & BOVERIS, A. 1979. Hydroperoxide metabolism in mammalian organs. *Physiological Reviews*, 59:527-605.
- CHENG, Y. & PRUSOFF, W. 1973. Relationship between the inhibition constant ( $K_i$ ) and the concentration of inhibitor which causes 50 per cent inhibition ( $I_{50}$ ) of an enzymatic reaction. *Biochemical Pharmacology*, 22:3099-3108.

- CHIMENTI, F., FIORAVANTI, R., BOLASCO, A., CHIMENTI, P., SECCI, D., ROSSI, F., YANEZ, M., ORALLO, F., ORTUSO, F., ALCARO, S., CIRILLI, R., FERRETTI, R. & SANNA, M.L. 2010. A new series of flavones, thioflavones, and flavonones as selective monoamine oxidases-B inhibitors. *Bioorganic & Medical Chemistry*, 18:1273-1279.
- CHIUEH, C.C., KRISHNA, G., TULSI, P., OBATA, T., LANG, K., HUANG, S.J. & MURPHY, D.L. 1992. Intracranial microdialysis of salicylic acid to detect hydroxyl radical generation through dopamine autooxidation in the caudate nucleus. Effects of MPP+. *Free Radical Biology and Medicine*, 13:581-583.
- CICCHETTI, F., DROUIN-OUELLET, J. & GROSS, R.E. 2009. Environmental toxins and Parkinson's disease: what have we learned from pesticide-induced animal models? *Trends in Pharmacological Sciences*, 30:475-483.
- COMMONER, B., TOWNSEND, J. & PAKE, G.E. 1954. Free radicals in biological materials. *Nature*, 174:689-691.
- COOKE, M.S., EVANS, M.D., DIZDAROGLU, M. & LUNEC, J. 2003. Oxidative DNA damage: mechanisms, mutation, and disease. *FASEB Journal*, 17:1195-1214.
- CORBETTA, M., PATEL, G. & SHULMAN, G.L. 2008. The reorienting system of the human brain: From environment to theory of mind. *Neuron*, 58:306-624.
- CRAWFORD, D.R., SUZUKI, T., SESAY, J. & DAVIES, K.J. 2002. Analysis of gene expression following oxidative stress. *Methods in Molecular Biology*, 196:155-162.
- CROMPTON, M. 1999. The mitochondria permeability transition pore and its role in cell death. *Biochemical Journal*, 341:233-249.
- CUI, K., LUO, X., XU, K. & VEN MURTHY, M.R. 2004. Role of oxidative stress in neurodegeneration: recent developments in assay methods for oxidative stress and nutraceutical antioxidants. *Progress in Neuro-Psychopharmacology & Biological Psychiatry*, 28:771-799.
- DALLE-DONNE, I., SCALONI, A. & BUTTERFIELD, D.A., eds. 2006. Redox proteomics: From protein modifications to cellular dysfunction and diseases. New York : Wiley Press. pp 563-603.

- DALLE-DONNE, I., SCALONI, A., GIUSTARINI, D., CAVARRA, E., TELL, G., LUNGARELLA, G., COLOMBO, R., ROSSI, R. & MILZANI, A. 2005. Proteins as biomarkers of oxidative/nitrosative stress in diseases: the contribution of redox proteomics. *Mass Spectrometry Reviews*, 24:55-99.
- DANIELSON, S.R. & ANDERSEN, J.K. 2008. Oxidative and nitrative protein modifications in Parkinson's disease. *Free Radical Biology and Medicine*, 44:1787-1794.
- DAVIES, K.J. 1995. Oxidative stress: the paradox of aerobic life. *Biochemical Society Symposia*, 61:1-31.
- DESCHNER, E.E., RUPERTO, J., WONG, G. & NEWMARK, H.L. 1991. Quercetin and rutin as inhibitors of azoxymethanol-induced colonic neoplasia. *Carcinogenesis*, 12:1193-1196.
- DESIDERI, N., BOLASCO, A., FIORAVANTI, R., MONACO, L.P., ORALLO, F., YÁÑEZ, M., ORTUSO, F. & ALCARO, S. 2011. Homoisoflavonoids: Natural scaffolds with potent and selective monoamine oxidase-B inhibition properties. *Journal of Medicinal Chemistry*, 54:2155-2164.
- DEXTER, D.T., WELLS, F.R., LEES, A.J., AGID, F., AGID, Y., JENNER, P. & MARSDEN, C.D. 1989. Increased nigral iron content and alterations in other metal ions occurring in brain in Parkinson's disease. *Journal of Neurochemistry*, 52:1930-1936.
- DIMMOCK, J.R., ELIAS, D.W., BEAZELY, M.A. & KANDEPU, N.M. 1999. Bioactivities of chalcones. *Current Medicinal Chemistry*, 6:1125-1149.
- DIMMOCK, J.R., JHA, A., ZELLO, G.A., QUAIL, J.W., OLOO, E.O., NIENABER, K.H., KOWALCZYK, E.S., ALLEN, T.M., SANTOS, C.L., DE CLERCQ, E., BALZARINI, J., MANAVATHU, E.K. & STABLES, J.P. 2002. Cytotoxic *N*-[4-(3-aryl-3-oxo-1-propenyl)phenylcarbonyl]-3,5-bis(phenylmethylene)-4-piperidones and related compounds. *European Journal of Medicinal Chemistry*, 37:961-972.
- DIXON, R.A. & PAIVA, N.L. 1995. Stress-induced Phenylpropanoid metabolism. *Plant Cell*, 7:1085-1097.
- DRAKE, J., LINK, C.D. & BUTTERFIELD, D.A. 2003. Oxidative stress precedes fibrillar deposition of Alzheimer's disease amyloid beta-peptide (1-42) in transgenic *Caenorhabditis elegans* model. *Neurobiology of Aging*, 24:415-420.

- DRAPER, H.H. & HADLEY, M. 1990. Malondialdehyde determination as index of lipid peroxidation. *Methods in Enzymology*, 186:421-431.
- DRECHSEL, D.A. & PATEL, M. 2008. Role of reactive oxygen species in the neurotoxicity of environmental agents implicated in Parkinson's disease. *Free Radical Biology and Medicine*, 44:1873-1886.
- DUYAO, M., AMBROSE, C., MYERS, R., NOVELLETTO, A., PERSICHETTI, F., FRONTALI, M., FOLSTEIN, S., ROSS, C., FRANZ, M., ABBOT, M., et al. 1993. Trinucleotide repeat length instability and age of onset in Huntington's disease. *Nature Genetics*, 4:387-392.
- EDMONDSON, D.E., BINDA, C. & MATTEVI, A. 2007. Structural insights into the mechanism of amine oxidation by monoamine oxidases A and B. *Archives of Biochemistry and Biophysics*, 464:269-276
- ELANGO VAN, V., SEKAR, N. & GOVINDASAMY, S. 1994. Chemopreventive potential of dietary bioflavonoids against 20-methylcholanthrene-induced tumorigenesis. *Cancer Letters*, 87:107-113.
- ESTERBAUER, H. & CHEESEMAN, K.H. 1990. Determination of aldehydic lipid peroxidation products: malonaldehyde and 4-hydroxynonenal. *Methods in Enzymology*, 148:407-421.
- ESTERBAUER, H., SCHAUR, R.J. & ZOLLNER, H. 1991. Chemistry and biochemistry of 4-hydroxynonenal, malonaldehyde and related aldehydes. *Free Radical Biology and Medicine*, 11:81-128.
- FAHN, S. & SULZER, D. 2004. Neurodegeneration and Neuroprotection in Parkinson Disease. *The Journal of the American Society for Experimental NeuroTherapeutics*, 1:139-154.
- FOLEY, P., GERLACH, M., YODIM, M.B.H. & RIEDERER, P. 2000. MAO-B inhibitors: multiple roles in the therapy of neurodegenerative disorders? *Parkinsonism and Related Disorders*, 6:25-47.
- FOWLER, C.J., CALLINGHAM, B.A., MANTLE, T.J. & TIPTON, K.F. 1980. The effect of lipophilic compounds upon the activity of rat liver mitochondrial monoamine oxidase-A and -B. *Biochemical Pharmacology*, 29:1177-1183.
- FRIDOVICH, I. 1995. Superoxide radical and superoxide dismutases. *Annual Review of Biochemistry*, 64:97-112.

- FUKAI, T. 2009. Extracellular SOD and aged blood vessels. *American Journal of Physiology. Heart and Circulatory Physiology*, 297:H10-H12.
- GANTET, P. & MEMELINK, J. 2002. Transcription factors: tools to engineer the production of pharmacologically active plant metabolites. *Trends in Pharmacological Sciences*, 23:563-569.
- GEHA, R.M., REBRIN, I., CHEN, K. & SHIH, J.C. 2001. Substrate and inhibitor specificities for human monoamine oxidase A and B are influenced by a single amino acid. *Journal of Biological Chemistry*, 276:9877-9882.
- GELDENHUYS, W.J., MALAN, S.F., BLOOMQUIST, J.R., MARCHAND, A.P. & VAN DER SCHYF, C.J. 2005. Pharmacology and Structure activity relationships of bioactive polycyclic cage compounds: A Focus on Pentacycloundecane Derivatives. *Medicinal Research Reviews*, 25:21-48.
- GESI, M., SANTINAMI, A., RUFFOLI, R., CONTI, G. & FORNAI, F. 2001. Novel aspects of dopamine oxidative metabolism (cofounding outcomes take place of certainties). *Pharmacology & Toxicology*, 89:217-224.
- GIL, B., SANZ, M.J., TERCENIO, M.C., FERRÁNDIZ, M.L., BUSTOS, G., PAYÁ, M., GUNASEGARAN, R. & ALCARAZ, M.J. 1994. Effects of flavonoids on *Naja naja* and human recombinant synovial phospholipases A2 and inflammatory responses in mice. *Life Sciences*, 54:333-338.
- GIUSEPPE, P., GIUSEPPE, P., VALERIA, P. & FRANCESCA, M.R. 2011. Mitochondrial dysfunction in brain aging: Role of oxidative stress and cardiolipin. *Neurochemistry International*, 58:447-457.
- GLABE, C.C. 2005. Amyloid accumulation and pathogenesis of Alzheimer's disease: significance of monomeric, oligomeric and fibrillar ABeta. *Subcellular Biochemistry*, 38:167-177.
- GOEDERT, M. 2001. Alpha-synuclein and neurodegenerative diseases. *Nature Reviews Neuroscience*, 2:492-501.
- GONZALEZ-POLO, R.A., SOLER, G., RODRIGUEZ MARTIN, A., MORAN, J.M. & FUENTES, J.M. 2004. Protection against MPP<sup>+</sup> neurotoxicity in cerebellar granule cells by antioxidants. *Cell Biology International*, 28:373-380.

- GRAHAM, D.G. 1978. Oxidative pathways for catecholamines in the genesis of neuromelamin and cytotoxic quinones. *Molecular Pharmacology*, 14:633-643.
- GREEN, D.R. & REED, J.C. 1998. Mitochondria and apoptosis. *Science*, 281:1309-1312.
- GREENACRE, S.A. & ISCHIROPOULOS, H. 2001. Tyrosine nitration: localisation, quantification, consequences for protein function and signal transduction. *Free Radical Research*, 34:541-581.
- GRIMSBY, F., CHEN, K., WANG, L.J., LAN, N.C. & SHIH, J.C. 1991. Human monoamine oxidase A and B genes exhibit identical exon-intron organization. *Proceedings of the National Academy of Sciences USA*, 88:3637-3641.
- GUTTERIDGE, J.M. 1995. Lipid peroxidation and antioxidants as biomarkers of tissue damage. *Clinical Chemistry* 41:1819-1828.
- GUTTERIDGE, J.M.C. 1988. Lipid peroxidation: some problems and concepts. (In HALLIWELL, B., ed. *Oxygen Radicals and Tissue Injury*. Kansas : Allen Press. pp 9-19).
- HALLIWELL, B. & CHIRICO, S. 1993. Lipid peroxidation: its mechanism, measurement and significance. *The American Journal of Clinical Nutrition*, 57:715S-724S.
- HALLIWELL, B. & GUTTERIDGE, J.M. 1990. Role of free radicals and catalytic metal ions in human disease: an overview. *Methods in Enzymology*, 186:1-85.
- HALLIWELL, B. & GUTTERIDGE, J.M. 1989. Free radicals, aging and disease. (In HALLIWELL, B. & GUTTERIDGE, J.F., eds. *Free radicals in Biology and Medicine*. 2<sup>nd</sup> ed. Oxford : Clarendon Press. pp 446-493).
- HALLIWELL, B. & GUTTERIDGE, J.M.C. 1984. Oxygen toxicity, oxygen radicals, transition metals and disease. *Biochemical Journal*, 219:1-14.
- HARBORNE, J.B. 1986. Nature, distribution, and function of plant flavonoids. (In CODY, V., MIDDLETON, Jr, E. & HARBORNE, J.B., eds. *Plant flavonoids in biology and medicine: Biochemical, Pharmacological and Structure-activity relationships*. New York : Alan R. Liss, Inc. pp. 15-24).
- HARMAN, D. 1956. Aging: a theory based on free radical and radiation chemistry. *The Journals of Gerontology*, 11:298-300.



- HEFFNER, J.E. & REPINE, J.E. 1989. Pulmonary strategies of antioxidant defense. *American Review of Respiratory Disease*, 140:531-554.
- HEIKKILA, R.E., MANZINO, L., CABBAT, F.S. & DUVOISIN, R.C. 1984. Protection against the dopaminergic neurotoxicity of 1-methyl-4-phenyl-1,2,5,6-tetrahydropyridine by monoamine oxidase inhibitors. *Nature*, 311:467-469.
- HELY, M.A., FUNG, V.S.C. & MORRIS, J.G.L. 2000. Treatment of Parkinson's disease. *Journal of Clinical Neuroscience*, 7:484-494.
- HENCHCLIFFE, C. & BEAL, M.F. 2008. Mitochondrial biology and oxidative stress in Parkinsons disease pathogenesis. *Nature Clinical Practice Neurology*, 4:600-609.
- HERRAIZ, T. & GUILLÉN, H. 2011. Inhibition of the bioactivation of the neurotoxin MPTP by antioxidants, redox agents and monoamine oxidase inhibitors. *Food and Chemical Toxicology*, 49:1773-1781.
- HODARA, R., NORRIS, E.H., GIASSEN, B.I., MISHIZEN-EBERZ, A.J., LYNCH, D.R., LEE, V.M. & ISCHIROPOULOS, H. 2004. Functional consequences of alpha-synuclein tyrosine nitration: diminished binding to lipid vesicles and increased fibril formation. *Journal of Biological Chemistry*, 279:47746-47753.
- HUBÁLEK, F., BINDA, C., KHALIL, A., LI, M., MATTEVI, A., CASTAGNOLI, N. & EDMONDSON, D.E. 2005. Demonstration of Isoleucine 199 as a structural determinant for the selective inhibition of human monoamine oxidase b by specific reversible inhibitors. *Journal of Biological Chemistry*, 280:15761-15766.
- IVERSON, S.L. & ORRENIUS, S. 2004. The cardiolipin-cytochrome c interaction and the mitochondrial regulation of apoptosis. *Archives of Biochemistry and Biophysics*, 423:37-46.
- JENNER, P., DEXTER, D.T., SIAN, J., SCHAPIRA, A.H. & MARSDEN, C.D. 1992. Oxidative stress as a cause of nigral cell death in Parkinson's disease and incidental Lewy body disease. The Royal Kings and Queens Parkinson's disease Research Group. *Annals of Neurology*, 32:S82-S87.
- JOHNSTON, J.P. 1968. Some observations upon a new inhibitor of monoamine oxidase in brain tissue. *Biochemical Pharmacology*, 17:1285-1297.

- KAKKAR, T., BOXENBAUM, H. & MAYERSOHN, M. 1999. Estimation of  $K_i$  in a competitive enzyme-inhibition model: comparisons among three methods of data analysis. *Drug metabolism and disposition*, 27:756-762.
- KALGUTKAR, S.A., CASTAGNOLI, J.N. & TESTA, B. 1995. Selective inhibitors of monoamine oxidase (MAO-A and MAO-B) as probes of its catalytic site and mechanism. *Medicinal Research Reviews*, 15:325-388.
- KALIR, A., SABBAGH, A. & YODIM, M.B.H. 1981. Selected acetylenic suicide and reversible inhibitors of monoamine oxidase types A and B. *British Journal of Pharmacology*, 73:55-64.
- KEARNEY, E.B., SALACH, J.I, WALKER, W.H., SENG, R.L., KENNEY, W., ZESZOTEK, E & SINGER, T.P. 1971. The covalently-bound flavin of hepatic monoamine oxidase: 1. Isolation and sequence of a flavin peptide and evidence for binding at the 8 $\alpha$  position. *Journal of Biochemistry*, 24:321-327.
- KNEGTEL, R.M.A., KUNTZ, I.D. & OSHIRO, C.M. 1997. Molecular docking to ensembles of protein structures. *Journal of Molecular Biology*, 266:424-440.
- KNOLL, J. & MAGYAR, K. 1972. Some puzzling pharmacological effects of monoamine oxidase inhibitors. *Advances in Biochemical Psychopharmacology*, 5:393-408.
- KOPIN, I.J. 1985. Catecholamine metabolism, Basic aspects and clinical significance. *Pharmacological Review*, 37:338-364.
- KUHN, D.M., ARTHUR, Jr, R.E., THOMAS, D.M. & ELFERINK, L.A. 1999. Tyrosine hydroxylase is inactivated by catechol-quinones and converted to redox-cycling quinoprotein: possible relevance to Parkinson's disease. *Journal of Neurochemistry*. 73:1309-1317.
- KUMAR, M.J., NICHOLLS, D.G. & ANDERSEN, J.K. 2003. Oxidative (alpha)-ketoglutarate dehydrogenase inhibition via subtle elevations in monoamine oxidase B levels results in loss of spare respiratory capacity: implications for Parkinson's disease. *Journal of Biological Chemistry*, 278:46432-46439.
- LAN, N.C., HEINZMANN, C., GAL, A., KLISAK, I., ORTH, U., LAI, E., GRIMSBY, J., SPARKES, R.S., MOHANDAS, T. & SHIH, J.C. 1989. Human monoamine oxidase A and B genes map to Xp 11.23 and are deleted in a patient with Norrie disease. *Genomics*, 4:552-559.

- LANG, A.E. & LOZANO, A.M. 1998. Parkinson's disease: first of two parts. *The New England Journal of Medicine*, 339:1044-1053.
- LANGSTON, J.W., BALLARD, P., TETRUD, J.W. & IRWIN, I. 1983. Chronic Parkinsonism in humans due to a product of meperidine-analog synthesis. *Science*, 219:979-980.
- LANGSTON, J.W., IRWIN, I., LANGSTON, E.B. & FORNO, L.S. 1984. 1-Methyl-4-phenylpyridinium ion (MPP<sup>+</sup>): Identification of a metabolite of MPTP, a toxin selective to the substantia nigra. *Neuroscience Letters*, 48:87-92.
- LAUDERBACK, C.M., HACKETT, J.M., HUANG, F.F., KELLER, J.N., SZWEDA, L.I., MARKESBERY, W.R. & BUTTERFIELD, D.A. 2001. The glial glutamate transporter, GLT-1, is oxidatively modified by 4-hydroxy-2-nonenal in the Alzheimer's disease brain: the role of Abeta 1-42. *Journal of Neurochemistry*, 78:413-416.
- LEE, D.-H., KIM, C.-S. & LEE, Y.J. 2011. Astaxanthin protects against MPTP/MPP<sup>+</sup>-induced mitochondrial dysfunction and ROS production in vivo and in vitro. *Food and Chemical Toxicology*, 49:271-280.
- LEUNG, A.W. & HALESTRAP, A.P. 2008. Recent progress in elucidating the molecular mechanism of the mitochondrial permeability transition pore. *Biochimica et Biophysica Acta*, 1777:946-952.
- LI, M., BINDA, C., MATTEVI, A. & EDMONDSON, D.E. 2006. Functional role of the "aromatic cage" in human monoamine oxidase B: Structures and catalytic properties of Tyr435 mutant proteins. *Biochemistry*, 45:4775-4784.
- LINDEN, A., GÜLDEN, M., MARTIN, H., MASER, E. & SEIBERT, H. 2008. Peroxide-induced cell death and lipid peroxidation in C6 glioma cells. *Toxicology in Vitro*, 22:1371-1376.
- LINNANE, A.W., MARZUKI, S., OZAWA, T. & TANAKA, M. 1989. Mitochondrial DNA mutations as an important contributor to ageing and degenerative diseases. *Lancet*, 1:642-645.
- LIU, R.H. 2004. Potential synergy of phytochemicals in cancer prevention: mechanism of action. *Journal of Nutrition*, 134:3479S-3485S.

- LOVELL, M.A., XIE, C. & MARKESBERY, W.R. 2001. Acrolein is increased in Alzheimer's disease brain and is toxic to primary hippocampal cultures. *Neurobiology of Aging*, 22:187-194.
- LOURENS, A.C.U. 2008. Structural and synthetic studies of sesquiterpenoids and flavonoids isolated from *Helichrysum* species. University of KwaZulu-Natal: Pietermaritzburg. (Thesis – Ph.D.) p181-182.
- LU, C. & LIU, Y. 2002. Interaction of lipoic acid radical cations with vitamins C and E analogue and hydroxycinnamic acid derivatives. *Archives of Biochemistry and Biophysics*, 406(1):78-84.
- MADESH, M. & HAJNÓCZKY, G. VDAC-dependent permeabilization of the outer mitochondrial membrane by superoxide induces rapid and massive cytochrome c release. *Journal of Cell Biology*, 155:1003-1015.
- MAKER, H.S., WEISS, C., SILIDES, D.J. & COHEN, G. 1981. Coupling of dopamine oxidation (monoamine oxidase activity) to glutathione oxidation via the generation of hydrogen peroxide in rat brain homogenates. *Journal of Neurochemistry*, 36:589-593.
- MANETTI, D., MARTINI, EL., GHELARDINI, C., DEI, S., GALEOTTI, N., GUANDALINI, L., ROMANELLI, M.N., SCAPECCHI, S., TEODORI, E., BARTOLINI, A. & GUALTIERI, F. 2003. 4-Aminopiperidine derivatives as a new class of potent cognition enhancing drugs. *Bioorganic & Medicinal Chemistry Letters*, 13:2303-2306.
- MARANGONI, A.G. 2003. Enzyme kinetics: A modern approach. New York : John Wiley & Sons. pp 50-78.
- MARCHITTI, S.A., DEITRICH, R.A. & VASILIOU, V. 2007. Neurotoxicity and metabolism of the catecholamine-derived 3,4-dihydroxyphenylacetaldehyde and 3,4-dihydroxyphenylglycoaldehyde: the role of aldehyde dehydrogenase. *Pharmacological Reviews*, 59:125-150.
- MARKESBERY, W.R. & CARNEY, J.M. 1999. Oxidative alterations in Alzheimer's disease. *Brain Pathology*, 9:133-146.
- MARKESBERY, W.R. 1997. Oxidative stress hypothesis in Alzheimer's disease. *Free Radical Biology and Medicine*, 23:134-147.

- MARKESBERY, W.R., MONTINE, T.M. & LOVELL, M.A. 2001. Oxidative alterations in neurodegenerative diseases. (In MATTSON, M.P., eds. Pathogenesis of neurodegenerative disorders. New Jersey : Humana Press. pp. 21-52).
- MARTÍNEZ-CAYUELA, M. 1995. Oxygen free radicals and human disease. *Biochimie*, 77:147-161.
- MATSUMOTO, T., SUZUKI, O., FURUTA, T., ASAI, M., KUROKAWA, Y., NIMURA, Y., KATSUMATA, Y. & TAKAHASHI, I. 1985. A sensitive fluorometric assay for serum monoamine oxidase with kynuramine as substrate. *Clinical Biochemistry*, 18:126-129.
- MAZZULLI, J.R., MISHIZEN, A.J., GIASSON, B.I., LYNCH, D.R., THOMA, S.A., NAKASHIMA, A., NAGATSU, T., OTA, A. & ISCHIROPOULOS, H. 2006. Cytosolic catechols inhibit alpha-synuclein aggregation and facilitate the formation of intracellular soluble oligomeric intermediates. *The Journal of Neuroscience*, 26:10068-10078.
- MIDDLETON, Jr, E., KANDASWAMI, C. & THEOHARIDES, T.C. 2000. The effect of plant flavonoids on mammalian cells: implications for inflammation, heart disease, and cancer. *Pharmacological Reviews*, 52:673-751.
- MOSHAROV, E.V., STAAL, R.G., BOVE, J., PROU, D., HANANIYZ, A., MARKOV, D., POULSEN, N., LARSEN, K.E., MOORE, C.M., TROYER, M.D., EDWARDS, R.H., PRZEDBORSKI, S. & SULZER, D. 2006. Alpha-synuclein overexpression increases cytosolic catecholamine concentration. *The Journal of Neuroscience*, 26:9304-9311.
- MUNOZ, E., OLIVA, R., OBACH, V., MARTI, M.J., PASTOR, P., BALLESTA, F. & TOLOSA, E. 1997. Identification of Spanich familial Parkinson's disease and screening for the Ala53Thr mutation of the alpha-synuclein gene in early onset patients. *Neuroscience Letters*, 235:57-60.
- MURPHY, M.P. 2009. How mitochondria produce reactive oxygen species. *Biochemical Journal*, 417:1-13.
- MURPHY, M.P., PACKER, M.A., SCARLETT, J.L. & MARTIN, S.W. 1998. Peroxynitrite: a biologically significant oxidant. *General Pharmacology*, 31:179-186.
- NAARDING, P., KREMER, H.P.H. & ZITMAN, F.G. 2001. Huntington's disease: a review of the literature on prevalence and treatment of neuropsychiatric phenomena. *European Psychiatry*, 16:439-445.

- NAKAMURA, Y., WATANABE, S., MIYAKE, N., KOHNO, H. & OSAWA, T. 2003 . Dihydrochalcones: evaluation as novel radical scavenging antioxidant. *Journal of Agricultural and Food Chemistry*, 51:3309-3312.
- NAOI, M., MARUYAMA, W., SHAMOTO-NAGAI, M., YI, H., AKAO, Y. & TANAKA, M. 2005. Oxidative stress in mitochondria: decision to survive and death of neurons in neurodegenerative disorders. *Molecular Neurobiology*, 31:82-93.
- NAPPI, A.J. & VASS, E. 1998. Hydroxyl radical formation resulting from the interaction of nitric oxide and hydrogen peroxide. *Biochimica et Biophysica Acta*, 1380:55-63.
- NIGAM, S. & SCHEWE, T. 2000. Phospholipase A2s and lipid peroxidation. *Biochimica et Biophysica Acta*, 1488:167-181.
- NOHL, H. & STOLZE, K. 1992. Ubisemiquinones of the mitochondrial respiratory chain do not interact with molecular oxygen. *Free Radical Research Communications*, 16:409-419.
- NORRIS, E.H., GIASSEN, B.I., HODARA, R., XU, S., TROJANOWSKI, J.Q., ISCHIROPOULOS, H. & LEE, V.M. 2005. Reversible inhibition of alpha-synuclein fibrillization by dopamine-chrom-mediated conformational alterations. *Journal of Biological Chemistry*, 280:21212-21219.
- NYIREDY, S.Z., ERDELMEIER, C.A.J., MEIER, B. & STICHER, O. 1985. "Prisma": ein modell zur optimierung der mobilen phase für die Dünnschichtchromatographie, vorgestellt anhand verschiedener naturstofftrennungen. *Planta medica*, 241-246.
- OKADO-MATSUMOTO, A. & FRIDOVICH, I. 2001. Subcellular distribution of superoxide dismutases (SOD) in rat liver: Cu, Zn-SOD in mitochondria. *Journal of Biological Chemistry*, 276:38388-38393.
- OTTINO, P. & DUNCAN, J.R. 1997. Effect of  $\alpha$ -tocopherol succinate on free radical and lipid peroxidation levels in BL6 melanoma cells. *Free Radical Biology & Medicine*, 22:1145-1151.
- PACZAL, A., BÉNYEI, A.C. & KOTSCHY, A. 2006. Modular synthesis of heterocyclic carbene precursors. *Journal of Organic Chemistry*, 71:5969-5979.
- PAMPLONA, R. 2008. Membrane phospholipids, lipoxidative damage and molecular integrity: a causal role in aging and longevity. *Biochimica et Biophysica Acta*, 1777:1249-1262.

- PARADIES, G., PETROSILLO, G., PARADIES, V. & RUGGIERO, F.M. 2011. Mitochondrial dysfunction in brain aging: Role of oxidative stress and cardiolipin. *Neurochemistry International*, 58:447-457.
- PARSONS, C.G., DANYSZ, W. & QUACK, G. 1999. Memantine is a clinically well tolerated N-methyl-D-aspartate (NMDA) receptor antagonist – Review of preclinical data. *Neuropharmacology*, 38:735-767.
- PAULSEN, J.S. 2009. Functional imaging in Huntington's disease. *Experimental Neurology*, 216:272-277.
- PETERSON, J. & DWYER, J. 1998. Flavonoids: dietary occurrence and biochemical activity. *Nutrition Research*, 18:1995-2018.
- POCERNICH, C.B. & BUTTERFIELD, D.A. 2003. Acrolein inhibits NADH-linked mitochondrial enzyme activity: implications for Alzheimer's disease. *Neurotoxicity Research*, 5:515-520.
- POLYMEROPOULOS, M.H., LAVEDAN, C., LEROY, E., IDE, S.E., DEHEJIA, A., DUTRA, A., PIKE, B., ROOT, H., RUBENSTEIN, J., BOYER, R., STENROOS, E.S., CHANDRASEKHARAPPA, S., ATHANASSIADOU, A., PAPAPETROPOULOS, T., JOHNSON, W.G., LAZZARINI, A.M., DUVOISIN, R.C., DI LORIO, G., GOLBE, L.I. & NUSSBAUM, R.L. 1997. Mutation in the alpha-synuclein gene identified in families with Parkinson's disease. *Science*, 276:2045-2047.
- PRINS, L.H.A., PETZER, J.P. & MALAN, S.F. 2010. Inhibition of monoamine oxidase by indole and benzofuran derivatives. *European Journal of Medicinal Chemistry*, 45:4458-4466.
- RABEY, J.M., SAGI, I., HUBERMAN, M., MELAMED, E., KORCZYN, A., GILADI, N., INZELBERG, R., DJALDETTI, R., KLEIN, C. & BERECH, G. 2000. Rasagiline mesylate, a new MAO-B inhibitor for the treatment of Parkinson's disease: a double-blind study as adjunctive therapy to levodopa. *Clinical Neuropharmacology*, 23:324-330.
- RADAK, Z., KUMAGAI, S., NAKAMOTO, H. & GOTO, S. 2007. 8-Oxoguanosine and uracil repair of nuclear and mitochondrial DNA in red and white skeletal muscle of exercise-trained old rats. *Journal of Applied Physiology*, 102:1696-1701.
- RADI, R., BECKMEN, J.S., BUCH, K.M. & FREEMAN. 1991. Peroxynitrite induced membrane lipid peroxidation: the cytotoxic potential of superoxide and nitric oxide. *Archives of Biochemistry and Biophysics*, 288:481-487.

- RAHMAN, I., BISWAS, S.K. & KODE, A. 2006. Oxidant and antioxidant balance in the airways and airway diseases. *European Journal of Pharmacology*, 533:222-239.
- REAL, J.T., MARTÍNEZ-HERVÁS, S., TORMOS, M.C., DOMENECH, E., PALLARDO, F.V., SÁEZ-TORMO, G., REDON, J., CARMENA, R., CHAVES, F.J., ASCASO, J.F. & GARCÍA-GARCÍA, A.-B. 2010. Increased oxidative stress levels and normal antioxidant enzyme activity in circulating mononuclear cells from patients of familial hypercholesterolemia. *Metabolism Clinical and Experimental*, 59:293-298.
- REBRIN, I., GEHA, R.M., CHEN., K. & SHIH, J.C. 2001. Effects of carboxyl-terminal truncations on the activity and solubility of human monoamine oxidase B. *Journal of Biological Chemistry*, 276:29499-29506.
- REDDY, P.H. 2009. Amyloid beta, mitochondrial structural and functional dynamics in Alzheimer's disease. *Experimental Neurology*, 218:286-292.
- REED, T.T. 2011. Lipid peroxidation and neurodegenerative disease. *Free radical biology & medicine*, 51:1302-1319.
- REQUENA, J.R., DIMITROVA, M.N., LEGNAME, G., TEIJEIRA, S., PRUSINER, S.B. & LEVINE, R.L. 2004. Oxidation of methionine residues in the prion protein by hydrogen peroxide. *Archives of Biochemistry and Biophysics*, 432:188-195.
- RHEE, S.G., CHAE, H.Z. & KIM, K. 2005. Peroxiredoxins: a historical overview and speculative preview of novel mechanisms and emerging concepts in cell signaling. *Free Radical Biology and Medicine*, 38:1543-1552.
- ROBAK, J. & GRYGLEWSKI, R.J. 1996. Bioactivity of flavonoids. *Polish Journal of Pharmacology*, 48:555-564.
- RODWELL, V.W. 1993. Enzymes: kinetics. (In MURRAY, R.K., GRANNER, D.K., MAYES, P.A., RODWELL, V.W., eds. *Harper's Biochemistry*, 23<sup>rd</sup> ed. Connecticut : Appleton and Lange. pp. 71-85).
- ROSCHEK, Jr, B., FINK, R.C., MCMICHAEL, M.D., LI, D. & ALBERTE, R.S. 2009. Elderberry flavonoids bind to and prevent H1N1 infection in vitro. *Phytochemistry*, 70:1255-1261.



- RUMP, A.F., SCHUSSLER, M., ACAR, D., CORDES, A., RATKE, R., THEISOHN, M., ROSEN, R., KLAUS, W. & FRICKE, U. 1995. Effects of different inotropes with antioxidant properties on acute regional myocardial ischemia in isolated rabbit hearts. *General Pharmacology*, 26:603-611.
- SALMI, M., YEGUTKIN, G.G., LEHVONEN, R., KOSKINEN, K., SALMINEN, T. & JALKANEN, S. 2001. A cell surface amine oxidase directly controls lymphocyte migration. *Immunity*, 14:265-276.
- SARKELA, T.M., BERTHIAUME, J., ELFERING, S., GYBINA, A.A. & GIULIVI, C. 2001. The modulation of oxygen radical production by nitric oxide in mitochondria. *The Journal of Biological Chemistry*, 276:6945-6949.
- SAURA, J., LUQUE, H.M., CESURA, A.M., DA PRADA, M., CHAN-PALAY, V., HUBER, G., LOFFLER, J. & RICHARDS, J.G. 1994. Increased monoamine oxidase B activity in plaque-associated astrocytes of Alzheimer brains revealed by quantitative enzyme radioautography. *Neuroscience*, 62:15-30.
- SDBSWeb : <http://riodb01.ibase.aist.go.jp/sdbs/> (National Institute of Advanced Industrial Science and Technology) Date of access: October 2011.
- SEET, R.C.S., LEE, C.-Y.J., LIM, E.C.H., TAN, J.J.H., QUEK, A.M.L., CHONG, W.-L., LOOI, W.-F., HUANG, S.-H., WANG, H., CHAN, Y.-H. & HALLIWELL, B. 2010. Oxidative damage in Parkinson disease: Measurement using accurate biomarkers. *Free Radical Biology and Medicine*, 48:560-566.
- SEGEL, I.H. 1993. Enzyme kinetics. New York : John Wiley & Sons. pp. 100-125.
- SELKOE, D.J. 2001. Alzheimer's disease: genes, proteins, and therapy. *Physiological Reviews*, 81:741-766.
- SEWERYNEK, E., POEGGELER, B., MELCHIORRI, D. & REITER, R.J. 1995. H<sub>2</sub>O<sub>2</sub>-induced lipid peroxidation in rat brain homogenates is greatly reduced by melatonin. *Neuroscience Letters*, 195:203-205.
- SHIH, J.C., CHEN, K. & GEHA, R.M. 1998. Determination of regions important for monoamine oxidase (MAO) A and B substrate and inhibitor selectivities. *Genomics*, 4:552-559.

- SIDDAIAH, V., RAO, C.V., VENKATESWARLU, S., KRISHNARAJU, A.V. & SUBBARAJU, G.V. 2006. Synthesis, stereochemical assignments, and biological activities of homoisoflavonoids. *Bioorganic & Medicinal Chemistry*, 14:2545-2551.
- SIMPSON, J.A., CHEESEMAN, K.H., SMITH, S.E. & DEAN, R.T. 1988. Free-radical generation by copper ions and hydrogen peroxide. *Biochemical Journal*, 254:519-513.
- SMITH, T.S. & BENNETT, J.P. 1997. Mitochondrial toxins in models of neurodegenerative diseases.1. In vivo brain hydroxyl radical production during systemic MPTP treatment or following microdialysis infusion of methylpyridinium or azide ions. *Brain Research*, 765:183-188.
- SOFIC, E., RIEDERER, P., HEINSEN, H., BECKMANN, H., REYNOLDS, G.P., HEBENSTREIT, G. & YODIM, M.B. 1988. Increased iron (III) and total iron content in post mortem substantia nigra of parkinsonian brain. *Journal of Neural Transmission*, 74:199-205.
- SPILLANTINI, M.G., SCHMIDT, M.L., LEE, V.M., TROJANOWSKI, J.Q., JAKES, R. & GOEDERT, M. 1997. Alpha-synuclein in Lewy bodies. *Nature*, 388:839-840.
- STADTMAN, E.R. & LEVINE, R.L. 2003. Free radical-mediated oxidation of free amino acid and amino acid residues in proteins. *Amino Acids*, 25:207-218.
- STRYDOM, B., MALAN, S.F., CASTAGNOLI, Jr, N., BERGH, J.J. & PETZER, J.P. 2010. Inhibition of monoamine oxidase by 8-benzoyloxycaffeine analogues. *Bioorganic & Medicinal Chemistry*, 18:1018-1028.
- SULTANA, R. & BUTTERFIELD, D.A. 2009. Oxidatively modified, mitochondria-relevant brain proteins in subjects with Alzheimer' disease and mild cognitive impairment. *Journal of Bioenergetics and Biomembranes*, 41:441-446.
- SULTANA, R., BOYD-KIMBALL, D., POON, H.F., CAI, J., PIERCE, W.M., KLEIN, J.B., MERCHANT, M., MARKESBERY, W.R. & BUTTERFIELD, D.A. 2006. Redox proteomics identification of oxidized proteins in Alzheimer's disease hippocampus and cerebellum: an approach to understand pathological and biochemical alterations in AD. *Neurobiology of Aging*, 27:1564-1576.
- SULTANA, R., POON, H.F., CAI, J., PIERCE, W.M., MERCHANT, M., KLEIN, J.B., MARKESBERY, W.R. & BUTTERFIELD, D.A. 2006b. Identification of nitrated proteins in Alzheimer's disease brain using a redox proteomics approach. *Neurobiology of Disease*, 22:76-87.

KOPPENOL, W.H., MORENO, J.J. & PRYOR, W.A. 1992. Peroxynitrite, a cloaked oxidant formed by nitric oxide and superoxide. *Chemical Research in Toxicology*, 5:834-842.

TAMAGNO, E., PAROLA, M., BARDINI, P., PICCINI, A., BORGHI, R., GUGLIELMOTTO, M., SANTORO, G., DAVIT, A., DANNI, O., SMITH, M.A., PERRY, G. & TABATON, M. 2005. Beta-site APP cleaving enzyme up-regulation induced by 4-hydroxynonenal is mediated by stress-activated protein kinases pathways. *Journal of Neurochemistry*, 92:628-636.

TANG, S.C., LATHIA, J.D., SELVARAJ, P.K., JO, D.G., MUGHAL, M.R., CHENG, A., SILER, D.A., MARKESBERY, W.R., ARUMUGAM, T.V. & MATTSON, M.P. 2008. Toll-like receptor-4 mediates neuronal apoptosis induced by amyloid beta-peptide and the membrane lipid peroxidation product 4-hydroxynonenal. *Experimental Neurology*, 213:114-121.

TARIOT, P.N., LOY, R., RYAN, J.M., PORSTEINSSON, A. & ISMAIL, S. 2002. Mood stabilizers in Alzheimer's disease: symptomatic and neuroprotective rationales. *Advanced Drug delivery reviews*, 54:1567-1577.

THE PARKINSON STUDY GROUP. 1993. Effect of tocopherol and deprenyl on the progression of disability in early Parkinson's disease. *New England Journal of Medicine*, 328:176-183.

TIPTON, K.F., BOYCE, S., O'SULLIVAN, J., DAVEY, G.P. & HEALY, J. 2004. Monoamine oxidases: certainties and uncertainties. *Current Medicinal Chemistry*, 11:1965-1982.

TSANG, A.H.K. & CHUNG, K.K.K. 2009. Oxidative and nitrosative stress in Parkinson's disease. *Biochimica et Biophysica Acta*, 1792:643-650.

TSUGENO, Y., HIRASHIKI, I., OGATA, F. & ITO, A. 1995. Regions of the molecule responsible for substrate specificity of monoamine oxidase A and B: a chimeric enzyme analysis. *The Journal of Biochemistry*, 118:974-980.

TURRENS, J.F. 2004. Oxidative stress and antioxidant defenses: a target for the treatment of diseases caused by parasitic protozoa. *Molecular Aspects of Medicine*, 25:211-220.

TURRENS, J.F., ALEXANDRE, A. & LEHNINGER, A.L. 1985. Ubisemiquinone is the electron donor for superoxide formation by complex III of heart mitochondria. *Archives of Biochemistry and Biophysics*, 237:408-414.

- URSINI, F., MAIORINO, M., BRIGELIUS-FLOHÉ, R., AUMANN, K.D., ROVERI, A., SCHOMBURG, D. & FLOHÉ, L. 1995. Diversity of glutathione peroxidases. *Methods in Enzymology*, 252:38-53.
- VAN DEN BERG, D. 2006. Inhibition of monoamine oxidase B by substituted benzamindazole analogues. North-West University: Potchefstroom campus. (Dissertation – M.Sc.) p27-30.
- VENKAT RATNAM, D., ANKOLA, D.D., BHARDWAJ, V., SAHANA, D.K. & RAVI KUMAR, M.N.V. 2006. Role of antioxidants in prophylaxis and therapy: A pharmaceutical perspective. *Journal of Controlled Release*, 113:189-207.
- VERTUANI, S., ANGUSTI, A. & MANFREDINI, S. 2004. The antioxidants and pro-antioxidant network: an overview. *Current Pharmaceutical Design*, 10:1677-1694.
- WALLING, C. 1975. Fenton reagent: V. Hydroxylation and side-chain cleavage of aromatics. *Accounts of Chemical Research*, 8:125-131.
- WANG, W., YUAN, X., JIN, Z., TIAN, Y. & SONG, H. 2007. Free radical and reactive oxygen species scavenging activities of peanut skins extract. *Food Chemistry*, 104:242-250.
- WEI, Y.H. 1992. Mitochondrial DNA alterations as ageing-associated molecular events. *Mutation Research*, 275:145-155.
- WEISSHAAR, B. & JENKINS, G.I. 1998. Phenylpropanoid biosynthesis and its regulation. *Current Opinion in Plant Biology*, 1:251-257.
- WICKENS, A.P. 2001. Ageing and the free radical theory. *Respiration Physiology*, 128:379-391.
- WOLLENWEBER, E. & DIETZ, H.V. 1981. Occurrence and distribution of free flavonoid aglycones in plants. *Phytochemistry*, 20:869-932.
- WOUTERS, J. 1998. Structural aspects of monoamine oxidase and its reversible inhibition. *Current Medicinal Chemistry*, 5:137-162.
- YAMADA, Y. & HARASHIMA, H. 2008. Mitochondrial drug delivery systems for macromolecule and their therapeutic application to mitochondrial diseases. *Advanced Drug Delivery Reviews*, 60:1439-1462.

YOSHINAGA, N., MURAYAMA, T.E. & NOMURA, Y. 2000. Apoptosis induction by a dopaminergic neurotoxin, 1-methyl-4-phenylpyridinium (MPP+), and inhibition by epidermal growth factor in GH3 cells. *Biochemistry and Pharmacology*, 60:111-116.

YOUDIM, M.B.H., FRIDKIN, M. & ZHENG, H. 2004. Novel bifunctional drugs targeting monoamine oxidase inhibition and iron chelation as an approach to Neuroprotection in Parkinson's disease and other neurodegenerative diseases. *Journal of Neural Transmission*, 111:1455-1471.

YU, B. 1994. Cellular defences against damage from reactive oxygen species. *Physiological Reviews*, 74:139-162.

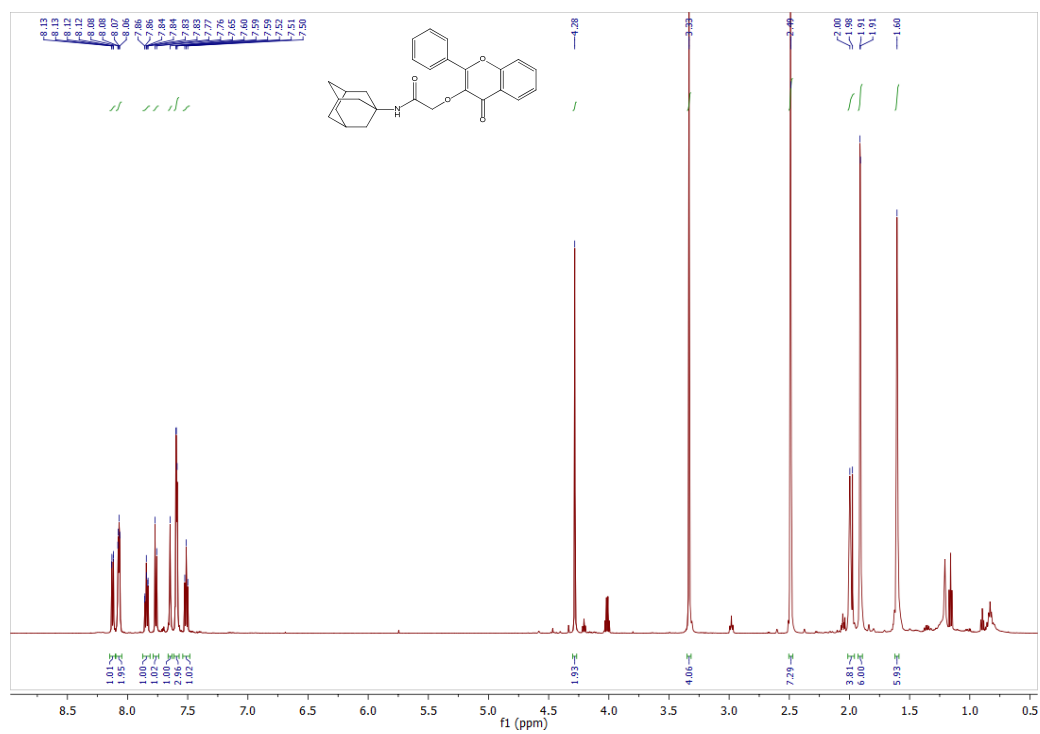
ZHOU, J., ZHONG, B. & SILVERMAN, R. 1996. Direct continuous fluorometric assay for monoamine oxidase. *Analytical Biochemistry*, 234:9-12.

## Appendix

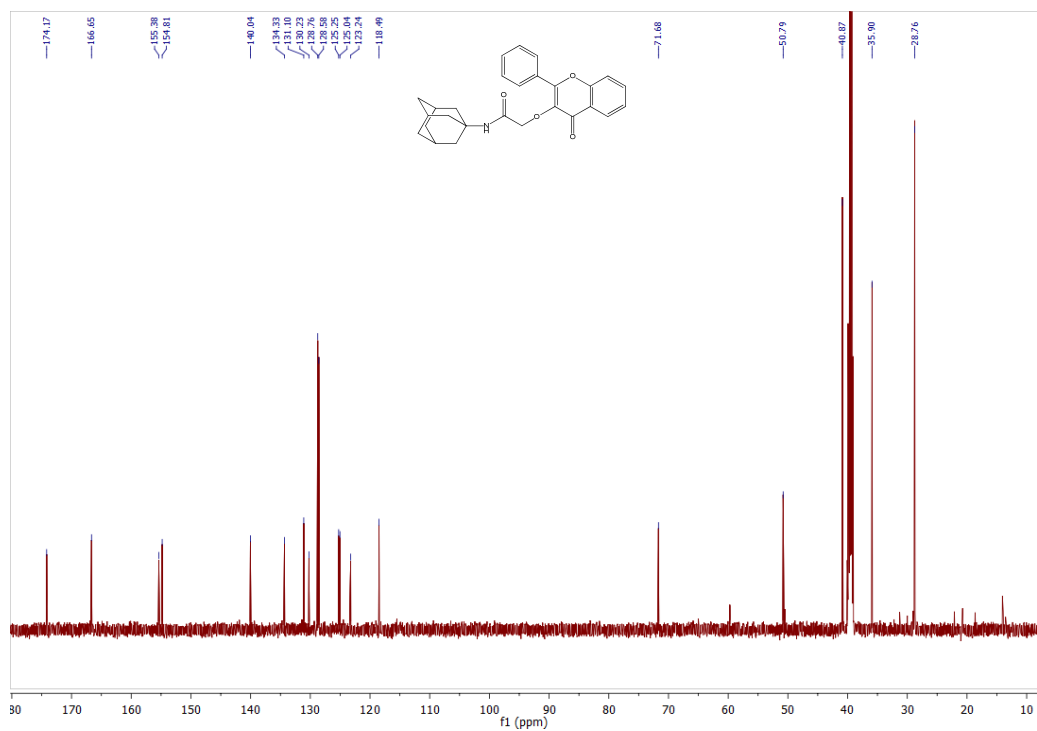
Spectral Data:

$^1\text{H}$  NMR,  $^{13}\text{C}$  NMR, DEPT, COSY, HSQC, HMBC, MS, IR

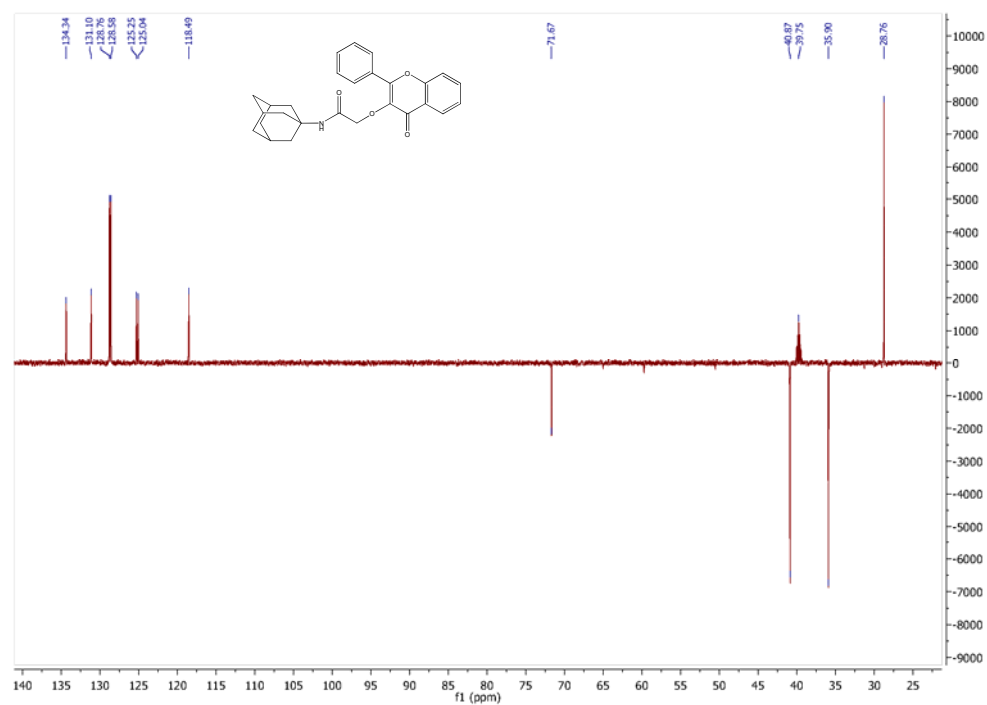
Spectrum 1  $^1\text{H}$  of N-(adamantan-1-yl)-2-[(4-oxo-2-phenyl-4H-chromen-3-yl)oxy]acetamide



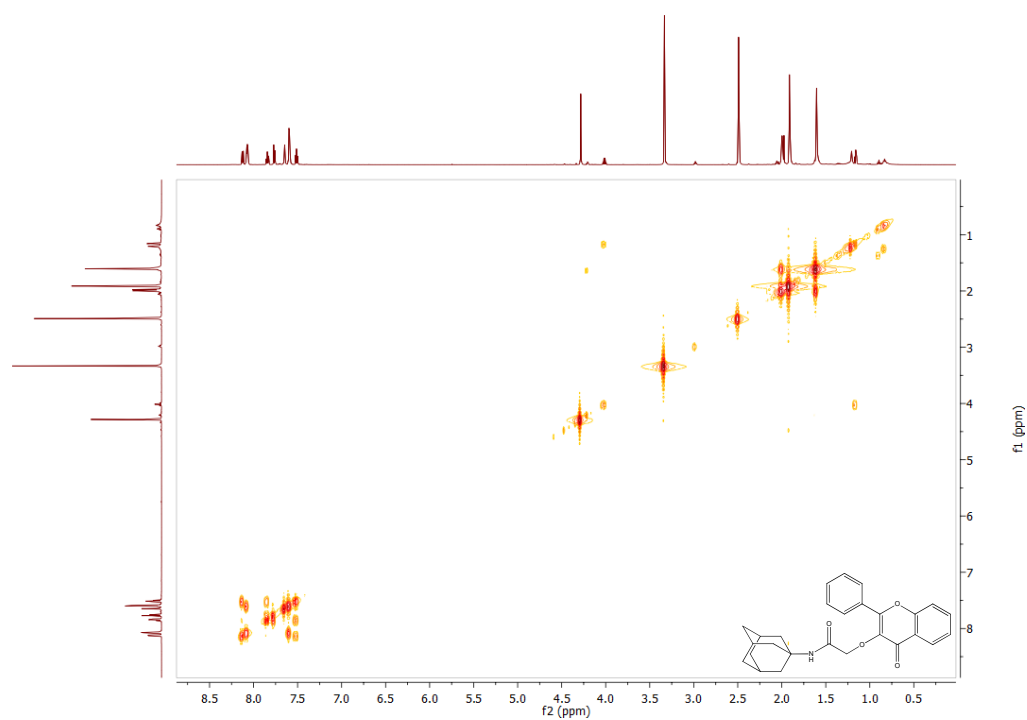
Spectrum 2  $^{13}\text{C}$  of N-(adamantan-1-yl)-2-[(4-oxo-2-phenyl-4H-chromen-3-yl)oxy]acetamide



Spectrum 3 DEPT of N-(adamantan-1-yl)-2-[(4-oxo-2-phenyl-4H-chromen-3-yl)oxy]acetamide

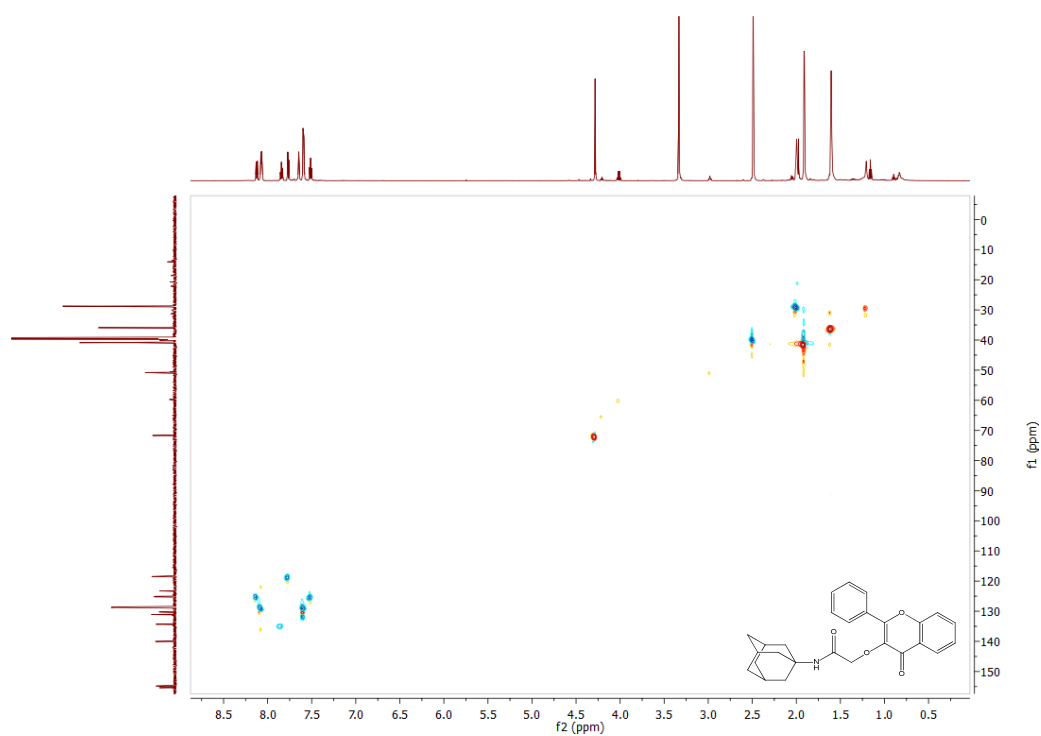


Spectrum 4 COSY of N-(adamantan-1-yl)-2-[(4-oxo-2-phenyl-4H-chromen-3-yl)oxy]acetamide

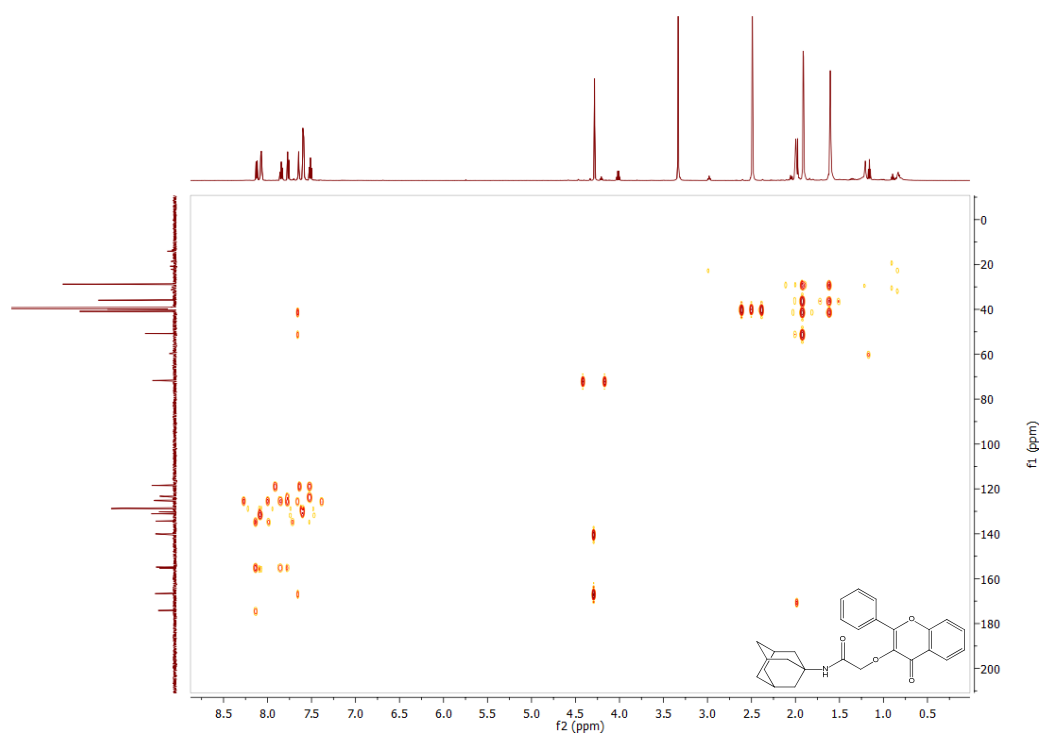




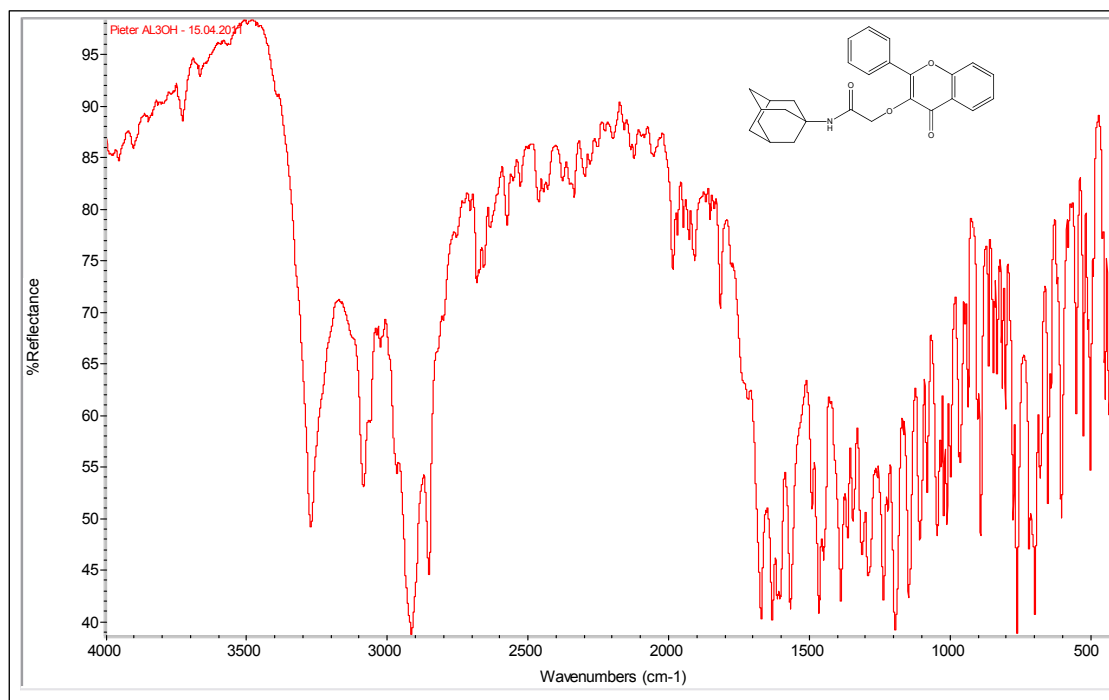
Spectrum 5 HSQC of N-(adamantan-1-yl)-2-[(4-oxo-2-phenyl-4H-chromen-3-yl)oxy]acetamide



Spectrum 6 HMBC of N-(adamantan-1-yl)-2-[(4-oxo-2-phenyl-4H-chromen-3-yl)oxy]acetamide

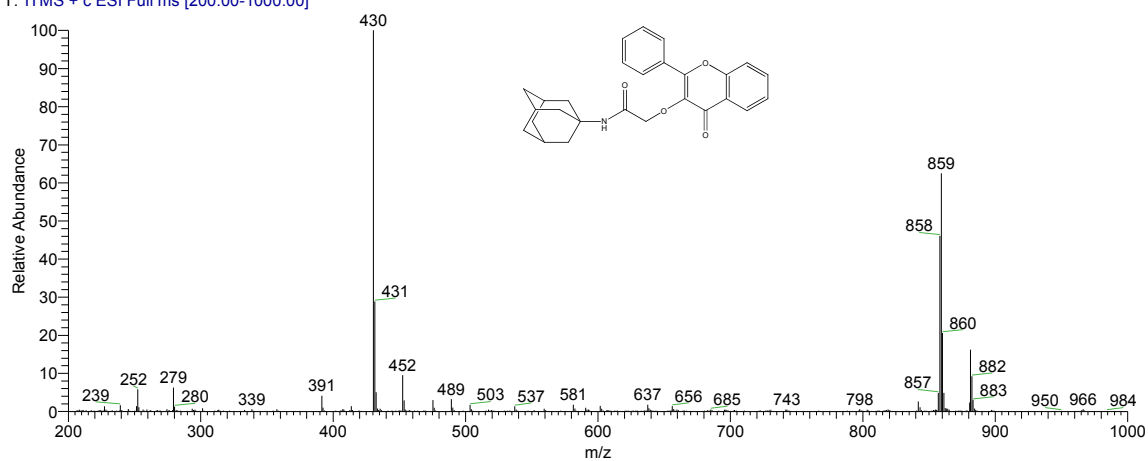


Spectrum 7  $\nu_{\max}$  of N-(adamantan-1-yl)-2-[(4-oxo-2-phenyl-4H-chromen-3-yl)oxy]acetamide



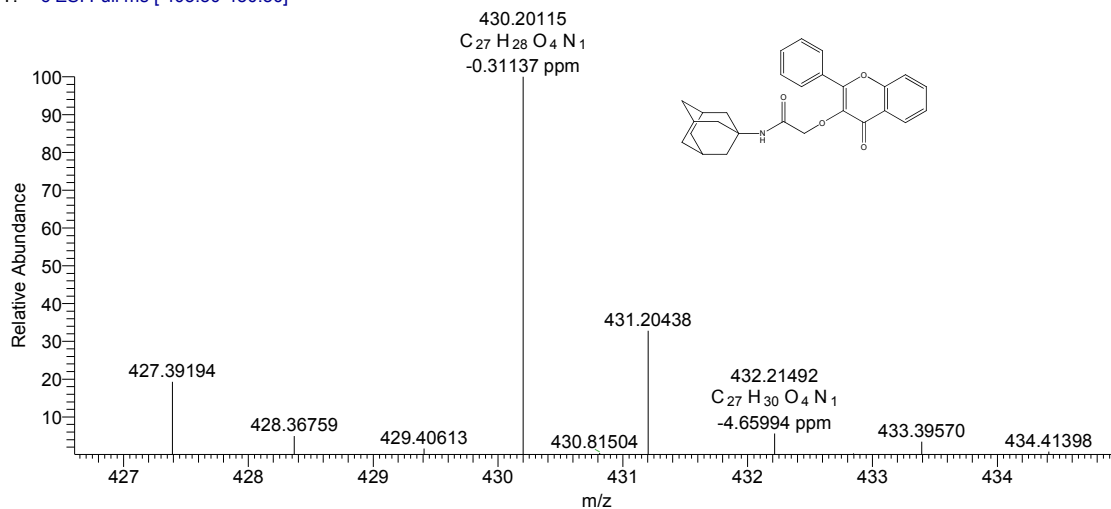
Spectrum 8 ESI MS of N-(adamantan-1-yl)-2-[(4-oxo-2-phenyl-4H-chromen-3-yl)oxy]acetamide

amantadineal3ohflavone #10-32 RT: 0.35-1.12 AV: 23 NL: 3.45E4  
T: ITMS + c ESI Full ms [200.00-1000.00]

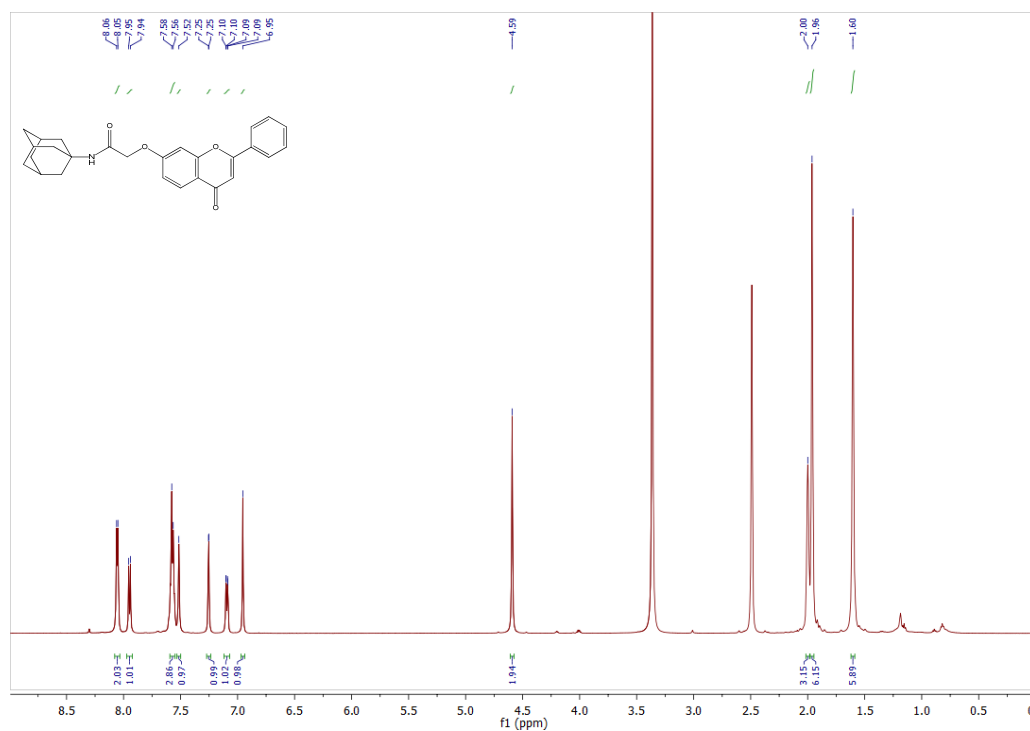


Spectrum 9 HRESIMS of N-(adamantan-1-yl)-2-[(4-oxo-2-phenyl-4H-chromen-3-yl)oxy]acetamide

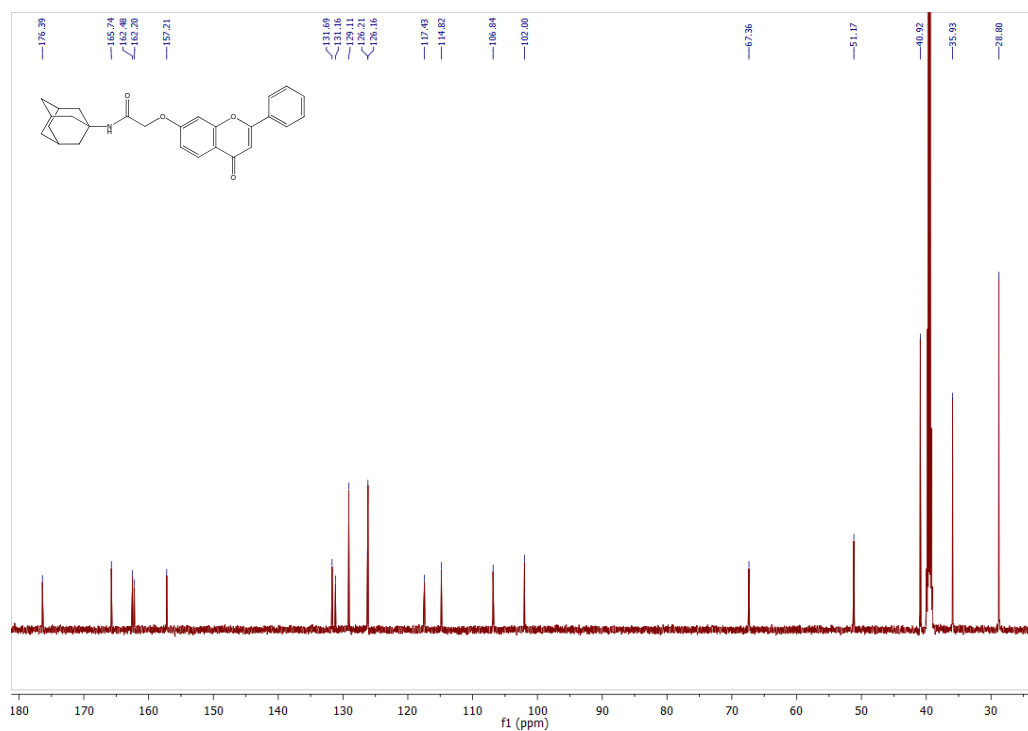
PF01\_HRESI-c1 #25 RT: 0.55 AV: 1 NL: 1.83E6  
T: + c ESI Full ms [ 403.50-450.50]



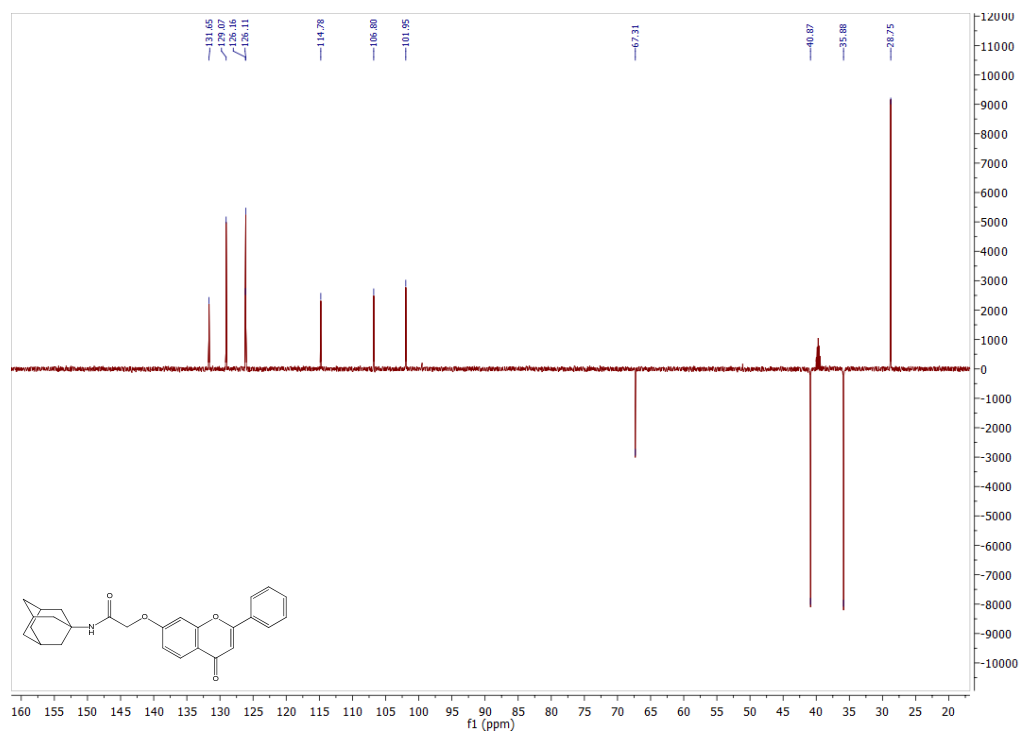
Spectrum 10  $^1\text{H}$  of N-(adamantan-1-yl)-2-[(4-oxo-2-phenyl-4H-chromen-7-yl)oxy]acetamide



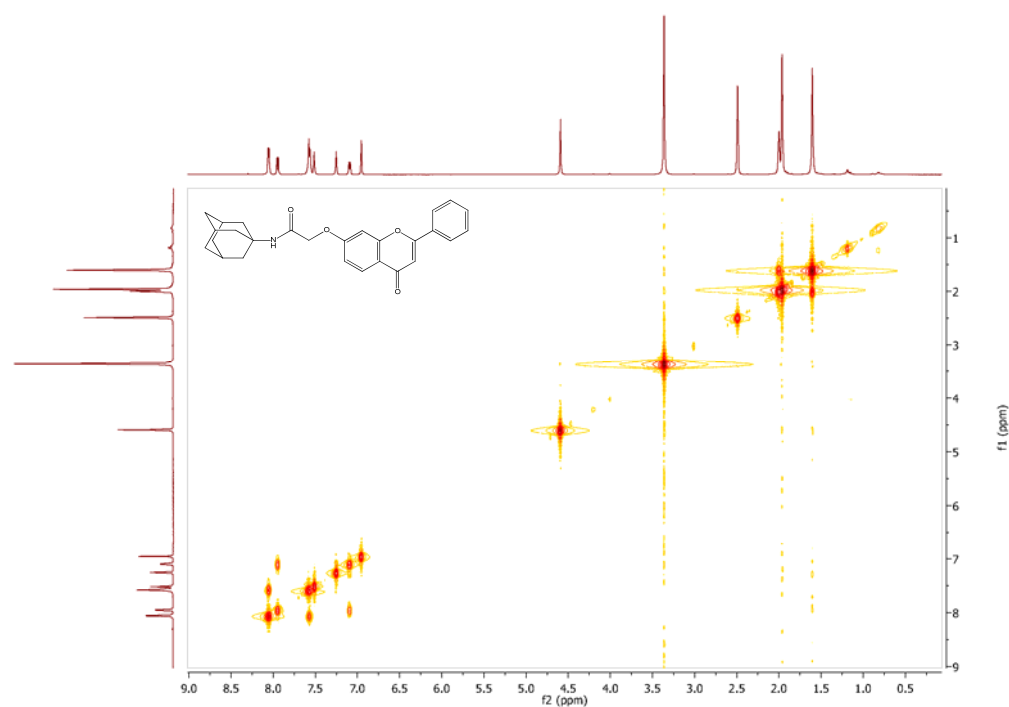
Spectrum 11  $^{12}\text{C}$  of N-(adamantan-1-yl)-2-[(4-oxo-2-phenyl-4H-chromen-7-yl)oxy]acetamide



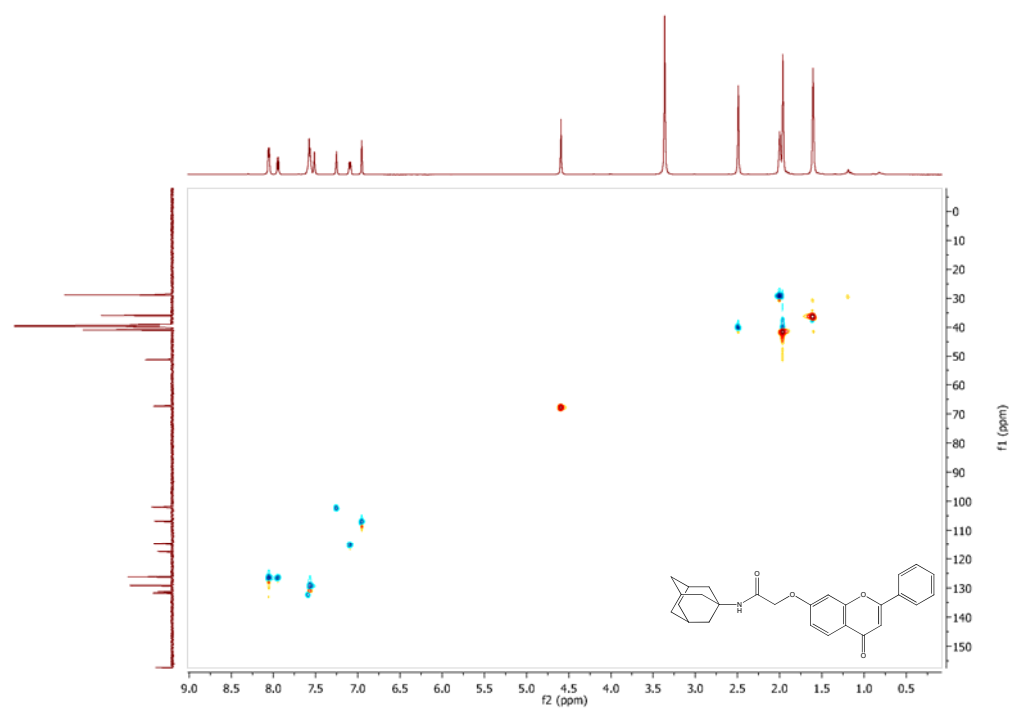
Spectrum 12 DEPT of N-(adamantan-1-yl)-2-[(4-oxo-2-phenyl-4H-chromen-7-yl)oxy]acetamide



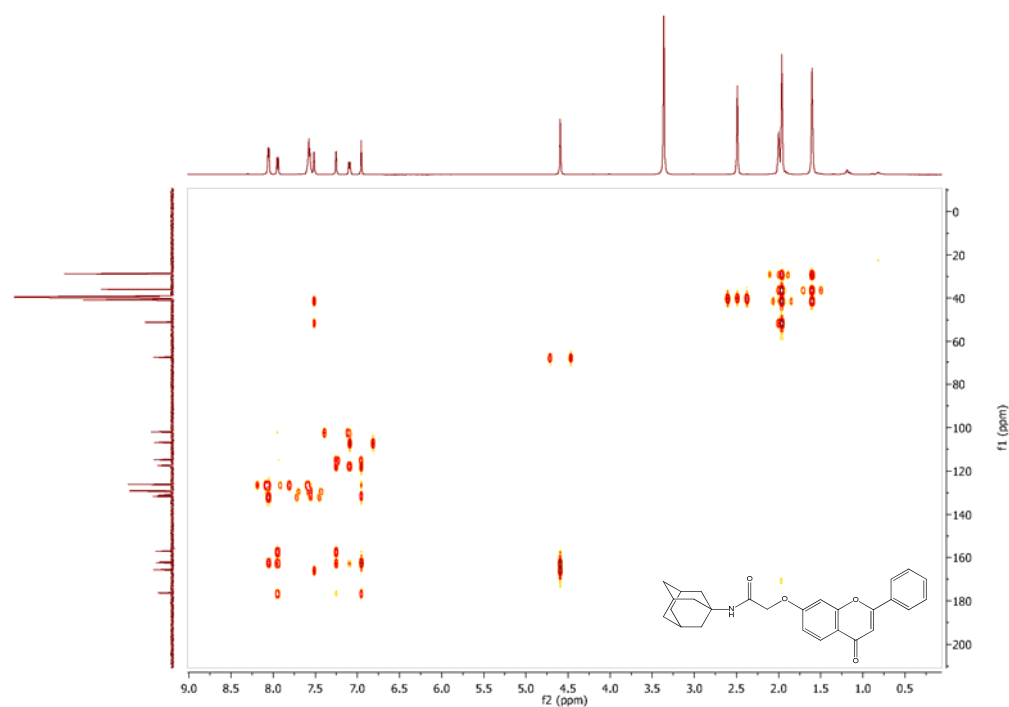
Spectrum 13 COSY of N-(adamantan-1-yl)-2-[(4-oxo-2-phenyl-4H-chromen-7-yl)oxy]acetamide



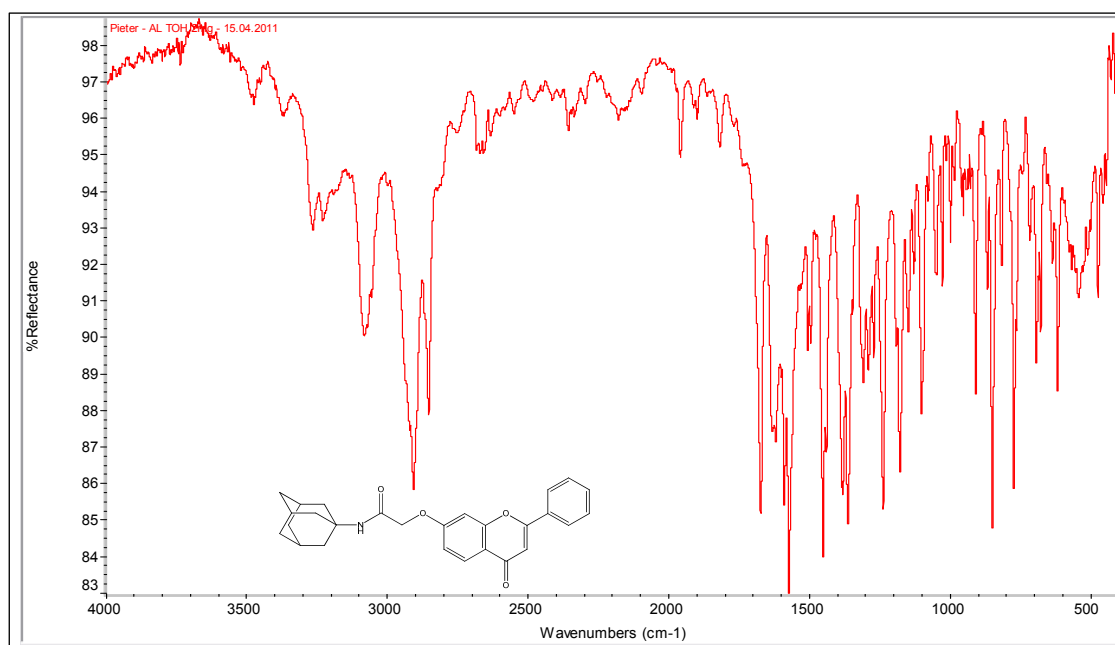
Spectrum 14 HSQC of N-(adamantan-1-yl)-2-[(4-oxo-2-phenyl-4H-chromen-7-yl)oxy]acetamide



Spectrum 15 HMBC of N-(adamantan-1-yl)-2-[(4-oxo-2-phenyl-4H-chromen-7-yl)oxy]acetamide

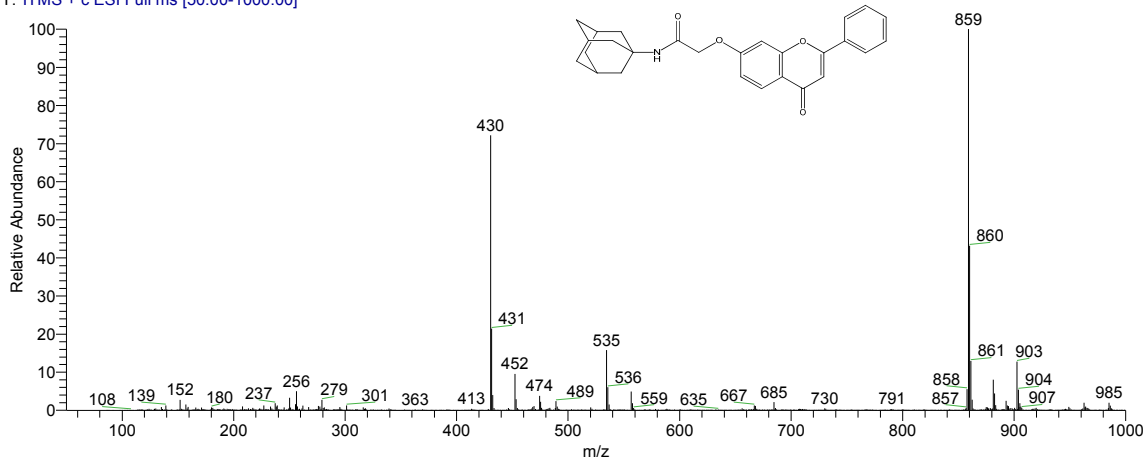


Spectrum 16  $\nu_{\max}$  of N-(adamantan-1-yl)-2-[(4-oxo-2-phenyl-4H-chromen-7-yl)oxy]acetamide



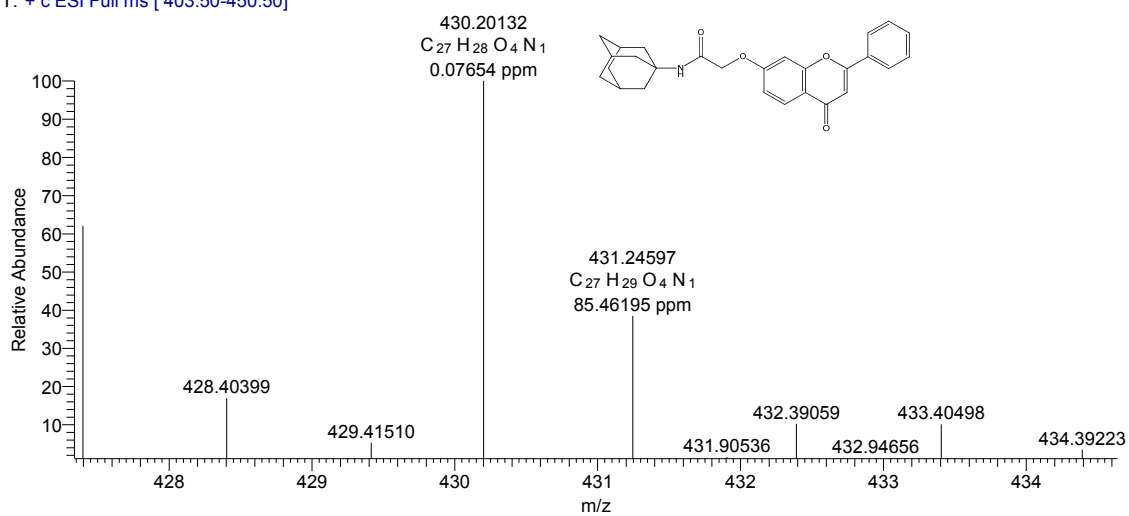
Spectrum 17 ESI MS of N-(adamantan-1-yl)-2-[(4-oxo-2-phenyl-4H-chromen-7-yl)oxy]acetamide

AL70HF #9-20 RT: 0.32-0.74 AV: 12 NL: 9.72E3  
T: ITMS + c ESI Full ms [50.00-1000.00]

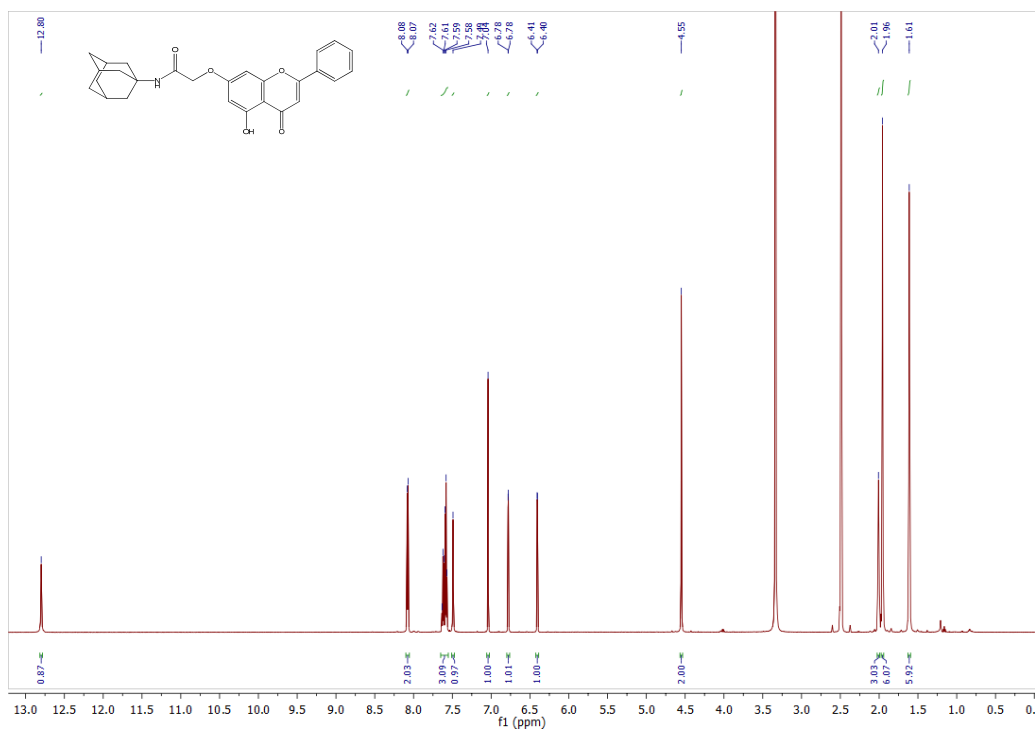


Spectrum 18 HRESIMS of N-(adamantan-1-yl)-2-[(4-oxo-2-phenyl-4H-chromen-7-yl)oxy]acetamide

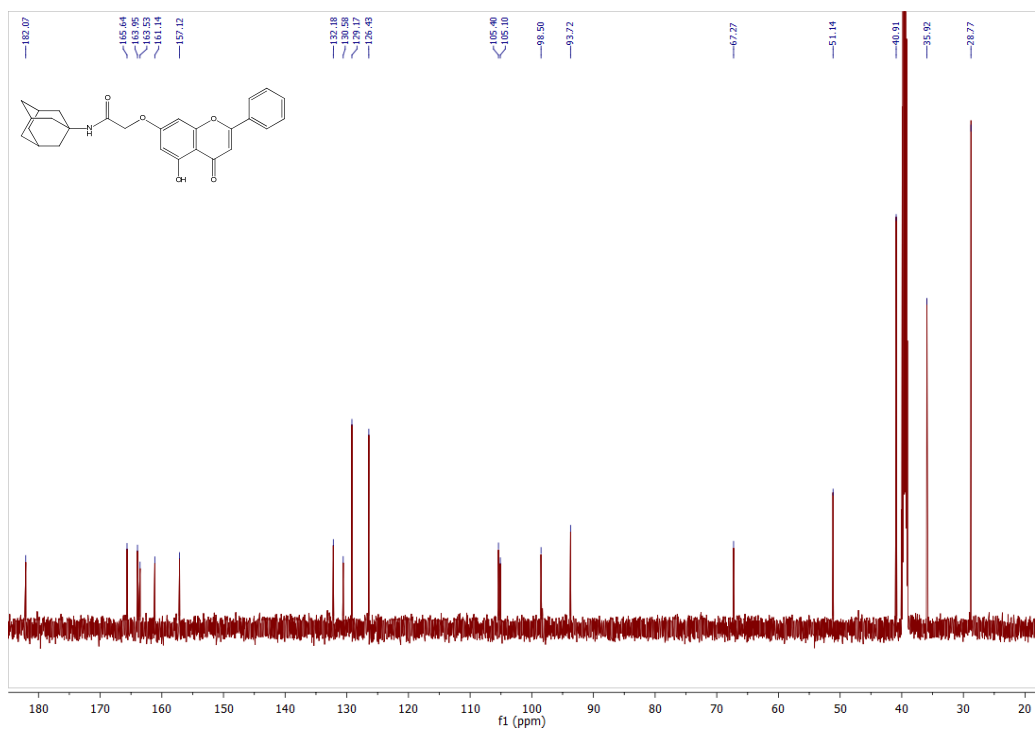
PF03\_HRESI-c1 #39 RT: 0.87 AV: 1 NL: 6.29E5  
T: + c ESI Full ms [403.50-450.50]



Spectrum 19  $^1\text{H}$  of N-(adamantan-1-yl)-2-[(5-hydroxy-4-oxo-2-phenyl-4H-chromen-7-yl)oxy]acetamide

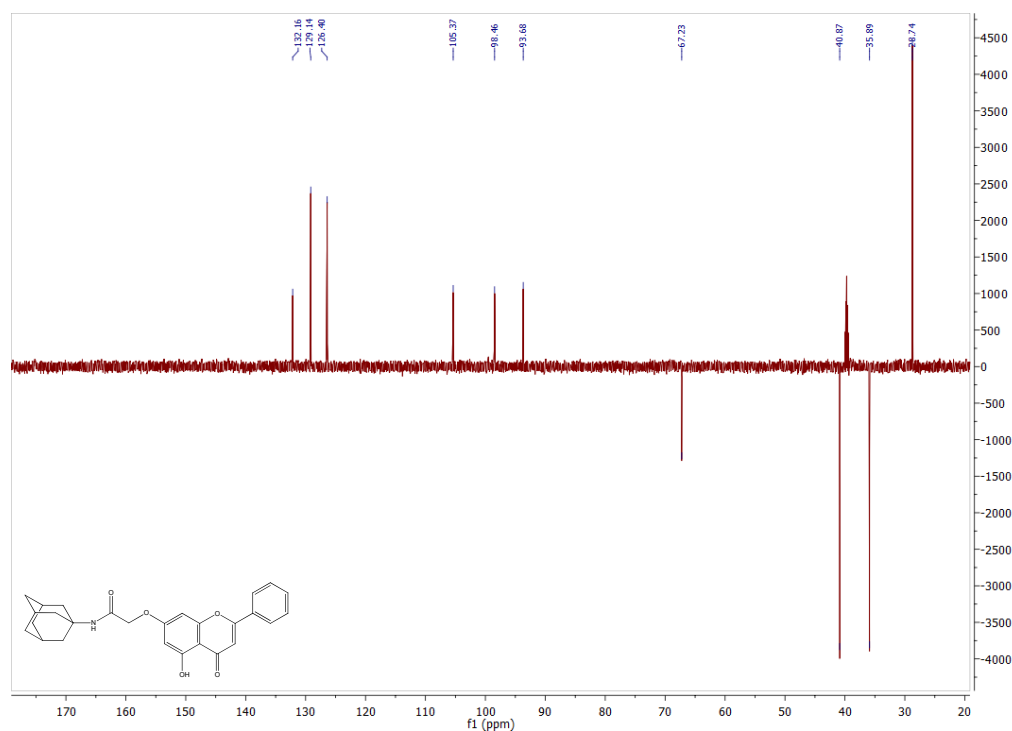


Spectrum 20  $^{13}\text{C}$  of N-(adamantan-1-yl)-2-[(5-hydroxy-4-oxo-2-phenyl-4H-chromen-7-yl)oxy]acetamide

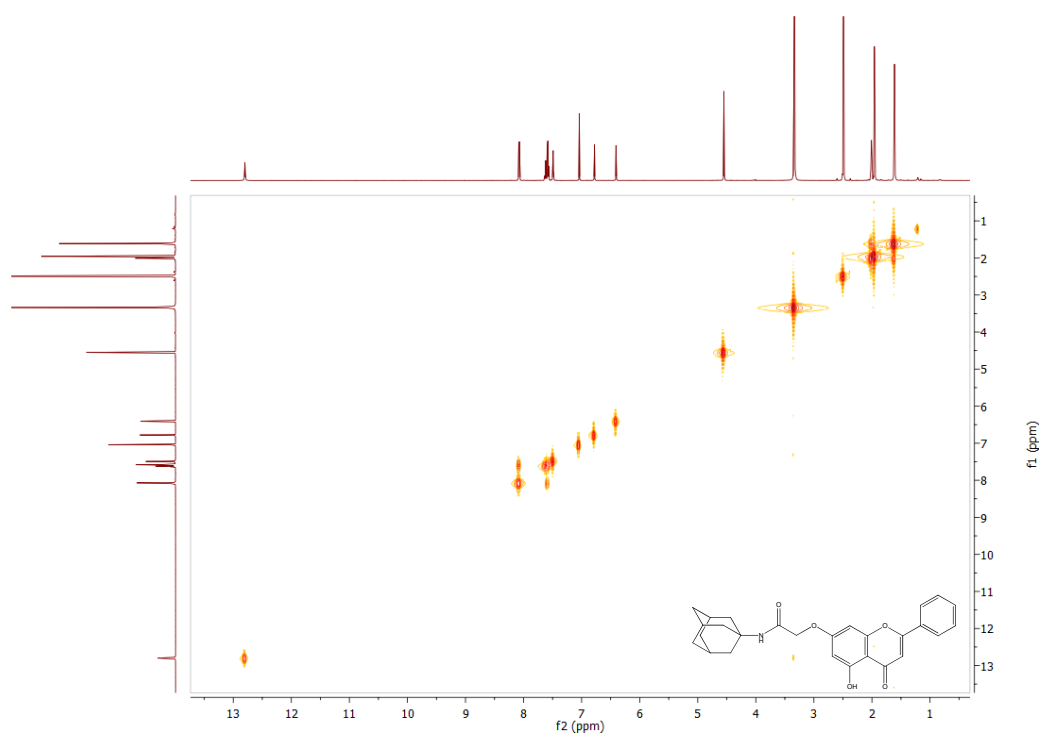




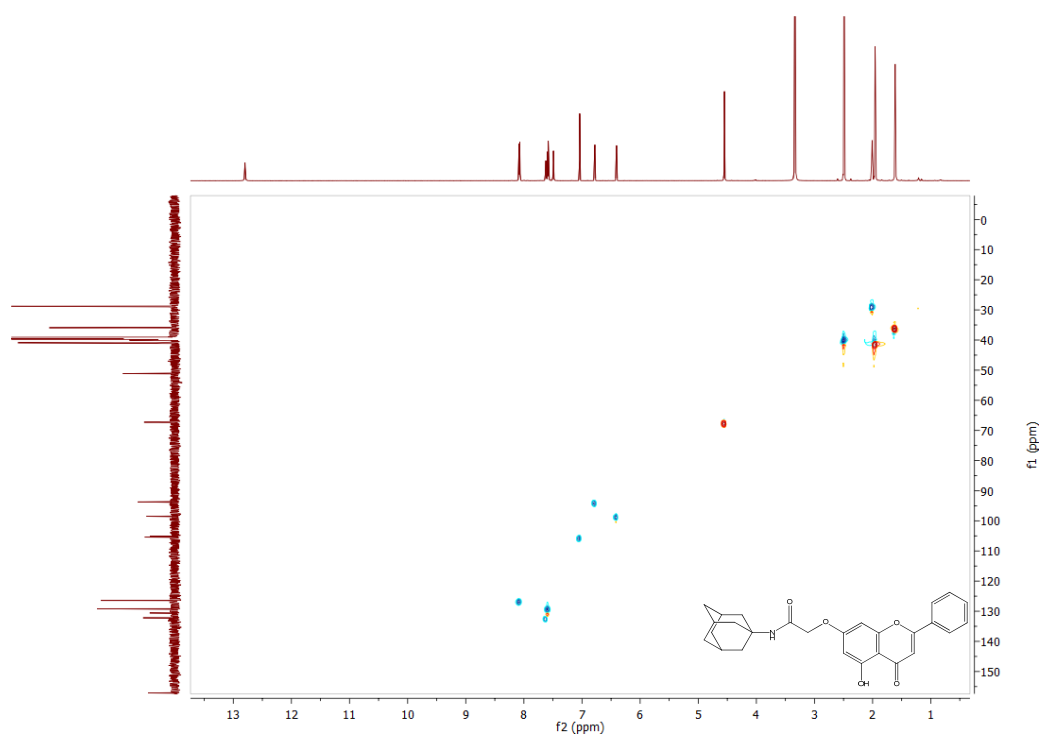
Spectrum 21 DEPT of N-(adamantan-1-yl)-2-[(5-hydroxy-4-oxo-2-phenyl-4H-chromen-7-yl)oxy]acetamide



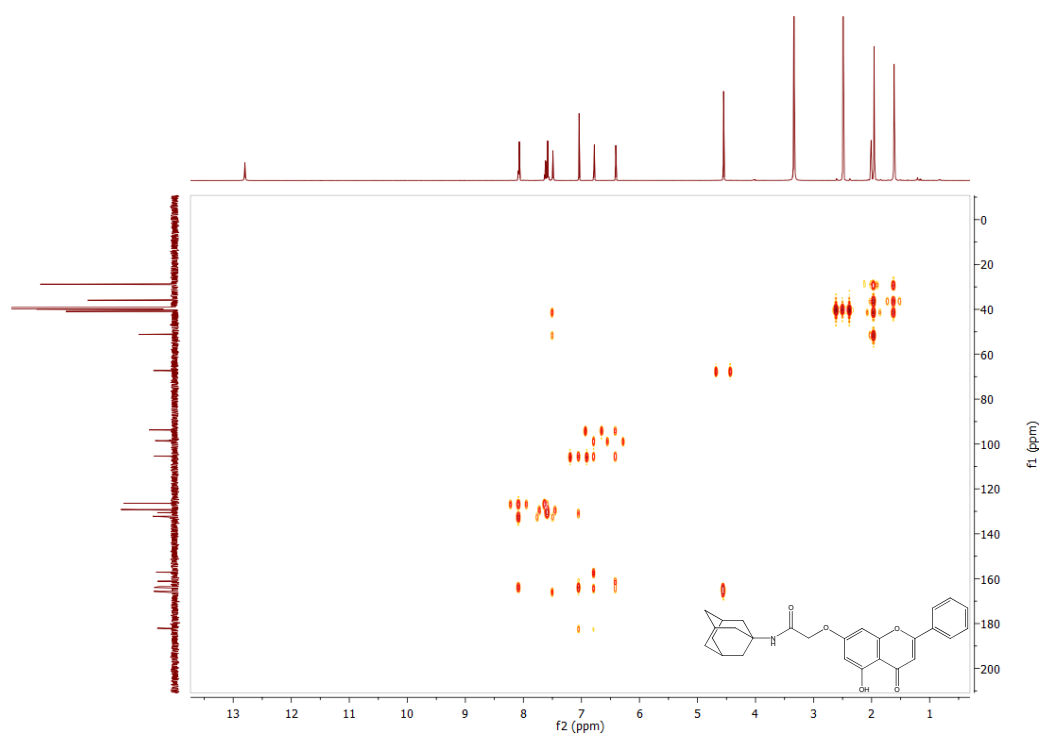
Spectrum 22 COSY of N-(adamantan-1-yl)-2-[(5-hydroxy-4-oxo-2-phenyl-4H-chromen-7-yl)oxy]acetamide



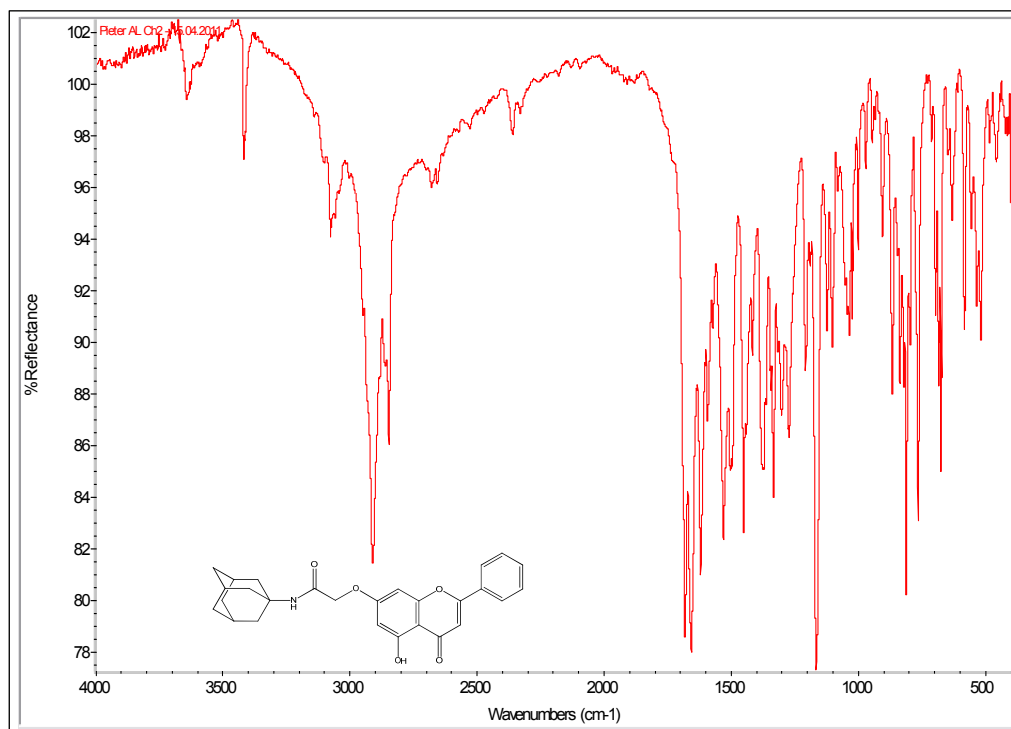
Spectrum 23 HSQC of N-(adamantan-1-yl)-2-[(5-hydroxy-4-oxo-2-phenyl-4H-chromen-7-yl)oxy]acetamide



Spectrum 24 HMBC of N-(adamantan-1-yl)-2-[(5-hydroxy-4-oxo-2-phenyl-4H-chromen-7-yl)oxy]acetamide

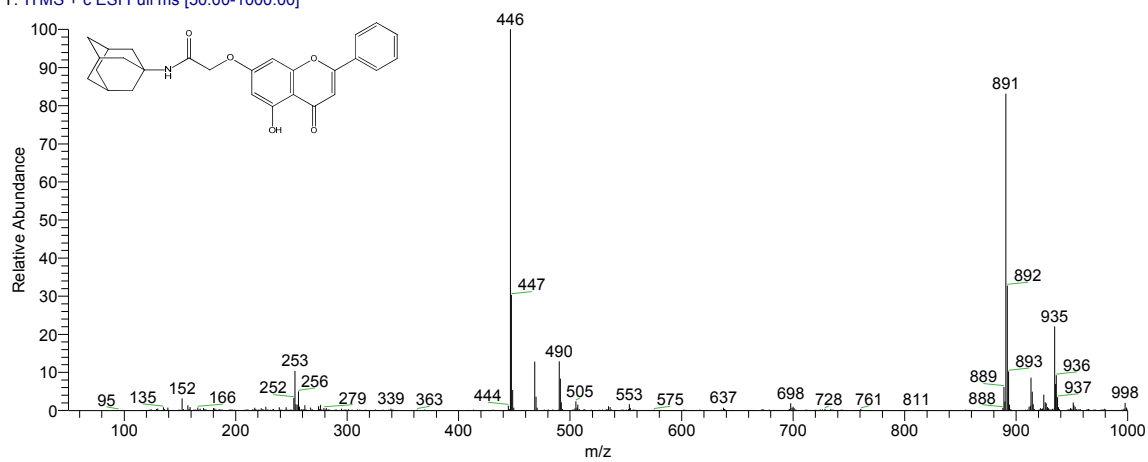


Spectrum 25  $\nu_{\max}$  of N-(adamantan-1-yl)-2-[(5-hydroxy-4-oxo-2-phenyl-4H-chromen-7-yl)oxy]acetamide



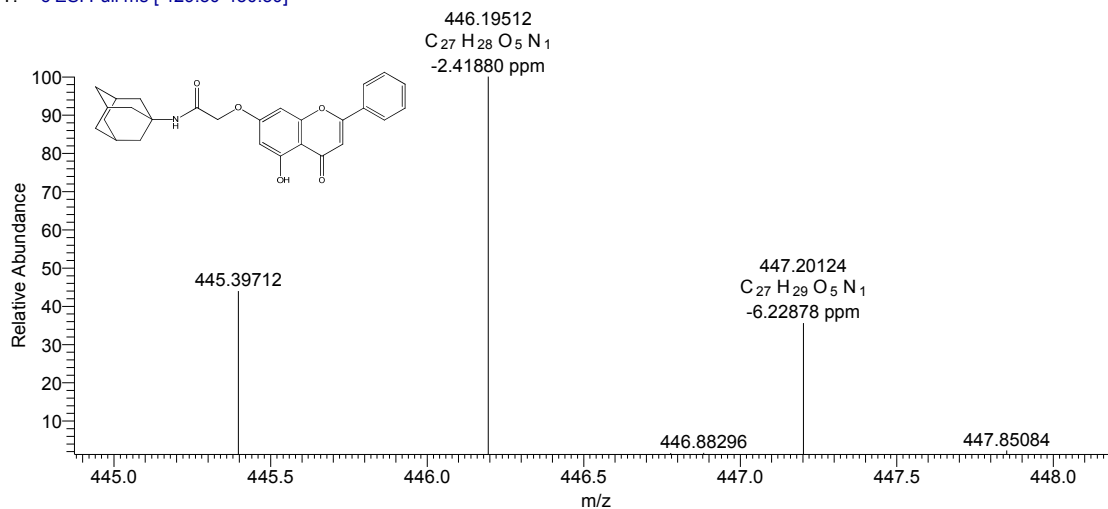
Spectrum 26 ESI MS of N-(adamantan-1-yl)-2-[(5-hydroxy-4-oxo-2-phenyl-4H-chromen-7-yl)oxy]acetamide

ALCrysin #9-20 RT: 0.32-0.74 AV: 12 NL: 9.22E3  
T: ITMS + c ESI Full ms [50.00-1000.00]

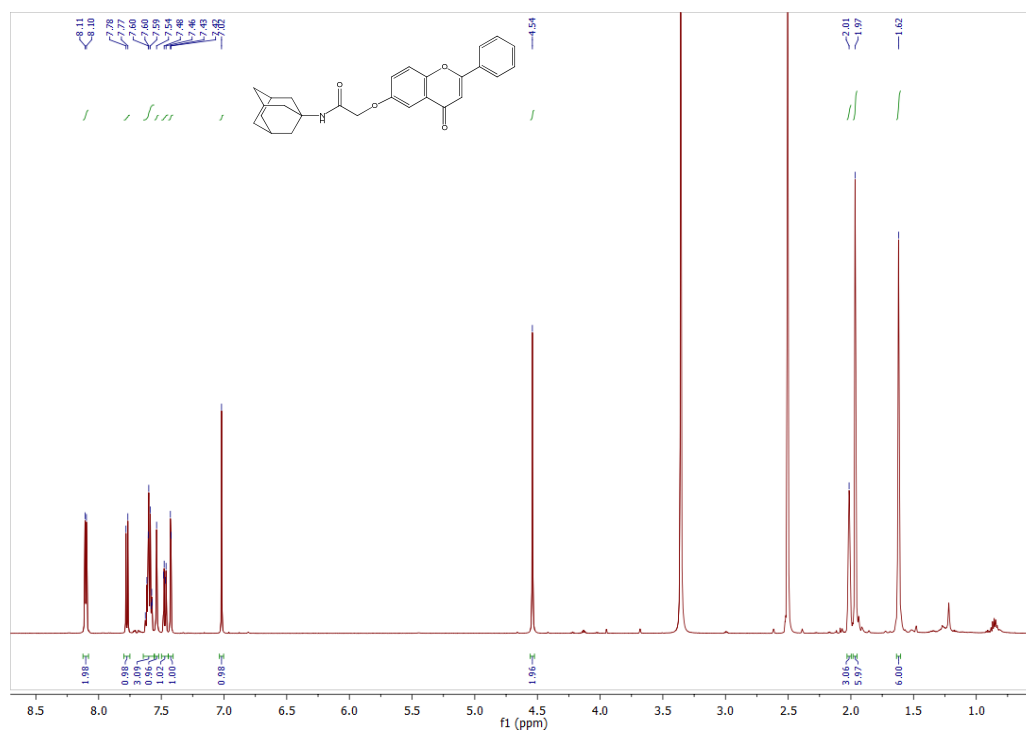


Spectrum 27 HRESIMS of N-(adamantan-1-yl)-2-[(5-hydroxy-4-oxo-2-phenyl-4H-chromen-7-yl)oxy]acetamide

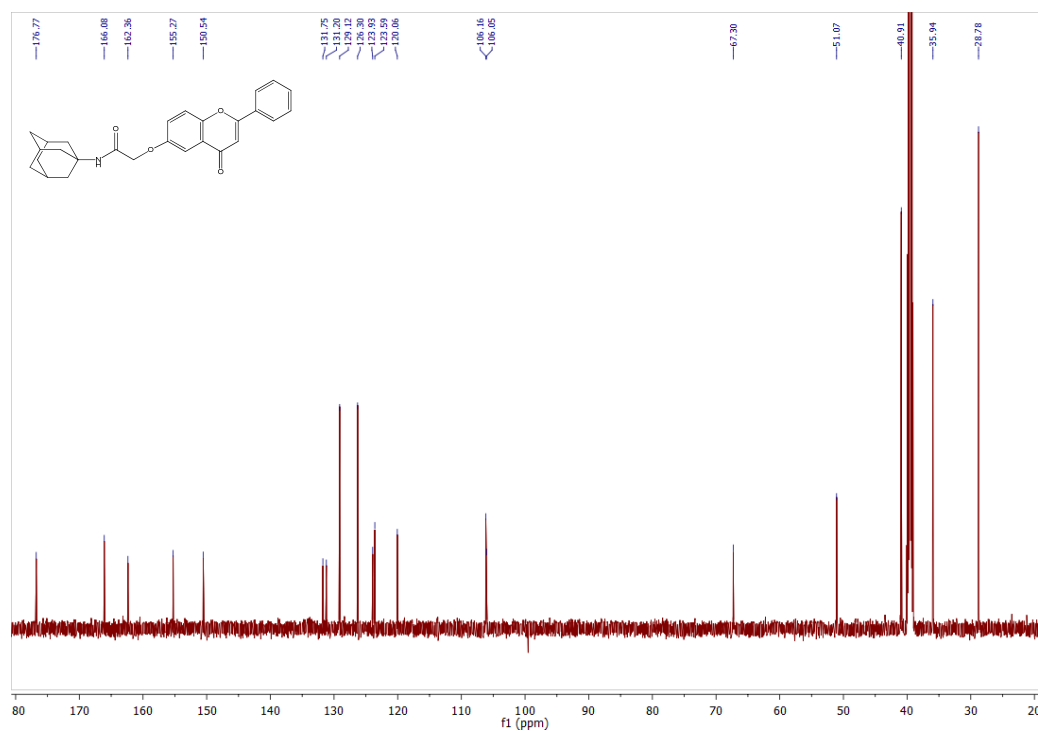
PF02\_HRESI-c1 #186 RT: 2.16 AV: 1 NL: 2.93E5  
T: + c ESI Full ms [ 429.50-450.50]



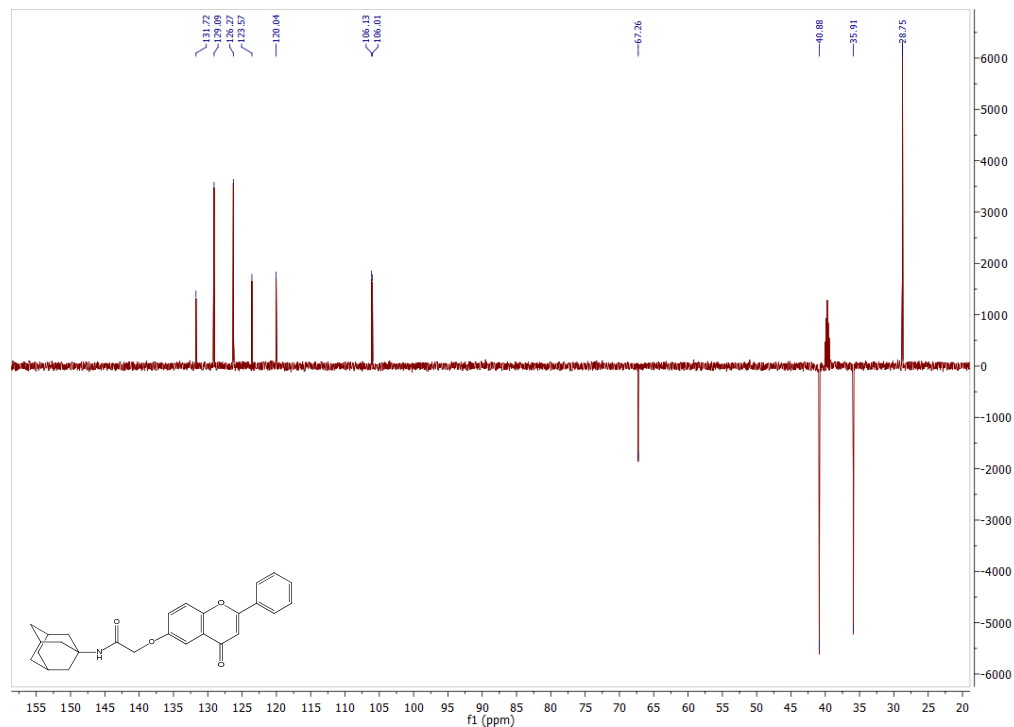
Spectrum 28 <sup>1</sup>H of N-(adamantan-1-yl)-2-[(4-oxo-2-phenyl-4H-chromen-6-yl)oxy]acetamide



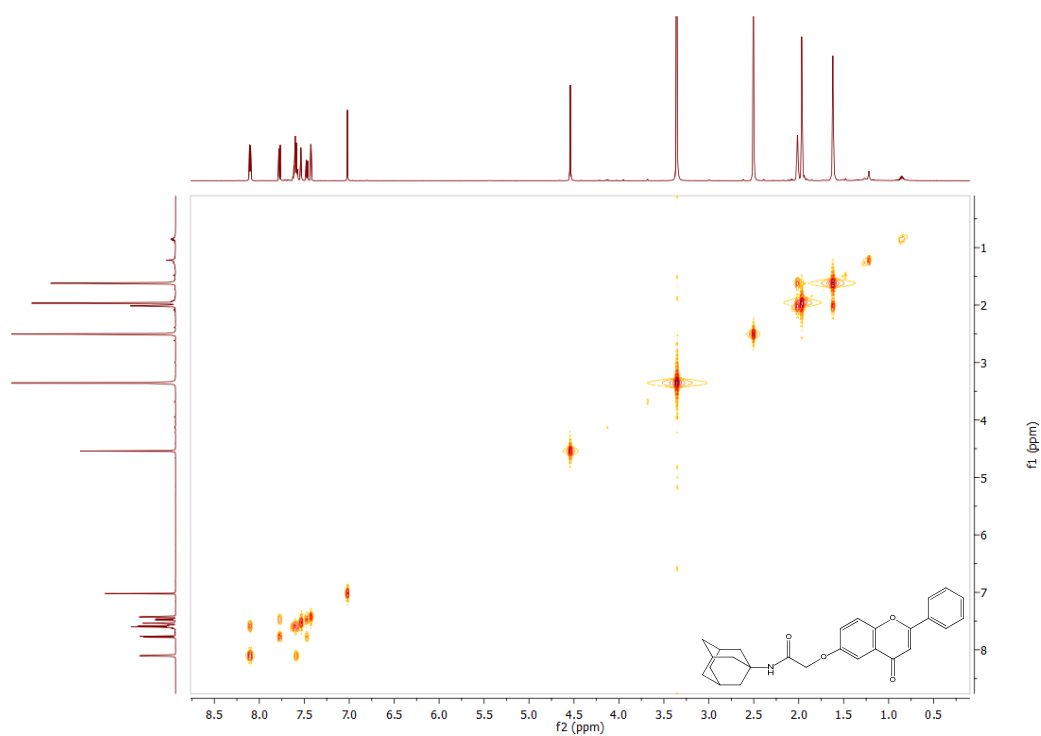
Spectrum 29  $^{13}\text{C}$  of N-(adamantan-1-yl)-2-[(4-oxo-2-phenyl-4H-chromen-6-yl)oxy]acetamide



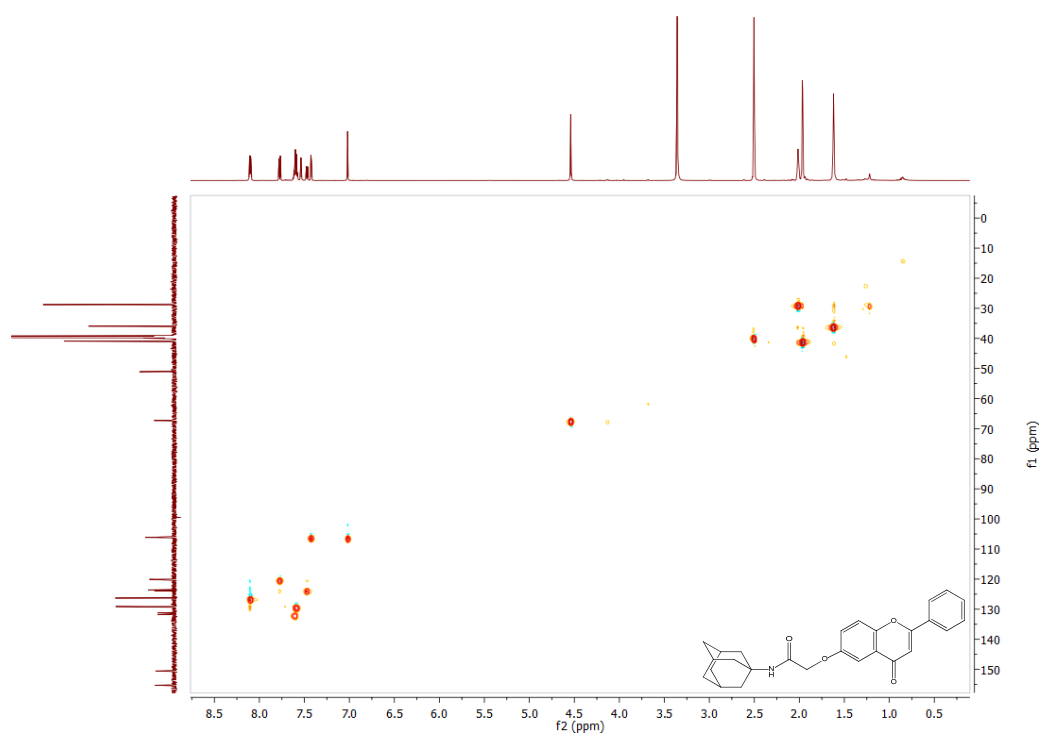
Spectrum 30 DEPT of N-(adamantan-1-yl)-2-[(4-oxo-2-phenyl-4H-chromen-6-yl)oxy]acetamide



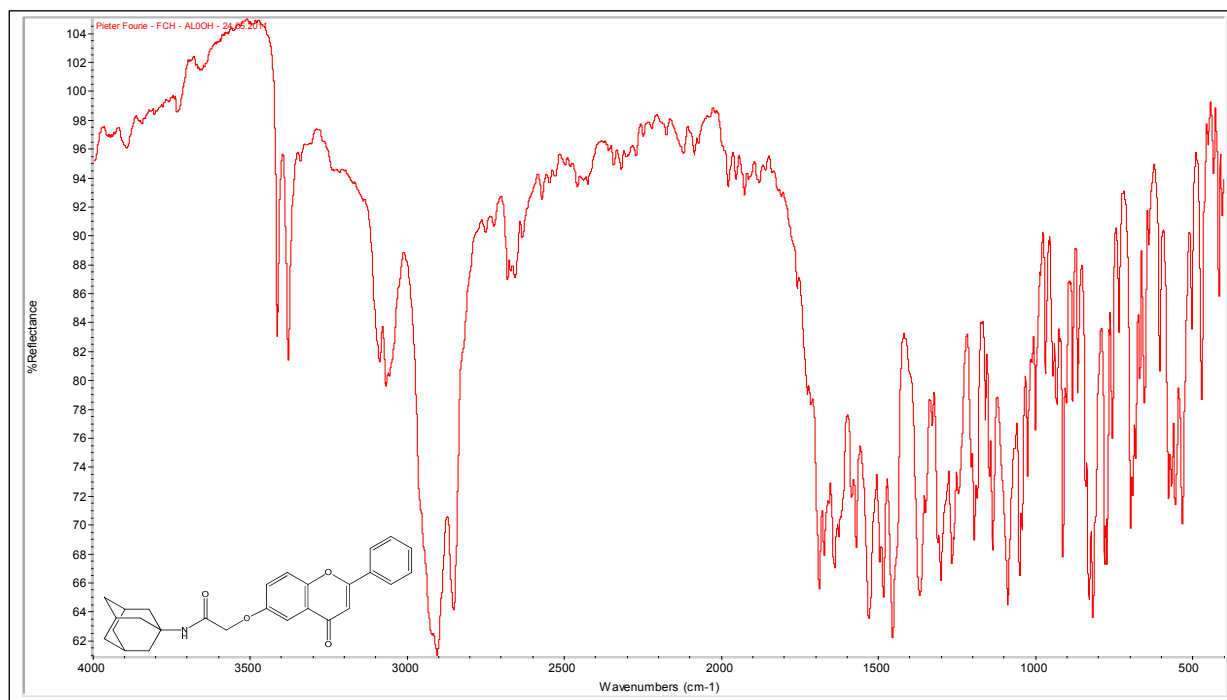
Spectrum 31 COSY of N-(adamantan-1-yl)-2-[(4-oxo-2-phenyl-4H-chromen-6-yl)oxy]acetamide



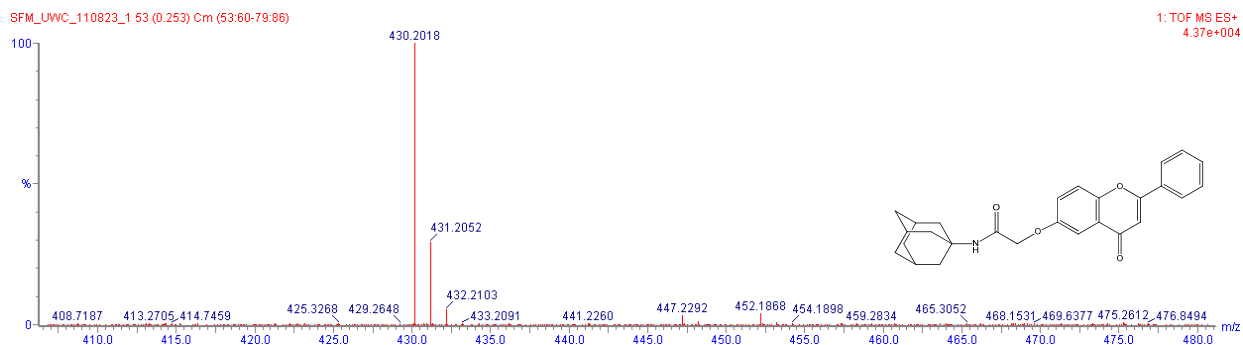
Spectrum 32 HSCQ of N-(adamantan-1-yl)-2-[(4-oxo-2-phenyl-4H-chromen-6-yl)oxy]acetamide



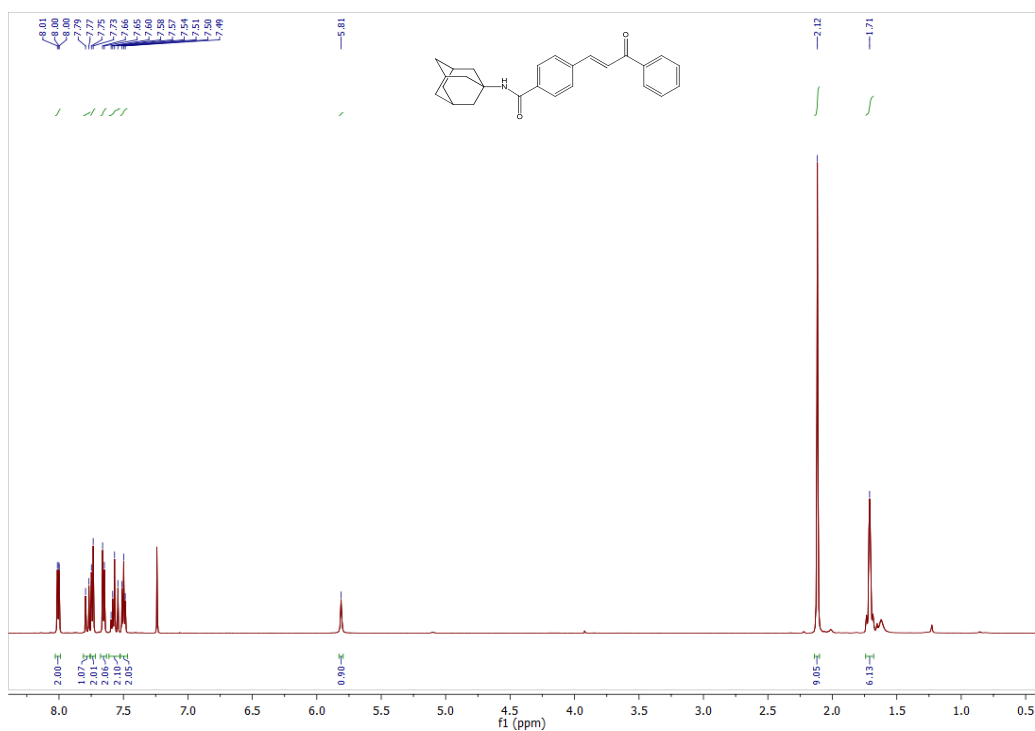
Spectrum 33  $\nu_{\max}$  of N-(adamantan-1-yl)-2-[(4-oxo-2-phenyl-4H-chromen-6-yl)oxy]acetamide



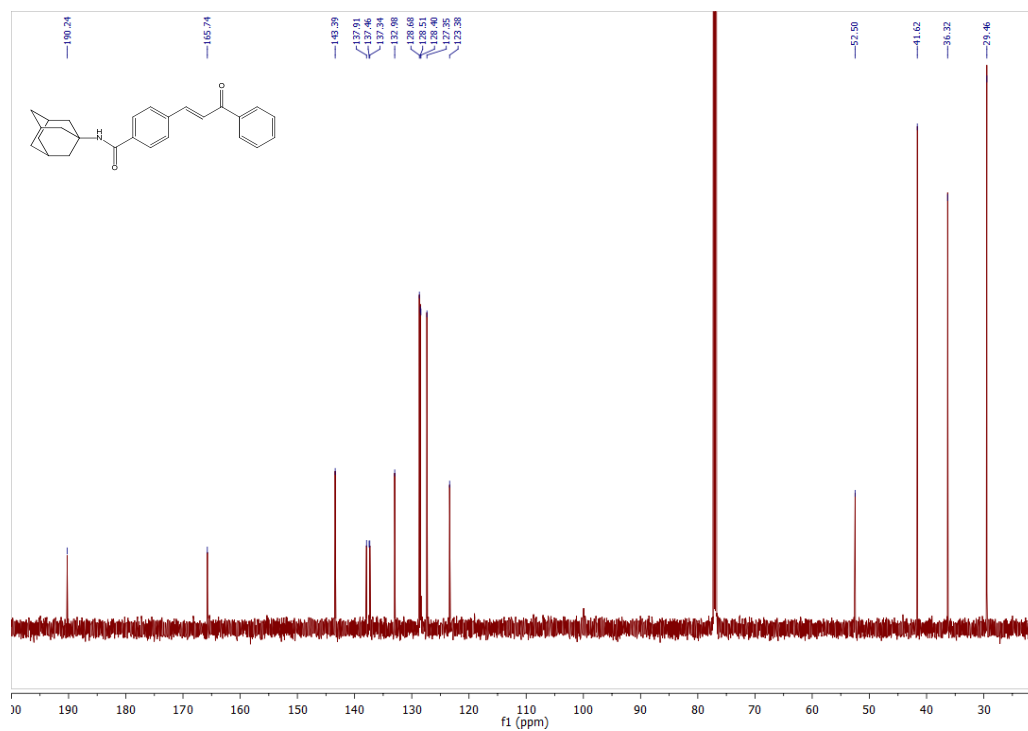
Spectrum 34 HRESIMS of N-(adamantan-1-yl)-2-[(4-oxo-2-phenyl-4H-chromen-6-yl)oxy]acetamide



Spectrum 35  $^1\text{H}$  of N-(adamantan-1-yl)-4-[(1E)-3-oxo-3-phenylpro-1-en-1-yl]benzamide

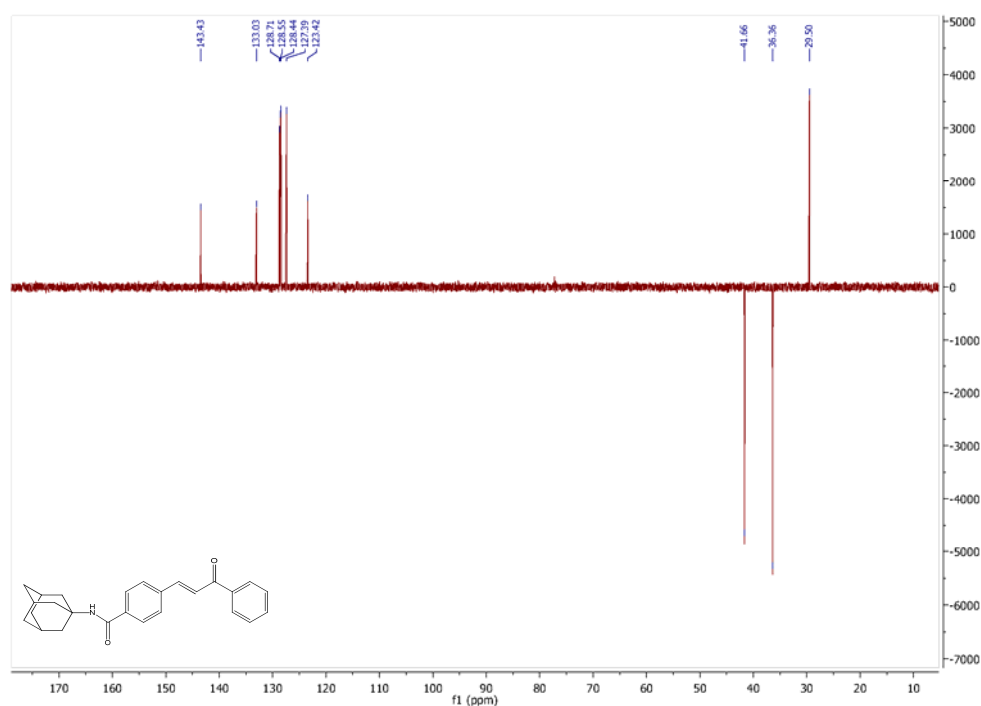


Spectrum 36  $^{13}\text{C}$  of N-(adamantan-1-yl)-4-[(1E)-3-oxo-3-phenylpro-1-en-1-yl]benzamide

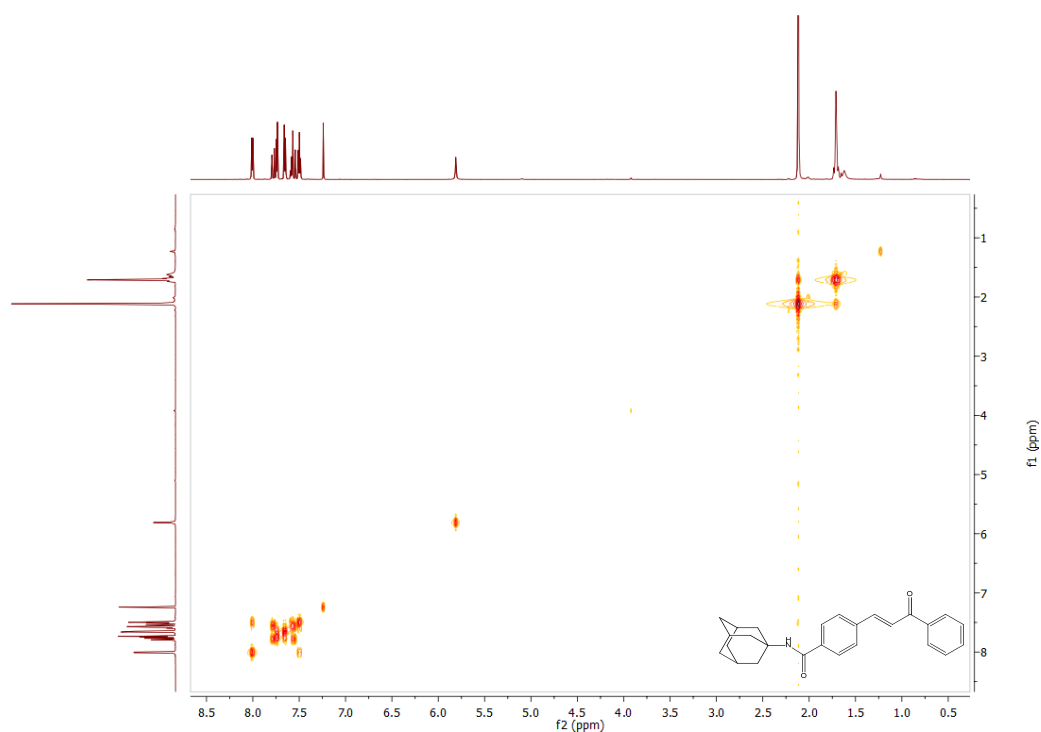




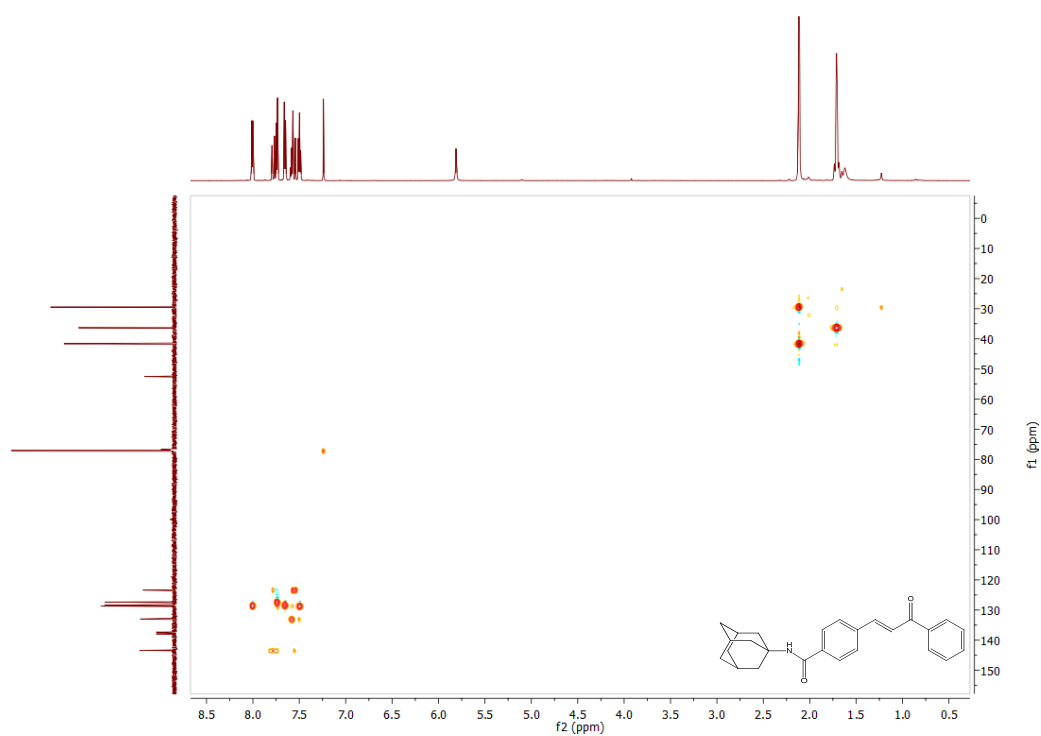
Spectrum 37 DEPT of N-(adamantan-1-yl)-4-[(1E)-3-oxo-3-phenylpro-1-en-1-yl]benzamide



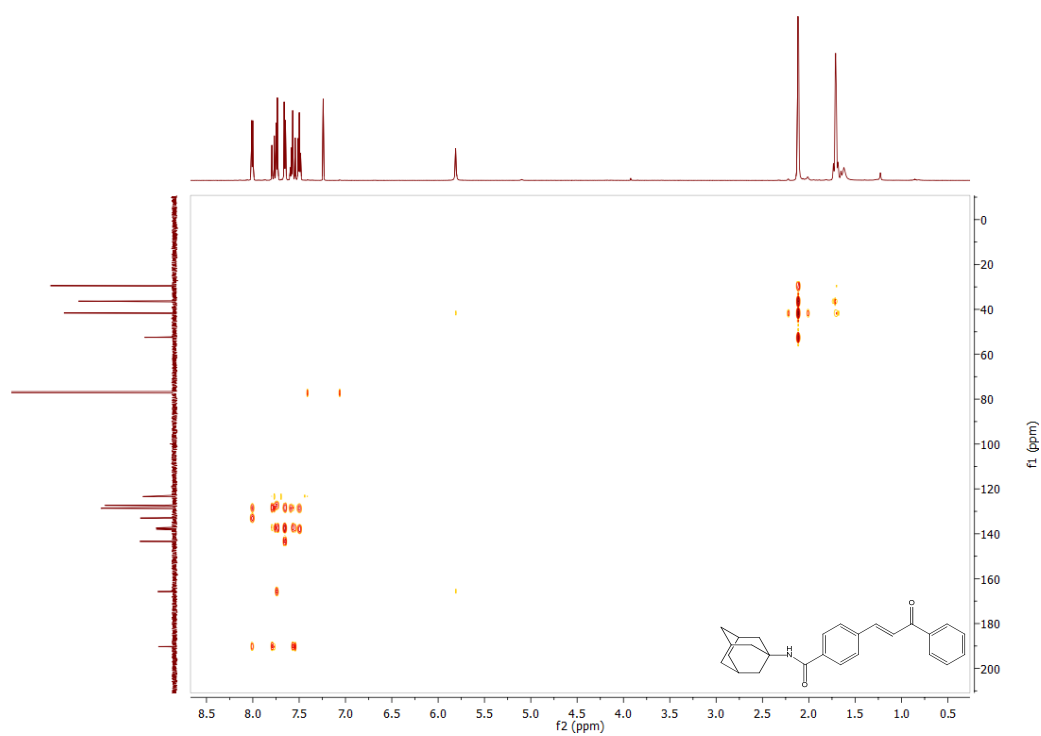
Spectrum 38 COSY of N-(adamantan-1-yl)-4-[(1E)-3-oxo-3-phenylpro-1-en-1-yl]benzamide



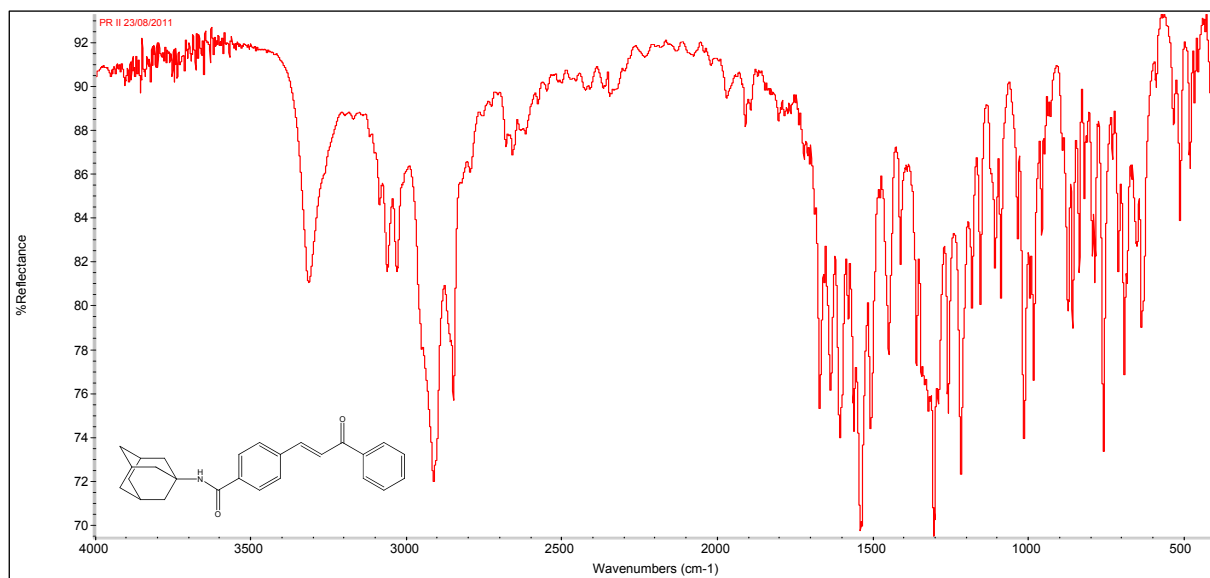
Spectrum 39 HSQC of N-(adamantan-1-yl)-4-[(1E)-3-oxo-3-phenylpro-1-en-1-yl]benzamide



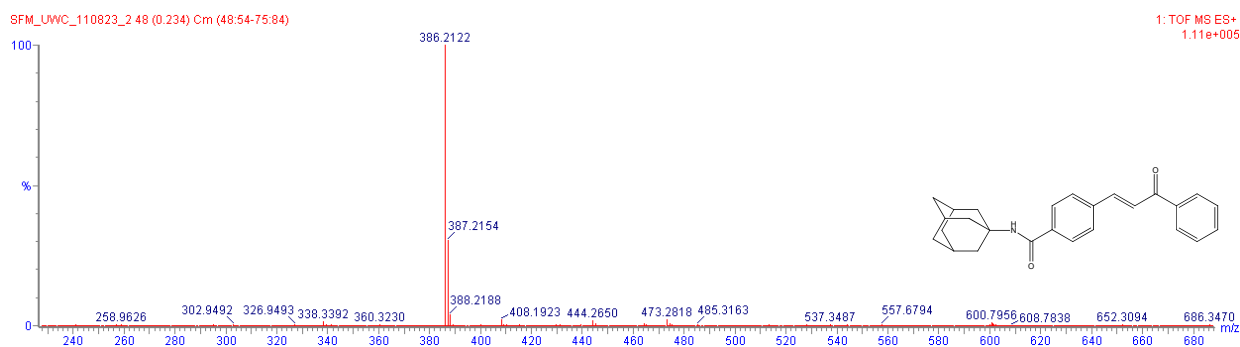
Spectrum 40 HMBC of N-(adamantan-1-yl)-4-[(1E)-3-oxo-3-phenylpro-1-en-1-yl]benzamide



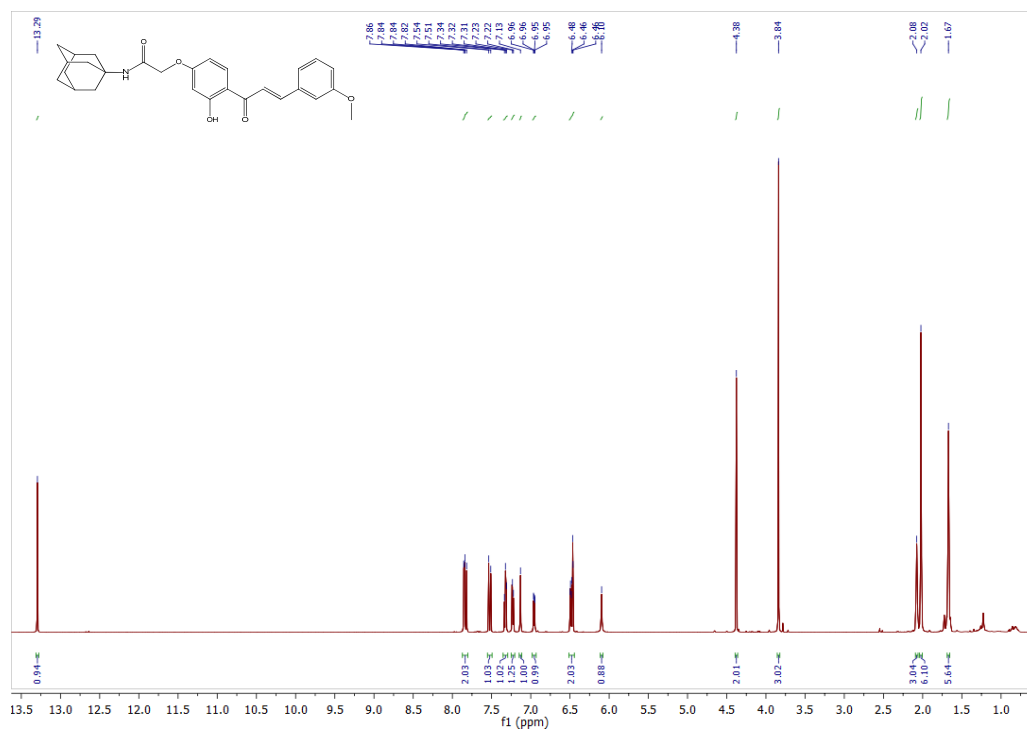
Spectrum 41  $\nu_{\max}$  of N-(adamantan-1-yl)-4-[(1E)-3-oxo-3-phenylpro-1-en-1-yl]benzamide



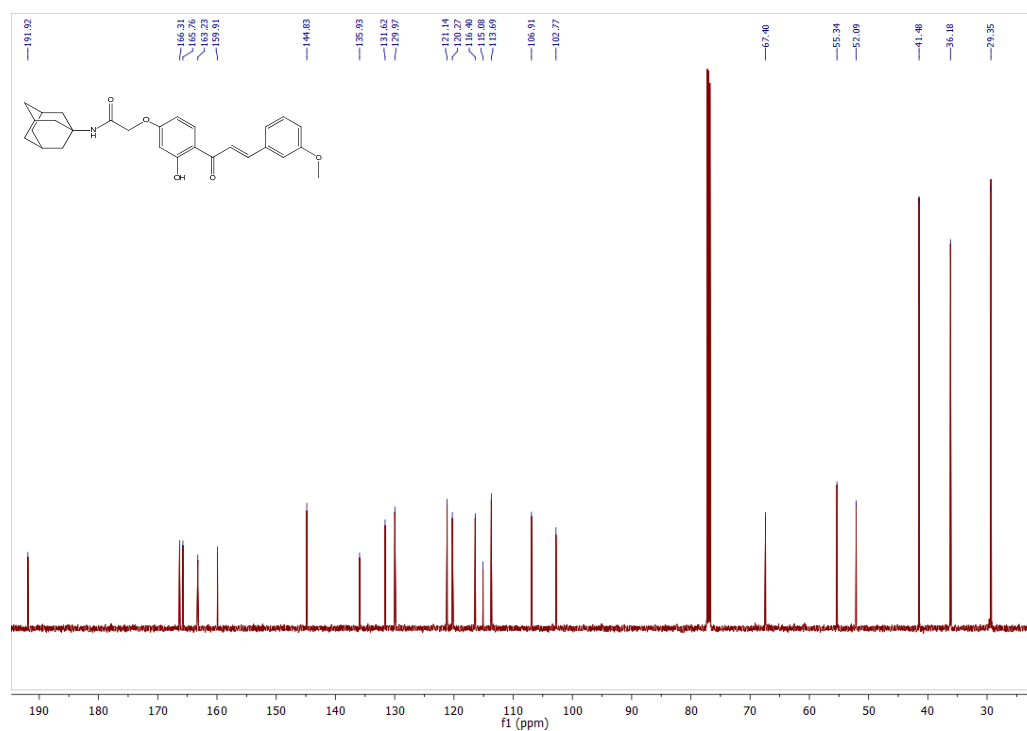
Spectrum 42 HRESIMS of N-(adamantan-1-yl)-4-[(1E)-3-oxo-3-phenylpro-1-en-1-yl]benzamide



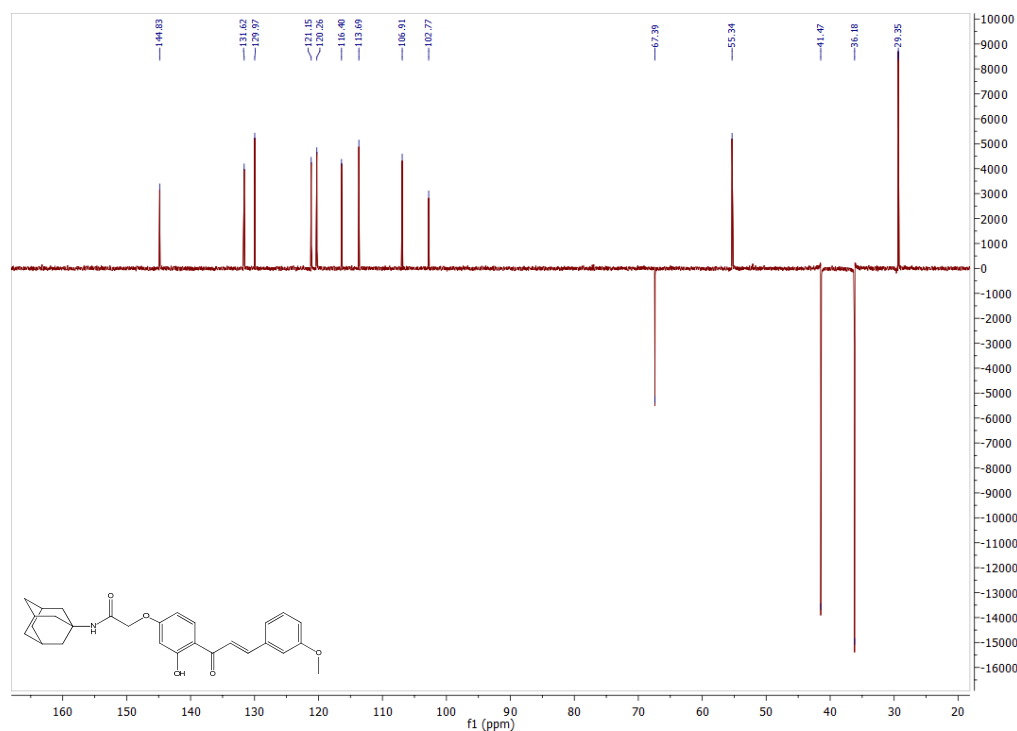
Spectrum 43  $^1\text{H}$  of N-(adamantan-1-yl)-2-{3-hydroxy-4-[(2E)-3-(3-methoxyphenyl)pro-2-enoyl]phenoxy}acetamide



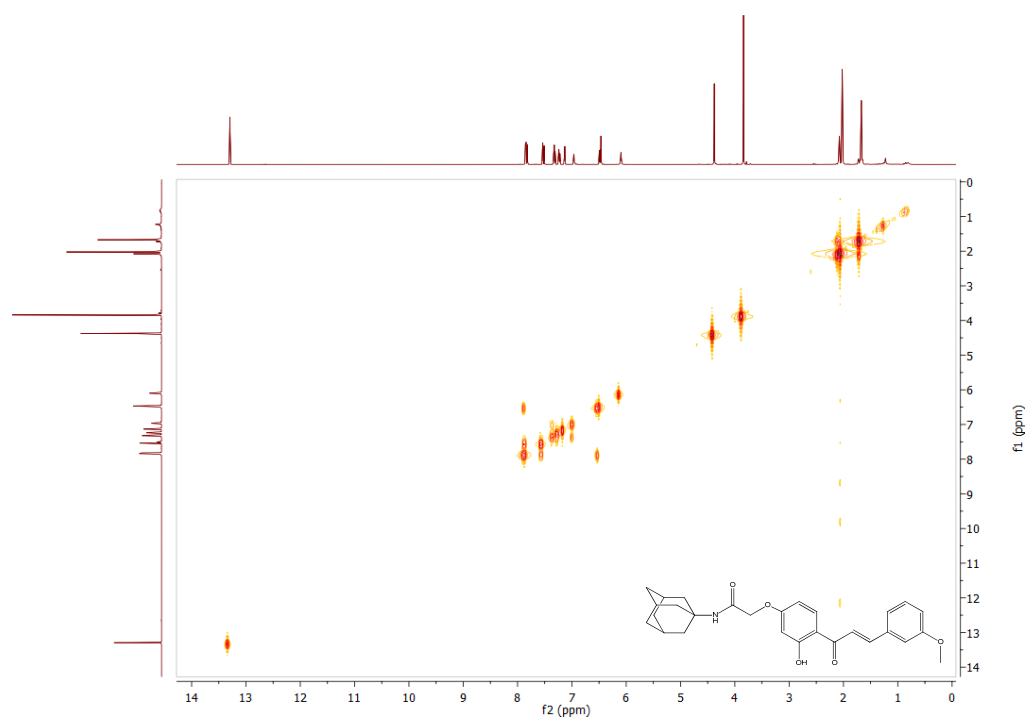
Spectrum 44  $^{13}\text{C}$  of N-(adamantan-1-yl)-2-{3-hydroxy-4-[(2E)-3-(3-methoxyphenyl)pro-2-enoyl]phenoxy}acetamide



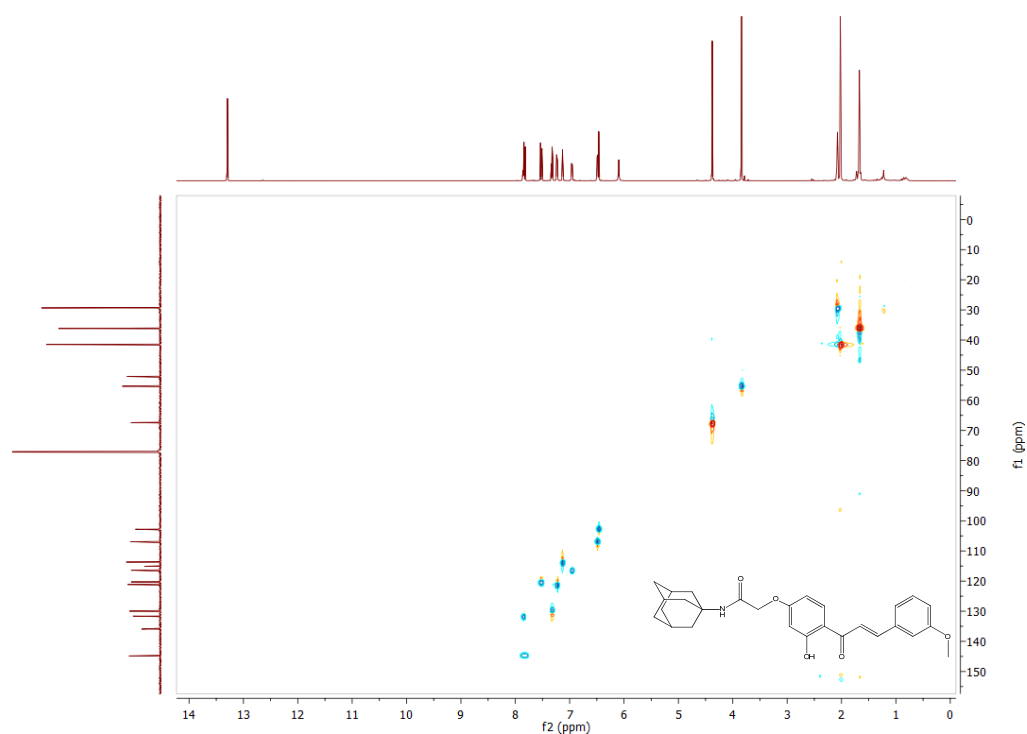
Spectrum 45 DEPT of N-(adamantan-1-yl)-2-{3-hydroxy-4-[(2E)-3-(3-methoxyphenyl)pro-2-enoyl]phenoxy}acetamide



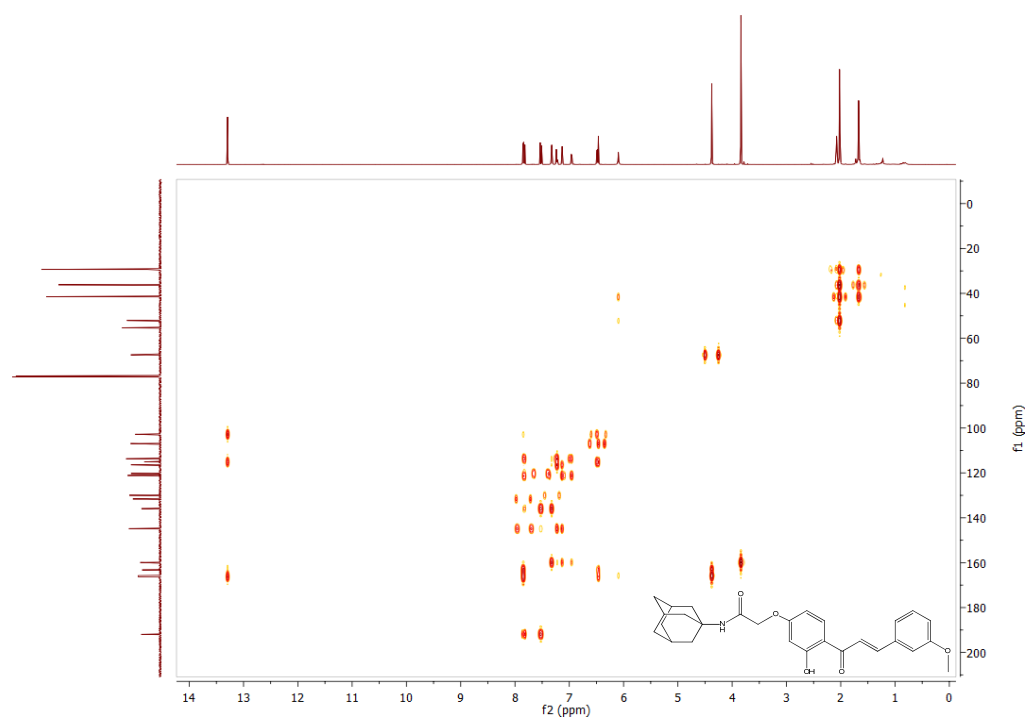
Spectrum 46 COSY of N-(adamantan-1-yl)-2-{3-hydroxy-4-[(2E)-3-(3-methoxyphenyl)pro-2-enoyl]phenoxy}acetamide



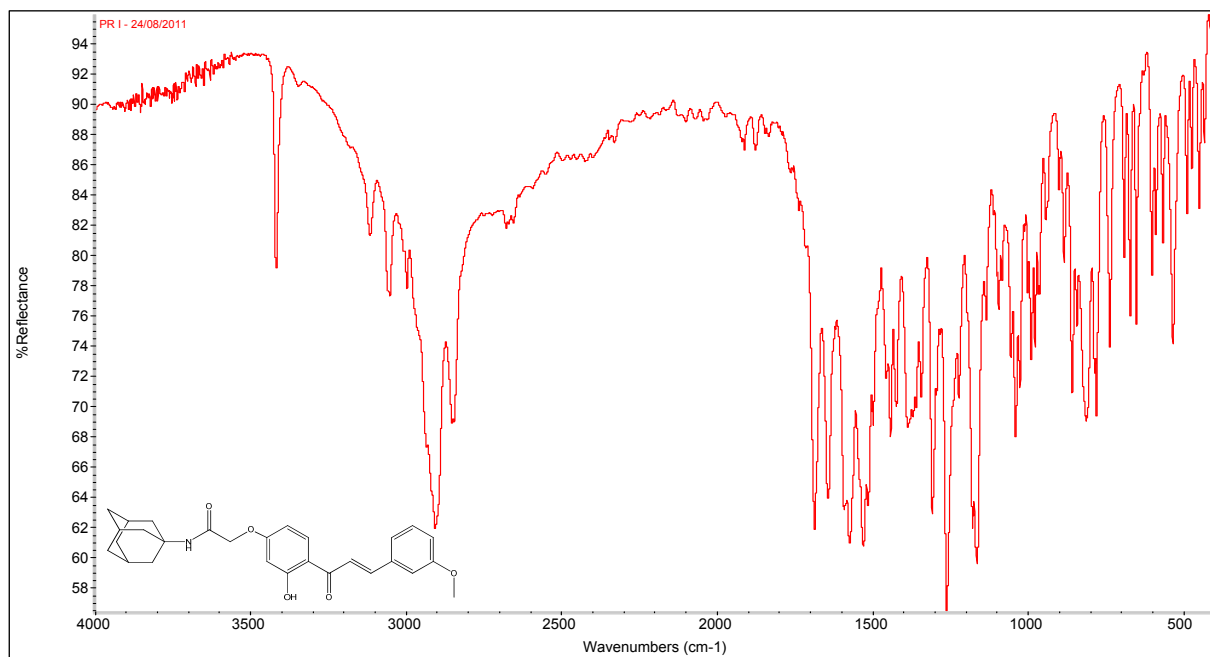
Spectrum 47 HSCQ of N-(adamantan-1-yl)-2-{3-hydroxy-4-[(2E)-3-(3-methoxyphenyl)prop-2-enoyl]phenoxy}acetamide



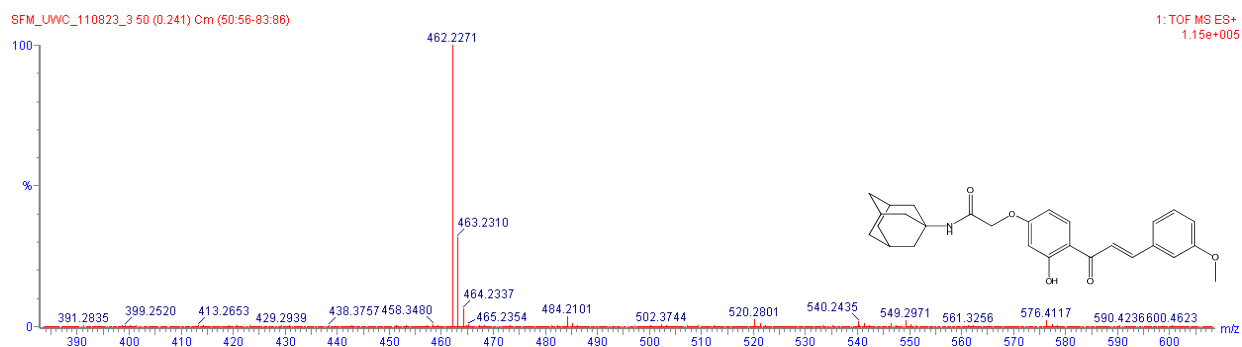
Spectrum 48 HMBC of N-(adamantan-1-yl)-2-{3-hydroxy-4-[(2E)-3-(3-methoxyphenyl)prop-2-enoyl]phenoxy}acetamide



Spectrum 49  $\nu_{\text{max}}$  of N-(adamantan-1-yl)-2-{3-hydroxy-4-[(2E)-3-(3-methoxyphenyl)pro-2-enoyl]phenoxy}acetamide



Spectrum 50 HRESIMS of N-(adamantan-1-yl)-2-{3-hydroxy-4-[(2E)-3-(3-methoxyphenyl)pro-2-enoyl]phenoxy}acetamide



## Acknowledgements

I would like to express my sincere gratitude to the following people and organisations for their support and assistance in helping me complete this dissertation:

- School of Pharmacy, UWC:

Prof. Sarel Malan.

- Department of Pharmaceutical Chemistry, NWU, Potchefstroom:

Prof. Sandra van Dyk

Prof. D.W. Oliver

Arina Lourens

Bennie Repsold

Nellie Scheepers

Jacques & Anèl Petzer

Samuel Mokobane

Andre Joubert

- Mr. Cor Bester, Mr. Petri Bronkhorst and Mrs. Antionette Fick for their invaluable assistance in the handling of the animals during the biological assay.
- Wessel Roux, for assisting me during my study and his friendship throughout the study period.
- Mr Andre Joubert and Mr Marius Brits, for determining the IR spectra.
- Mrs. Marelize Ferreira (WITS) and Dr. Marietjie Stander (Stellenbosch) for the skilled recording of mass spectrometry.
- The National Research Foundation, Academy of Pharmaceutical Sciences and North West University for financial support.
- My parents, Peet and Fransie Fourie, for giving me this amazing opportunity and for always believing in me.